School of Earth and Planetary Sciences

New Insights into the Structural and Stratigraphic Evolution of the Northern Sumatra Basin, Aceh

Muchlis

0000-0002-4391-0325

This thesis is presented for the Degree of

Doctor of Philosophy

of

Curtin University

December 2022

Declaration

To the best of my knowledge and belief, this thesis contains no material previously published by any other person except where due acknowledgment has been made.

This thesis contains no material which has been accepted for the award of any other degree or diploma in any university.

Signature:

Date: 21/12/2022

ABSTRACT

The Northern Sumatra Basin (NSB) is a Paleogene-Neogene basin in a back-arc setting relative to the volcanic arc along the Barisan Mountains. The arc forms the spine of west Sumatra and marks the position of the Sumatra Fault System. The North Sumatra Basin forms a prolific hydrocarbon province, evidenced by the giant Arun gas field and other petroleum fields. However, the NSB is underexplored due to the long periods of domestic war. This thesis aims to investigate the geology of the North Sumatra Basin based on available existing data.

SRTM data and regional 2D seismic profiles have been used to examine surface and subsurface structures in the onshore part of the basin and a marine 2D seismic survey has been used to study structures in the offshore parts of the basin. There are three stages involved in the evolution of the NSB: rifting, post-rift sagging (tectonic quiescence), and compression. Both onshore and offshore areas were initiated as a rift basin in the Oligocene and are dominated by north-south trending extensional faults, although NW-SE trending faults are also present adjacent to the Barisan foothills in the onshore NSB. Both the onshore and offshore parts of the basin then experienced a period of thermal subsidence from the Miocene onwards, resulting in the thickening of strata into the basin centre.

The onshore and offshore areas have different histories related to compression. In the onshore area, compressional structures only developed during the Pliocene to Recent. They predominantly occur close to the Barisan Mountains and are expressed as anticlines and synclines on SRTM data. Due to the uplift, most post-rift sedimentary rocks are exposed and eroded at the surface. Most of these structures have a predominantly northwest-southeast trend, similar to the regional tectonic trend defined by the Barisan Mountains, the main Sumatra Fault and the Indian Ocean subduction trench, Compressional structures have caused the area to be geologically complex, which has made seismic imaging challenging. However, seismic data show that these structures mainly formed as detachment folds above thick Miocene shale sequences. Further into the basin limited inversion of original rift-related extension faults resulted in the development of fault propagation folds with lower relief and a north-south orientation reflecting the orientation of the underlying faults

By contrast, compression in the offshore North Sumatra Basin occurred in several episodes in different areas. The first occurred in the early Miocene, in the north of the offshore North Sumatra Basin. The event inverted the syn-rift successions into the anticline structures associated with fault propagation folds and detachment folds. The second was in the late Miocene and occurred in the northwest, toward the Mergui Ridge/Platform. The inversion formed a symmetrical anticline and inverted the post-rift sedimentary rocks above the horst block. The last was in the Pliocene-Pleistocene and occurred in the

south of the offshore basin, towards the coastline, close to the surface expression of the Barisan Mountains. Similar to the onshore NSB a thin-skinned fold and thrust belt is developed, detached on thick Miocene shales. However, in this area uplift is less and the fold belt remains below sea level.

In the offshore area small scale planar and listric extensional faults developed during the Pliocene-Pleistocene. Some planar faults reactivated older faults and formed monoclines above the tips of faults. Strike-slip faults also developed during this period.

Earthquake data indicate that the basin is still active in the onshore area. The data shows that most earthquakes are related to compressional stress, with the major trends being northwest-southeast. Some onshore interpreted faults identified in this thesis are located close to the earthquakes' epicentres. Although the faults are not directly linked to the earthquakes, they may act as a potential source for future earthquakes.

In addition, the potential of petroleum resources and reserves in the North Sumatra Basin remains promising, especially in the western margin of the onshore North Sumatra Basin. Using passive seismic, a low frequency (1 to 6 Hz) anomaly shows the possibility of hydrocarbon accumulations in the area of a carbonate build-up. In other places, several seismic lines suggested the presence of carbonate build-ups both onshore and offshore, which may also host the hydrocarbon.

Some of the key findings of this research provide a new perspective on our current knowledge of the geology of the North Sumatra Basin. These revisions cover new interpretations of structural relationships and basement configuration.

ACKNOWLEDGEMENTS

The author would like to thank Lion Energy and Aceh for providing the seismic data used in this study. I am very grateful for the support of the Australia Award Scholarships in Indonesia and Curtin University for granting me a Ph.D. scholarship. Schlumberger is acknowledged for granting an education license for the Petrel software used for seismic interpretation.

In particular, I would like to thank Chris Elders (Curtin University) for supervising this project. He has taught me so many things that are not only related to seismic interpretation. I am also grateful to Jane Cunneen and Greg Smith (Curtin University) for their kind advice and discussions regarding some aspects of this project.

Most importantly, I would like to thank my family, especially my mother, my father, my wife (Nurul), and my children (Luna and Ibrahim), for their unconditional support. Without them, this project could never have been accomplished. Also, Alfi syahrin for special helps in drawing the cartoons.

ATTRIBUTION STATEMENT

This thesis is the product of work that I undertook in a Petrel project which contained seismic and well data. The data was provided by Lion Energy. I undertook all of the seismic interpretation myself. I then wrote and prepared the first draft of the dissertation and prepared all the figures. Discussion of the first draft occurred between myself and my supervisor, Professor Elders. A final draft of the thesis was proof read by Mr John Fielder, an approved proof reader arranged by Curtin International.

During preparation and development of ideas I had regular discussions with my supervisory panel. This includes the preparation of documents for several conferences as paper or poster presentations, some involving oral presentations.

Student Name: Muchlis

Signature…….

Contents

`

LIST OF FIGURES

LIST OF TABLES

1 INTRODUCTION

1.1 Location of Study Area

The North Sumatra Basin (NSB) is situated in the Northeast of Sumatra Island, Indonesia, and extends offshore to the northwest into the Mergui Basin, offshore Thailand. Both basins are part of the same structural unit (Andreason, Mudford et al, 1997; Davies, 1984; Meckel et al., 2012). The Indonesian part of the basin covers an area of 60,000 km2, both onshore and offshore (Hidayatillah et al., 2017). To the south, the NSB is bounded by the Barisan Mountains, which are cut by the Sumatra Fault System (SFS). To the northwest, the North Sumatra and Mergui basins are separated from the Andaman Sea basins by the Mergui Ridge (Figure 1-1). To the southeast, the Asahan Arch (also known as the Tebing Tinggi High) separates the NSB from the Central Sumatra Basin (CSB) (Figure 1-2). The NSB is Paleogene-Neogene in age and has a complex tectonic history related to its location in a back-arc setting relative to the Sunda subduction system (Figure 1-1).

The first commercial hydrocarbon discovery in this basin was the Telaga Said field, made by Royal Dutch Shell in 1885. In 1929 another giant field, Rantau, was discovered, which made the basin well-known. Both fields are shallow, with the oil trapped in anticlinal structures (Koesoemadinata, 1969). The most significant discovery that of the Arun field (Carbonate build-up reservoir), was made in 1971 by Exxon Mobil. The Arun and Rantau fields are both located in Aceh province (Figure 1-3). However, after the discovery of the Arun field exploration activity within this basin was reduced due to the geopolitical situation (Banukarso et al, 2013). Thus, some areas of this basin are considered a “green field” because of the gap in exploration and recent geological research. This is demonstrated by the renewed interest in the basin that has resulted in the recent offshore discoveries of Timpan-1 drilled by Harbour Energy in 2022 and Layaran-1 drilled by Mubadala Energy in 2023.

1.2 Aims and Objectives

The overall aim of this thesis is to investigate the structural and stratigraphic evolution of the Northern Sumatra Basin. Because of the location of the North Sumatra Basin in a back-arc setting relative to the Sunda volcanic arc and it proximity to the strike-slip Sumatra Fault and the compressional structures of the Barisan Mountains, specific objectives (outlined in section 2.5) include determining the interaction between extensional, compressional and strike-slip components of deformation, the way in which they are distributed in the basin and their relationship to regional plate tectonic evolution. New insights gained from this study will give a

more thorough understanding of the basin, fill the gap in the previous studies, and open opportunities for more exploration in the future. AusAid funded this project to develop skills and competency in geoscience in Aceh and to encourage research to develop new knowledge of structural geology and stratigraphy in the region.

This thesis used all available data, such as seismic, well data, SRTM (Shuttle Radar Topography Mission) data, surface geological information (geological maps, remote sensing imagery), and earthquake data, to interpret the geological structure and evolution of the North Sumatra Basin from the Oligocene to the Recent. This research examines the timing of extension, compression, and strike-slip deformation and relates these different phases of deformation to the evolution of the Sumatra/Sunda margin. Of particular interest is the partitioning of extensional, compressional and strike slip deformation, and how this changes through time. Recent earthquake data is also incorporated to investigate neo-tectonic deformation.

In addition, this study will provide a better understanding of the hydrocarbon potential, which will provide significant knowledge for future exploration. Thus, the result of this research will enhance understanding of this basin and help encourage exploration for hydrocarbons, which in turn will help to develop the economy of Indonesia and Aceh in particular.

1.3 Thesis Structure

The thesis comprises seven chapters, including the Introduction (Chapter 1) and Conclusion (Chapter 7). A detailed literature review is presented in Chapter 2, which summarizes the present understanding of the study area regarding the tectonic elements, regional tectonic evolution, basin development, and the general stratigraphic fill of the basin. The main tectonic features presented in chapter 2 are the Sumatra Fault System, the Barisan Mountains, and the Barisan Foothills, as well as the North Sumatra Basin itself.

Chapter 3 presents the data and methodology. This is followed by the main results, which are the core of this study, and are described in chapters 4, 5, and 6.

Chapter 4 focuses on seismic interpretation in the onshore North Sumatra Basin constrained by well data and the interpretation of SRTM images to reveal a new perspective that updates the work from previous authors. Chapter 4 identifies structural elements that differ from those in the current literature and presents a new interpretations of the basin evolution and the style of structures in the basin.

Chapter 5 focuses on the interpretation of seismic data from the offshore North Sumatra Basin.

Chapter 5 discuses basin evolution, structural styles, and the distinctive geological features observed in the data.

Chapter 6 discusses hydrocarbon potential using passive seismic in the western onshore part of the North Sumatra Basin. The acquisition was done over an area of approximately 64 km2, with 78 measurements, around the Sigli well. The result shows that there are high anomalies indicating hydrocarbon occurrence to the north of the Sigli well.

Chapter 7 is the discussion and conclusion of the thesis. In the discussion part, the deformation and evolution of the onshore and offshore areas are compared. This discussion offers new insights into these two areas. The conclusion draws together all the work that has been done in the the North Sumatra Basin. Some suggestions for future work are presented to address gaps in this research. Suggestions to make the North Sumatra Basin more attractive for future exploration are also given.

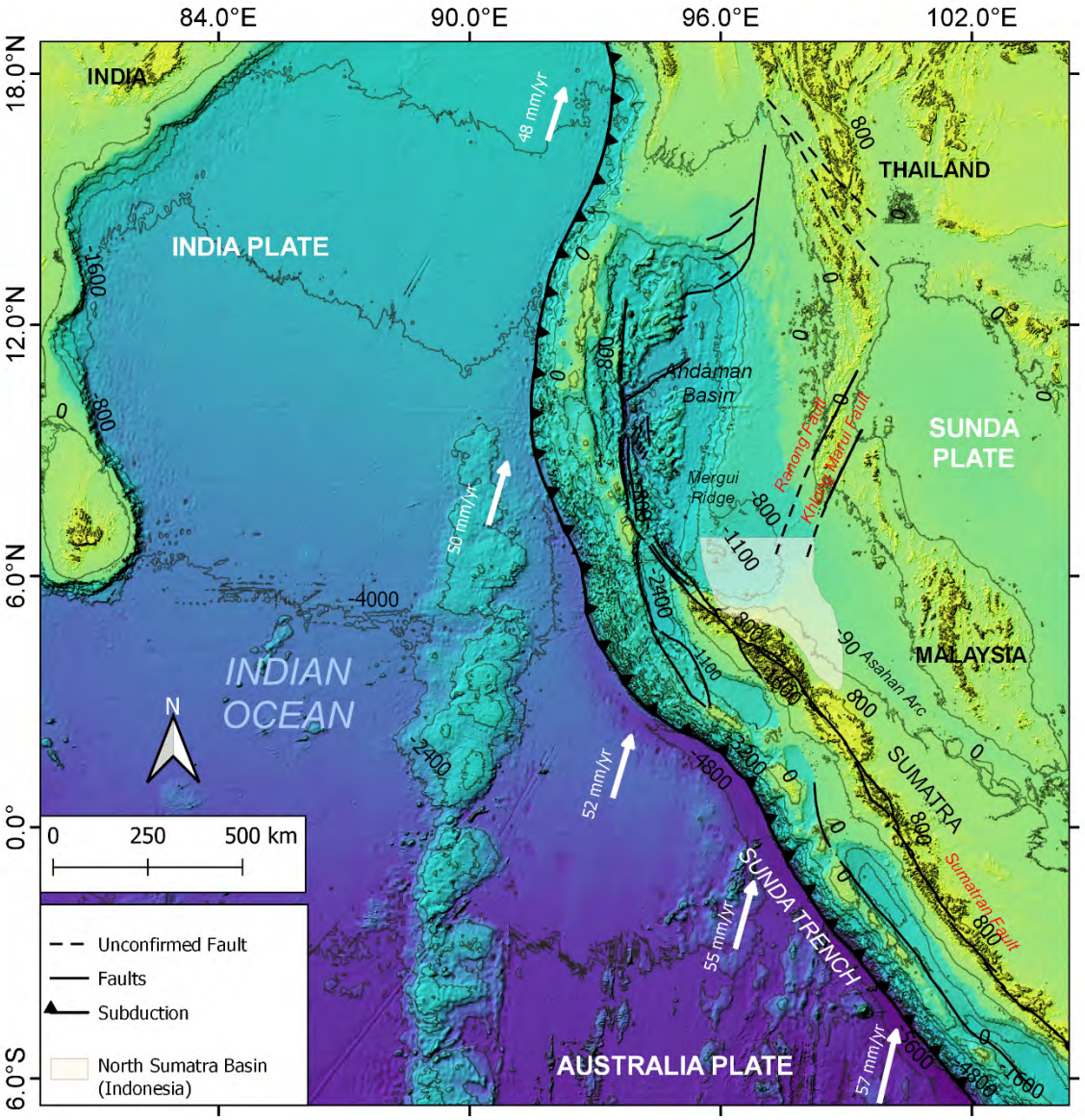

Figure 1-1 Regional tectonic setting of Northern Sumatra, showing the major fault in the Sumatra mainland (Sumatran Fault System) and plate convergences vector at the Sunda Trench. Other tectonic elements such as the Andaman Basin, Ranong and Khlong-Marui Faults are also shown in this map. The dashed lines are the possible continuation of the Ranong and Khlong-Marui faults into the offshore North Sumatra Basin as proposed by Davies (1984). The elevations are in meters (m). The map is compiled from Acocella, Bellier, Sandri, Sébrier, & Pramumijoyo (2018) Carton et al. (2014), Cattin et al. (2009), Curray (2005), Davies (1984), Morley (2001) and Watkinson, Elders, & Hall (2008)

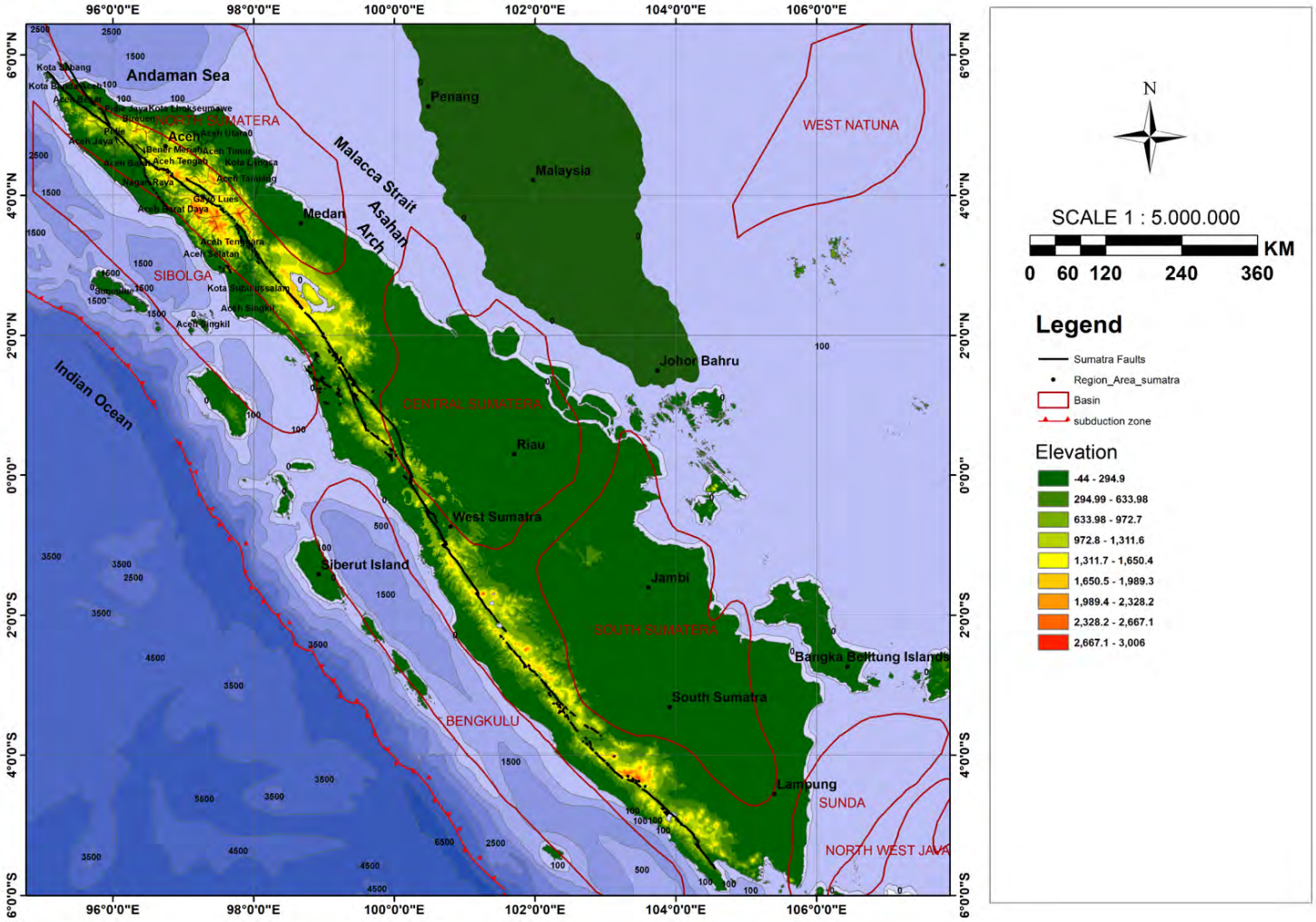

Figure 1-2 Map shows the location of the North Sumatra Basin. The area of the basin is approximately 60,000 km2. The offshore North Sumatra Basin extends to the offshore area of Thailand. The Trench at the southern part is the boundary between the Indian Ocean, subducting the Sunda margin (part of the Eurasia plate. Red lines show the location of seismic data used in this study. There also location of several petroleum basins in Sumatra; North Sumatra Basin, Central Sumatra, and South Sumatra Basin. The Great Sumatra Faults (black lines), situated along the Barisan Mountains extend from the province of Aceh to the region of Lampung in Indonesia

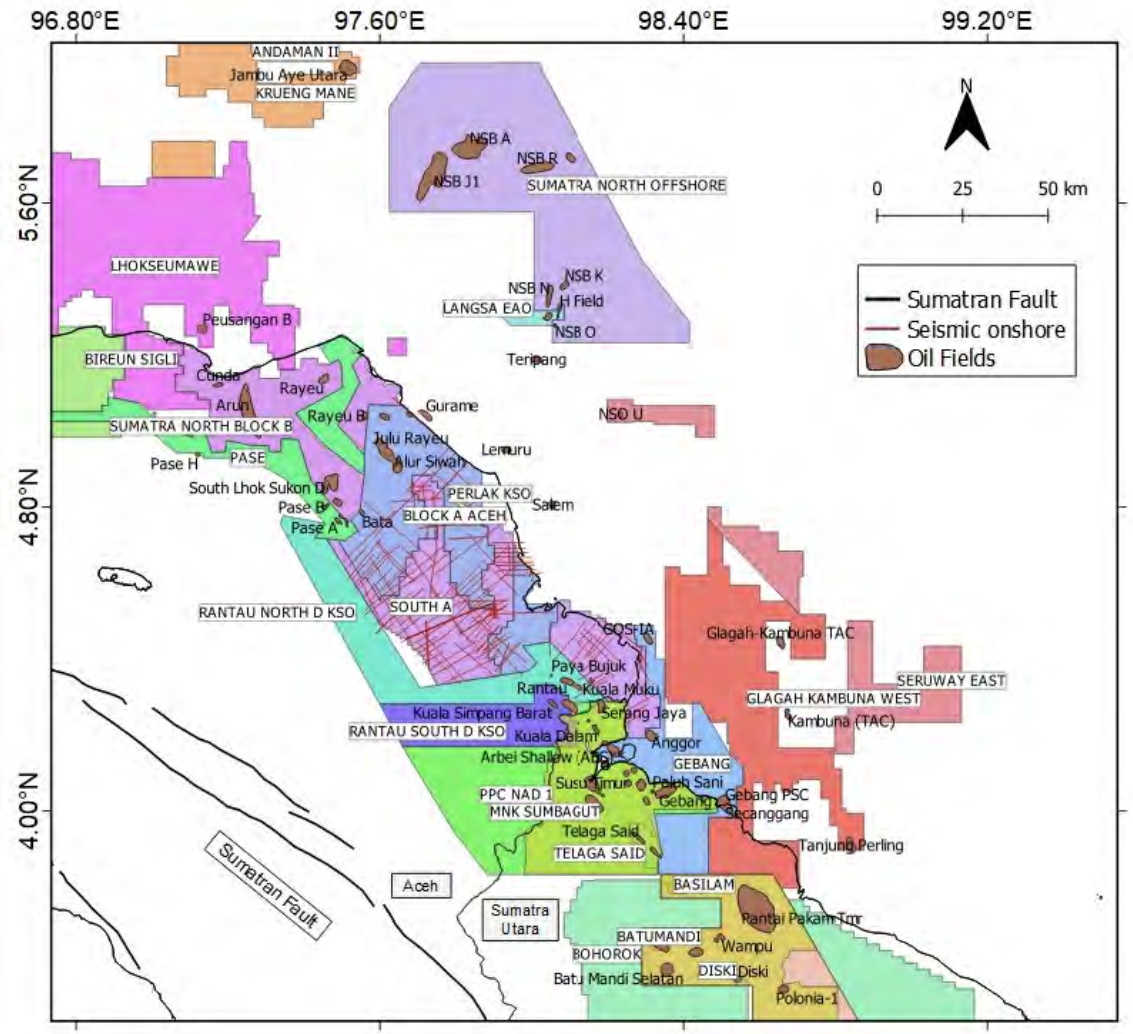

Figure 1-3 Map showing the distribution of hydrocarbon fields in the North Sumatra Basin (Aceh and Sumatra Utara province). Most of the fields are mature because they were discovered in 1960's to 1970's. Concessions are also shown. Pertamina is the operator of Block B, PPC NAD, and Sumatra North offshore. The onshore study area is in Southeast Aceh (Pertamina, 2017)

2 GEOLOGICAL SETTING

2.1 Major tectonic elements

The North Sumatra Basin is surrounded by several prominent geological features. To the south-west, the Sunda Trench marks the main tectonic boundary between the Indian-Australian plate and the Eurasian plate. The Sibolga fore-arc basin lies between the Sunda Trench and the Barisan Mountains, which contains uplifted basement rock and volcanic centres of the volcanic arc (Figure 2-1). The Barisan Mountains are cut by the Sumatra Fault, a major strike-slip fault which lies on the western side of the island and follows the same trend as the volcanic arc. The Barisan Foothills are an area of lower relief that marks the transition from the Barisan Mountains to the North Sumatra Basins (Figure 2-1) and contain deformed North Sumatra Basin sediments. The topographic distinction between the Barisan Mountains and the Foothills is not always obvious in all places. The North Sumatra Basin continues north into Thailand as the Megui Basin and is separated from the basins of the Andaman Sea by the Mergui Ridge. The Thai Peninsula lies to the north-east and is cut by the Ranong and Khlong-Marui Faults. It is not clear whether or not these faults extend into the Mergui Basin.

2.1.1 Sunda Subduction Trench

The Sunda Trench is the region where the India-Australia plate subducts beneath the Eurasian (Sunda) plate. This trench spans from the East Himalayas region in India to the Banda Arc in Indonesia (Figure 1-1). A magnitude 9.1 earthquake, the largest magnitude earthquake along this zone, occurred close to Aceh Province, in December 2004. The earthquake also triggered a tsunami and created a massive catastrophe along the northern part of Sumatra and in neighbouring regions such as Thailand and Sri Lanka.

According to Davies (1984), the convergence between the India-Australia plate and the Eurasian (Sunda) plate started in the Early Miocene. However, Hall (2002) stated that subduction did not begin until the late Miocene when Sumatra rotated anti-clockwise and created convergence oblique to the India-Australia plate. Based on tomographic imaging beneath the Sunda plate in the Sumatra region, Widiyantoro and van der Hilst (1996) showed that subduction has taken place since the closing of the Mesozoic Tethys Ocean circa 135 Ma ago (Fan, Niu, Liu, & Hao, 2021). The tomographic images also showed that the lithospheric slab penetrates 1,500 kilometers into the mantle. They also found that the deep slab detached from the upper mantle slab beneath Sumatra, and while this may, in part, be related to the oblique subduction and/or the anticlockwise rotation of Sumatra, they also conclude that there

is currently insufficient data to determine the significance of this observation.

Oblique subduction is a distinctive feature of the Andaman-Sunda-Java trench. The rate of subduction is 48 mm/year and is highly oblique east of the Andaman Sea. Meanwhile, south west of Sumatra, the velocity is 55 mm/year and the angle of convergence is 40°.

2.1.2 Andaman Sea

The Andaman Sea is situated along a segment of markedly oblique convergence between the northeastern advancing Sunda-Indian plate and the relatively stationary Southeast Asian plate. The Andaman Sea extends from Sumatra in the south to Thailand to the east and Myanmar to the north.

While the east Anderman Sea comprises thick sedimentary sequences deposited above the extended continental crust, the nature of the area of thinned crust to the west is the subject of much controversy (Curray, 2015; Morley & Alvey, 2015). Curray et al. (1979b) postulated that the opening of this part of the basin was initiated by seafloor spreading at 11 Ma. However, more recent interpretations (Morley & Alvey, 2015; Raju, Ramprasad, Rao, Rao, & Varghese, 2004) suggest seafloor spreading initiated at 4 Ma, and there is further debate as to whether it has been continuous or episodic since that time. As the Andaman Sea lies between the Sagaing Fault to the north and the Sumatra Fault to the southeast, a proper understanding of the basin could have implications for understanding the evolution of these strike-slip fault systems.

2.1.3 Barisan Mountains

The Barisan Mountains are situated in the heart of Sumatra Island. The mountains extend about 1800 km from Banda Aceh in the north to Lampung in the south (Figure 1-2). They consist of basement rocks of the Palaeozoic and Mesozoic ages (N. Cameron et al., 1983) and also contain Permian and Recent volcanic rocks (N. R. Cameron, Clarke, Aldiss, Aspden, & Djunuddin, 1980). The Recent volcanoes in the Barisan Mountains are related to the subduction of the Australia-India plate beneath Sumatra (Gasparon, 1993).

The Sumatra basement was formed by several pre-tertiary crustal blocks that rifted from Gondwana and were accreted to the Sunda plate (Barber & Crow, 2003; Hutchison, 1994; Metcalfe, 1996; Pulunggono & Cameron, 1984). The blocks are the Devonian Indochina block, the Permian Sibumasu block, the Triassic West Sumatra block, and the Woyla Nappe, an oceanic arc that was accreted to the western part of Sundaland in the Cretaceous (Barber,

2000; Hall, 2002, 2012; Hall & Morley, 2004) (Figure 2-2).

There is still a debate as to when the Barisan Mountains developed. Morton, Humphreys, and Dharmayanti (1994) suggested that the Barisan Mountains were uplifted and were a significant sediment source for the North Sumatra Basin in the middle Miocene. This suggestion is based on their study of the Middle Miocene Keutapang Formation where they found large amounts of chrome spinel sourced from ophiolites within these sediments. However, chrome spinel is not present in younger sediments. It is suggested that an ophiliotic terrain had probably been eroded, implying an uplift of the Barisan Mountains in the middle Miocene. Alternatively, the source may have moved away due to the movement of the Sumatra Fault System. On the other hand, De Smet and Barber (2005) suggest that the Barisan Mountains developed in the late Oligocene-early Miocene as a volcanic feature, based on the evidence from volcanic materials such as tuffs found in late Oligocene sediments.

The Barisan Mountains are cut by the dextral Sumatra fault, as discussed in the next section. In addition some lineaments, such as faults and bedding, can be observed in the Barisan Mountains and the Barisan front. The trends are shown as river directions, saddle and sag, and topographic escarpments. These contours have a dominant NW-SE direction, the same orientation as the main Sumatra Fault (Figure 2.1).

2.1.4 Sumatra Fault System

The Sumatra Fault System (SFS) is a critical tectonic element in Sumatra. The SFS is a dextral strike-slip fault with an NW-SE orientation that lies along the centre of the Barisan Mountains (Figure 2-1). It extends from the Andaman Sea in the northwest to the Sunda Straits in the southeast. It dramatically varies in deformation, geometry, and width along strike (McCarthy & Elders, 1997).

The initiation of the Sumatra Fault System is still debated. Some authors suggested that the SFS was initiated in the mid-Miocene at the same time that the spreading centre in the Andaman Sea was initiated (Curray et al., 1979a; Morley, 2002). However, as discussed above, the timing and significance of spreading in the Andaman Sea is hotly debated. Alternatively, De Smet and Barber (2005) suggested that the Sumatra Fault was initiated in the late Oligocene-Early Miocene, at about the same time as the development of the Barisan Mountains. This is based on the observation that some NNW-SSE structures were imprinted over N-S trending horst and grabens in several Sumatra Basins. In addition, the forearc region has expanded about 460 km northwest to the Andaman Sea relative to Sumatra since the early

Miocene (25 Ma) along the Sumatra Fault Zone.

From Figure 2-1, it can be seen that the Sumatra Fault System consists of several splay faults. The splays are located in the Barisan Mountains and extend into the onshore North Sumatra Basin (Cameron et al., 1983). These splay faults have created areas of subsidence (extension) such as the Kutacane Graben (Figure 2-1) and regions of uplift (compression), which are attributed to transtensional and transpressional movement (Holder, Walker, Gafoer, Amin, & Andi Mangga, 1995).

Right stepping of the dextral Sumatra Fault caused the Kutacane Graben. The trace of the fault is rotated 20° in a clockwise sense relative to the main trend of the Sumatra Fault and is continuously curved away from the main trace of the fault. This divergent bend determines the extent of the offset area. A schematic diagram showing the subsidence and extension due to the right stepping of the Sumatra Fault can be seen in Figure 2-3. The Kutacane Graben contains Quaternary to Recent alluvium at the surface (N. Cameron, 1982). However, there is no seismic line or subsurface well data available from Kutacane Graben to help constrain the age of the oldest sediment in the basin. If there was, this could help determine the timing of movement on the Sumatra Fault.

Uplift occurs where left stepping of the Sumatra dextral fault generates contractional bends, and the trace of the fault is rotated anti-clockwise by about 30° from the main fault. with an orientation of WNW-SSE. A schematic diagram of the uplift along a strike-slip fault is shown in Figure 2-4.

Besides these features, Sosromihardjo (1988) stated that NNE-SSW trends in the region, such as the Julu Rayeu Fault, which is antithetic to the Sumatra Fault, extend into the onshore North Sumatra Basin (Figure 2-1). This trend is not easy to recognize because it is masked by the high density of vegetation or covered by the recent sediments. Sosromihardjo (1988) also showed that the Lhokseumawe Fault extends into the onshore North Sumatra Basin. This fault has an NW-SE trend and propagates to the coastline of Aceh. The Lhokseumawe and Julu Rayeu faults are believed to be the splays of the Kutacane Fault.

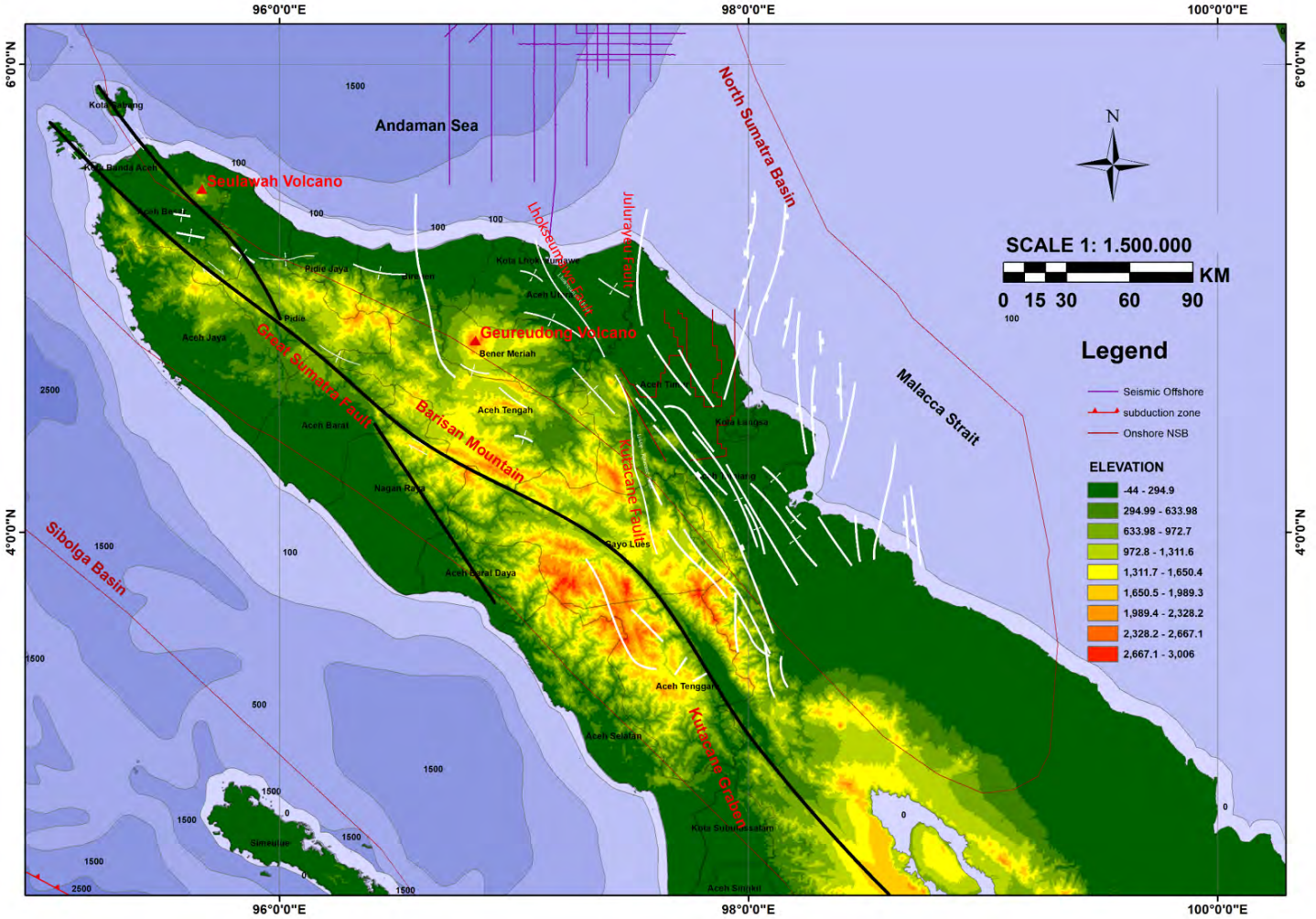

Figure 2-1 SRTM image showing the major structural elements such as the Barisan mountain and the Great Sumatra Fault System. The map also shows the Barisan Foothills (contrast in elevation is shown by colour bars), the onshore and the offshore North Sumatra Basin in Aceh.

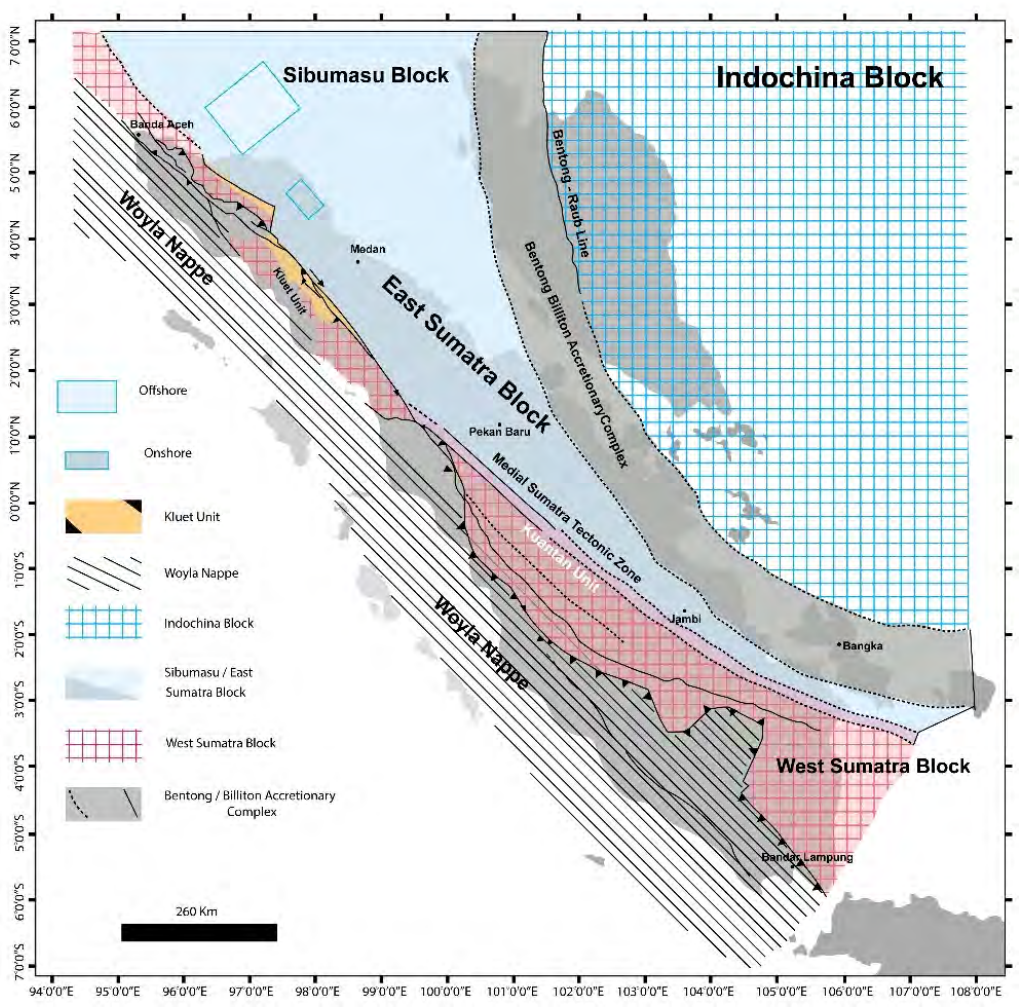

Figure 2-2 Pre-tertiary blocks/terranes that form the basement of Sumatra (Barber & Crow, 2003; Hutchison, 1994, 2014; Metcalfe, 1996; Pulunggono & Cameron, 1984). Onshore and offshore areas of this study overlie the Sibumasu/East Sumatra Basement of the Permian age.

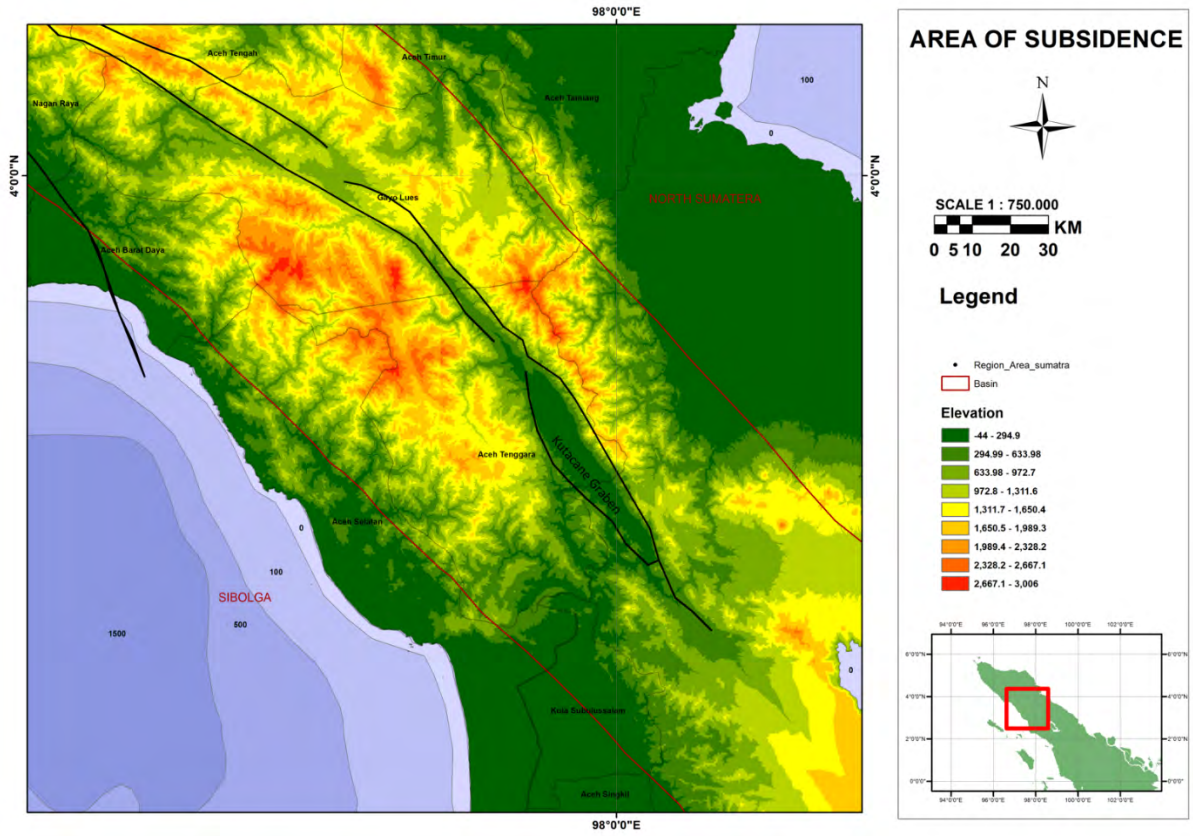

Figure 2-3 Diagram showing off right stepping releasing bends on a dextral strike-slip fault that provides an analogue for subsidence areas along the Sumatra Fault in the Kutacane graben (McClay & Bonora, 2001; Van der Pluijm & Marshak, 2004)

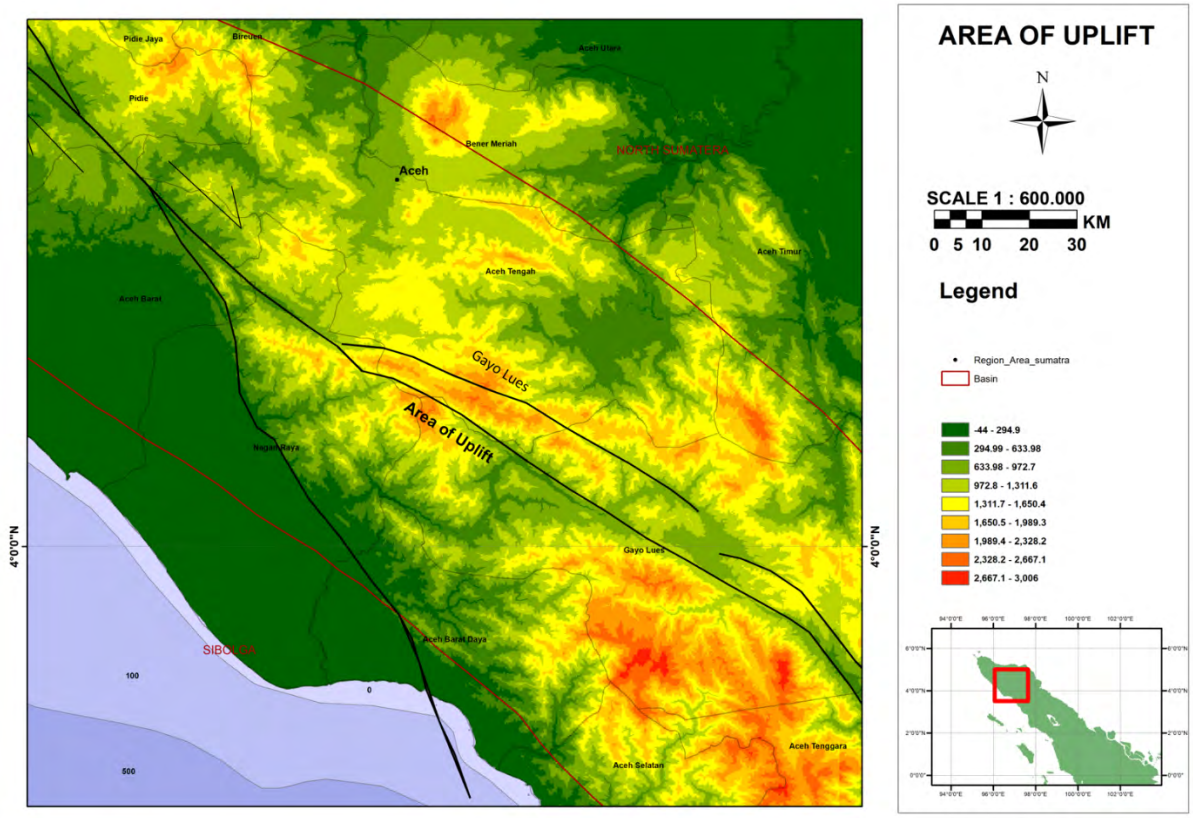

Figure 2-4 Diagram showing left stepping restraining bends on a dextral strike-slip fault that provides an analogue of the uplifted areas along the Sumatra Fault (McClay & Bonora, 2001; Van der Pluijm & Marshak, 2004)

2.1.5 Barisan Foothills

The Barisan Foothills is the most deformed area of the North Sumatra Basin and contains outcrops of the basement and the overlying North Sumatra Basin sediments. According to Cameron et al. (1980), the basement is highly jointed and faulted (see Figures 2-5).

The oldest sediments in the North Sumatra Basin belong to the Meucampli Formation (late Eocene to early Oligocene age) and are exposed in the northwestern part of Sigli (Figure 2-5) in fault-bounded or tilted horst blocks (Bennett et al., 1981; Keats et al., 1981). This stratigraphic unit is absent in East Aceh, both in the wells or at the surface, although there are outcrops of the Bampo and Peutu formations, of Oligocene and early Miocene ages respectively, in the Barisan Foothills in East Aceh.

Cameron et al. (1980) found Miocene sediment overlying the basement during their field mapping in the Tamiang River, in the south of the area (Tamiang Deep), and that Oligocene age sediments were missing. He suggested that the Oligocene sediments may have been eroded due to early Miocene tectonism. Alternatively, this may be because the early Miocene sediments onlap onto the fault block at the margin of the basin. In the study area, it can be seen from the Peulalu 3 well (Figure 3-2) that the Bampo and Peutu stratigraphic units are present above the basement.

The middle Miocene to Pleistocene units form outcrops in anticlines and synclines and as eroded dipping beds that characterise the Barisan Foothills (Bachtiar et al, 2012) (Figure 2-6).

2.1.6 North Sumatra Basin

The North Sumatra Basin extends from onshore, where it corresponds to relatively flat and low-lying topography, northward into present-day deep waters of the North Aceh Sea. The offshore area is considered a green area for exploration due to the absence of oil and gas fields and has been the site of significant recent exploration activity. As a consequence, there is a lack of publicly available detailed geological and geophysical information.

The North Sumatra Basin has two distinct parts with different subsidence histories. The first is in the Lhoksukon and Bireun Deep, and the second is in the Tamiang Deep (Meckel, 2013; Sosromihardjo, 1988). Subsidence was greater in the Bireun and Lhoksukon deeps. This area also forms the southern limit of the Mergui Basin, which merges into the western part of the North Sumatra Basin (Figure 2-5). This western margin of Bireun Deep is formed by the Sigli High (part of the Mergui Ridge).

To the east of the Bireun Deep is the Arun High, associated with the Arun Field. To the east of Arun High and west of the Alur Siwah High is the Lhoksukon Deep, which is the location of the depocenter containing the excellent source rock for the giant Arun gas field (Andreason et al., 1997; Fuse et al., 1996; Kingston, 1978; Meckel et al., 2012). The Lhoksukon and Bireun deeps contain the thickest sedimentary sequences with a basement observed at 6 seconds two-way time on seismic data (Wang, Budijanto, Johnson, & Siringoringo, 1989).

The Tamiang Deep forms the eastern part of the North Sumatra Basin. It consists of a number of horsts and grabens between the Alur Siwah High and the Malacca Platform to the east. It covers the largest area of the onshore North Sumatra Basin and extends offshore where the basement is observed at between 3 and 5 seconds two-way time on seismic data (Figure 2-5). It forms the kitchen that is associated with the Rantau, Kuala Simpang, and Telaga Said oil fields (Clure, 2005; Kingston, 1978).

2.1.7 Ranong and Khlong Marui Faults

In addition to the Sumatra Fault, the Khlong Marui Fault (KMF) and Ranong Fault (RF) are significant strike-slip faults with a NNE-SSW orientation that cut the Thai Peninsula (Figure 1-1). They are conjugate to other major strike-slip faults in SE Asia, such as the Mai Ping and Red River faults, a show a similar reversal of movement, but with an opposite sense. The Khlong Marui and Ranong faults originated as dextral faults in proximity to the southern edge of a Late Cretaceous–Paleocene orogen, potentially influenced by fluctuations in the subduction rate at

the leading edge of the India-Australia plate (Watkinson, Elders, & Hall, 2008). Before the reactivation of the subduction zone adjacent to southern Sundaland in the Eocene, north-south compression led to extensive deformation in the overriding plate, including sinistral transpression along the KMF and RF (Watkinson, Elders, & Hall, 2008).

Davies (1984) and Lunt (2019) suggests that the Ranong and Khlong Marui faults extend into the Northern Sumatra Basin and possibly connect to the Sumatra Fault. However, there is little evidence to support this, although the faults may explain some of the segmentation in the North Sumatra and Mergui basins.

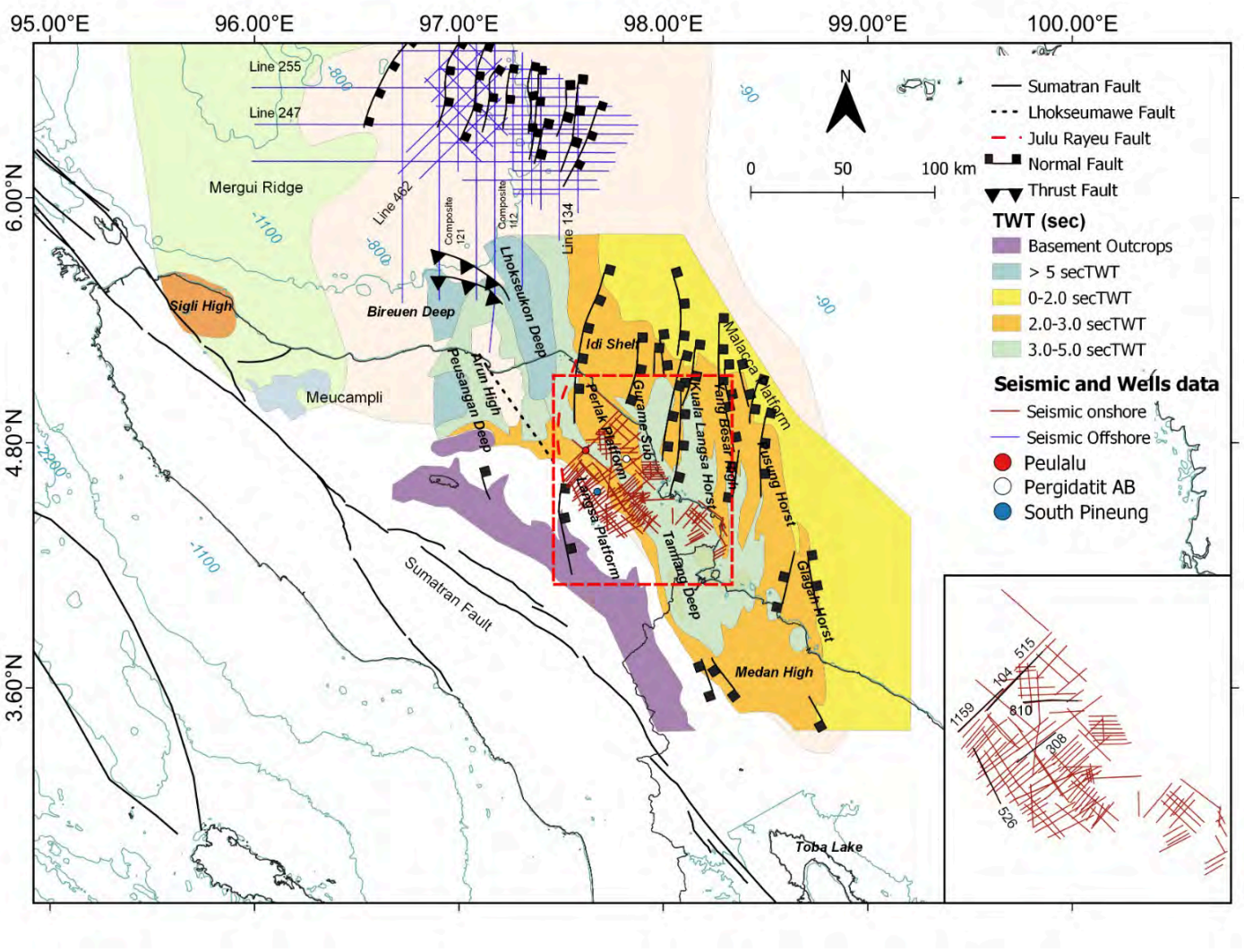

Figure 2-5 Structural elements of the North Sumatra Basin including the Sigli High, the Mergui Ridge, the Arun High, the Alur Siwah High and the Malaca Platform. The locations of the Bireuen Deep, the Lhoksukon Deep, and the Tamiang Deep are also shown This map is compiled from Anderson et al, (1993), Davies, (1984), Kamili et al. (1976) and Sosromihardjo (1988) for basement map (horst and graben) in TWT, Cameron et al (1983) for onshore geology and Muchlis & Elders (2020) for faults in offshore area . The red lines indicate the onshore seismic lines used in this study, while the blue lines indicate the offshore seismic lines. The location of wells (dots with colour) is shown.

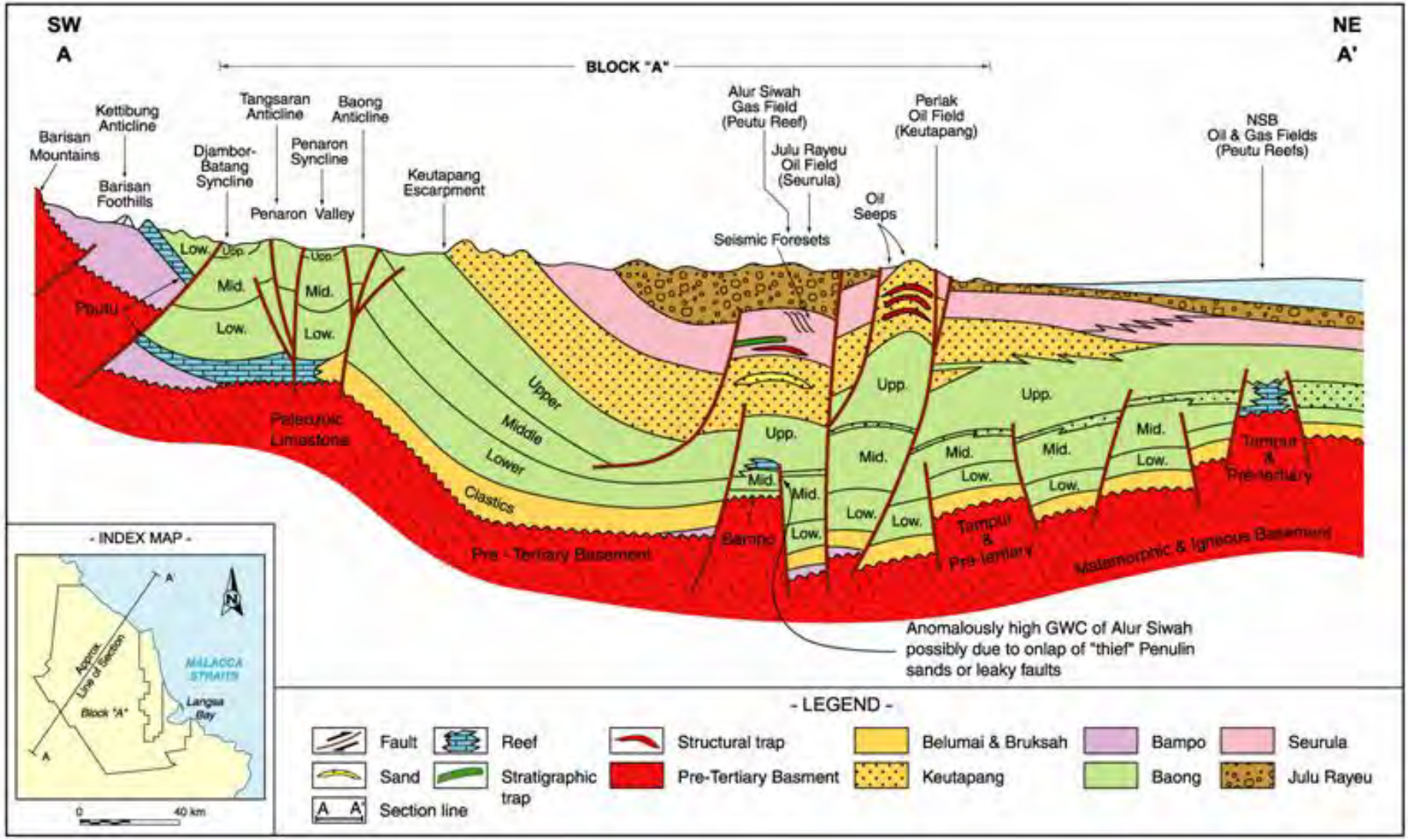

Figure 2-6 Geoseismic interpretation of a seismic line crossing from the Barisan Foothills to the offshore of North Sumatra Basin from Pertamina-Beicip (Caughey & Wahyudi, 1993). The location of this section is similar to the seismic composite line 1 in Figure 4-1.

2.2 Regional Tectonic Evolution

Plate tectonic reconstructions provide useful context for understanding basin evolution. In the case of SE Asia, a number of different reconstructions have been proposed. The most widely used ones are Hall (2002, 2012), which are primarily based on geological and geophysical observations, while others, such as Brune et al (2016), are kinematic reconstructions based on seafloor magnetic anomalies, plate velocities and coherent poles of rotation.

The oldest event to have affected the southwest margin of Sumatra is the collision of the Woyla terrain. The Woyla terrain is an intra-ocean volcanic arc that rifted from the margin of Gondwana (Barber, 2000; Barber & Crow, 2003; Hall, 2002, 2012). Based on the Hall (2012) model, the Woyla terrane rifted from the Gondwana margin, began moving north at about 160 Ma (Figure 2-7a) and collided with Sumatra at 90 Ma (Figure 2-8a). Brune et al (2016) also show a number of different terranes north of Australia at 150 Ma that had migrated significant distances to the north by 90 Ma, but had not yet been accreted to SE Asia. Brune et al (2016) also showed that Sumatra was oriented east-west (Figure 2-7b) at 150 Ma, implying much greater subsequent rotation than Hall (2012). They also appear to show that the western half of Sumatra had rifted away from eastern Sumatra by 90 Ma (Figure 2-8b).

Hall (2012) shows that subduction beneath Indonesia resumed at 45 Ma following the collision of the Woyla Terrane. This is related to the initial contact of an enlarged Greater India with Asia, reducing subduction to the northwest and increasing subduction to the SE as a result of the Australian plate moving northward, a process that has continued until the present day (Figure 2-9a). This may also have initiated extension and strike-slip events in some parts of Sundaland. Brune et al. (2016) show a much smaller extent of Greater India which consequently remained separate from Asia at this time, despite sharing a similar latitude to that in the Hall (2012) reconstruction at 45 Ma. They also show that by this time the West Sumatra Block has moved north and had been accreted to East Sumatra, creating a similar outline as today but still with an east-west orientation (2-9b).

Both (Hall, 2012) and Brune, Williams, Butterworth, and Müller (2016) show that the South China Sea began to open at 30 Ma in the early Oligocene (Figure 2-10 a, b) and ceased at 16 Ma in the Middle Miocene (Figure 2-12a,b). The timing of the South China Sea opening corresponds to the start of Cenozoic sedimentary basin formation in Sumatra and other parts of Southeast Asia (Daly et al., 1991; Davies, 1984), suggesting that this, rather than subduction, may be an important control on basin formation.

Both Hall (2012) and (Brune et al., 2016) show that Sumatra rotated anti-clockwise from the late Oligocene (25 Ma), associated in part with the opening of the South China Sea, until the late Miocene (10 Ma) when it largely achieved its current orientation (Figure 2-11a, Figure 2-13a). The northward movement of Greater India and its collision and continued indentation into Asia may also have contributed to this rotation. Davies (1984) proposed a similar timing for the onset of rotation but proposed that it continues until the present day. This is supported by GPS measurements which suggest that the Sunda plate, including east Sumatra, is rotating slowly clockwise by 30 mm/year (Rangin et al., 1999).

At 16 Ma the Sula Spur (part of the Australian continent) collided with eastern Indonesia, causing the anticlockwise rotation of Borneo (Figure 2-12a, b, 2-13a,b), setting up compressional stresses that have affected many SE Asian basins since that time. It is important to note that the deformation of Sundaland is the result of the interaction of processes operating at several different plate boundaries, and not just a consequence of the subduction of the Indian Ocean Plate.

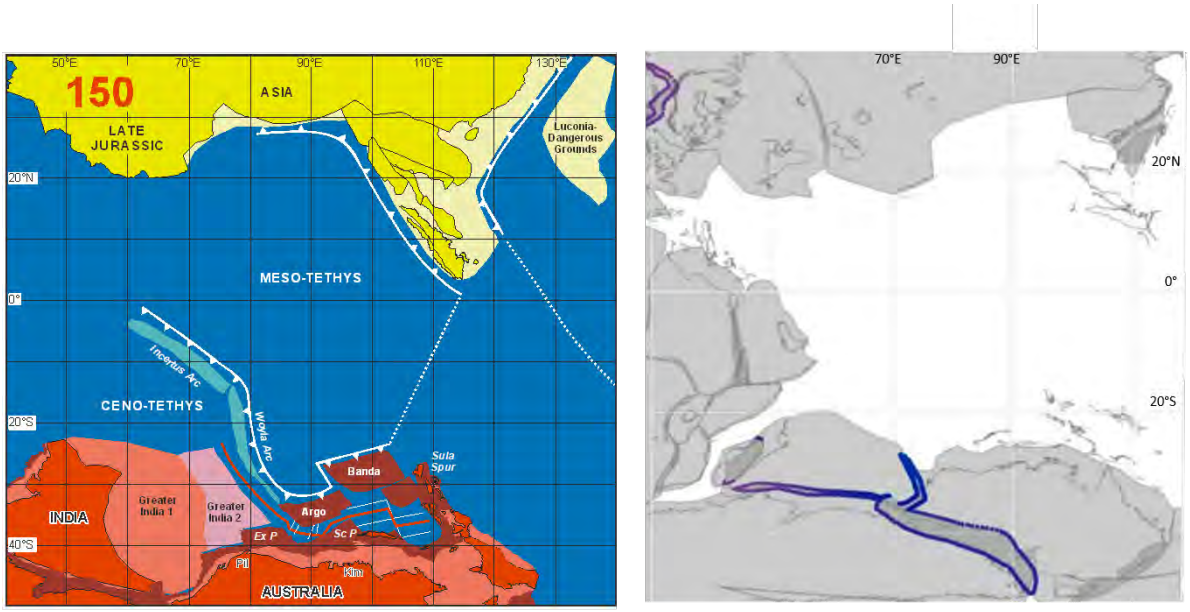

Figure 2-7a. (Hall, 2012) the model shows the Woyla intra terrain was moving northeast due to the spreading of Ceno-Tethys at 150Ma. b (Brune et al, 2016) model shows at 150Ma Sumatra was in an East-West orientation, meanwhile, the rifting occurred in the Antarctic area.

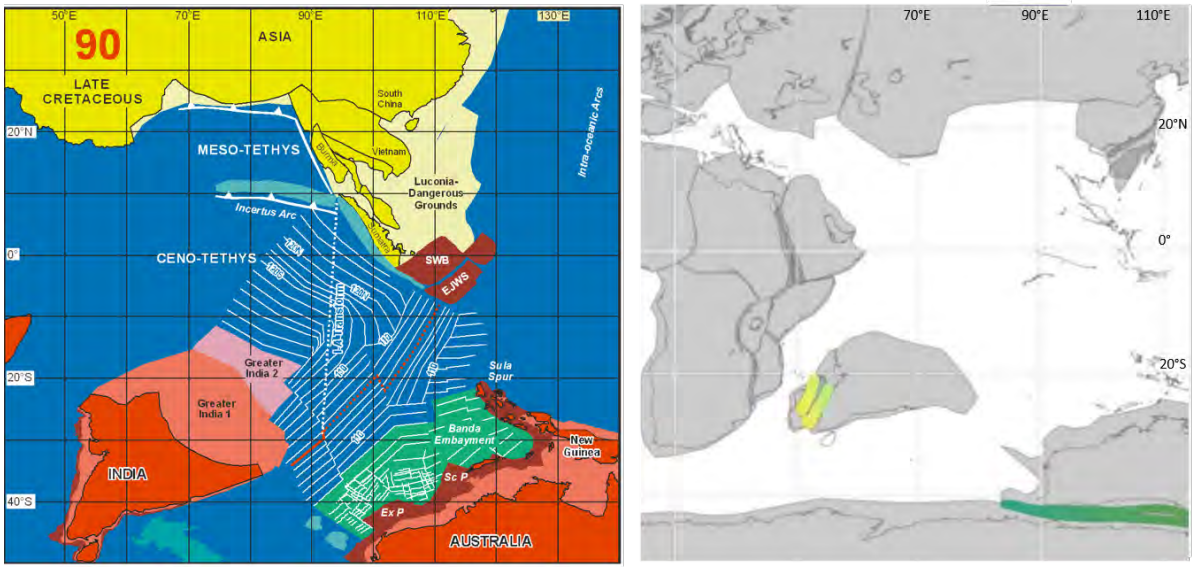

Figure 2-8a. Hall model at 90Ma, The Woyla terrain collided with West Sumatra. The Meso-Tethys subduction under Sumatra ceased. India and Australia continued to separate by spreading on a ridge southeast of India with a strike-slip motion along the I-A transform. b. Brune model at 90 Ma, the part of West Sumatra block rifted and moved away south from Sumatra. Furthermore, the Indian plate moved northward toward Asia.

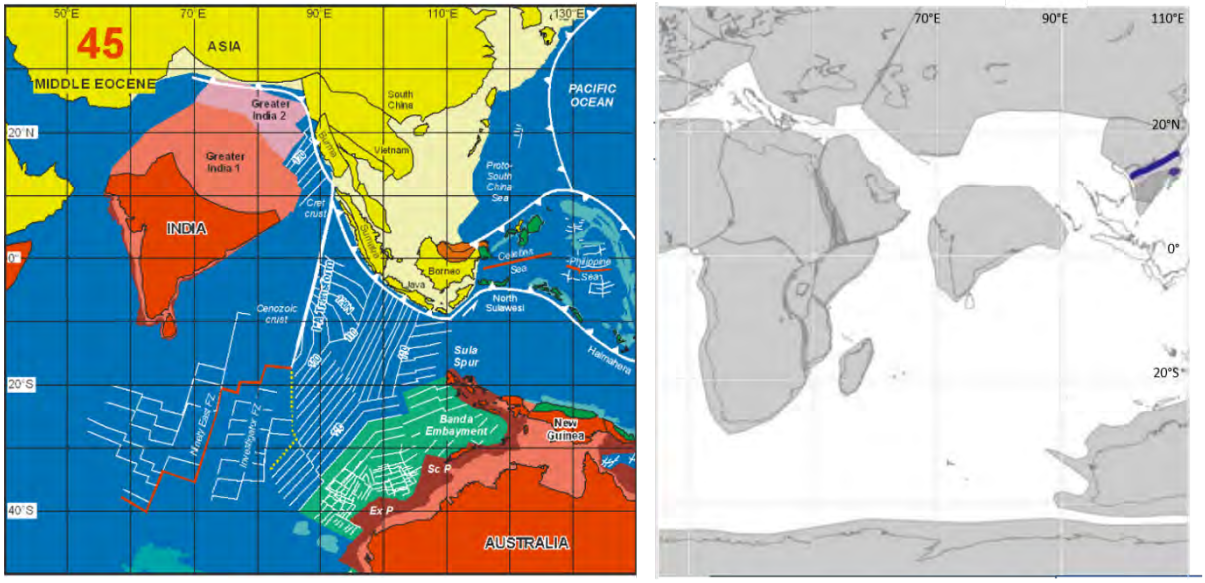

Figure 2-9a. Hall model at 45 Ma, the subduction began again in Indonesia due to the Australia plate moving northward. b. Brune model at 45 Ma, The West Sumatra Block moved north and joined the East Sumatra, creating a similar outline of Sumatra as today but with an east-west orientation

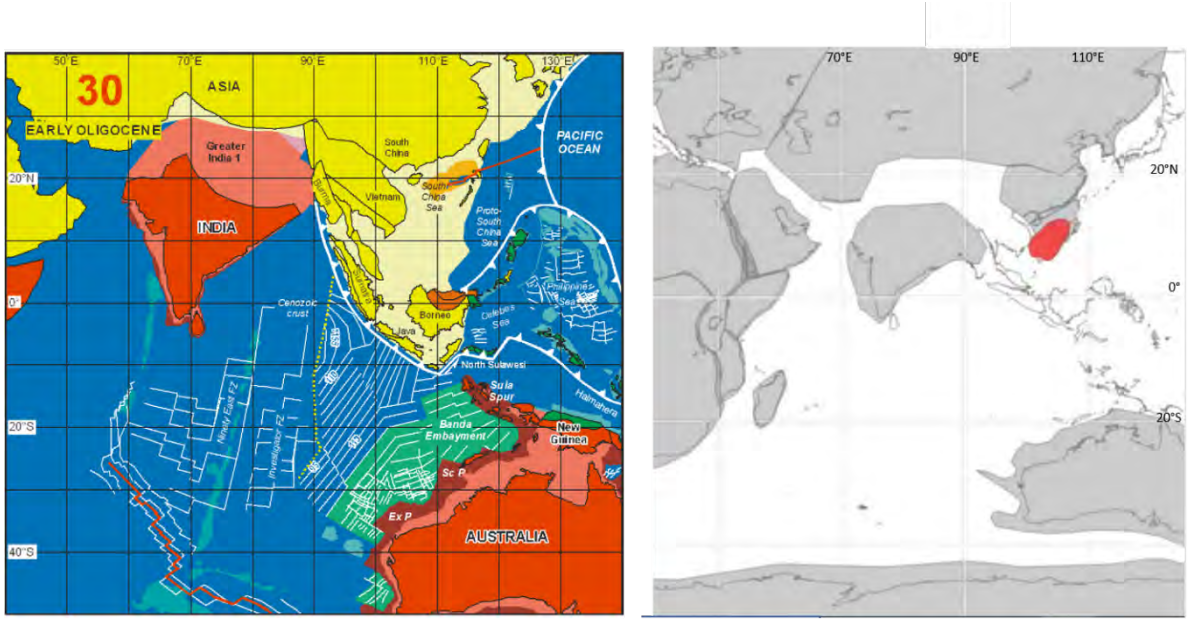

Figure 2-10a. Hall's model at 30 Ma, the South China Sea began to open and form ocean crust. b. Brune's model also shows the China Sea started to open and formed the Basin at 30Ma.

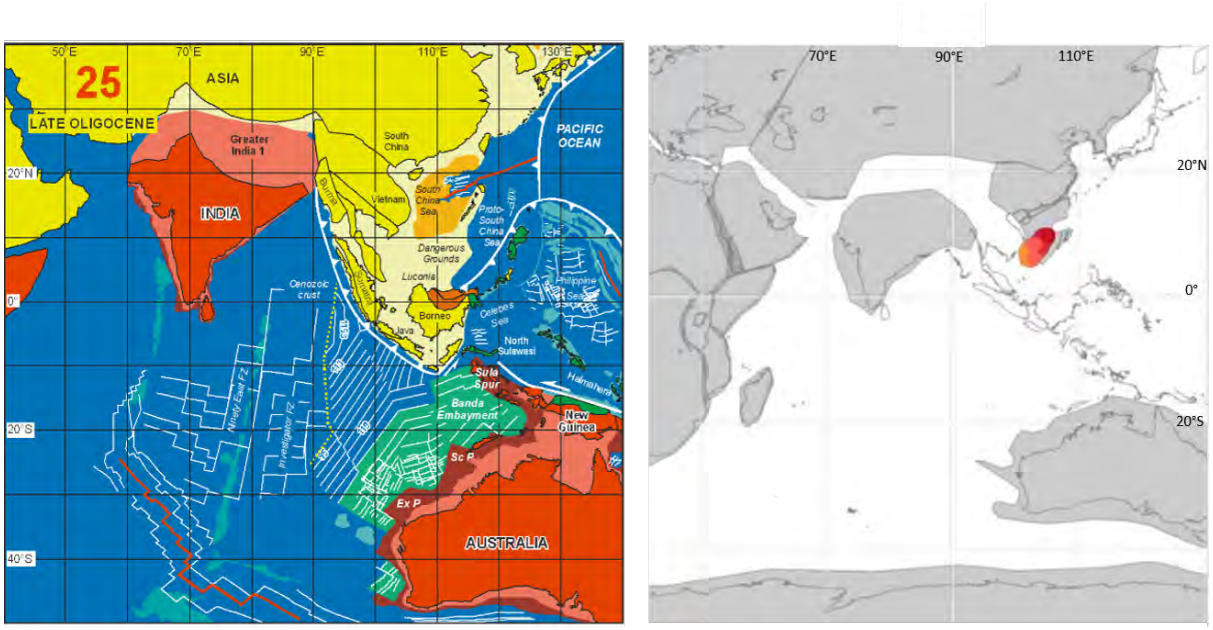

Figure 2-11 a. a. Hall model at 25Ma, Sumatra and east Indonesia (Borneo, Jawa, and Sulawesi) started rotating anti-clockwise. b. In contrast, the Brune model shows that Sumatra started to rotate a clockwise rotation in 25 Ma

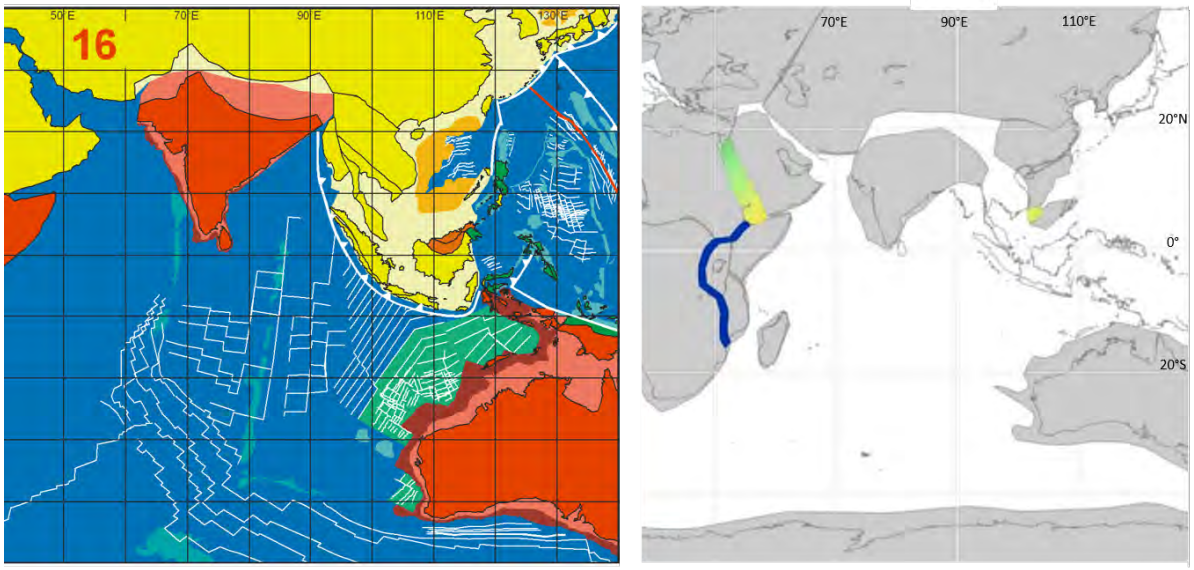

Figure 2-12 a. Hall's model y at 16 Ma. The spreading of South China ended b. Similarly, the Brune model shows China Sea had developed and formed the basin by 16Ma. Meanwhile, both models show India started to collide with the Eurasia plate.

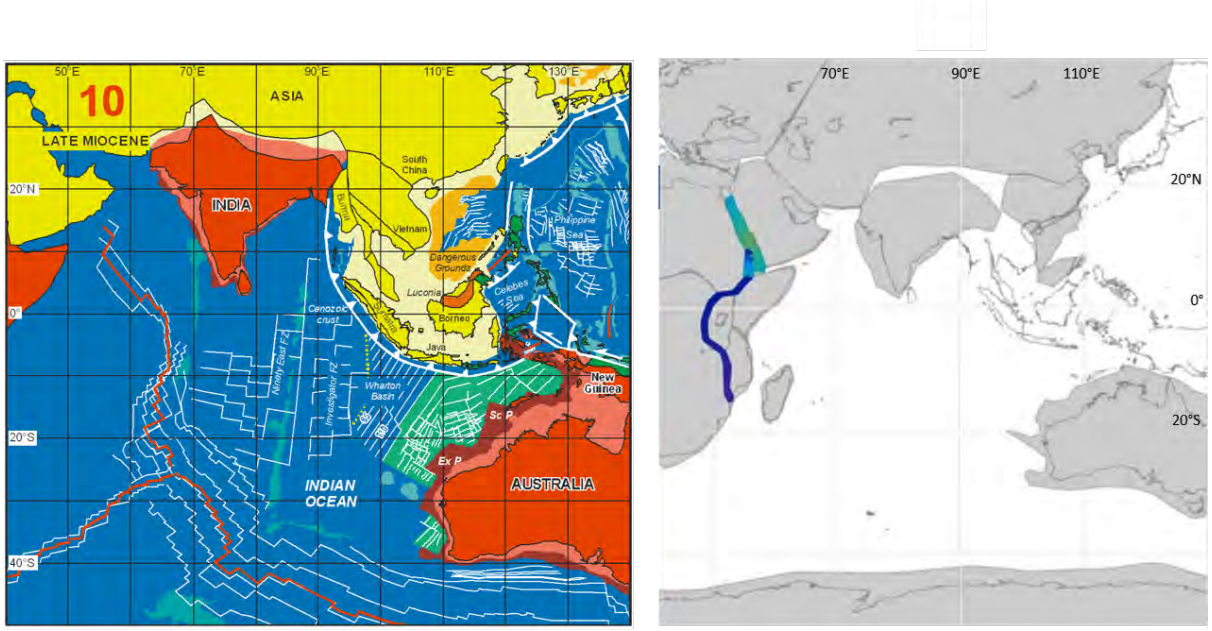

Figure 2-13 a. Hall model at 10 Ma showing spreading in the Andaman Sea. Sumatra and Borneo have formed similar to their present position. Meanwhile, India had already collided with the Eurasia plate b. the Brune model at 10 Ma shows Sumatra and Borneo have formed similar to their present position, while the east part of India's plate has not yet collided with Asia. This model does not show the Andaman Sea opening.

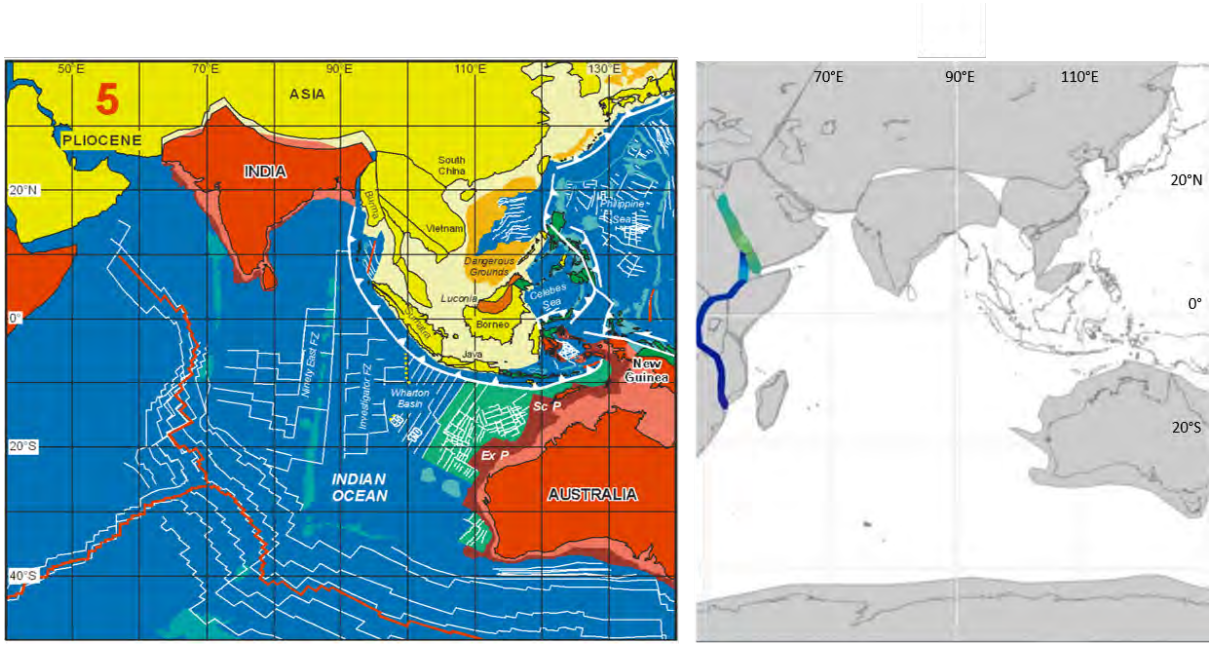

Figure 2-14 a. At 5 Ma, Hall 2012 shows a significant roll-back of Indian Ocean subduction under Indonesia. b. The Brune model shows that all parts of the Indian plate had collided with the Eurasian Plate. This model did not specifically show the evolution of the Sumatra Fault.

2.3 Evolution of the North Sumatra Basin

The Cenozoic history of the North Sumatra Basin began with extension during the Oligocene (Doust & Sumner, 2007; Morley, 2002). This was followed by the displacement of the Sumatra Fault System, which may have started at 13 Ma. The most recent tectonic event in the basin is compression which results from the change of orientation and the rates of convergence between the Indian Ocean Plate and Sundaland, resulting in rapid uplift during the late Miocene-early Pliocene (Collins, Kristanto, Bon, & Caughey, 1996; Davies, 1984).

2.3.1 Pre-rift

From the late Cretaceous until the middle-late Eocene, Western Sundaland was a stable craton. Fractured granites and metasediments of Mesozoic age characterize the basement of the NSB. It has been suggested that late Cretaceous-early Eocene sediments were deposited but were subsequently eroded (Cameron et al., 1980). However, the oldest sedimentary record is that of the Tampur limestone was which was deposited on the eroded basement during the late Eocene (Cameron et al., 1980; Ryacudu & Sjahbuddin, 1994; Sosromihardjo, 1988).

2.3.2 Rifting phase (35 Ma-23 Ma; Early Oligocene-Early Miocene)

Rifting in the NSB occurred during the early Oligocene to early Miocene. This event creates a series of horst and grabens oriented north-south. The orientation is possibly due to west-to-east subduction and the rotated position of Sumatra at this time. During the early phase of rifting, clastic sediments were sourced from exposed highlands to the east and northeast (Banukarso, Meckel, Citajaya, & Raharjo, 2013; A. J. Barber, Crow, & Milsom, 2005; Davies, 1984; Meckel, 2013).

2.3.3 Post-Rift phase (23Ma-11.2 Ma; Early – Late Miocene)

In the early Miocene, the rifting process ceased. Some authors suggest that in the Middle Miocene, oblique subduction of the Indian-Australian oceanic plate beneath the Eurasian plate arc resulted in extension and the commencement of sea-floor spreading in the Andaman Sea (Curray et al., 1979a; Curray, 2005; Morley& Alvey, 205; Raju et al, 2004) and that the development of transform faults from the Andaman Sea spreading centre particularly affected northern Sumatra and the Sumatra forearc basin (Barber & Crow, 2003; Curray, 2005), causing displacement along segments of the Sumatra Fault Zone in the Mid-Miocene. Alternatively, movement on the Sumatra Fault can be explained by oblique subduction of the Indian-Australian Plate. This event coincides with rapid subsidence in the NSB, which outpaced sedimentation resulting in the

drowning of the horst blocks, the Barisan Mountains, and the Malacca plateau (Syafrin, 1995; Ricky Andrian Tampubolon et al., 2018). A global rise in sea level also coincided with continuing subsidence to create the maximum transgression. At this stage, the main target reservoir, carbonate reefs, developed on horsts in the NSB (McArthur & Helm, 1982; Tsukada et al., 1996).

2.3.4 Compression (11.2 Ma- present day; Late Miocene – Present)

Compressional arc-related tectonics initiated and intensified during the late Miocene and Pliocene and continue to the present day. These events caused many structures to be inverted and reactivated previous structures. This event may be due to variations in the rates and angle of plate convergence (McCaffrey, 2009; McNeill & Henstock, 2014; Prawirodirdjo et al., 1997). It may be also due to the Cenozoic subduction that caused uplift in Sumatra at 20 Ma (Hall, 2012; Widiyantoro & van der Hilst, 1996).

Compressional tectonics also led to the uplift of the Barisan Mountain at the southern margin of the basin, which caused the primary source of sediment supply to be from the S-SW rather than from the N-NE (Hakim et al, 2014; Hakim et al, 2019; Rory, 1990). Furthermore, this event also eroded some of the Paleogene-Neogene sediments in the NSB (Hakim, Sibarani, & Syaiful, 2019).

2.4 General Stratigraphy

The stratigraphy of the North Sumatra Basin is divided into Pre-rift, Syn-rift, Post-rift, and Syn-inversion sequences. The ages of the sediments range from Oligocene to Pleistocene (Figures 2-15, and 2-16). Stratigraphic information is mainly derived from well and seismic data. However, this may have limitations because drilling only targeted traps located on horsts/basement highs where the oil and gas are dominantly discovered but where the stratigraphic record may be incomplete. In addition, the seismic horizons in the deep graben of the North Sumatra Basin are not well enough resolved to identify the boundary between the deepest sedimentary rocks and the basement.

Information is also available from the geological surface map (Figure 2-15) which shows early Permian metamorphic rocks belonging to the Kluet Formation (Cameron, 1980). This formation outcrops in the southwestern part of the research area, close to outcrops of the Oligocene Bampo Formation. Mesozoic rocks are not present in the area, probably due to erosion. However, they are preserved as the economic basement underlying the oldest sedimentary rocks in the North Sumatra Basin, McArthur and Helm (1982) reported that Triassic metamorphic rocks were penetrated in the NSB D well 1.

2.4.1 Pre-Rift Stratigraphy

Tampur/Meucampli formations (late Eocene)

The Tampur Formation is a limestone that was deposited in a shallow marine environment as carbonate/reef platforms on the margin of basement highs. The limestones are mixed with the dolomites and characterized by the presence of nodules of chert. The Tampur Formation outcrops near the Tampur River, in the Tamiang district in the southeast of the North Sumatra Basin (Cameron, Clarke, Aldiss, Aspden, & Djunuddin, 1980; Ryacudu & Sjahbuddin, 1994; Tarigan & Silaen, 2013; Wicaksono, Sijabat, Usman, Susanti, & Indrajaya, 2016). A lateral equivalent of the Tampur Formation is the Meucampli Formation which fills the grabens. In his geological map, Cameron et al. (1983) located this formation in the western part of the North Sumatra Basin, but other fieldwork has failed to encounter these rocks (Ryacudu et al., 1992). However, this formation is rarely observed and is only documented in oil and gas well reports (Meckel, 2013). Clastic sediments, sandstone, siltstone, and shale dominate this formation (Davies, 1984; Situmeang & Davies, 1986; Wicaksono et al., 2016). The depositional environment for this formation varies from fluvial to coastal/shelf.

2.4.2 Syn-Rift Stratigraphy

Parapat and Bampo Formations (Early to late Oligocene)

The Parapat Formation contains conglomerates and sandstone derived or transported from eroded local horsts. The depositional environment for this formation varies from fluvial through lacustrine to shallow marine (Bachtiar et al., 2014; Davies, 1984; Kamili et al., 1976; Meckel, 2013; Meckel et al., 2012; Tsukada et al., 1996). Whereas the Bampo Formation overlies the eroded Parapat Formation on horst blocks, it is deposited on top of the thick Parapat Formation within the grabens. The Bampo Formation is dominated by thick marine and lacustrine shales resulting from transgression and basin deepening (Buck & McCulloh, 1994; Kingston, 1978). However, sandstones contained within the Bampo Formation were most likely deposited by deep marine turbidity currents (personal communication with Harbour Energy, 2022).

The Bampo Formation is well-known for being the source rock for gas, such as in the Lhoksukon deep. In addition, this formation could be a candidate for unconventional gas plays in the future. It is an ideal petroleum source rock due to its TOC values ranging from 0.2 to 4.8% (Fuse et al., 1996; Kirby, Situmorang, & Setiardja, 1989). The potential of the Bampo Formation as a source of gas was demonstrated by the Timpan-1 discovery (Harbour Energy) in August 2022.

2.4.3 Post-Rift Stratigraphy

Peutu/Belumai Formation (Early to middle Miocene)

The Peutu Formation consists of various clastic lithologies such as sands and shales. This formation is also well-known for the limestones deposited as carbonate platforms/reef build-ups on the tops of basement highs (Cameron et al., 1980; Sosromihardjo, 1988). The basal thick sandstone members are exposed south of Lhokseumawe city toward the Barisan Foothills. The outcrops were deposited in fluvial or shallow marine environments, while the limestones in the upper part of the formation were also deposited in a shallow marine environment (Cameron et al., 1980; De Smet & Barber, 2005). The limestone has become the primary target for oil and gas exploration because it forms the reservoirs for most of the oil and gas fields in the North Sumatra Basin, including the Arun field (Jordan Jr & Abdullah, 1992; Meckel III & Banukarso, 2016).

In the offshore area, the Peutu Formation is known as the Belumai Formation. The formation is dominated by clastic sands and shales whose grainsize vary from very fine to coarse. (Cameron et al., 1980; Morton, Humphreys, & Dharmayanti, 1994). Only limited areas of limestones were identified from this formation in the offshore area, especially in the basinal areas, maybe because the environment was too deep for the carbonate to grow.

Baong Formation (Middle Miocene)

The Baong Formation (Middle Miocene) consists of thick calcareous shale rich in foraminifera, relating to a neritic marine depositional environment (Anderson, Bon, & Wahono, 1993; Fatrial Bahesti, Taufiqurrahman, Nuri, & Wahyudin, 2013; Cameron et al., 1980; Mulhadiono & Soedaldjo, 1978). The middle Baong Sandstone is a turbidite deposit within the marine shale of the Baong Formation (Mulhadiono & Soedaldjo, 1978; Syafrin, 1995).

The Baong Shale is an overpressured formation, which causes some problems with drilling in the basin (Aziz & Bolt, 1984; Buntoro et al., 2022). The overpressure is most likely due to rapid deposition with an estimated deposition rate of 0.45 mm/year resulting in the retention of fluids (De Smet & Barber, 2005). Besides acting as the seal, the Baong Shale is also recognized as the source of oil, with an average TOC value of 1.5% (F Bahesti, Subroto, Manaf, Sadirsan, & Wahyudin, 2013; Fuse et al., 1996; Kingston, 1978; Rizky, Fahmi, Amijaya, & Anggara, 2018; Sjahbuddin & Djaafar, 1993).

2.4.4 Syn-Inversion

Keutapang Formation (Late Miocene)

The Keutapang Formation consists of fluvial to inner neritic sandstone and fine clastics, which were mainly derived from the initial uplift of the Barisan Mountains to the southwest and from the Sunda shield to the east (Anderson et al, 1993; Humphreys et al, 1994; Kingston, 1978; Ronoatmojo et al, 2020). Mulhadiono and Soedaldjo (1978) identified four depositional environments of the lower Keutapang sandstone: shallow marine, interdeltaic, deltaic, and estuarine.

Sereula Formation (Early Pliocene)

The Seureula Formation is dominated by sandstones interbedded with shale and claystone. The grains are coarser due to the sediments being transported from the mountains into the alluvial fans (Cameron et al., 1980; De Smet & Barber, 2005; Kirby et al., 1989). The Seurula Formation marks significant uplift of the Barisan Mountains during the Pliocene.

Julu Rayeu Formation (Late Pliocene)

The Julu Rayeu Formation is the youngest Neogene sedimentary rock. The formation consists of thick sands mixed with volcanic material from the Barisan Mountains. The volcanic sediments may be derived from contemporaneous Late Pliocene volcanoes or from younger units. Grains comprise of tuff, tuffaceous sandstone, siltstone, claystone, and conglomerate. The Julu Rayeu Formation was deposited under fluvial to shallow water/shelf conditions (Anderson et al., 1993; Davies, 1984; De Smet & Barber, 2005).

Idi Formation (Pleistocene to Holocene)

The Idi formation is not widely recognized but is shown on geological maps in the northeast of the research area (Figure 2-15). The Formation is not found in wells, and is not included in the petroleum system of the North Sumatra Basin. It consists primarily of conglomeratic sandstone deposited in a terrestrial environment (Bennett et al., 1981; Cameron et al., 1980).

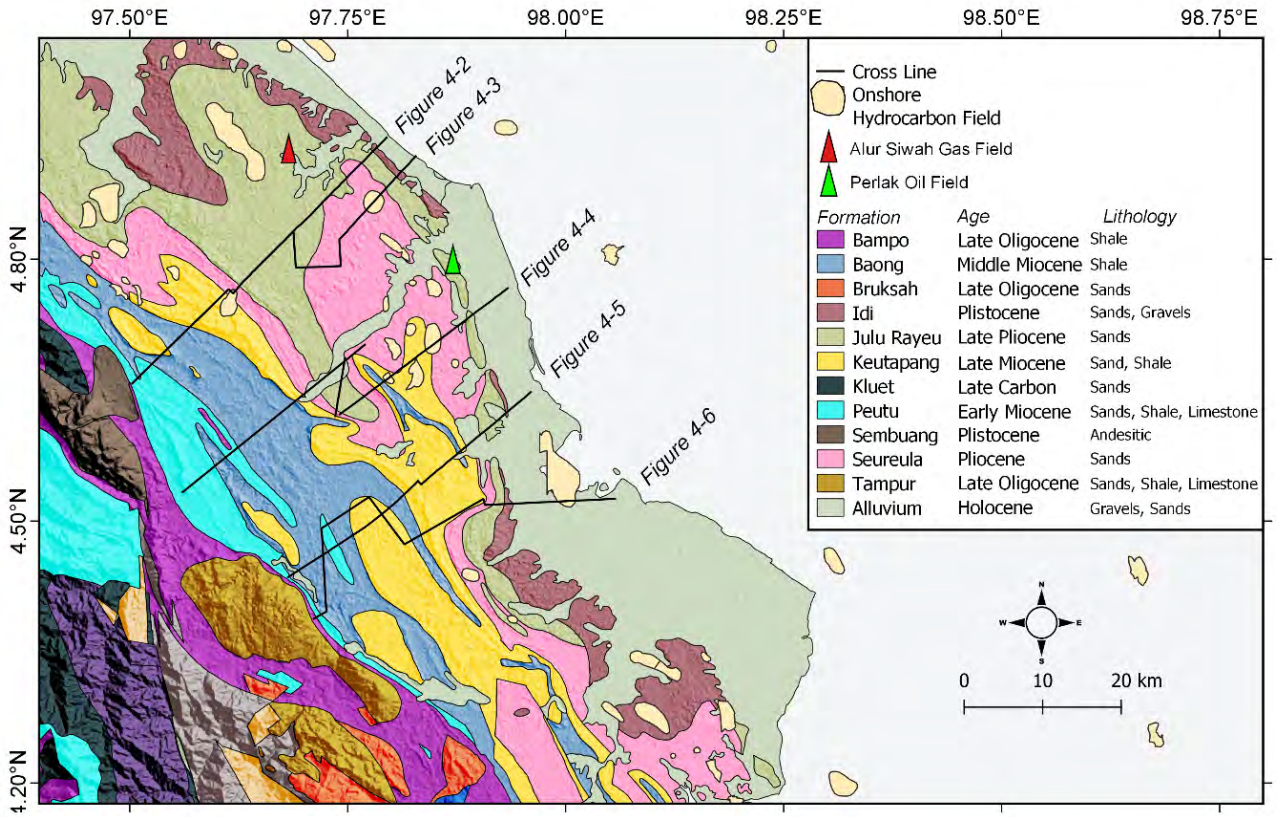

Figure 2-15 Geological maps of the research area. This map was digitized from the geology map of the Langsa sheet. (Bennett et al., 1981). The outcrops are dominated by the Paleogene-Neogene sedimentary rocks, with the oldest (Bampo/Bruksah/Tampur) in the southwest (toward the Barisan Mountains) and the youngest (Pliocene-Pleistocene) to the northeast (Idi/Julu Rayeu). Holocene to recent sediments (brown color) fills the northeast part of the basin toward the offshore. The oldest rock in the area is the Kluet formation, a Permian metamorphic rock. The Sembuang formation is a volcanic extrusive rock of Pleistocene age. The Kluet and Sembuang formations are located in the southeastern area adjacent to the Bampo Formation. Several oil and gas fields are also located in the research area. The fields were mainly discovered in the 1960s and 1970s. Only Alur Siwah (red triangle) and Perlak (green triangle) are still producing among those fields

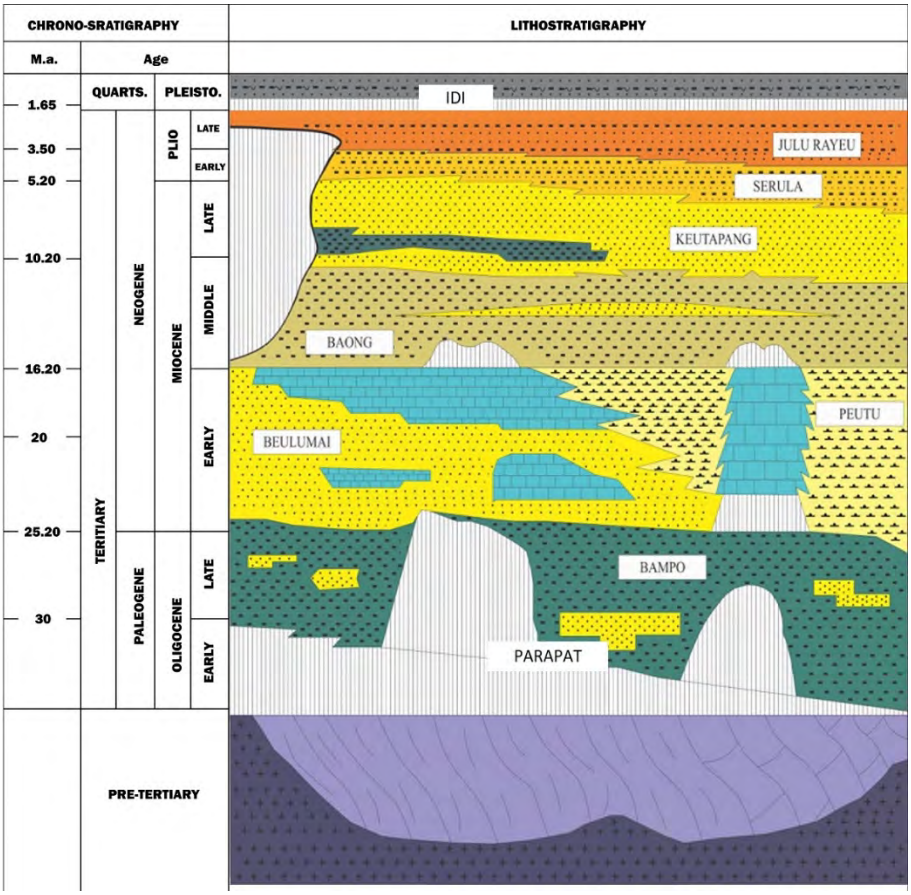

Figure 2-16 General stratigraphy of the North Sumatra Basin from the Barisan Foothills in the south to the Kuala Langsa area in the south (adapted from Sosromihardjo (1988).

2.5 Summary

This literature review highlights the fact that although the understanding of the plate tectonic evolution of SE Asia has received a lot of attention, there are relatively few detailed publications that specifically address the geology of the island of Sumatra. In particular, there are very few publications about the North Sumatra Basin, especially compared to other similar basins in Sumatra. Most publications come from oil and gas companies working in the area from the 1970s until the 1990s and consequently the evolution of the basin is only understood in general terms. The publication gap is also due to Aceh having experienced protracted conflicts. However, recent discoveries in the offshore part of the North Sumatra Basin have re-ignited interest in the area and it is therefore timely to re-evaluate our understanding of basin evolution. The following knowledge gaps have been identified that will be addressed in this thesis:

1) The north Sumatra Basin had experienced multiphase evolution including rifting, subsidence, and inversion. However, the timing of these episodes is still debated by some authors. By using the seismic data constrained by wells in both the onshore and offshore areas, this thesis will examine the evidence for the timing of the different phases of deformation and this will provide an important constraint for linking basin evolution to regional tectonics.
2) The subduction of the India ocean plate beneath the Sumatra is responsible for the formation and evolution of several regional tectonic elements such as strike-slip deformation associated with the Sumatra Fault System, compression and uplift in the Barisan Mountains, and extension in the Andaman Sea. The extent to which these different processes have influenced the evolution of the North Sumatra Basin has not been addressed, nor has the way in which their interaction may have influenced the structural styles in the North Sumatra Basin. Specific questions to be addressed include:
    a. How does the timing of the onset of extension in the North Sumatra Basin compare to other basins in the region, and can it be linked to similar back-arc processes?
    b. What affect do older basement structures, such as the Ranong and Klong Marui Faults, have on the basin? Are they responsible for segmentation of the basin?
    c. How is the compression associated with the formation of the Barisan Mountains expressed in the North Sumatra Basin, and how does it vary with distance from the Barisan Foothills?
    d. Is there any evidence that strike-slip deformation associated with the Sumatra Fault extends into the North Sumatra Basin?
3) There are no comprehensive and integrated studies which link the onshore and offshore parts of the basin. The structural evolution and styles of structure between the onshore and offshore areas, or between the Lhoksukon/Bireun Deep and the Tamiang Deep may be different. This may be due to the proximity of different tectonic elements to these different parts of the basin. This thesis will use structural and isochore maps to investigate these differences.

3 Data and Methodology

This chapter briefly describes the data and methodology utilized in this study.

3.1 Data

In Indonesia, oil and gas data is not publicly available and is considered highly classified (Sidauruk & Hamdi, 2015). Thus, it is very difficult to obtain permission to use seismic and well data, and to do so requires a long and complex bureaucratic process. Data is the responsibility of the Kementrian Energi dan Sumberdaya Mineral Indonesia (Ministry of Energy and Mineral Resources of Indonesia). Following these processes, permission was obtained to use seismic and well data for this thesis in late 2017.

The North Sumatra basin lies within Aceh Province. As Aceh is an autonomous province, it was given a mandate to regulate its oil and gas by the president of Indonesia (Kurniawan, 2018; Putuhena, 2015). Consequently, data from Aceh Province is kept by the government of Aceh through Dinas ESDM Aceh (Aceh Agency of Energy and Mineral Resources) and BPMA (Aceh Regulator of upstream oil and gas). After obtaining permission from the Ministry of Energy and Mineral Resources, it was then necessary to contact the head of BPMA and the oil companies operating in the area. As the author of this thesis works at Universitas Syiah Kuala, the main university in Banda Aceh, this was made a little easier, although a letter from the head of the university was also required, which gave a strong recommendation on the importance of the use of the data. It stated that Aceh needs new study/research of the North Sumatra Basin (NSB) after the long political conflict, with the hope that the research would open opportunities for new oil and gas discoveries in Aceh.

Permission was given to use seismic lines and wells in onshore South Block A covering the southern margin of the Tamiang Deep and parts of the Alur Siwah High and a regional offshore survey covering the northern extension of the Lhokseukon Deep (Figures 2-5 and 1-3) as at that time there was no exploration and no producing oil fields in those areas (although there has subsequently been the discovery by the Timpan-1 well in the area covered by the offshore data). Seismic lines and well data around the Arun field in Block B, the Rantau field in Block NAD, and the Sumatra North offshore block (locations are in Figure 1-3) were also requested. At that time, in 2017, all of these blocks were operated by Pertamina, although Block B containing Arun field was taken over by the Aceh State-owned enterprise in 2021. However, Pertamina did not approve the release of this data, despite the recommendation from the University.

3.1.1 Onshore data

The data used in the onshore includes Shuttle Radar Topography Mission (SRTM) data in GeoTIFF format, Digital Elevation Model (DEM), and Bathymetry. Those data were provided by the Badan Geologi Indonesia, in Bandung (Geospasial, 2018). In addition, the earthquakes data from the USGS website (USGS, 2023) were also used to observe present day deformation in the onshore area of NSB. The earthquakes are chosen from the year 1950 to 2022 with magnitude 2 to 8 Mw.

The seismic and well data from the onshore NSB were mainly acquired in the 1970s and 1980s. One hundred and sixty seismic lines cover an area of at least 4200 km^2 and were provided by Lion Energy, an oil company operating in the basin. Lion Energy does not have any information about the acquisition parameters or the total number of lines that have already been shot in the area and as the data were exported from a pre-existing seismic interpretation project, the typical headers that might contain this information are not available. The data available to them mainly covers the Alur Siwah High and adjacent parts of the Tamiang Deep (Figure 2-5). Northeast-southwest lines dominate the data and spacing between the lines is about 1.5 kms to 4 kms. Lines from different surveys have different vertical record lengths varying between 4000 and 5000 milliseconds two ways time (twt) (Figure 3-1).

The seismic lines are of different vintages and the quality of seismic images varies (see Figure 3-1). A frequency spectrum from a sample line is shown in Figure 3-6. The broad nature of the spectrum shows that there is little differentiation between reflectors and consequently reflections are not well resolved in some areas. This may be due to variations in acquisition and processing and the geological complexity of the area. For example, line 526 (Figure 3-1) is located close to the Barisan Foothills, where the area is structurally complex, and volcanic rocks such as the Sembuang Formation are present (Figure 2-15), reducing the resolution of the reflectors. There are also misties between some seismic lines.

Composite seismic lines were constructed to create regional geological cross-sections. The composite lines are oriented northwest-southeast and vary in length from 38 to 48 kilometers. Composite lines 1 and 2 (Figure 2-5) have a length of about 48 kilometers and a record length of 5000 milliseconds TWT. Most areas in lines 1 and 2 are well-imaged except the eastern part (Figures 4-4 and 4-5). Both lines have well-resolved reflections that define stratigraphic horizons and faults. Seismic composite lines 3, 4, and 5 have the same northwest-southeast orientation as composite lines 1 and 2 (Figure 4-1). Their lengths are about 40 to 50 kilometers (Figures 4-5,

4-6, and 4-7). Line 3 has a record length of 4000 milliseconds in the south and 5000 milliseconds in the north. Meanwhile, line 4 has a record length of 5000 milliseconds throughout.

Wells tops were provided from wells Peulalu3, Pergidatit, and South Pineung (Figure 3-2) and were used to tie the interpretation of the onshore lines to the regional stratigraphy. The only information from the Peulalu and South Pineung wells is a list of formation tops in the time domain. The South Pineung well also has a stratigraphic summary report. There was no other data (wireline logs, core or sidewall core descriptions, velocity surveys, etc.) available from these wells.

3.1.2 Offshore Data

Fifty-five lines of 2D seismic data offshore NSB covering about 10.000 km^2 were used to build offshore NSB horizon maps from the Oligocene to recent. The line length varies from 50 km to 180 km. The line spacing varies between 5 and 10 km (Figure 2-5) and the record length varies between 5000 milliseconds to 6000 milliseconds (ms) in two-way time (twt). Most lines are oriented E-W or N-S, but some NE-SW and NW-SE oriented lines are also present. A frequency spectrum from a sample line is shown in Figure 3-6. Compared to the onshore data, the frequency spectrum is much more sharply defined and the dominant frequency is lower, indicating the higher resolution of this data compared to the onshore lines. Consequently, the quality of the image varies from moderate to poor. For example, reflector imaging below 3 s TWT is poor, mainly corresponding to the base of the Paleogene sedimentary sequence and the Cretaceous basement (Figure 3-2). The seismic amplitudes vary significantly from one seismic line to another.

One well (BLD) was used to tie into the seismic interpretation to the regional stratigraphy. The well was spudded on a basement high (horst) and penetrated Cretaceous and older basement rocks (Figure 3-4). Only formation top information in time was provided for this well. As there are no wells in the grabens, the age of sediments filling the grabens is less well constrained.

In 2022, a section from the newest 3D seismic line in the offshore NSB was published by PGS (Figure 5-29) following the successful drilling of the Timpan-1 well and the commercial well test. The seismic shows very well-resolved reflectors and geological structures such as faults, beddings, and folds. A DHI (Direct Hydrocarbon Indicator) is also visible in the folded syn-rift Oligocene sedimentary rocks. However, the location of the line (longitudes and latitudes), the vertical scale, whether it is in-depth or time, and the key seismic horizons are not shown (PGS, 2022).

3.1.3 Passive Seismic data

Passive seismic was acquired by a team from Universitas Syiah Kuala (including the thesis author) in 2021. The purpose was to investigate the hydrocarbon potential in the Sigli High, in the onshore part of the western margin of the NSB (the survey area is in Figure 6-1). A hydrocarbon lead is shown by 2D seismic in the area (Figure 6-3). Based on that image, seventy-eight points in an area of 8 km x 8 km were acquired by seismographs to obtain amplitude vs. frequency data. This method uses the low seismic frequencies of 1 to 10 Hz. Because oil and gas absorb this frequency, this method has been widely used in Indonesia as a rapid and low-cost way to assess the presence of hydrocarbons.

3.2 Methodology

Conventional seismic interpretation was conducted for 2D seismic data sets onshore and offshore of the North Sumatra Basin using Petrel interpretation software provided by Schlumberger. The interpretation emphasizes the stratigraphic packages and the major structures recognizable across the study area. Two-way travel-time structure maps were generated by creating surfaces using standard gridding algorithms available within Petrel software. Given the wide spacing of the lines, particularly in the offshore area, this has the potential to create artefacts and prevents detailed mapping of structures. However, the maps provide a general understanding of the structural styles and evolution of the North Sumatra Basin. The 2D seismic data are also used to interpret more minor faults and anomalous Miocene geological bodies, but because of their scale, these features cannot be mapped laterally. However, with the onshore data, structural lineaments that appear at the surface were interpreted based on the SRTM data (Figures 2-4, 2-3, and 4-1) and were used to provide further control of the horizon and the structural interpretation of the seismic data (figure 3-5). Isochron maps were generated by calculating the difference between the structure maps that define the tops and bases of each sequence. Consequently, they measure vertical thickness (in time) rather than true stratigraphic thickness (in depth). Any artefacts due to the gridding method that are present in either surface will be propagated into the isochron map.

Ideally, the structure and isochore maps are shown in depth (meter/feet). However, time-depth conversions were not carried out in this study because of the limited amount of well information. The limited information from the wells is insufficient for creating velocity models that allow for velocity variations present in the large areas covered by the seismic interpretation. Therefore, all the seismic sections and maps (structural and isochron) are shown in the time domain (two-way times) but are still effective in demonstrating contrasting elevations and thickness.

Simplified paleo-reconstruction for each episode of the basin evolution were also created. The best seismic lines showing clear reflectors onshore and offshore were selected. Each horizon/formation was flattened to remove structures such as faults and folds. Flattening does not incorporate decompaction or make estimates of stratigraphy that is missing as a result of erosion. However, this does provide a visual estimate of the structure at the time when the deposition occurs.

Quantitative interpretations were not made, such as seismic attributes related to the deposition environment. This is because of the variations in amplitude between different seismic surveys and the spacing between lines which makes the creation of amplitude or attribute maps impractical.

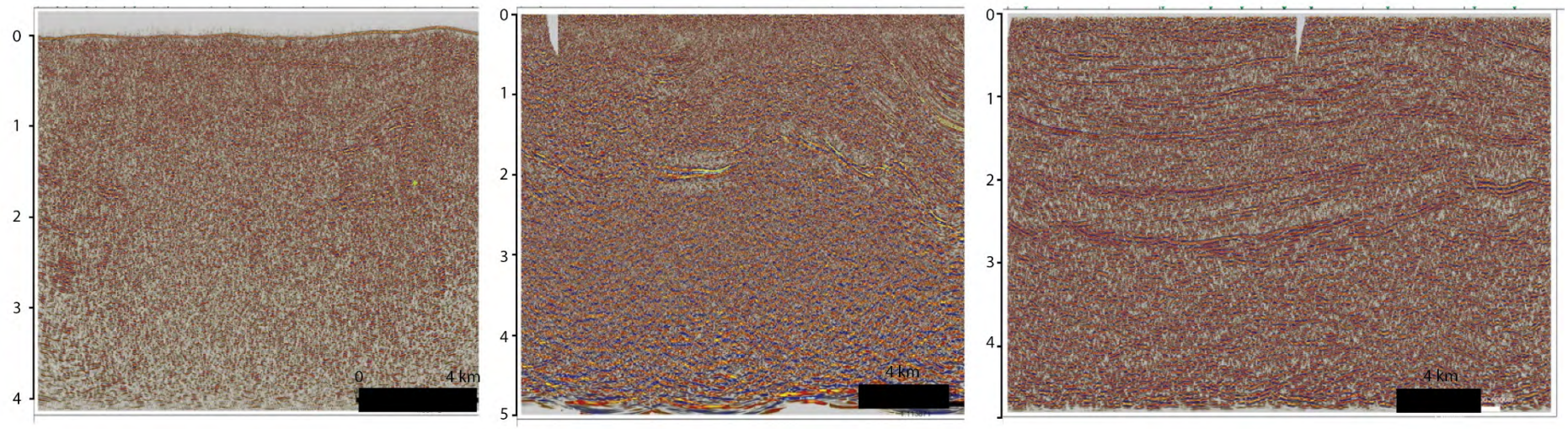

Figure 3-1 Samples of the seismic lines (left to right) in the study area (line 526; line 1159; line 104) show the quality of the images from poor, moderate, and good, respectively. The record length is not the same in each line, as, in lines 536 and 104, the two-way vertical time (TWT) ends at 4000 milliseconds(ms); meanwhile, line 1159 is 5000 ms. The location of these lines are shown in Figure 2-5.

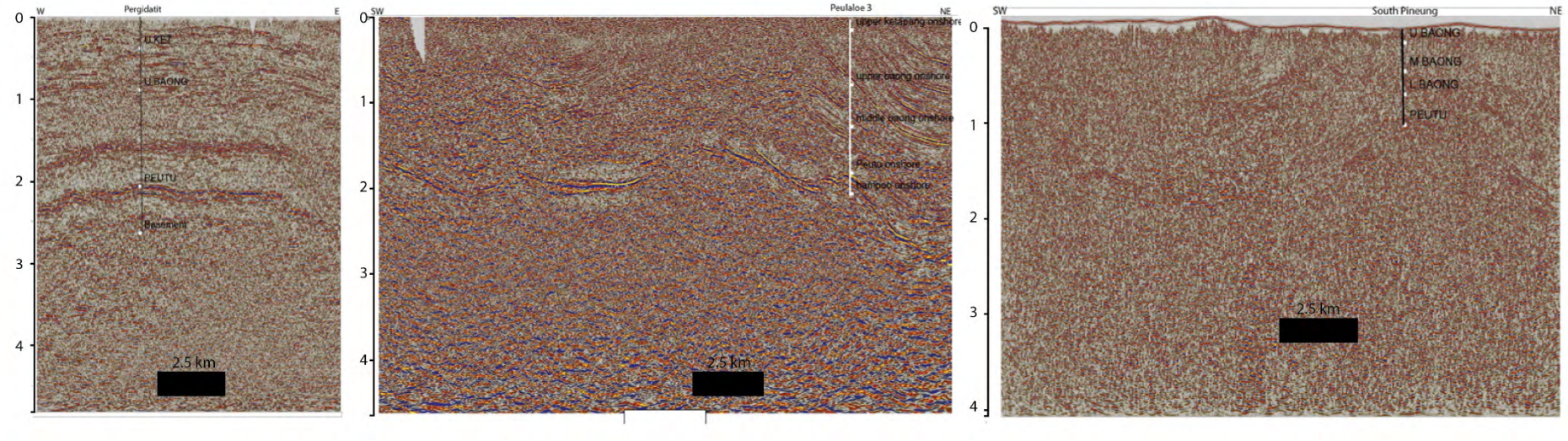

Figure 3-2 Seismic ties to formations tops in the onshore area (left to right Pergidatit AB at seismic line 810, Peulalu3 at seismic line 515, and South Pineung at seismic line 308). Only Pergidatid penetrated the basement. The location of these lines are in Figure 2-5. The vertical information is in TWT.

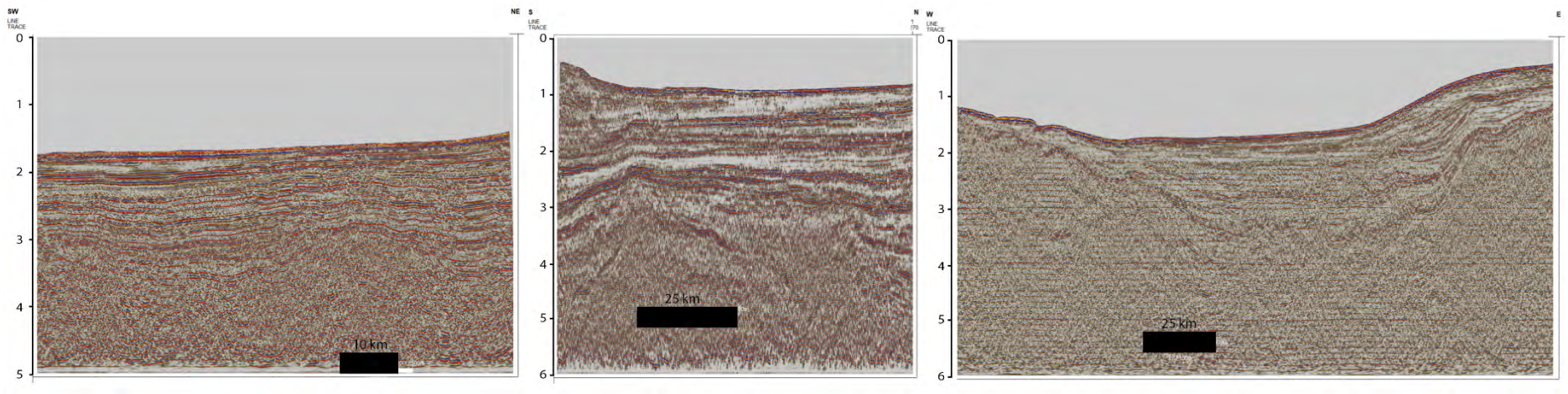

Figure 3-3 Seismic lines from the offshore study area (left to right line 462, line 134, and line 247) show the quality of the images as good, moderate, and poor, respectively. The record length is not the same in each line, as, in lines 134 and 247,the TWT is 6 s. Meanwhile, line 462 is 5 s. The images below 3 s show poorly resolved reflectors.

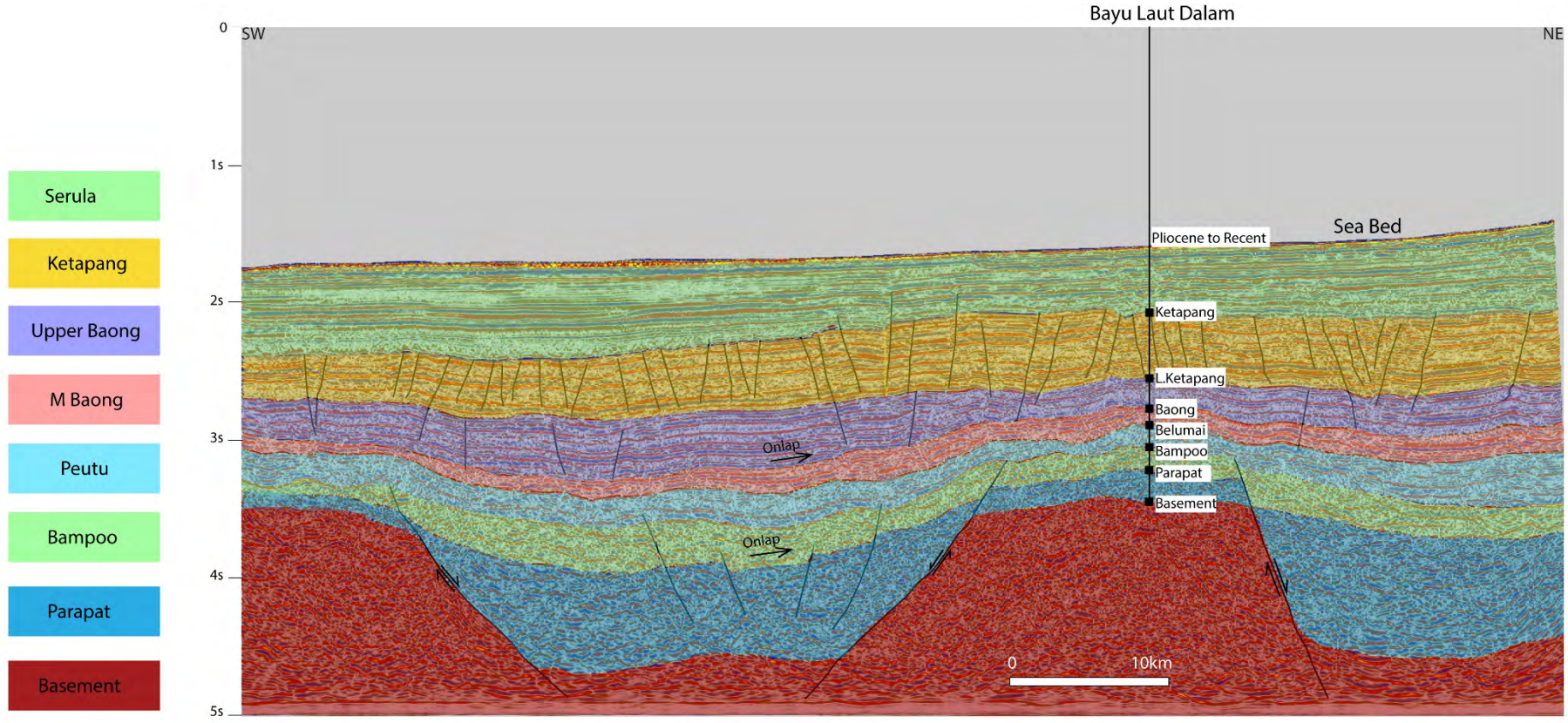

Figure 3-4 Seismic ties to formations tops in the Bayu Laut Dalam (BLD) well on line 462 in the offshore area. The wells penetrated from 1600 ms at the seabed to 3450 ms at the basement. The seismic is in TWT.

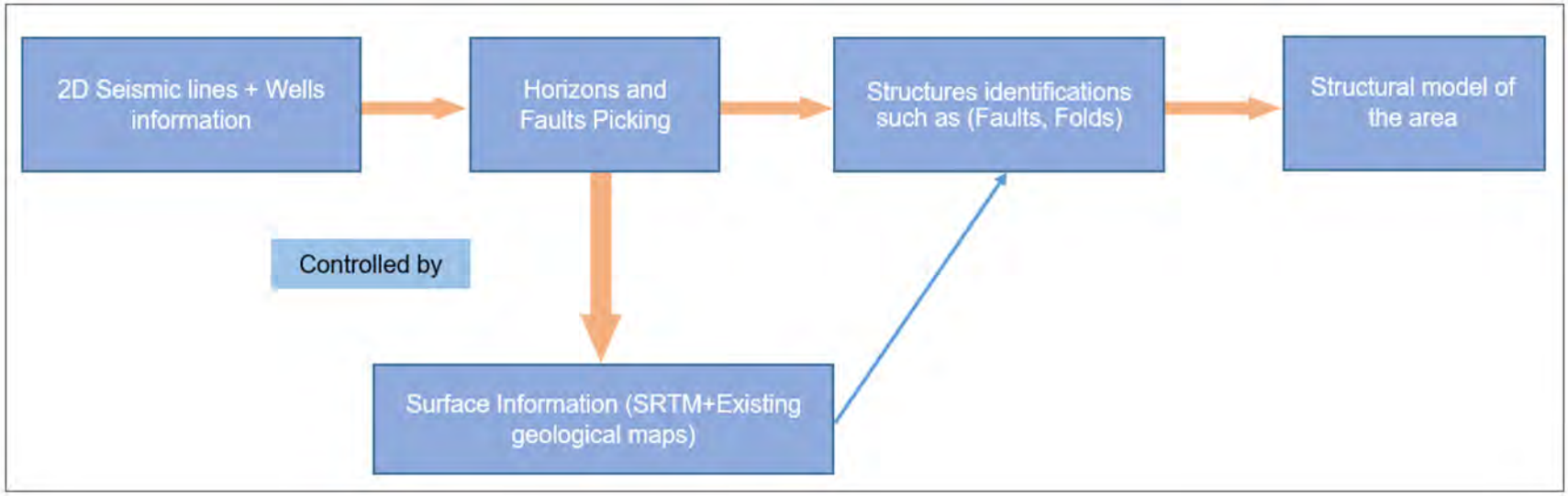

Figure 3-5 Flowchart of the structural model in the area by combination of seismic lines, wells information and the SRTM

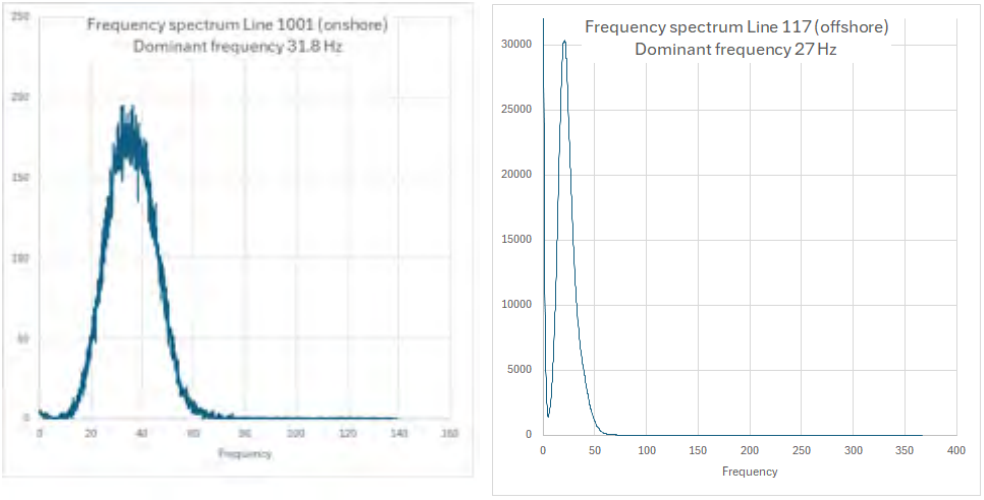

Figure 3-6 Examples of frequency spectra from the onshore (left) and offshore (right) data sets showing the difference in quality between the surveys.

4 Onshore North Sumatra Basin

The onshore North Sumatra Basin is located to the east of the Barisan Mountains (Figure 1-2, Figure 4-1). It is bounded by the Sigli High in the northwest and the Asahan Arch to the southeast which separates it from the Central Sumatra Basin (Figure 1-2). The northern limit is defined by the coastline.

Neogene sediments cover the onshore part of the North Sumatra Basin, as well as volcanic deposits, especially in areas close to active and paleo volcanoes (Cameron et al., 1980; Davies, 1984). For example, the area near Asahan and Medan is covered by volcanic ash from the eruption of the Toba super-volcano, approximately 300 km SE of the study area, 74,000 years ago (Cameron et al., 1980; C. Caughey & Sofyan, 1994; Setyobudi et al., 2016).

Sedimentary rocks that fill the onshore North Sumatra Basin range in age from Oligocene to Recent (Figure 4-2). The stratigraphy of the basin fill is based on outcrops that occur in the Barisan Foothills and on reports from wells drilled in East Aceh (Figure 3-2) in the 1970's provided by the oil companies that have concessions in parts of East Aceh. The available wells, such as Peulaloe 3, Pergidatit, and South Pineung (Figure 4-1), penetrated basement highs (horst) where prospects were identified (Figure 3-2). No wells targeted the syn-rift sediments in the grabens due to the lack of petroleum traps.

The study area is focused on the eastern part of the onshore North Sumatra Basin, on the western margin of the Tamiang Deep (Fig. 2.6). Five composite seismic sections were compiled from the available seismic data to investigate the seismic stratigraphy and structure of the basin (Figure 4-1). They extend from the Langsa Platform, on the western margin of the Tamiang Deep, and cross a variety of graben and half graben, reaching as far as the Perlak Platform and Langsa Horst, two of the intra-basinal highs that comprise the Tamiang Deep (Figures 4-1 and 2-5). Numerous structural features such as, anticlines, synclines and dipping bedding surfaces are exposed at the surface and are visible on SRTM maps (Figure 4-1). The observation of these features was incorporated into the seismic interpretation to assist identification of structures.

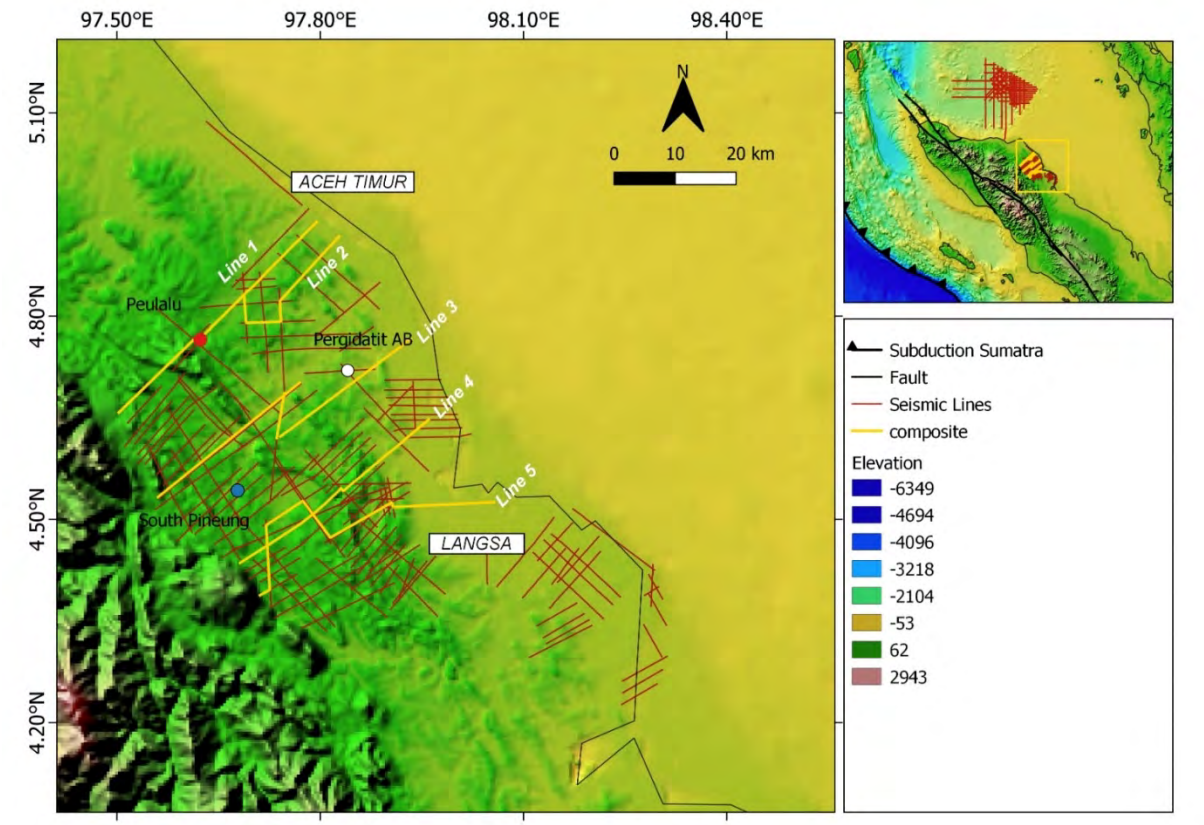

Figure 4-1 The seismic lines are shown in red while composite seismic are shown by yellow lines. The yellow box indicates the study area in onshore Aceh.

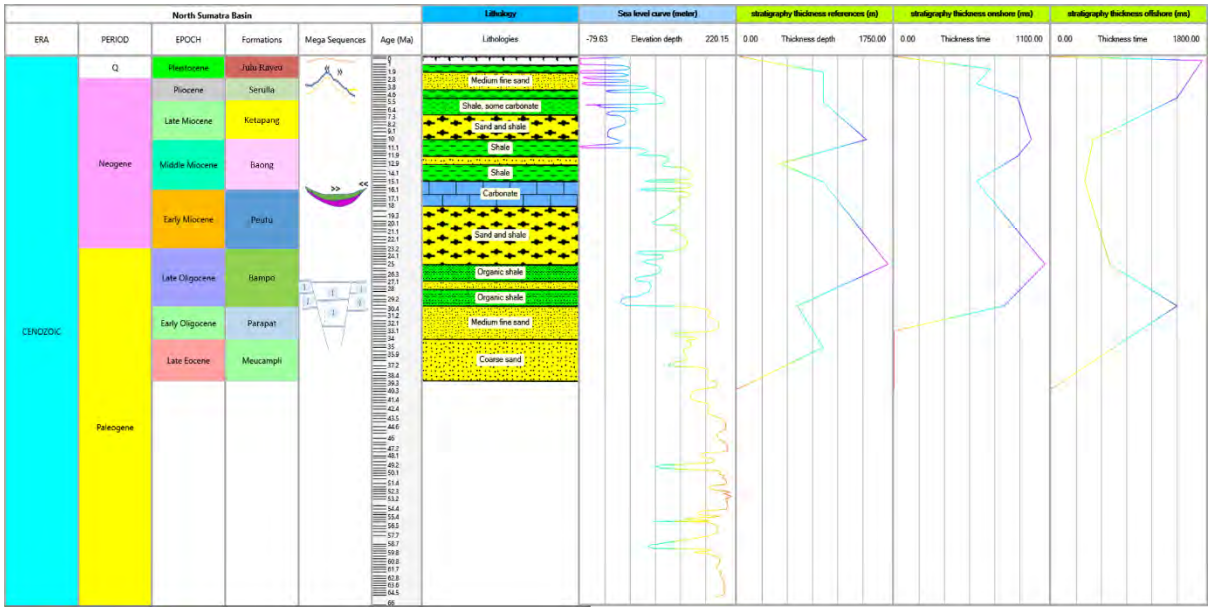

Figure 4-2 Stratigraphy of the North Sumatra Basin in east Aceh integrates with each horizon's thickness information. This map is a compilation of (Haq, Hardenbol, & Vail, 1987) for the global sea level curve, N. R. Cameron et al. (1980), Bennett et al. (1981), Keats et al. (1981), and Sosromihardjo (1988) for the general stratigraphy such as formation name, lithology, and thickness of formation (meter).

4.1 Seismic Stratigraphy

Paleogene to Neogene sedimentation in the North Sumatra Basin generally can be divided into pre-rift, syn-rift, post-rift (tectonic quiescence), and syn-inversion sequences. The composite seismic sections (Figures 4-3 to 4-7) are used to define these sequences.

4.1.1 Basement (Pre-rift)

The Basement sequence is characterized by chaotic and discontinuous reflectors. It is not easy to identify the unconformable contact between the basement and the overlying sediments. The tie to the Peulalu well on composite section 1 shows that it lies below high amplitude reflectors corresponding to the Petu Formation (Figure 4-3), which may reduce the seismic expression of the unconformity on the horsts. In addition, the top of the basement is just above the base of the seismic sections in the graben, where seismic imaging is poorer. For example, in composite line 3 (Figure 4-5), the top of the basement in the graben is at 4 seconds (s), whereas the record length of the seismic is 4.5s. Accurate identification of top of the basement top would benefit from better quality seismic data, if it were to be acquired, for future work.

4.1.2 Parapat and Bampo formation (Oligocene)

The Parapat Formation was deposited unconformably above the basement. It is characterised by subparallel, semi-continuous reflectors with moderate to strong amplitude (Figure 4-3 and table 4-1). It is interpreted as being present above the basement in the grabens where it is cut by faults, but it is thinner or is absent on the horsts (e.g. it is absent in the Peulalu well) located on the Langsa Platform at the southern end of composite line 1 (Figure 4-3). Where it is present on the horsts (Figures 4-3, 4-4, 4-5, 4-6), it is difficult to see from the seismic data whether or not there in any erosional truncation at the top of this unit and hence whether its absence or reduction in thickness is a result of erosion or non-deposition. It is also cut by a series of secondary faults on the Langsa Platform.

The Bampo Formation is present throughout the area. It overlies the Parapat Formation both in the grabens and on the horsts in places where the Parapat Formation is present. Elsewhere on the horsts the Bampo Formation lies unconformably on the basement. The seismic characteristics of the Bampo Formation are similar to the Parapat Formation (table 4-1). Generally, the Bampo Formation is thicker in the grabens that on the horsts and this is clearest on composite sections 1 and 2, but the difference is less noticeable than with the Parapat Formation. However, because

of the thickness changes and the presence of extensional faults, both formations are interpreted as syn-rift deposits.

4.1.3 Peutu/Belumai formation (Early Miocene)

The Peutu Formation was deposited above the Bampo Formation, and is most likely conformable with it. It is characterized by parallel and continuous reflectors. In addition, this unit also contains mounded, high amplitude reflectors which are characterised by internal discontinuous high amplitude reflections visible on composite lines 1 and 5 (Figure 4-3, Figure 4-7 and table 4-1). These are interpreted as carbonate platforms and occur on the margin of the horst towards the southwest, and above a second horst to the northeast, adjacent to graben bounding faults (Figure 4-7). Additional criteria for recognition of the build-up are provided by onlap and termination of overlying reflections on the flanks of the mounds. These features are discussed further in Section 4.5.3.

The Peutu Formation is of relatively uniform thickness, although it is deformed by reactivated faults and folds. It is interpreted as the start of the post-rift sequence. It is laterally equivalent to the Belumai Formation offshore.

4.1.4 Middle Baong and Upper Baong (Middle Miocene)

The Middle Baong Formation conformably overlies the Peutu Formation. The Middle Baong Formation has a uniform thickness and it is characterised by parallel and continuous reflectors with high amplitudes at the top and the base. Internally, the lower part, is characterized by low amplitude subparallel and discontinuous reflectors (Table 4-1). The upper part is characterized by parallel and semi-continuous reflectors which show variable moderate to high amplitudes, implying that his unit may consist of variable lithologies (Figure 4-2). Within the middle of this unit, some layers onlap and down-lap to the unit below. In addition, the middle layers also show top lap onto the above unit, which may indicate truncation (see Figure 4-3 and table 4-1).

An interesting feature can be observed in the Middle Baong Formation in Figure 4-8. It is characterized by isolated, laterally continuous, parallel high amplitude reflectors. It is similar to features interpreted by Hakim et al. (2019) as turbidite sands at the same stratigraphic interval in the offshore North Sumatra Basin.

This sequence shows subtle thickness changes across some faults (Figure 4-8), which may be due to differential compaction, also allowing propagation of the fault. More generally the sequence gradually thickens into the deeper part of the graben (e.g. Composite line 3, Composite line 4) and it is interpreted as part of the post-rift sequence.

Some sections show that the base of this unit is planar, while the upper surface is folded (Composite lines 3, 4 and 5) while other sections show that the upper surface is also planar, while the units above it are tightly folded (Composite lines 1 and 2). This implies that the Middle Baong unit is acting as a detachment for younger folds.

The Upper Baong Formation conformably overlies the Middle Baong Formation. It is characterized by semi-continuous, low to medium amplitude, sub-parallel to parallel reflectors (Figure 4-3 and table 4-1). The low amplitude parts of this sequence are possibly related to thick shales that characterise this formation.

The Upper Baong Fm forms the core of detachment folds in the southwest of the area (Figure 4-3). Elsewhere it is of relatively uniform thickness and forms part of the post-rift sequence (Figure 4-4).

4.1.5 Keutapang formation (Late Miocene)

The Keutapang Formation was deposited conformably above the upper Baong formation. It is characterised by high amplitude, parallel continuous reflectors. (Figure 4-3 and Table 4-1). The thickness of the formation is uniform across all the composite sections (Figures 4-3 to 4-7).

This unit is folded, particularly in the southwest of the area, where it is exposed at the surface (Figures 4-3 to 4-7). Towards the northeast it also show down-lap onto the Upper Baong Formation on some lines (Figure 4-5), possibly related to basinward progradation of deposition.

4.1.6 Seurula Formation (Early Pliocene)

The Seurula Formation conformably overlies the Keutapang Formation (Figure 4-3, 4-4, Table 4-1). Moderate to high amplitude, continuous parallel reflection patterns dominate this unit. However, some central areas show low amplitude reflections (table 4-1) and some sections show down-lap on to the Keutapang Formation in the north of the area. The sequences prograde from the south.

The thickness of this unit varies as a result of folding, exposure and erosion at the surface. It is eroded from the cores of anticlines in the southwest (Figure 4-3) and forms the surface outcrop

in the central areas as a result of uplift caused by inversion to the NE (Figure 4-3 & 4-5) that occurred after the deposition of this unit. This aspect of basin evolution will be discussed later.

4.1.7 Julu Rayeu formation (Late Pliocene)

The Julu Rayeu Formation was deposited conformably above the Seurula formation. The unit is located in the upper part of the seismic section and is exposed at the surface (Figure 4-3, 4-5, 4-6) and is the youngest of the Paleogene-Neogene sequences that fill the basin. It is characterised by continuous high amplitude reflections. There is limited evidence of onlap on to the anticline at the northeast end of composite lines 1 and 2 (Figure 4-3, 4-4), indicating that this unit is at least in part syn-inversion.

4.1.8 Summary of the seismic stratigraphy

The chronostratigraphic column of the North Sumatra Basin (Figure 2-16 and 4-2) extends from the pre-rift Mesozoic sequence until the late Neogene. The seismic stratigraphy in the onshore research area is summarized in Table 4-1 and Figure 4-2. The summary includes the seismic characteristics of each horizon and the structures.

In the grabens, the seismic interpretation shows thicker units of Paleogene rock, such as the Bampo Formation (Figures 2-16, 4-3, 4-4, 4-5, 4-6, and 4-7). Units older than than the Bampo Formation may exist in the deeper parts of the graben. However, the boundary of the basement and the sedimentary cover in the graben is not well imaged due to limitations in data processing. Besides, the interpretation is based on the information from wells that were drilled on the horsts.

The oldest sediments encountered in North Sumatra Basin belong to the Bampo, Parapat and Bruksah formations, which are Oligocene in age. The Bampo Formation is dominated by shale. However, some sandstones are locally developed and are referred to as either the Parapat or Bruksah Fm. These formations are thicker in graben and thin onto the horsts (Figure 2-16 and 4-3) indicating that they form the syn-rift sequence, with onlaps at the top of the Bampo Formation showing that the transition to the Parapat and Bruksah formations may represent the late syn-rift.

The first post-rift sediment is the Peutu Formation (early Miocene age), which was derived from the Malacca platform to the east (De Smet& Barber, 2005). At the start of the post-rift stage during the Early Miocene, the North Sumatra Basin experienced sagging due to thermal cooling (De Smet & Barber, 2005). The sagging resulted in marine transgression that drowned the

existing horsts. At the same time carbonate build-ups were developed in the Peutu Formation (Figure 4-9a, b, c) at the crests of some of the horsts.

The North Sumatra Basin experienced the maximum transgression in the Middle Miocene indicated by deposition of thick shales of the Baong Formation. A sandstone, known as the Middle Baong Sand (MBS), is interpreted as a basin floor fan (Syafrin, 1995) and is similar to features interpreted by Hakim et al. (2019) as turbidite sands in the same stratigraphic interval offshore. The sandstone is probably associated with the isolated high amplitude reflectors identified in this study (Figure 4-8).

The presence of folds that affect even the youngest stratigraphic units and the presence of Miocene age sediments at the surface show that the most recent stage of deformation is compression and uplift. Sandstones dominate the Keutapang, Seurula, and Julu Rayeu formations and are believed to be derived from uplift and erosion in the Barisan Mountains. However, the uniform thickness and parallel reflector geometries of the Ketapang and Serula Formation indicate that they pre-date inversion in the onshore Northern Sumatra Basin, and there is only limited evidence on onlap onto folds in the Julu Rayeu Formation, suggesting that inversion in the onshore Northern Sumatra Basin is Pliocene age and younger.

Horizons	Seismostratigraphy	Structures
Serula Fm.	• Moderate to high amplitude • Parallel with continuous reflectors	• Cut by reverse fault in the north east • Exposed to the surface forming eroded anticline in the southwest • Fold structure in the northeast
Ketapang Fm.	• High amplitude • Parallel with good continuity • Local down-laps related to basinward deposition	• Cut by a reverse fault in the north east • Exposed as anticline and syncline to the surface in the southwest • Fold structure in the northeast
Upper Baong Fm.	• Low amplitude in the southwest to medium in the centre • Sub-parallel with semi continuous reflectors • Thickening to the southwest	• Cut by reverse fault in the northeast • Formed as assymetrical fold in the southwest • Fold structure related to reactivation of basement bounded-fault
Mid. Baong Fm.	• Low amplitude in the lower part to higher amplitude in the upper part • Parallel with semi continuous reflectors • Uniform thickness • Local on-laps and down-laps	• Cut by basement bounding fault in the southwest and dip northeast • Cut by several reverse faults in the south east dipping southwest • Formed as fold structure in the northeast
Peutu Fm.	• High amplitude • Local mound with high amplitude associated with reef build-up in south horst area • Parallel with continuous reflectors • Uniform thickness	• Formed anticline in the northeast • Carbonate/reefs build-up in the south horst adjacent to the graben
Bampoo Fm.	• Moderate amplitude • Sub-parallel with semi continuous reflectors • Unconformity on basement boundary on the horst • Thickening in the graben and thinning on the horst	• Basement bounding faults forming horst-graben structure
Parapat Fm.	• Moderate amplitude • Sub parallel with semi continuous reflectors • Deposited in the graben and possibly eroded on the horst	• Basement bounding faults forming horst-graben structure
Basement Fm.	• Chaotic with discontinuous reflectors	• Basement bounding faults.

Table 4-1 The summary of Seismic Stratigraphy and structures of the onshore study area. The seismic characteristics and the structures are summarized in the table on the right of the seismic composite 1. The Parapat (syn-rift) sequence on the horst is not informed in the well. However, we distinguished the Parapat and Bampo formations in the syn-rift packages. Meanwhile, the Serula formation was interpreted based on the formation shown by the geological map.

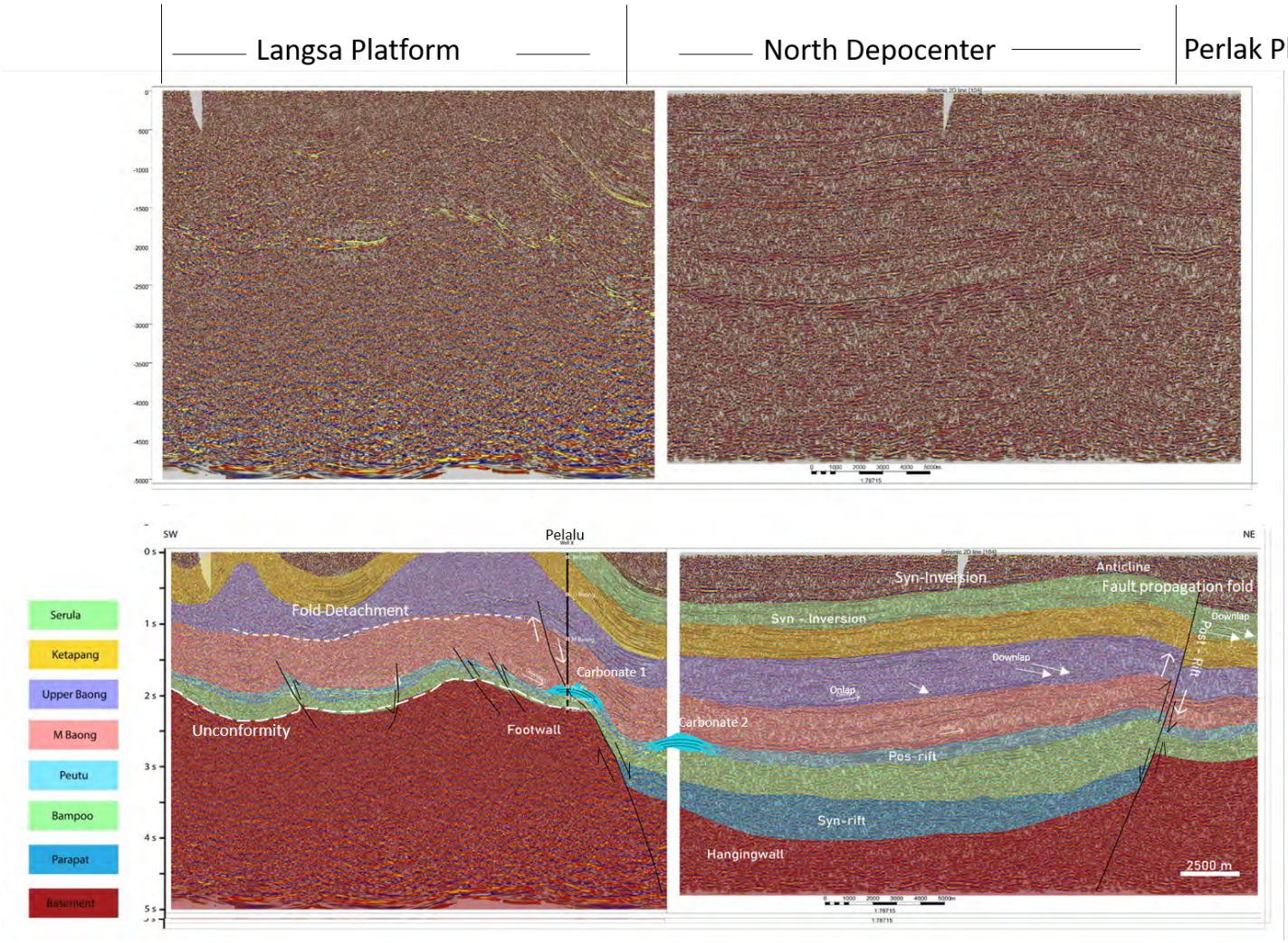

Figure 4-3 The composite line 1 in the onshore study area (lines 1159 and 104) shows the regional subsurface geology (location is in Figure 2-15). This line shows several structures, such as faults and folds. Two main faults are basement bounding faults creating the horst and graben/trough. Minor faults were also identified on the horst in the southwest. The folds in the southwest had elevated several formations to the surface. These folds are possibly related to the thrust fault that lies parallel in the upper Baong (royal blue color). The elevated Seurula fm (green in the upper part) close to the well marks the boundary between the high and fewer deformations area. The well penetrates two carbonate structures, and the other is identified to the northeast from the first build-up.

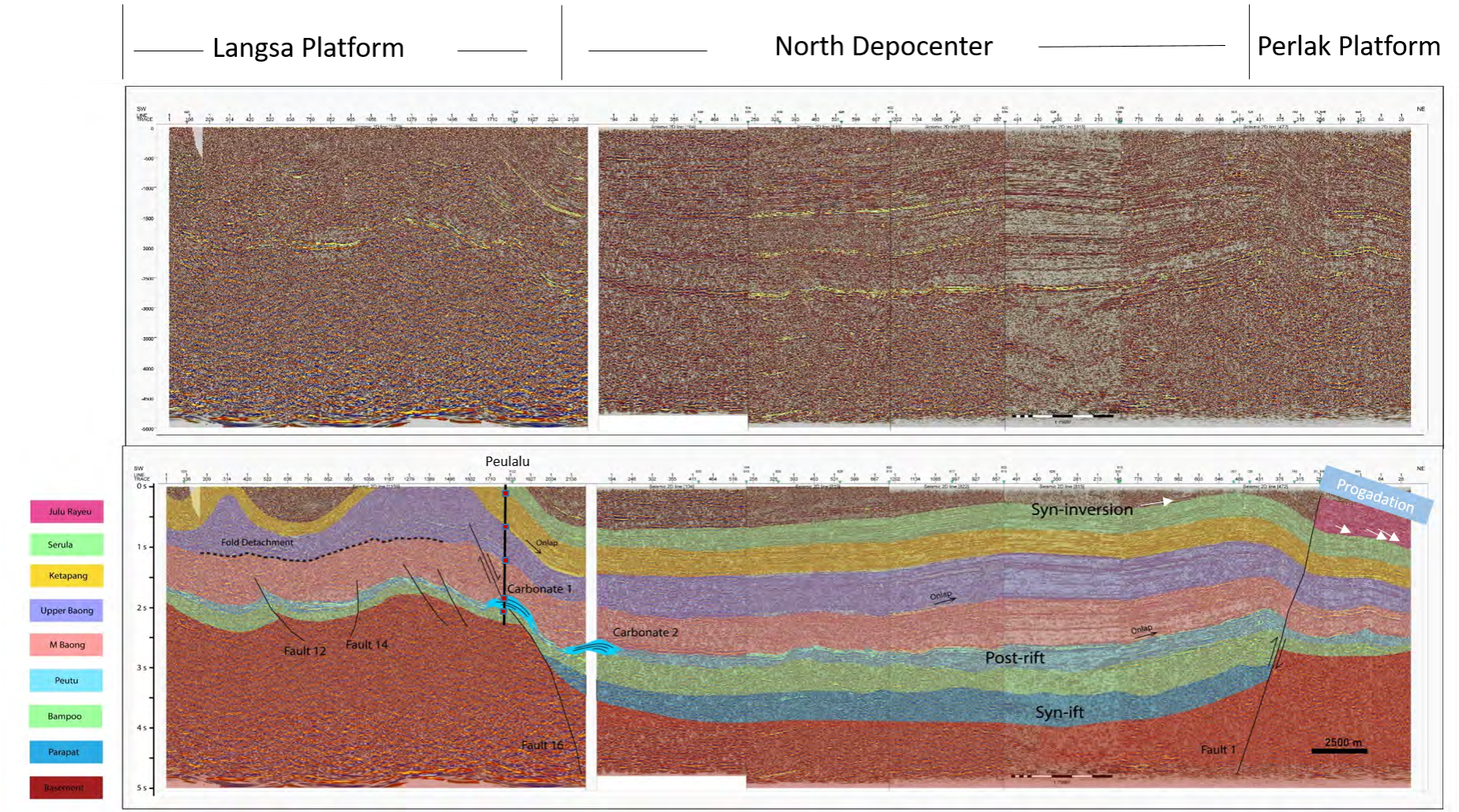

Figure 4-4 The composite line 2 in the onshore study area (lines 1159, 104, 819, 826, 815, and 472) shows the regional subsurface geology (in Figure 2-15). This line shows similar structures, such as in composite line 1. This line gives clearer seismic reflectors in the northeast so that the fold and fault are relatively clear to identify.

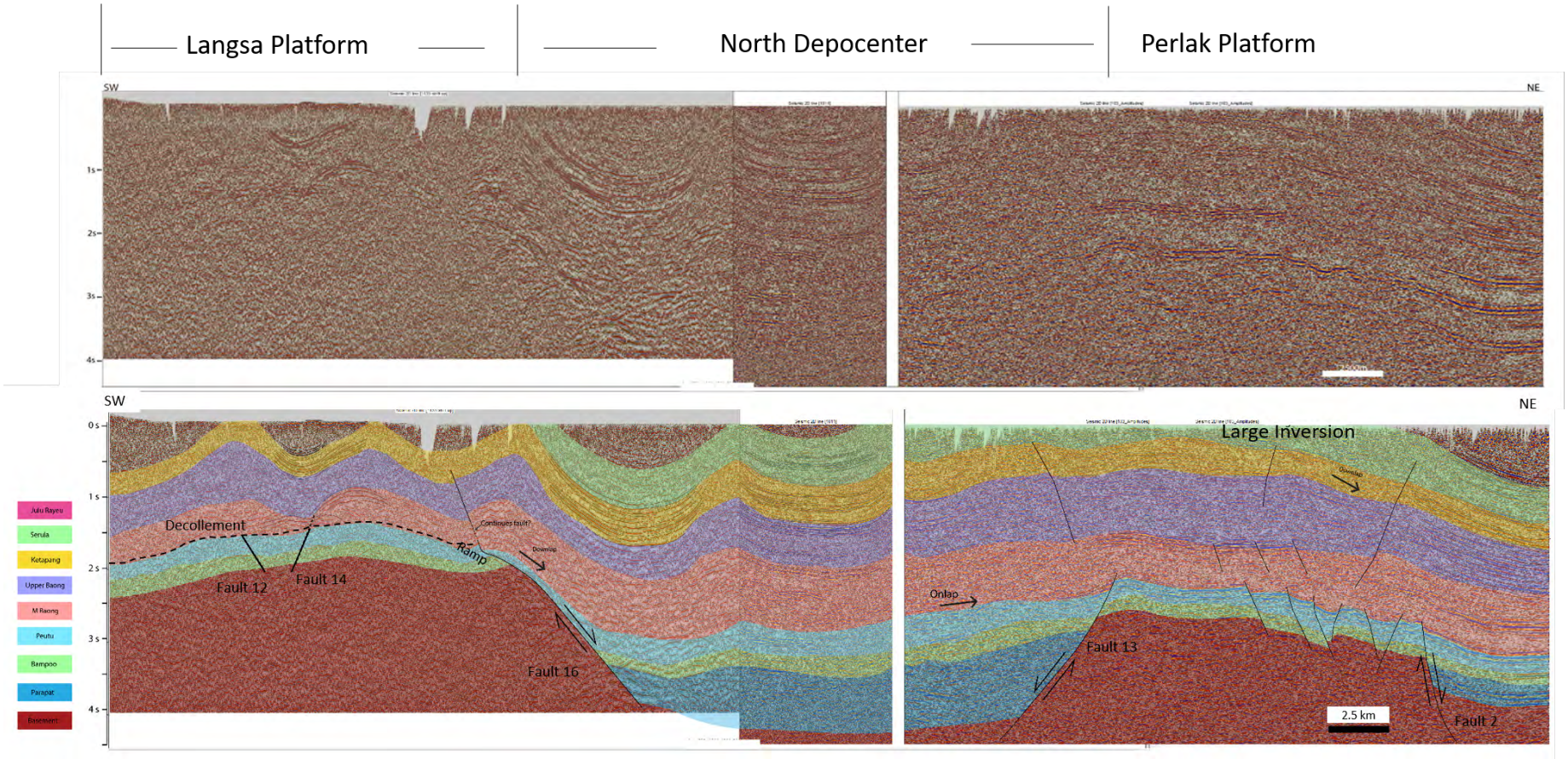

Figure 4-5 The composite line 3 in the onshore study area (line 1133, 1011, and 103) show the regional subsurface geology (location is in Figure 2-15). This line shows complex structures along the area. The lower part of the seismic shows the graben geometry, which is shaped by two main faults. The minor faults dominate from the center to the northeast in the lower and upper parts. The fold's structure is predominant along the lines, and they are exposed to the surface.

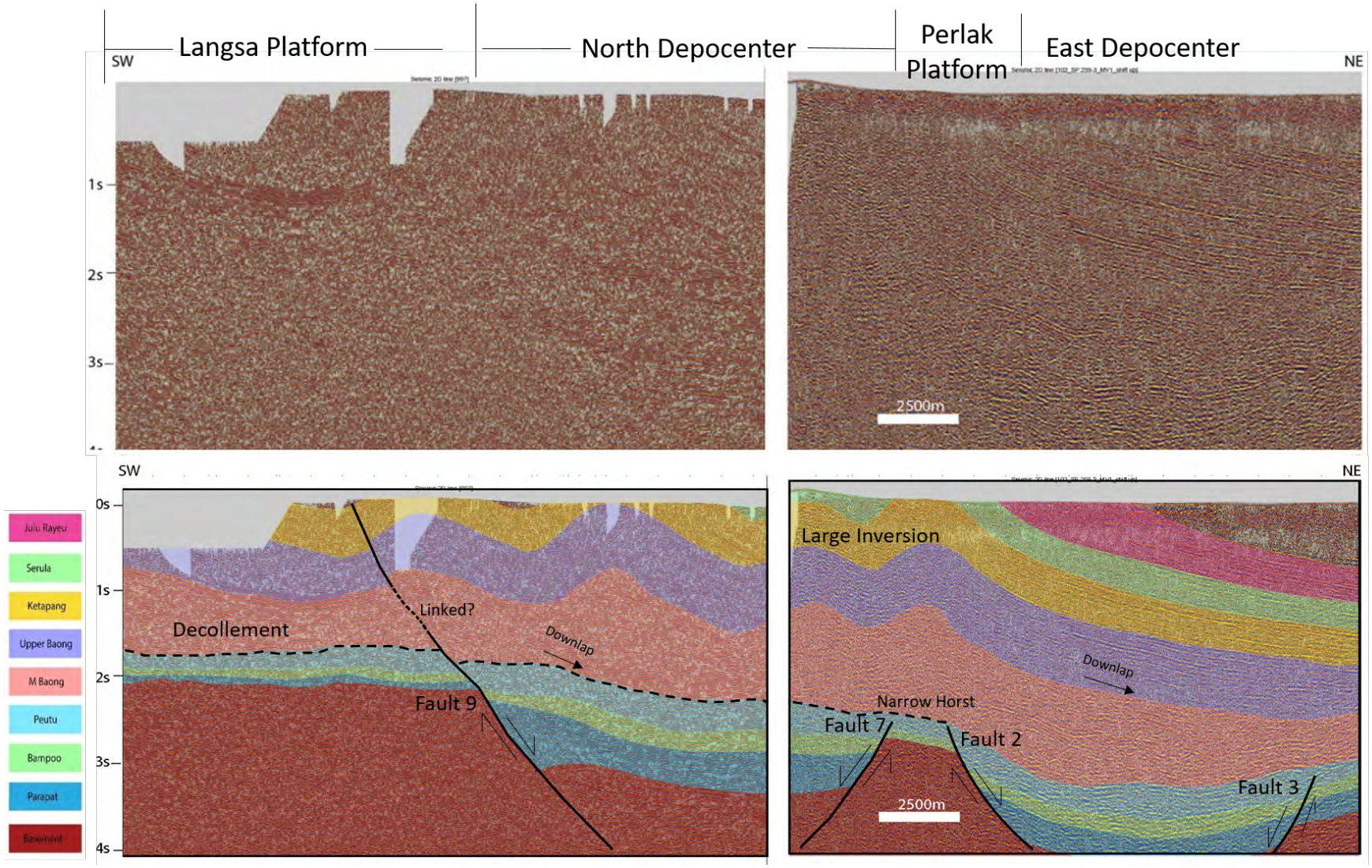

Figure 4-6 The composite line 4 in the onshore study area (lines 997 and 102sp) shows the regional subsurface geology (location is in Figure 2-15). This line shows complex structures along the area. The low part of the seismic shows two grabens geometry and a narro narrow horst in the middle shaped by several main faults. The record length of 4s has limited to observe the extensional of those faults to the lowest part. Fold structures dominate the upper section.

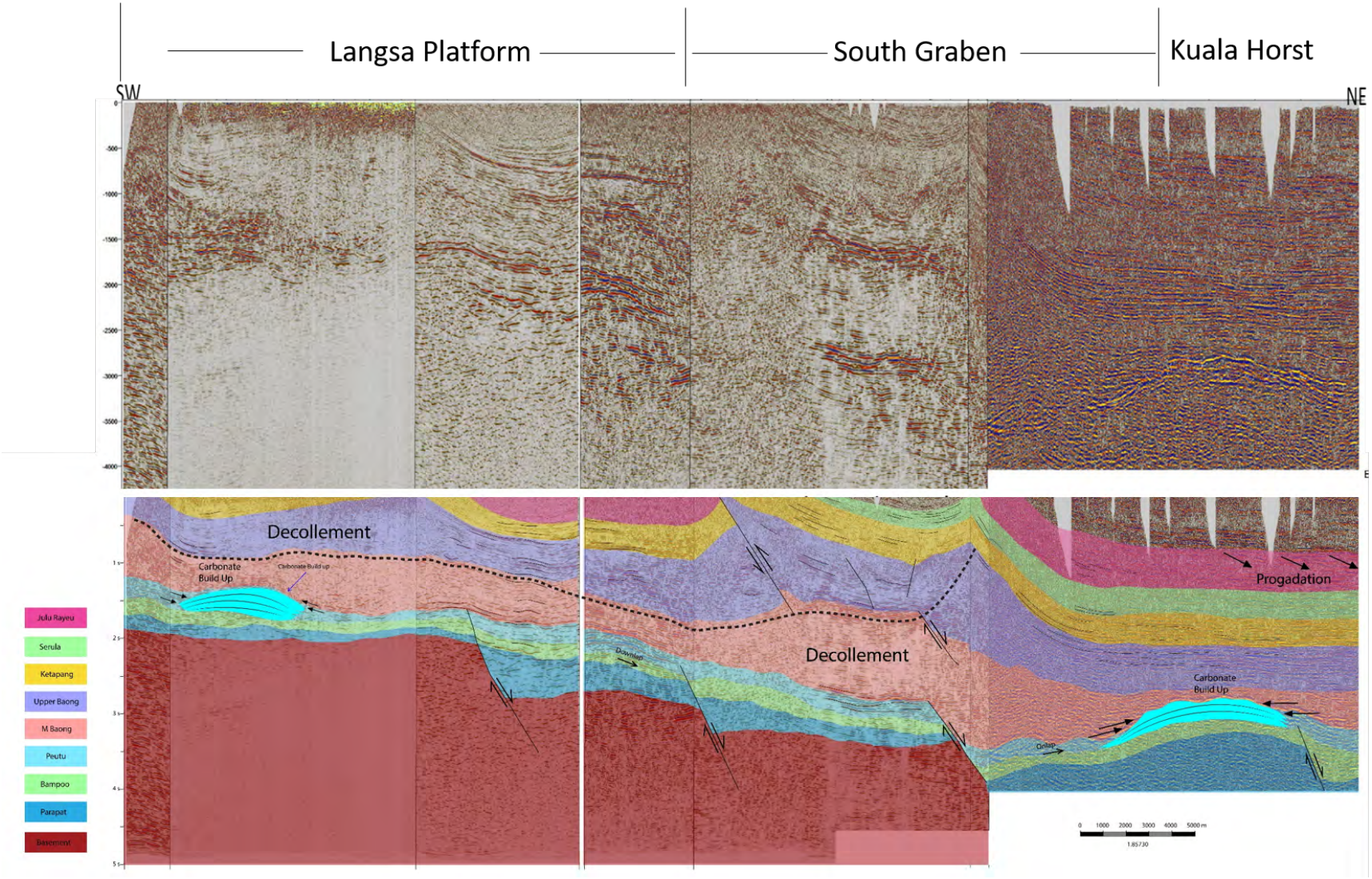

Figure 4-7 The composite line 5 in the onshore study area (line ree12_05_08_06_11_15_930sp, and 1002) shows the regional subsurface geology (location is in Figure 2-15). This line shows complex structures along the area in the upper part. Thrust/reverse faults were identified in the center. The lower part of the seismic shows half-grabens geometry on the horst. Two carbonates build-up was also identified in the horst's south and north seating .

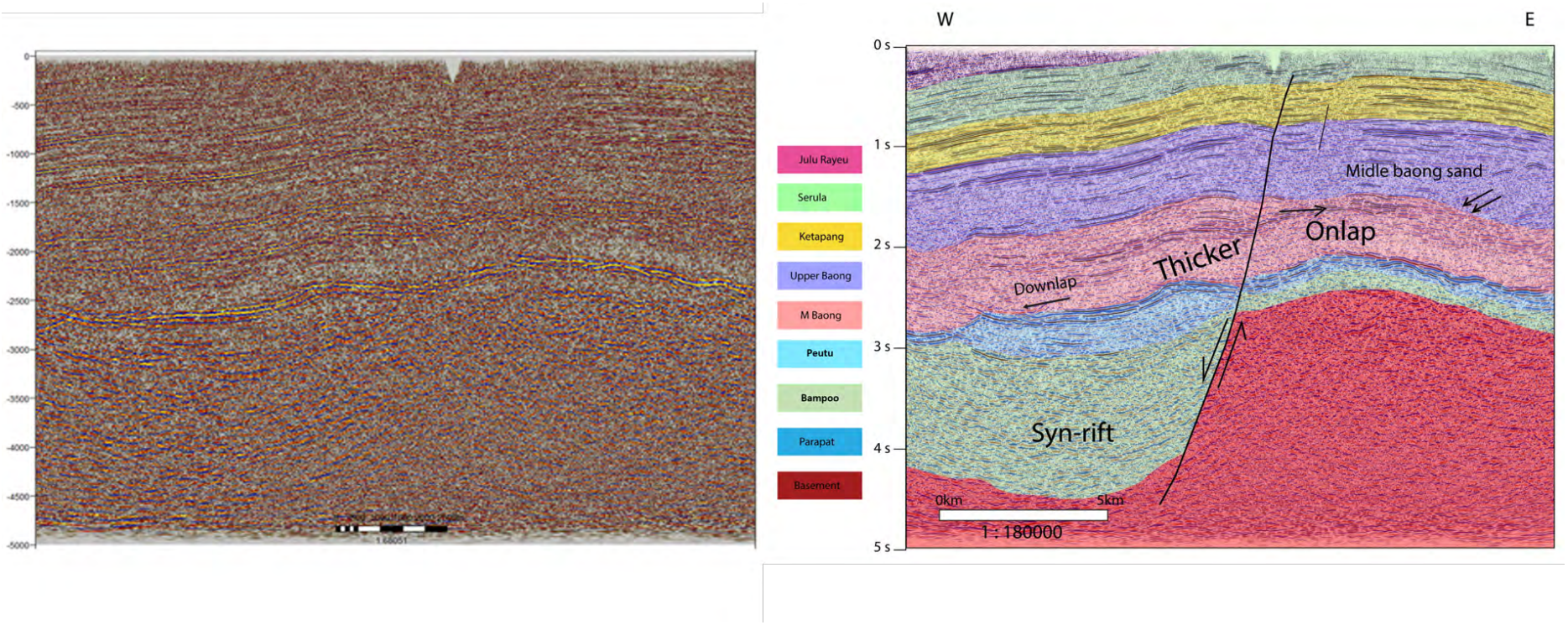

Figure 4-8 The interpretation of seismic line 818 shows an isolated and mounded thick sequence with a parallel configuration with good continuity and a high amplitude sequence that is thicker to the west of the fault than the east of the fault. The thickness is possibly related to the compaction creating the accommodation space, so the sediments fill thicker to the west. The compaction also creates the onlap features that perhaps erode the feature sequences. In addition, the compaction also perhaps caused the fault to rotate.

4.2 Carbonate/reef build-up

Carbonate build-up structure have been widely recognized by explorers and researchers in the North Sumatra Basin as the major contributor to oil and gas reservoirs. Arun and Alur Siwah are examples of gas fields that have produced multi-trillion cubic feet (tcf) of gas from carbonate reservoirs of the Peutu Formation (the location of Arun and Alur Siwah is shown in Figure 1-3).

The 2D data in this thesis shows the presence of other carbonate structure based on seismic characterization observed in composite lines 1 and 5 (Figures 4-3 and 4-7). Composite seismic line 1 shows two carbonate build-ups (Figures 4-3 and 4-9a). The first carbonate was drilled and is located close to the boundary between the horst and the graben. The build-up is 50 milliseconds (ms) thick in the center and 30 ms on the flanks, and it width is about 1.5 km. The second carbonate is approximately 5 km northeast of the first carbonate. This carbonate is situated in the graben or in the basinal area relative to the first carbonate location. This is not common in the North Sumatra Basin, as carbonates are usually present above the horst or on the slope. Therefore, it is proposed that this carbonate was possibly initially developed on the platform shelf or the platform ramp. However subsequent tectonic movement caused subsidence resulting in the more basinward position of the carbonate.

The composite line 5 shows two carbonate build-ups (Figures 4-7, and 4-9). The first is above the horst structure on the southwest edge of the area. This carbonate was possibly developed on the shelf platform. It is approximately 150 ms thick and 2.5 km wide (4-9b). The second carbonate formed above a narrow horst adjacent to a graben in the northeast of the area. This carbonate was possibly developed as a bank platform. This carbonate is the largest observed, approximately 300 ms thick and 6 km wide (4-9c).

The platform setting was the product of tectonic activities such as fault movements creating horst and graben structures. Based on the observations, the sequences from the Peutu and Middle Baong formations on-lapped to flanks of all the carbonate structures.

The platform setting could be associated with wave/wind energy. For example, the shelf carbonate could be associated with high energy conditions, while the carbonate in the basin may relate to low energy. The depositional energy can also be linked to the rock properties, because higher energy relates to larger grain size and larger grain size gives a better porosity.

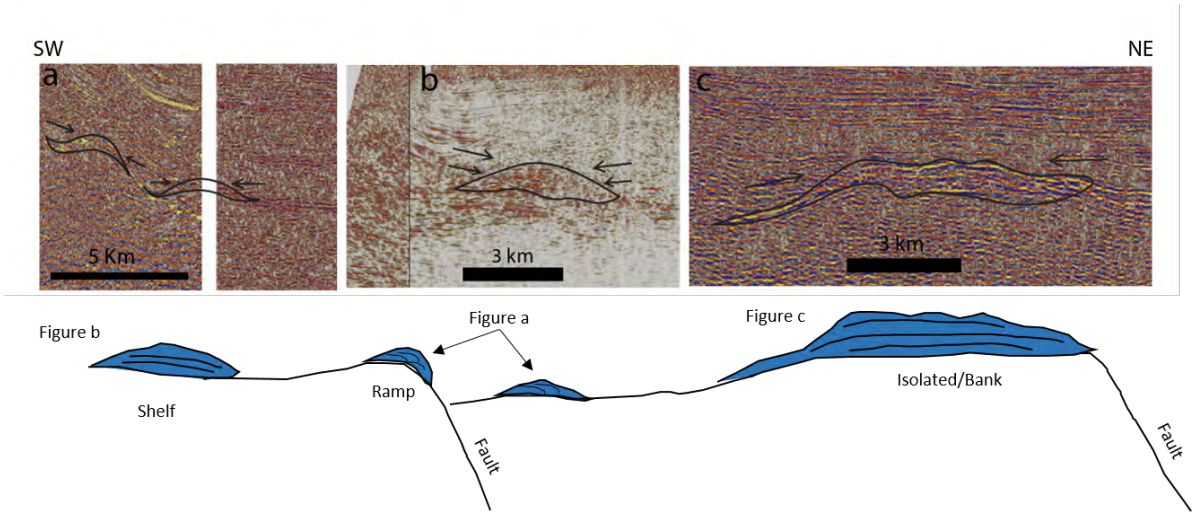

Figure 4-9a. The carbonate build-up in composite line 1, Figure 4-3. The first carbonate is located in the southwest, and the second in the northeast. b and c. The carbonate build-up is present in composite line 5, Figure 4-7, the first is in the southwest, and the second is in the northeast. d. In the illustration of the platform setting for carbonate development, the first carbonate from Figure (a) is developed on the shelf edges. In contrast, the second carbonate is situated in the basin. The carbonate in Figure (b) possibly formed on the shelf. Meanwhile, the carbonate in Figure (c) is developed on an isolated platform.

4.3 Structure of the Onshore North Sumatra Basin

4.3.1 Rift Structure

The rift structure is revealed by maps of the pre- and syn-rift horizons (top Basment, top Parapt and top Bampo, Figures 4-10 to 4-12). Large faults that can be correlated between seismic sections define the main components of the rift and show two dominant trends: northwest-southeast and north-south. Minor structures can be observed on individual sections.

A major NW-SE trending fault marks the boundary between the Langsa Platform and the North Depocentre. The offset of the basement across the fault is greater than one second TWTT implying a throw of at least 1.5 – 2 kms, depending on the seismic velocities in this part of the section, which are unknown. Smaller scale NW-SE trending faults define smaller less continuous grabens on the Langsa Platform. The eastern margin of the North Depocentre is separated from the Perlak Platform by a major N-S trending fault with a similar throw. Similarly oriented faults mark the boundary between the Perlak Platform and the East Depocentre, and between the East Depocentre and the Kuala Horst. The faults that bound the Southeast Depocentre also trend NW-SE, similar to the Langsa Platform.

None of the rift faults are exposed at the surface because of burial by younger post-rift sediments and hence are not visible on the SRTM map. The Kutacane Fault lies to the south and west of the area covered by seismic data, so it is not clear if it influences the structure of the rift. However, it is parallel to the north-south trending faults interpreted from seismic data to the east,

which suggests that there could be some basement fabrics that influence faults with this orientation.

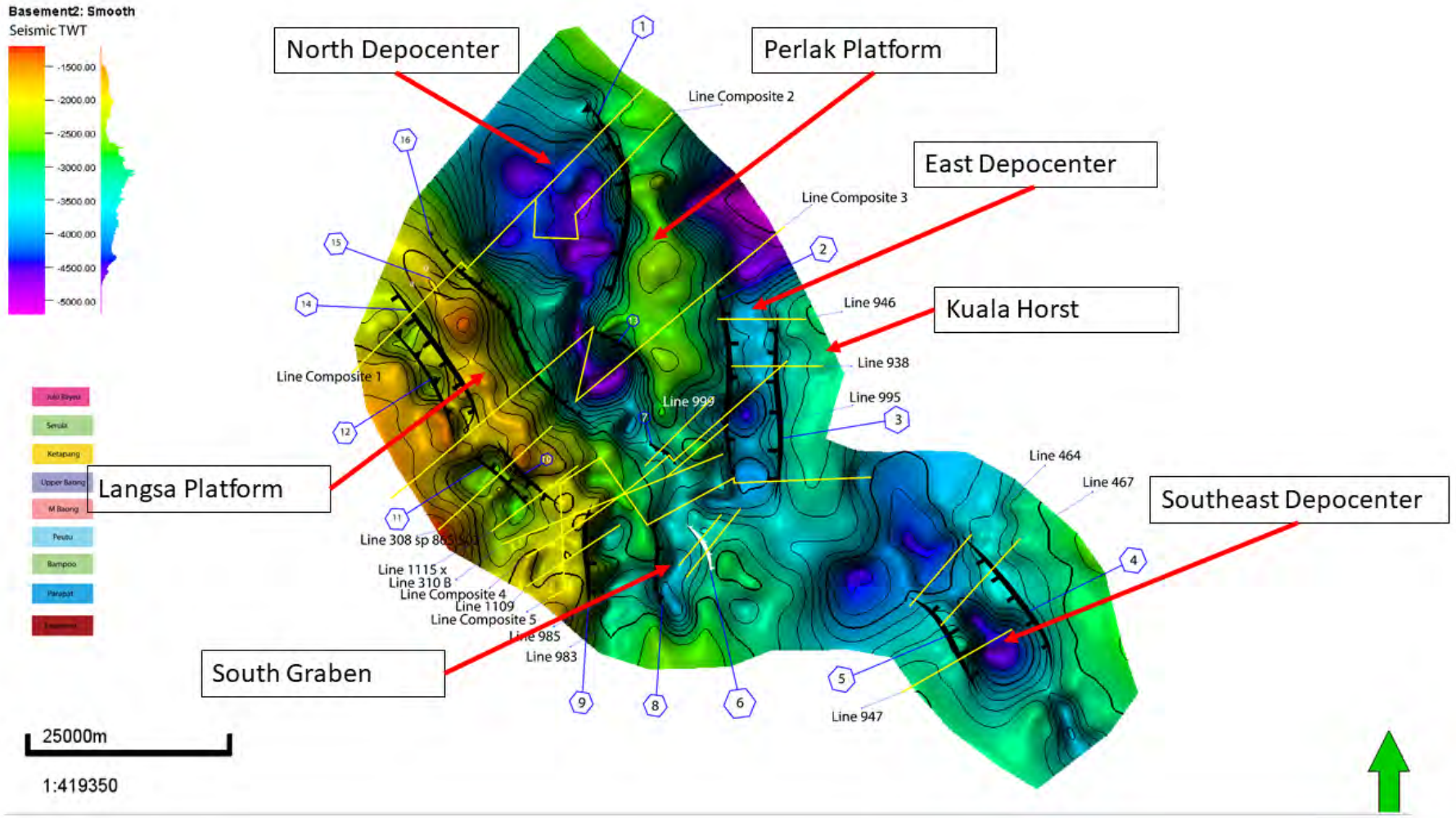

Figure 4-10 Time Structure map of Basement. This Figure is intended to show faults (1 to 16) observed in the onshore study area. In the middle is the basement map overlain by all identified faults. A series of horst-grabens structures trending north-south and northwest-southwest were identified. Previous pages show some faults in composite seismic lines (regional lines).

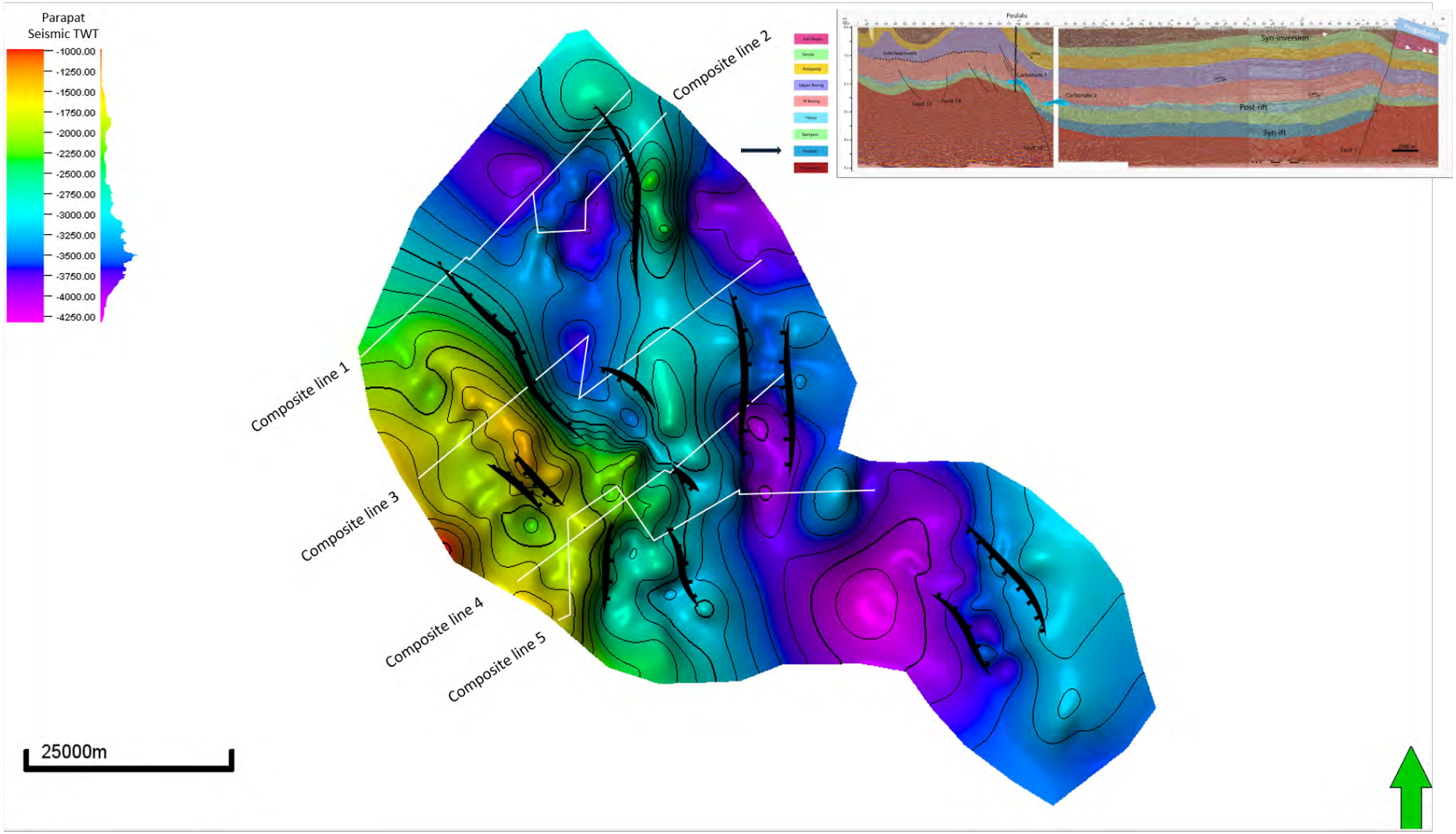

Figure 4-11 Time Structure map of Parapat fm/ Early Oligocene. The seismic profile is Composite line 2.

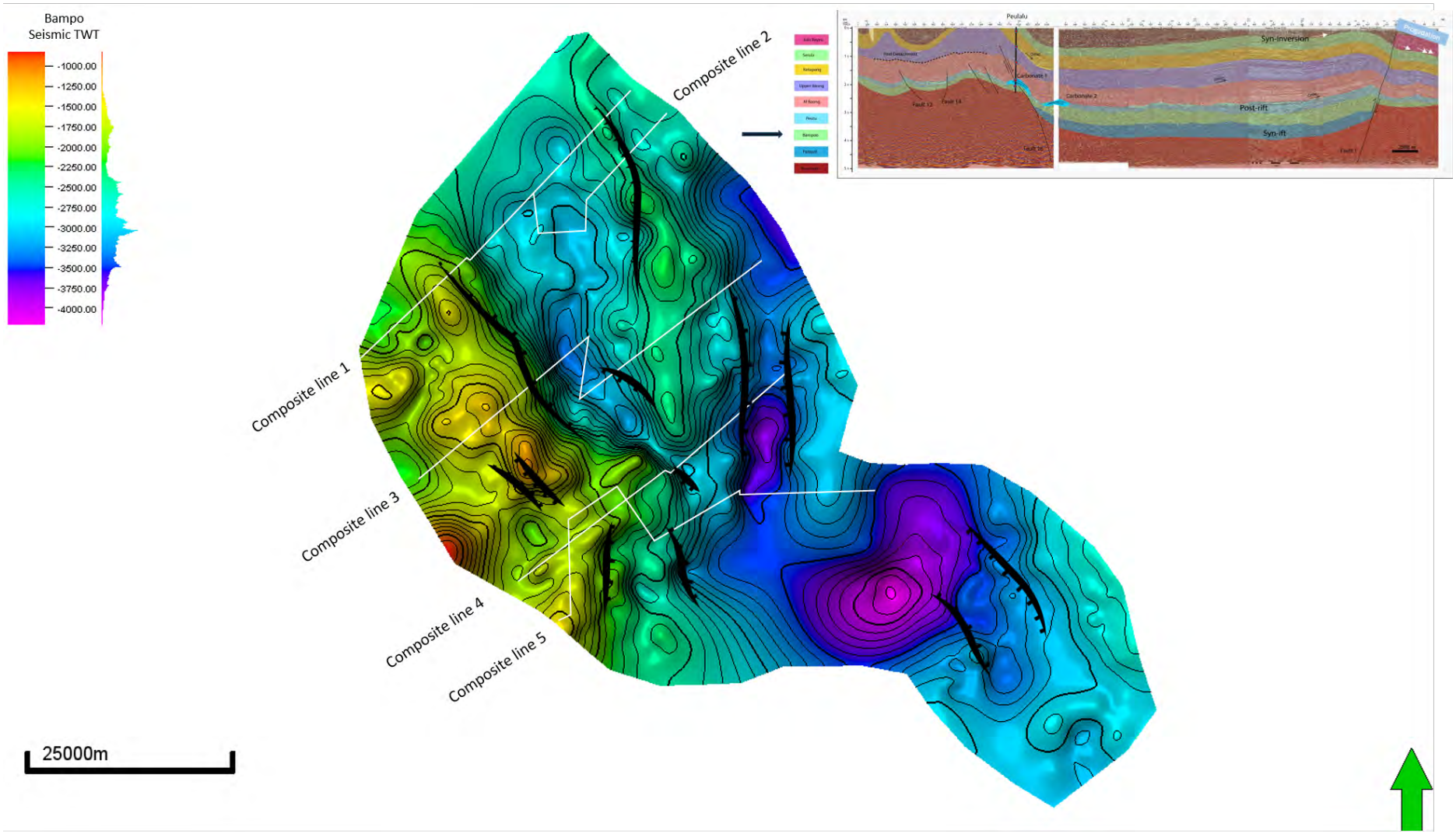

Figure 4-12Time Structure map of Bampo fm/ Late Oligocene. The seismic profile is Composite line 2.

4.3.2 Folds and Inverted faults

The Baong (Middle and upper Baong), Ketapang, Serula and Julu Rayeu formations are all deformed by folding (Figures 13 to 17). The folds occur at the surface and are also very well imaged by SRTM maps (Figure 4-18). The folds can be divided into two distinct zones. In the southwest, where they form the Barisan Foothills, the folds trend northwest-southeast, are relatively closely spaced, and the Keutapang and older formations form the cores of the anticlines. To the northeast, close to the coastline, the orientation of the folds is NNW-SSE. Formations younger than Keutapang, such as the Seurula and Julu Rayeu formations, form the cores of the anticlines. The folds in this region have much less topographic relief, and are less common that in the Barisan Foothills.

The 2D seismic sections also show a difference in structure between these two areas. The northwest-southeast orientated folds in the Barisan Foothills are symmetrical and are located above the basement high formed by the Langsa Platform (Figure 4-19 and 4-20). These folds are not associated with inverted extensional faults, but instead they appear to be detached from the flat lying Peutu, Bampo, Parapat and top Basement horizons beneath them. This detachment is located within the Baong Formation and is likely due to the presence of ductile material, such as shale as the formation is recognized to have very thick shales (De Smet, 2007). It would be interesting to know if there is evidence of duplication or complex folding within the shaley parts that might support diapirism or other processes related to those detachment folds (Buntoro et al., 2022; Lanin & Sone, 2022) (Figure 4-7). Therefore, it is proposed that the folds in the southwest are related to the thrust fault parallel to bedding within the Baong Formation and are directly related to the compression associated with the formation of the Barisan Mountains. Similar styles of fold are located in the east of the study area (Figure 4-19, Composite 3, 4, and 5, respectively), but here they are oriented north-south and there is a possibility of a thrust fault propagating trough younger formations (Middle Baong) with a low-angle dip (Figure 4-19, dashed line in composite 5 to the northeast).

The lower relief folds in the northeast of the area are related to the reverse fault formed due to the inversion of the pre-existing normal fault that separated the North Depocenter from the Perlak Platform (Figure 4-10, composite lines 1 and 2). This fold has steep slopes in the forelimb and gentle slopes in the back limb. This fold is oriented northwest-southeast and dips to the southwest. The folds occurred in all rock formations, including the syn-rift package and is clearly a result of the propagation of the extensional fault into the post-rift packages. It is interesting to note that none of the other major extensional faults show evidence of inversion.

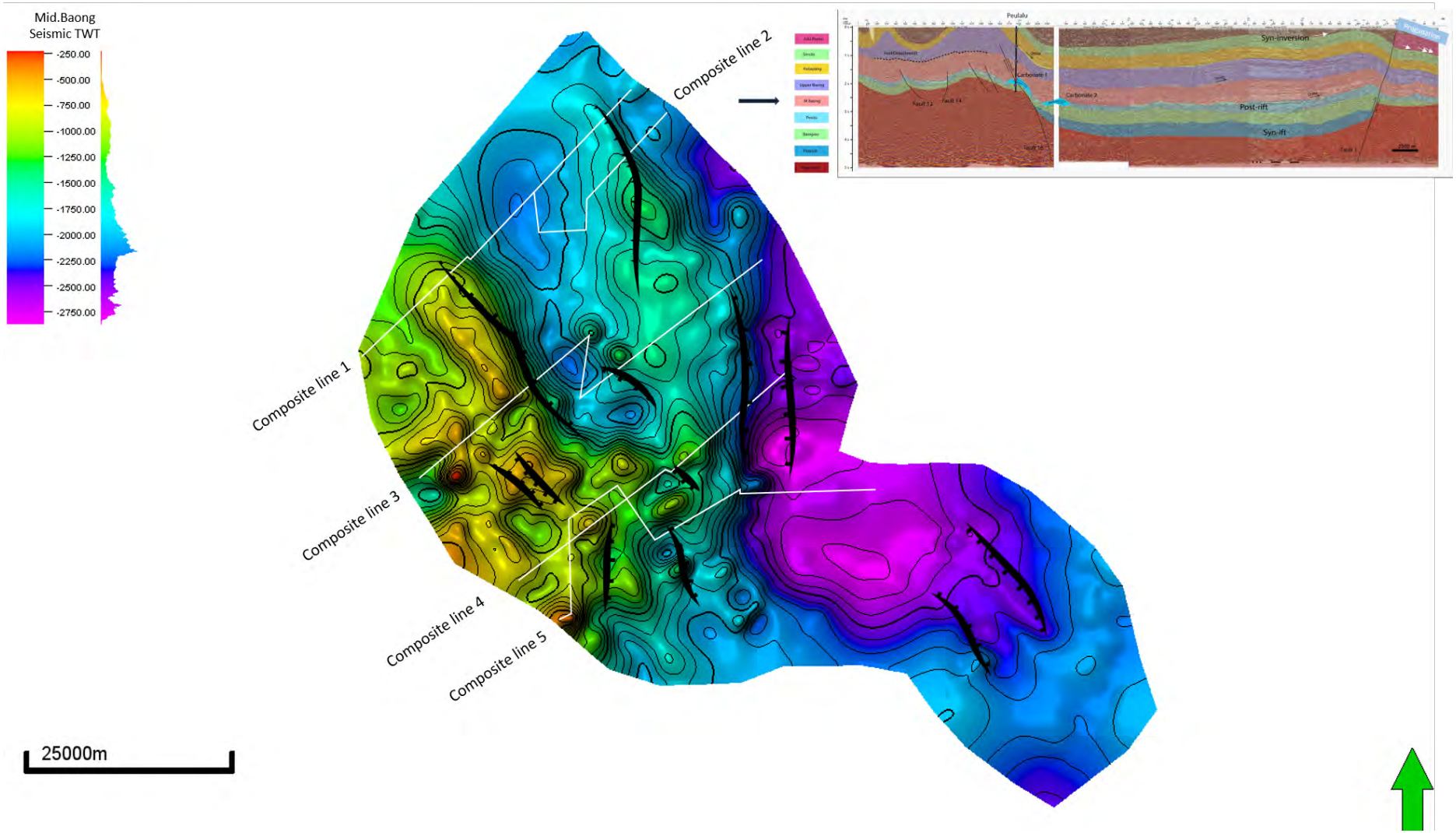

Figure 4-13 Time Structure map of middle Baong fm/ Middle Miocene. The seismic profile is Composite line 2.

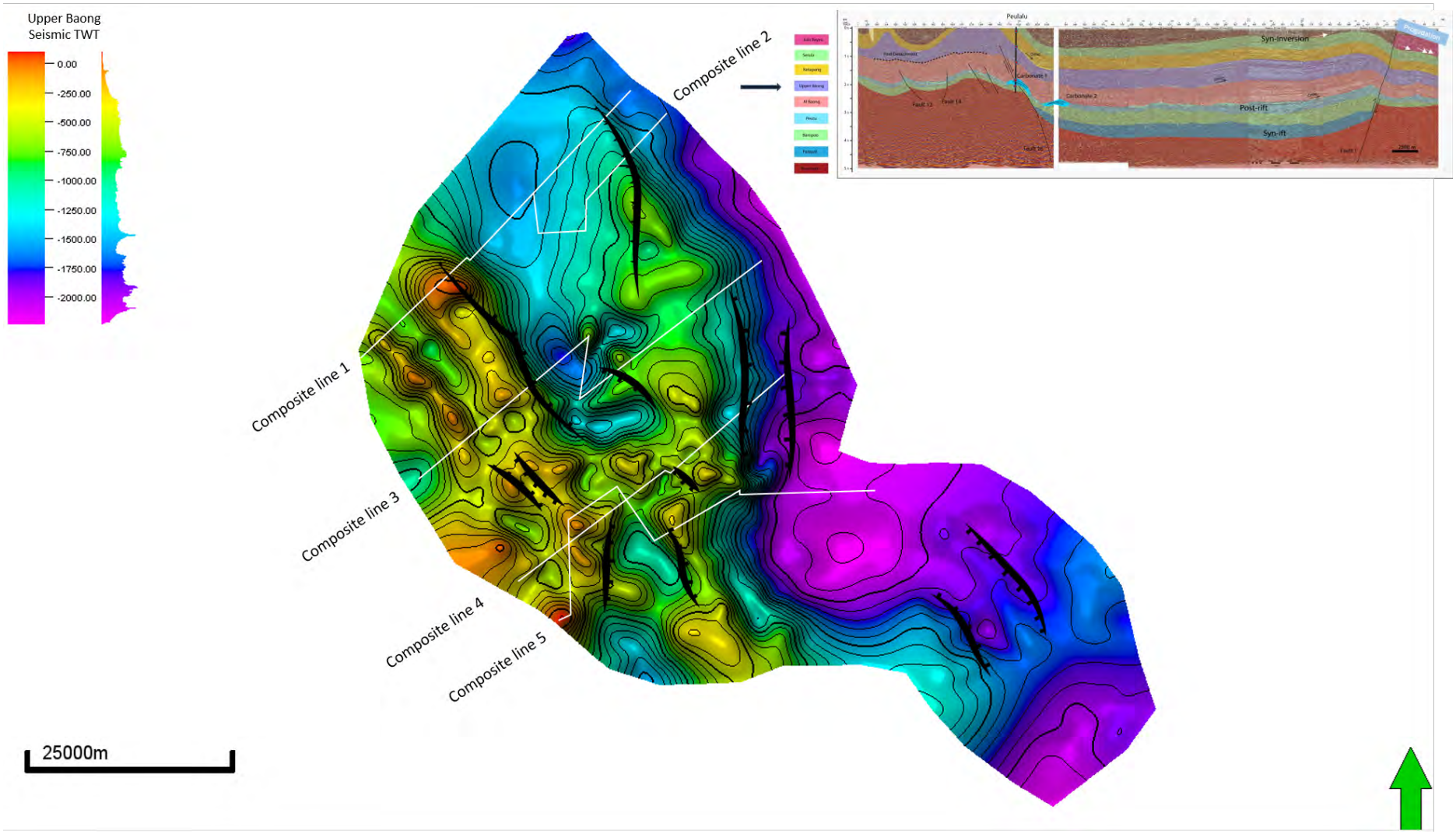

Figure 4-14Time Structure map of upper Baong fm/ Middle Miocene. The seismic profile is Composite line 2.

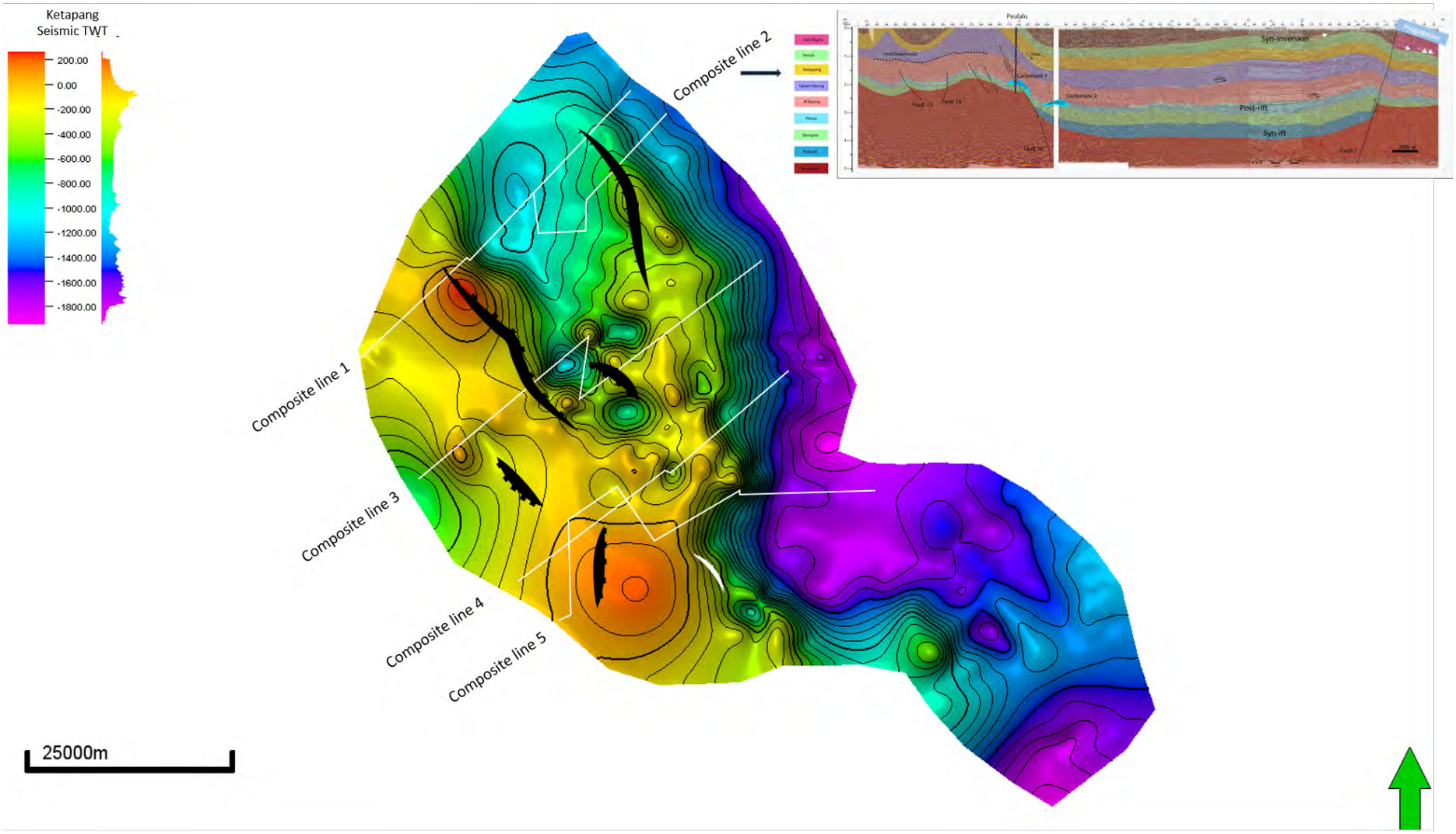

Figure 4-15 Time Structure map of Ketapang fm/ Late Miocene. The seismic profile is Composite line 2.

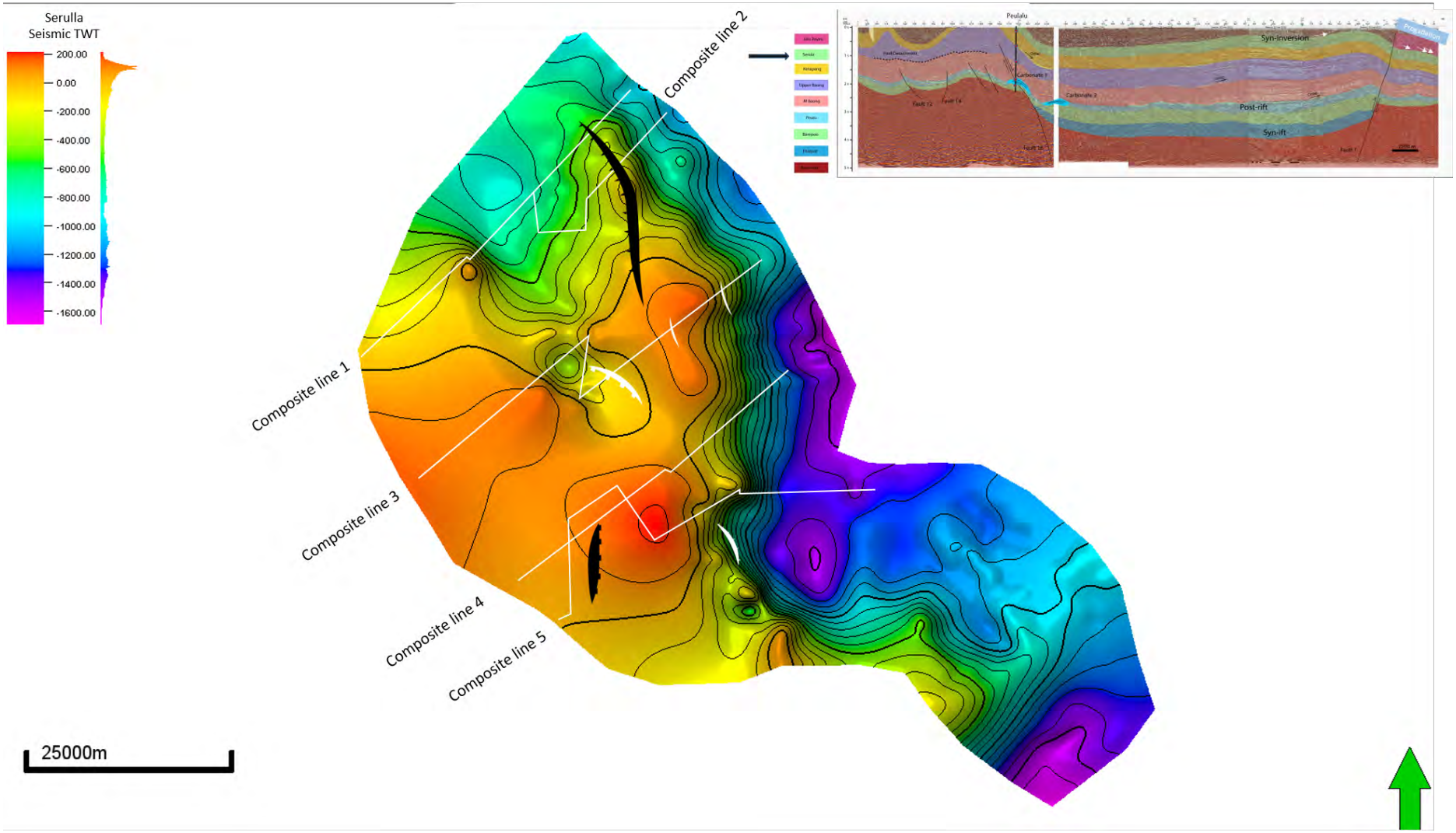

Figure 4-16 Time Structure map of Seurula fm/ Pliocene. The seismic profile is Composite line 2

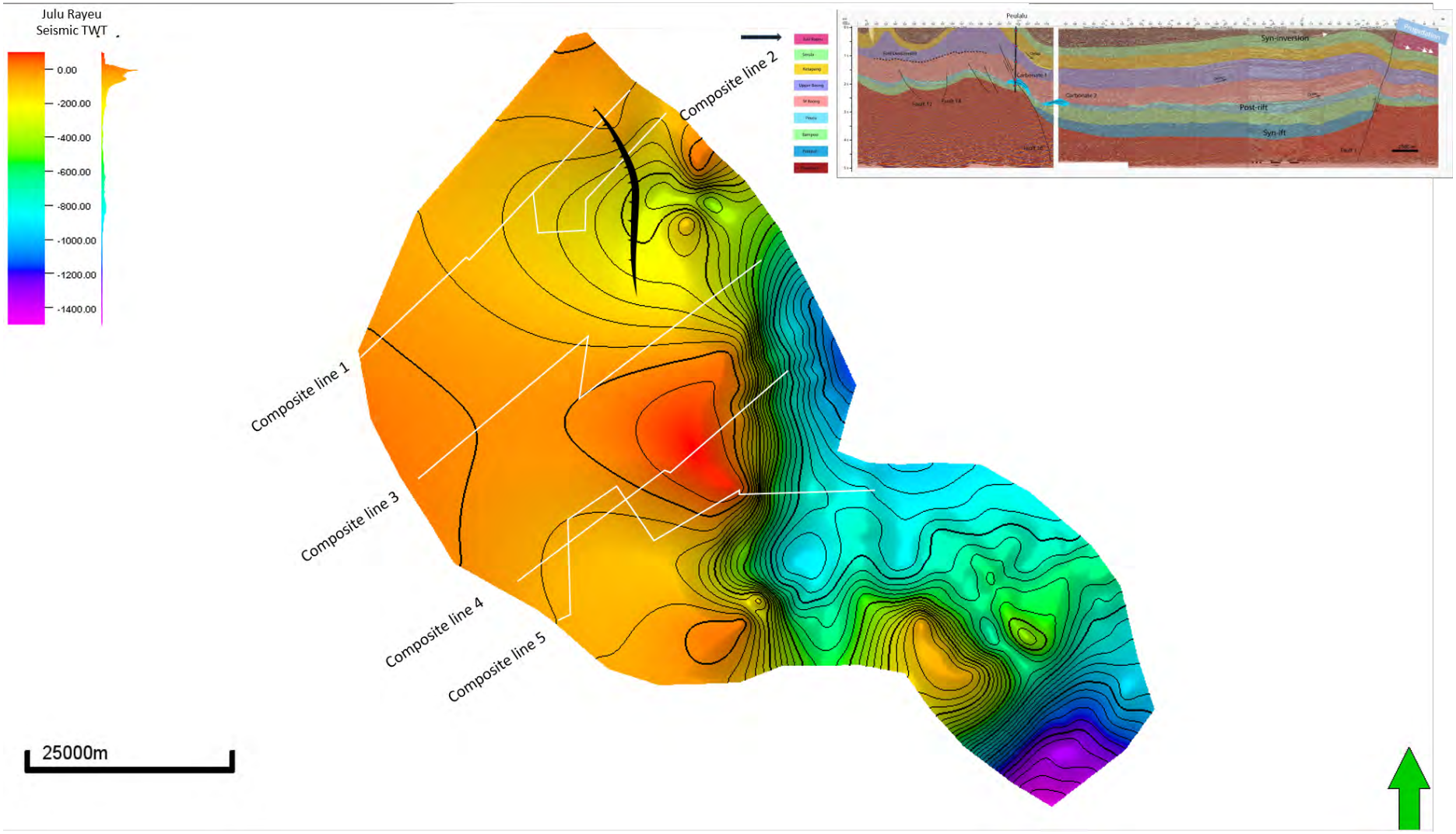

Figure 4-17 Time Structure map of Julu Rayeu fm/late Pliocene. The seismic profile is Composite line 2

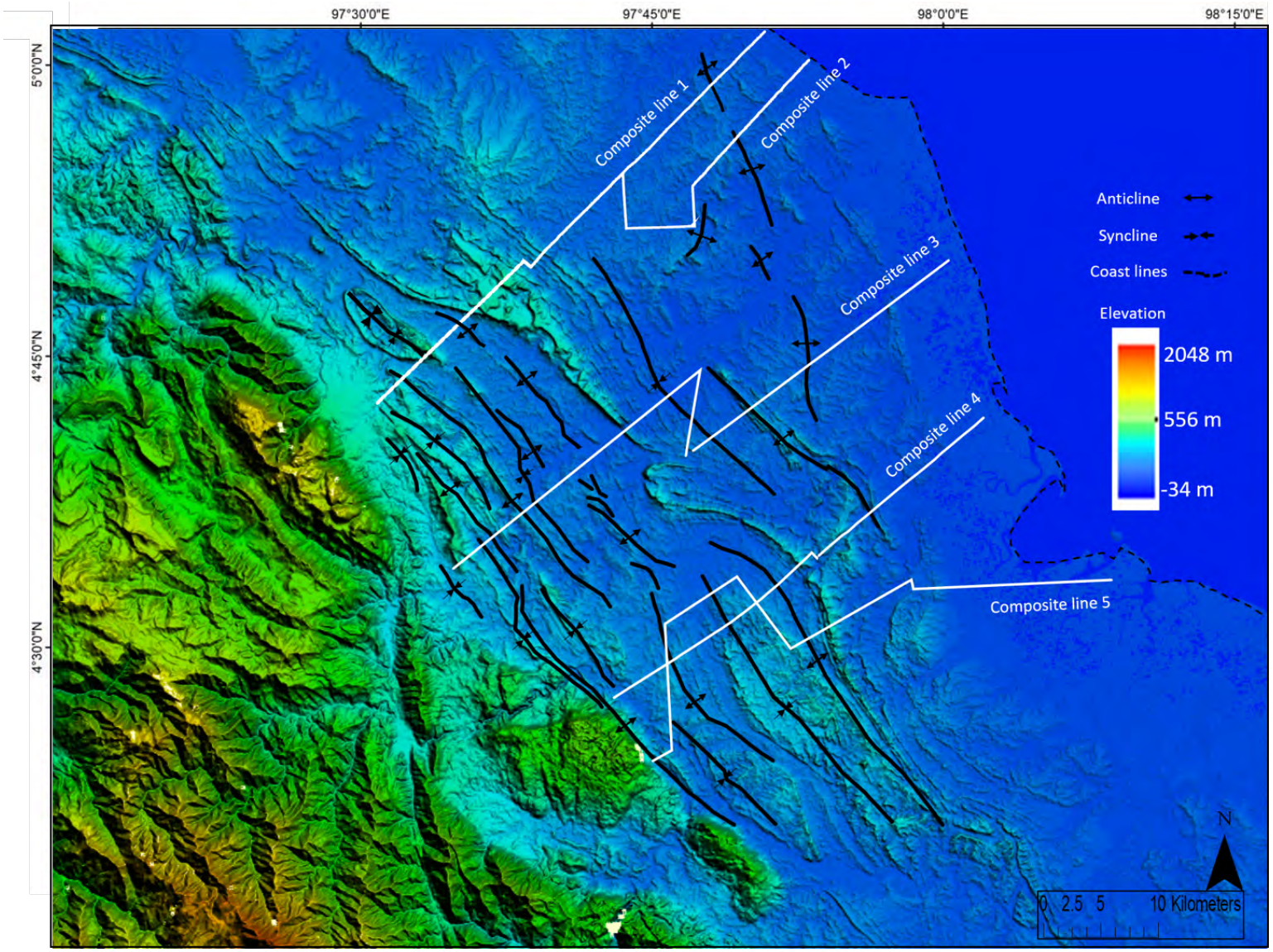

Figure 4-18 SRTM map showing fold interpretation

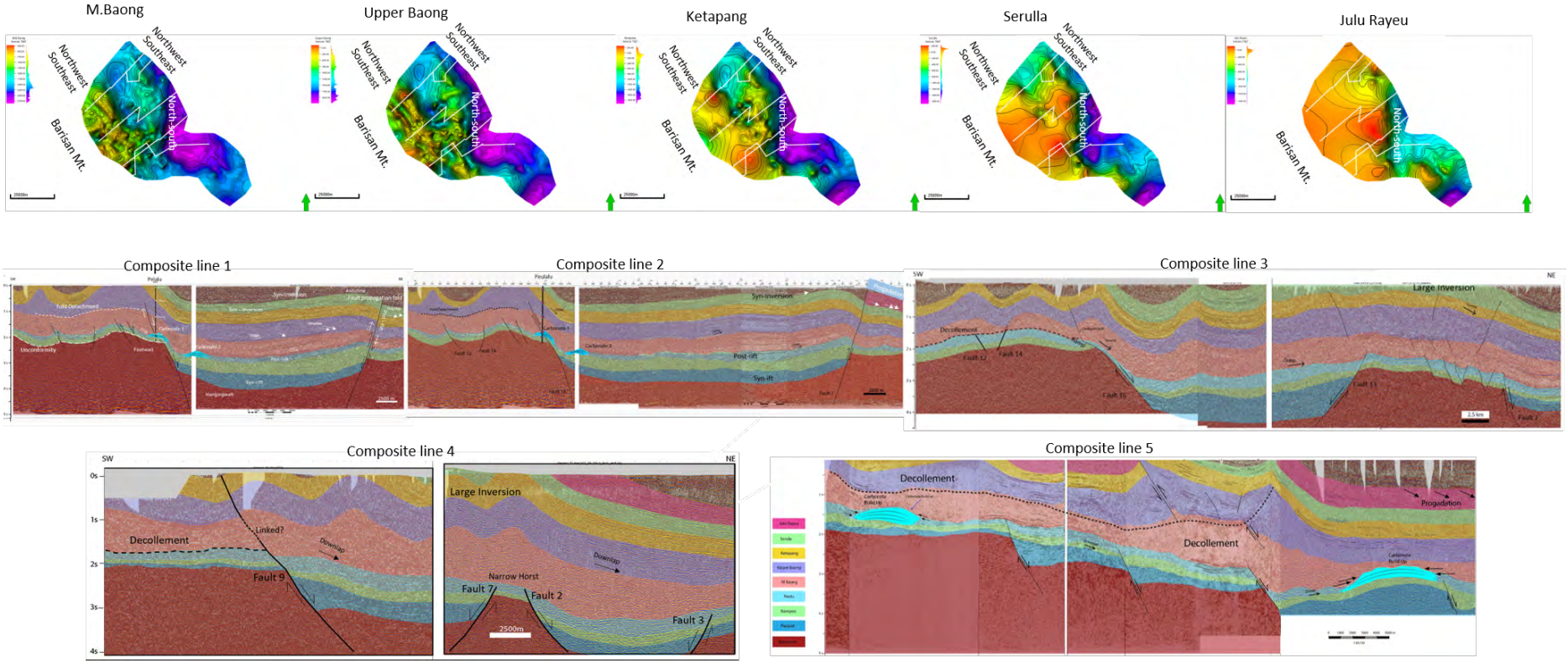

Figure 4-19 The Figure is intended to show the fold structures in the study area. All composite lines show that the fold structures (inversion) toward the Barisan hills possibly relate to the thrust fault detachment in the middle Baong shale formation. The structures are oriented northwest-southeast and are shown by time structural maps. Meanwhile, to the northeast, there are two trends of fold structure. The first is northwest-southeast, and the second is north-south. The first trend is related to the reverse fault (shown by composites 1 and 2), and the second is associated with the fold detachment (shown by composites 3, 4, and 5, respectively).

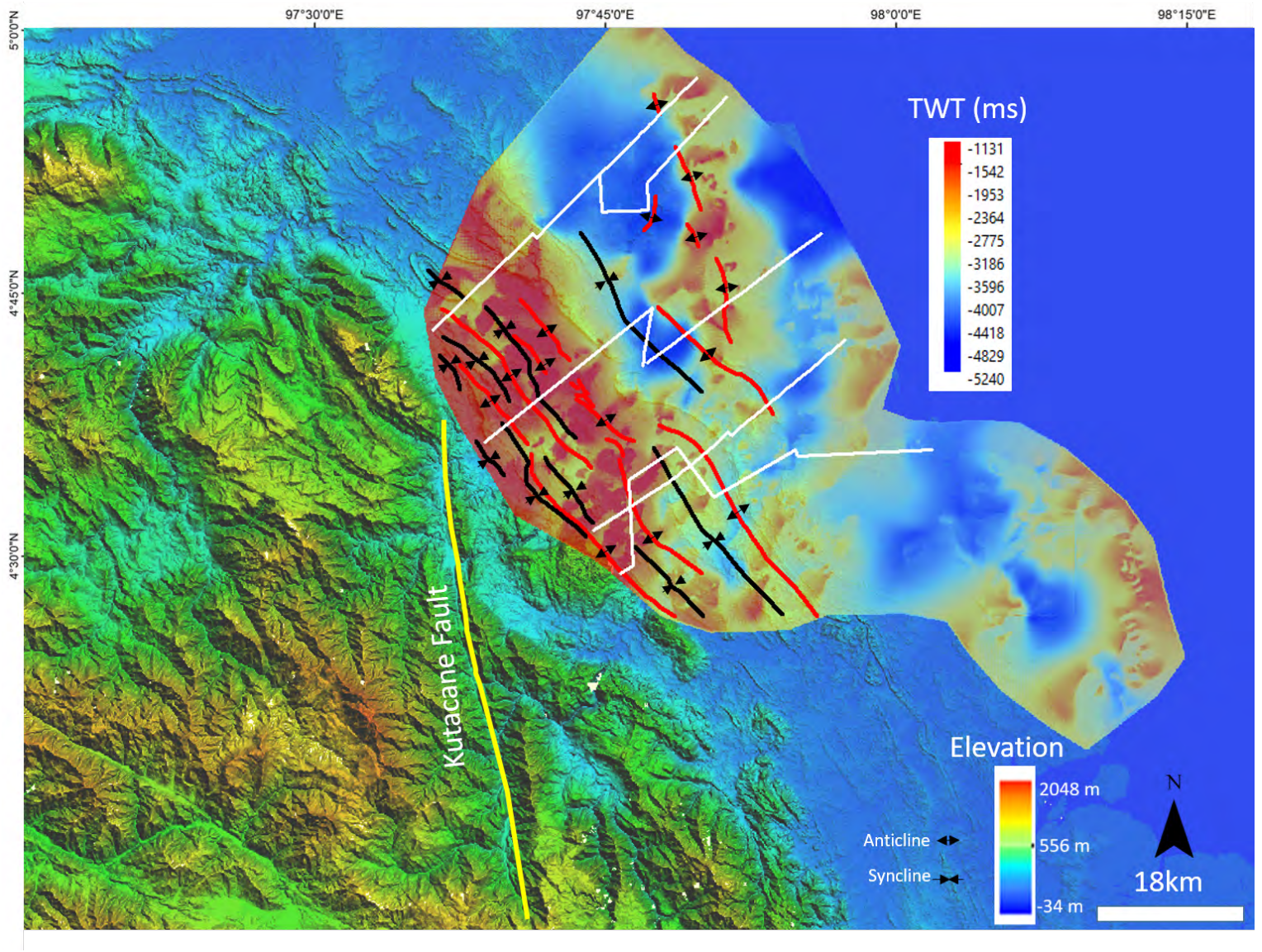

Figure 4-20 the figure showing basement horizon (TWT) superimposed on SRTM map.

4.4 Onshore Basin Evolution

The North Sumatra Basin has experienced several tectonic episodes that changed from rifting to post-rift sagging and inversion. Previous sub-chapters have explained the styles of structures, including the timing of the development of the structures. Although it is possible to recognise syn-rift deposits syn-inversion and syn-folding strata are more difficult to define. For example, sequences that onlap onto folds or the thinning sequence deposited above the folds were not well imaged. The other possibility is that the syn-inversion sequences may have been exposed to the surface and eroded. It has been shown in previous sub-chapters that some of the post-rift sedimentary sequences (including the syn-folding) have been folded and are exposed at the surface.

Therefore, another alternative to demonstrate the basin evolution is to create structural geology reconstruction. Each of the formations, including the structures, was flattened to visualise the original section at each stage of formation. Composite line 1 was chosen for the 2D reconstruction from Parapat/ Bampo Oligocene until the Middle Baong. However, the reconstruction could not be done for the younger formations because those formations outcrop to the surface. Alternatively, line 104 with a Southwest-Northwest direction (Figure 3-1, the location of the line is shown in Figure 2-5) was used these younger formations (Upper Baong until younger than Seurula).

The isochron maps were also incorporated to observe the paleogeography of onshore NSB. The highest isochron values correlate to the thickness associated with the basinal/low areas where the sediments were deposited. The lower values correspond to relative highs.

The earthquake focal mechanism was also input to see the deformation style associated with the strike, dip, and fault types. However, only some earthquakes in the study area have the focal mechanism data.

4.4.1 Pre-Rift

North Sumatra was assumed to be a flat, stable area, as shown by the flat basement (Figure 4-21a)

4.4.2 Rift (Early and Late Oligocene)

The rifting and basin formation, caused by extensional tectonics, began in the early Oligocene (ca 34 Ma) and was associated with the horst and graben structures. A series of horst and grabens were observed in the onshore study area. The trends of the rift faults are NNW-SSE and north-south (Figure 4-10 to 4-12).

The Parapat Formation filled the basin as the first syn-rift sequence during the Oligocene (Figure 4-21a, 4-21b, and 4-21c). The syn-depositional faults control the different thicknesses of the

Parapat in graben and on the horsts. In the late Oligocene (28-23 ma), rifting continued during the deposition of the Bampo Formation (Figures 4-21d and 4-21e). Several minor faults occurred, cutting the basement in the southwest platform (Langsa platform). During this period, the Parapat Formation in this area was probably eroded on some of the horsts.

The isochron map of the Parapat-Basement shows the greatest thickness located in depocentres to the north and the south. Meanwhile, the minimum values are in the west and east, corresponding to basement highs (Figure 4-22) which may have acted as a source of sediments to the lower grabens in the north and south.

Furthermore, the isochron map of the Bampo-Parapat formation shows the highest thickness in the north (Figure 4-23). Meanwhile, the rest of the area is filled with thinner sequences.

4.4.3 Post Rift (Early Miocene)

The beginning of a post-rift stage was shown by the deposition of the Peutu Formation in the early Miocene (23-16Ma) (Figure 4-21f). The Peutu Formation may be deposited unconformably overlain the Bampo Formation, especially on the horst. However, there is no evidence of the erosional truncation at the boundary between those formations on the seismic images.

During this period, almost no deformation occurred, shown by the absence of faults. The Peutu-Bampo isochron map also shows almost uniform thickness in all areas (Figure 4-24). This suggests a tectonically quiescent period.

4.4.4 Post Rift-Sagging (Middle Miocene)

During this period (11 until 15 Ma), the basin experiences a deepening due to the thick accumulation of sediments (Figure 4-21g). The basin changed from quiescent to a sag phase. The top Peutu shows the change, and Bampo formation shows a sagging shape (Figure 4-21g).

The Middle Baong Formation onlapped onto the carbonate platforms that developed during the early to middle Miocene (Figure 4-21g). The thickness of the Middle Baong Formation suggests that the Basin experienced transgression.

The Basin continued to subside and deepen during deposition of the Upper Baong Formation (Figure 4-21h). No structures were observed during this period.

The isochron maps of the Middle Baong-Peutu and the Upper Baong-Middle Baong show uniform thicknesses all over the area, except in the southeast and southwest (Figures 4-25, 4-26).

4.4.5 Late Miocene

Deposition of the Keutapang Formation in the onshore North Sumatra Basin shows a continuation of the subsidence during the late Miocene (ca 11 Ma) (Figure 4-21i). The structural reconstruction of this formation shows no significant deformation and the thickness is uniform in this section (Figure 4-27). The isochron maps of Keutapang-upper Baong shows variations in thickness (Figure 4-27,) due to exposure to the surface and erosion. However, there is no evidence that the fold structures formed during Keutapang deposition.

4.4.6 Pliocene

The Seurula Formation was deposited during the early Pliocene (5Ma) and marked the initiation of compresion in the North Sumatra Basin. The reconstruction shows that the fold started to develop in the south and in the north (Figure 4-21j). The basement bounding fault was also reactivated and started to invert the older rock formations.

The isochron map shows the thicker sediments in the northwest and northern areas (Figure 4-28). This is probably related to sediment supply from the south and is possibly associated with the initiation of Barisan uplift.

4.4.7 Late Pliocene

The reconstruction shows that most compresion occurred during the late Pliocene during deposition of the Julu Rayeu Formation (4-21k). This is indicated by the Julu Rayeu Formation onlapping and thinning above the folded Seurula Formation and thickening away from the fold (Figure 4-4). The basement bounding fault propagated from older rock formations and inverted those formations. The fault style changed from a normal to a reverse fault. The stress regime change is possibly related compression associated with development of the Barisan Mountains.

The isochron map shows that half of the area from the southwest to the centre contain very little sediment. The thinning is associated with the exposure to the surface and erosion. The thinning trend reflects the recent Barisan Mountains trend. Meanwhile, the thicker sediment is located east and north (Figure 4-29).

Figure 4-21a. Reconstruction of southwest-northeast Seismic composite line 1. The cartoon shows that the basement was assumed to be flat during pre-Paleogene.

Figure 4-21 b. The cartoon shows the Parapat fm deposited in early Oligocene time.

Figure 4-21 c. The cartoon shows the rifting formed the horst and graben structure while the Parapat fm filled the basin

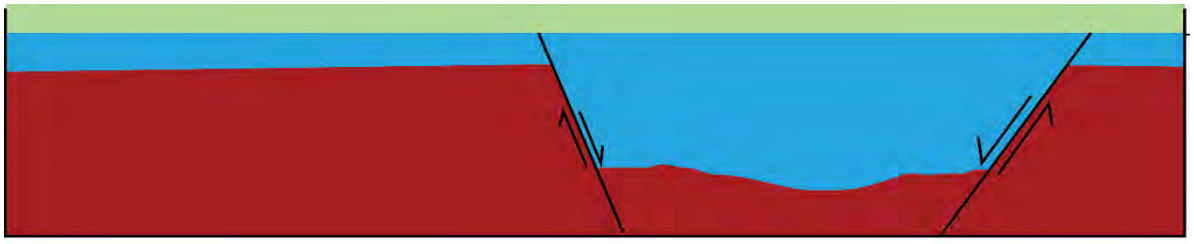

Figure 4-21 d. The Bampo fm started to deposit overlain the Parapat fm during the late Oligocene.

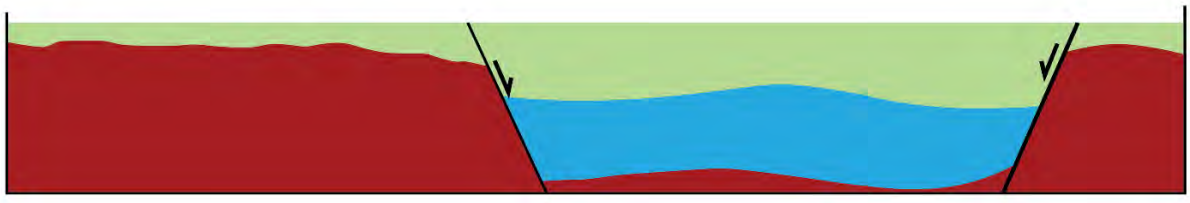

Figure 4-21 e. The rifting continued while the Bampo fm deposited during the late Oligocene. During this period, the Parapat fm was possibly eroded.

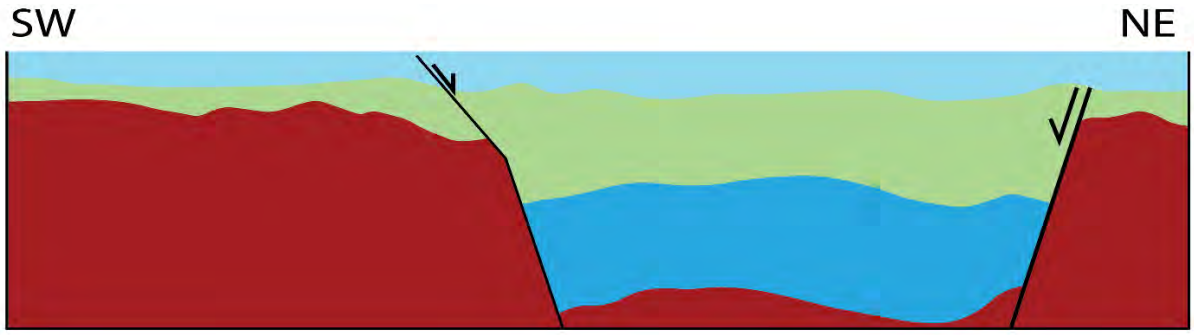

Figure 4-21 f. The rifting ceased, marked by the fault-basement bounding at the top of the Bampo formation. The Peutu fm marked the post-rift sediments in the Early Miocene, which overlain the Bampo fm. Almost no structures occurred during this period.

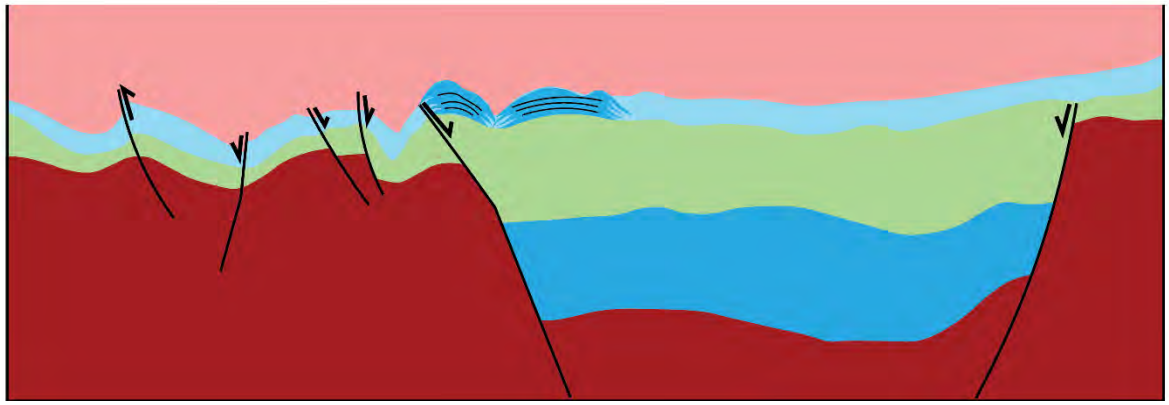

Figure 4-21 g. The reefs/carbonates build-ups during the early Miocene were shown by the Mid Baong fm on-laps. The sagging was also initiated during the deposition of Mid Baong fm.

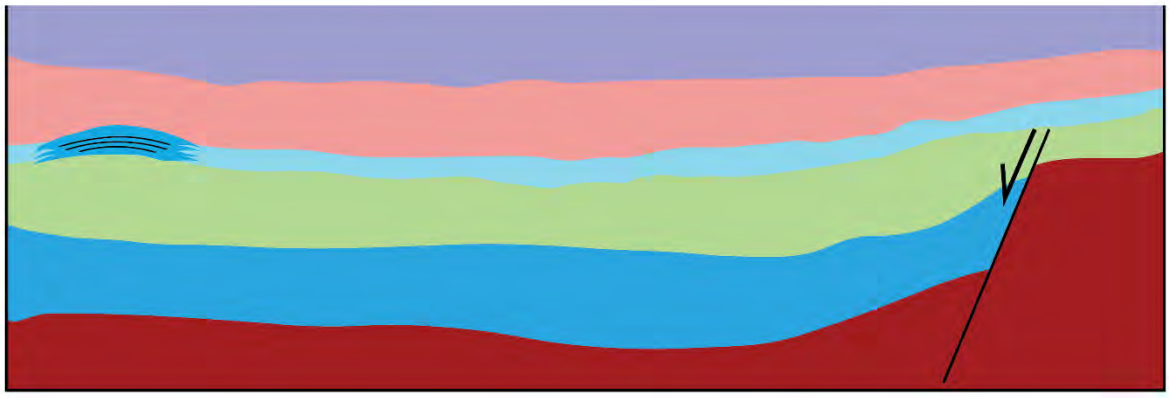

Figure 4-21 h. The Subsidence continued during the deposition of Upper Baong fm during the middle Miocene.

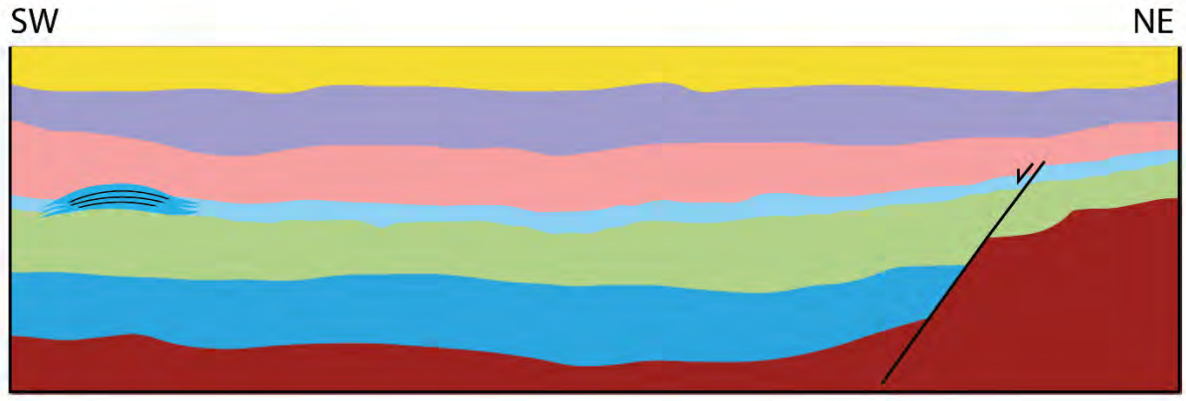

Figure 4-21 i. The Sagging continued while the deposition of Keutapang fm was during the late Miocene.

Figure 4-21 j. Inversion started during the deposition of Seurula fm during the Pliocene.

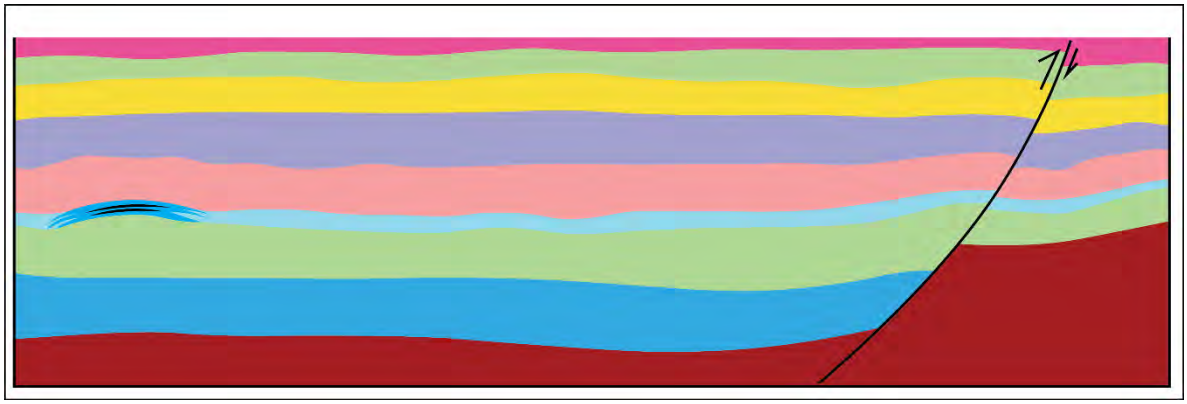

Figure 4-21 k. The inversion continued during the deposition of Julu Rayeu fm during the late Pliocene.

Figure 4-21 l. The Recent North Sumatra Basin based on line 104.

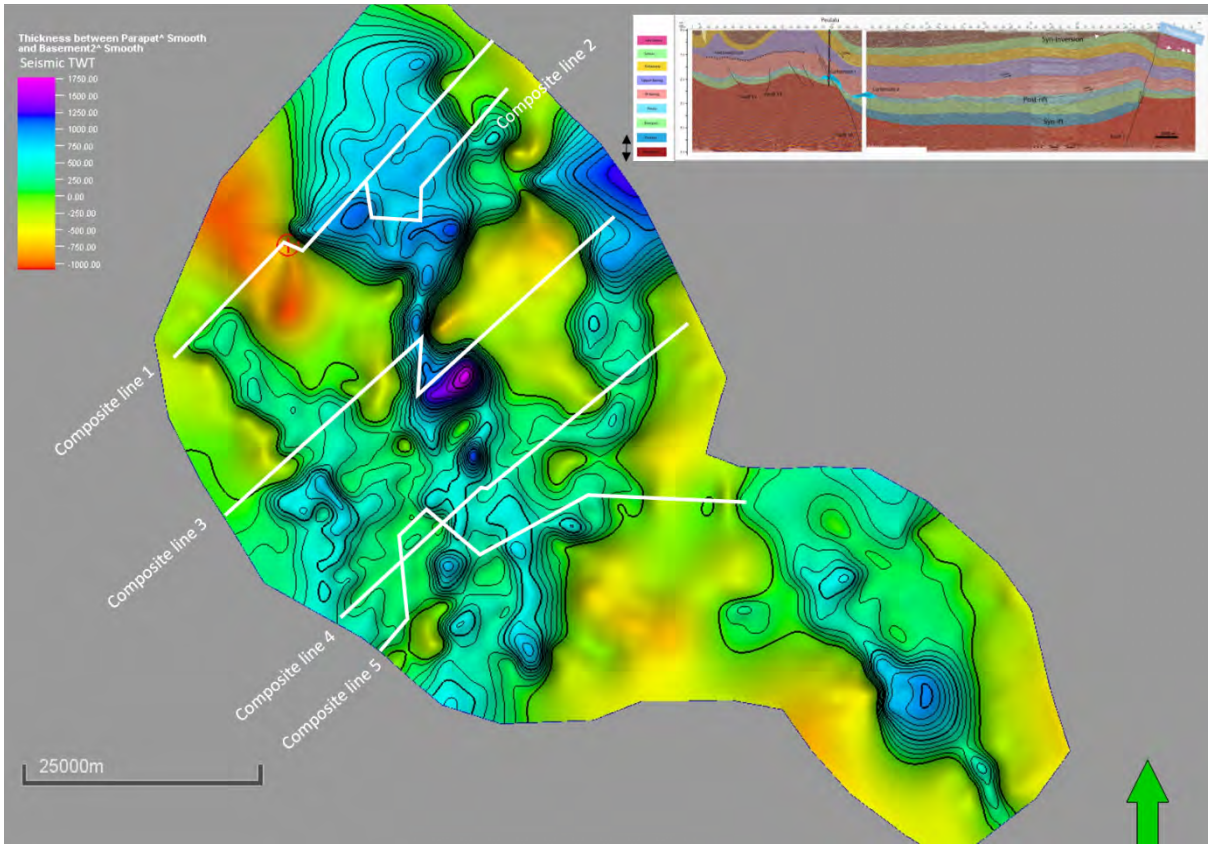

Figure 4-22 Isochron map showing the thickness of Parapat-Basement formation The pink colour shows zero thickness meaning the area was not deposited or eroded. Meanwhile, blue shows the highest thickness. The upper right is seismic composite line 2

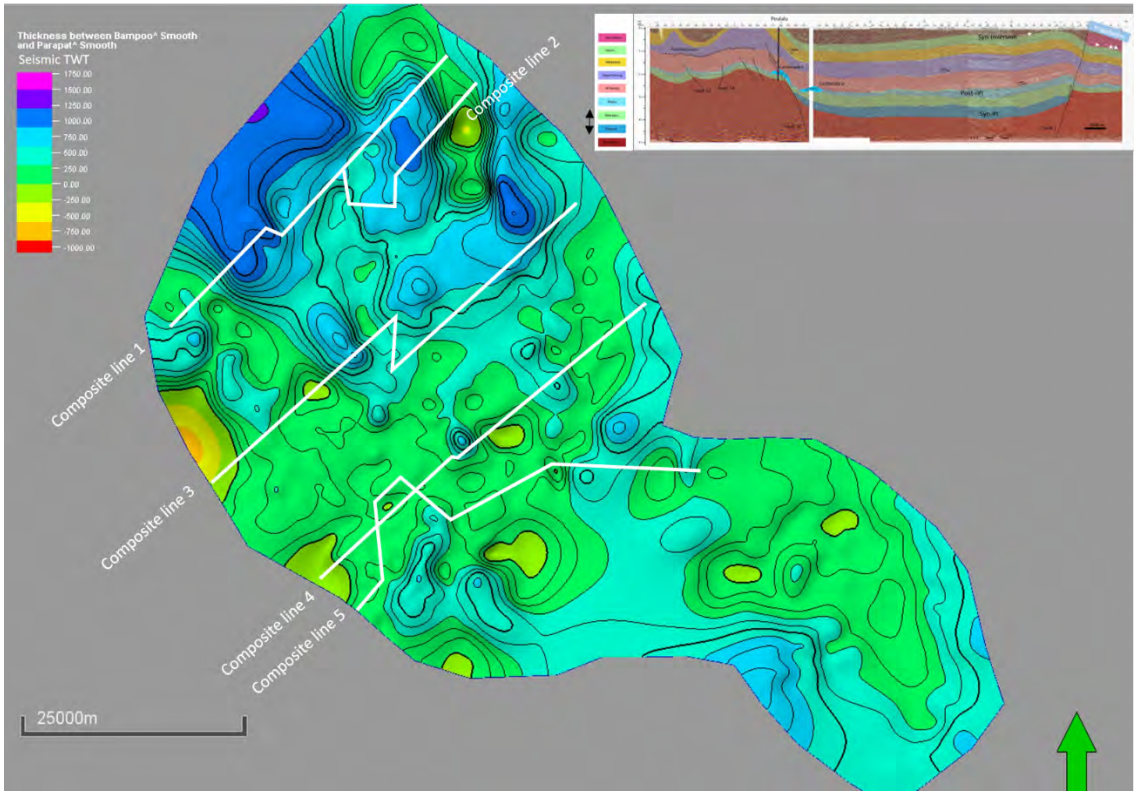

Figure 4-23 Isochron map showing the thickness of Bampo-Parapat formation. The green colour shows zero thickness meaning the area was not deposited or eroded. Meanwhile, blue shows the highest thicknesses. The upper right is seismic composite line 2.

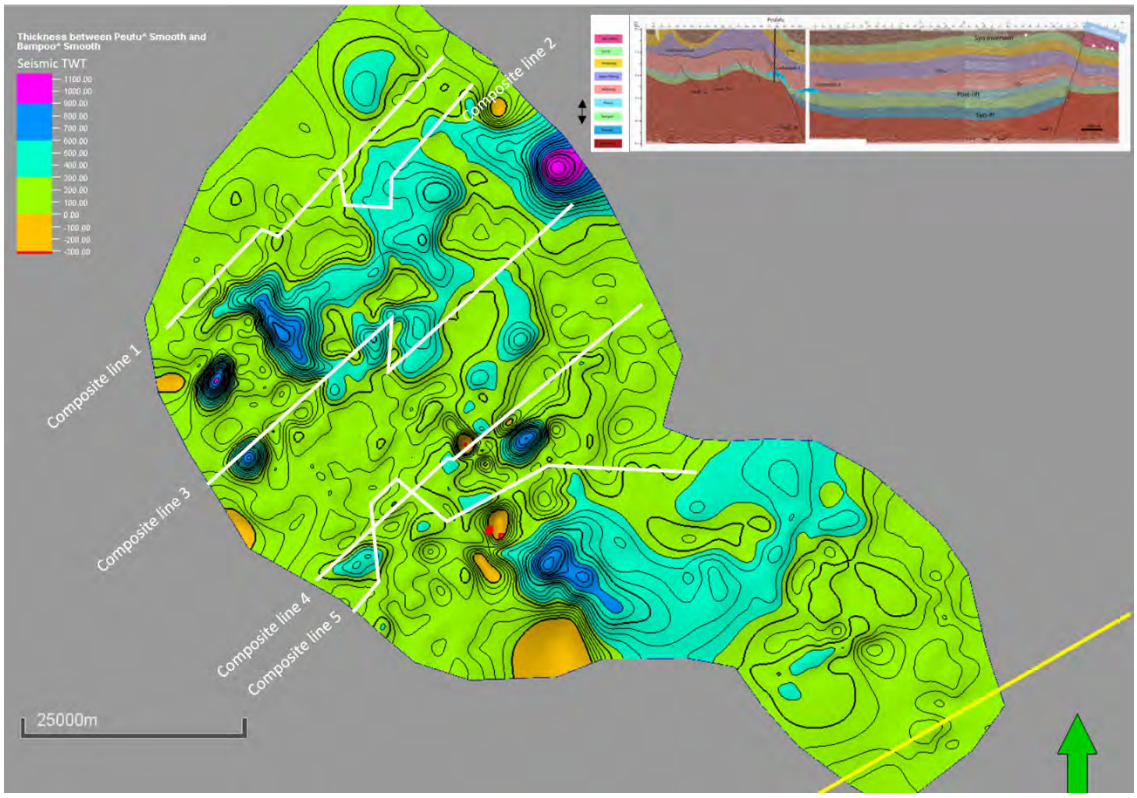

Figure 4-24 Isochron map Showing the thickness of Peutu-Bampo formation. The green color shows lower thicknesses; meanwhile, blue is the highest thickness. The upper right is seismic composite line 2.

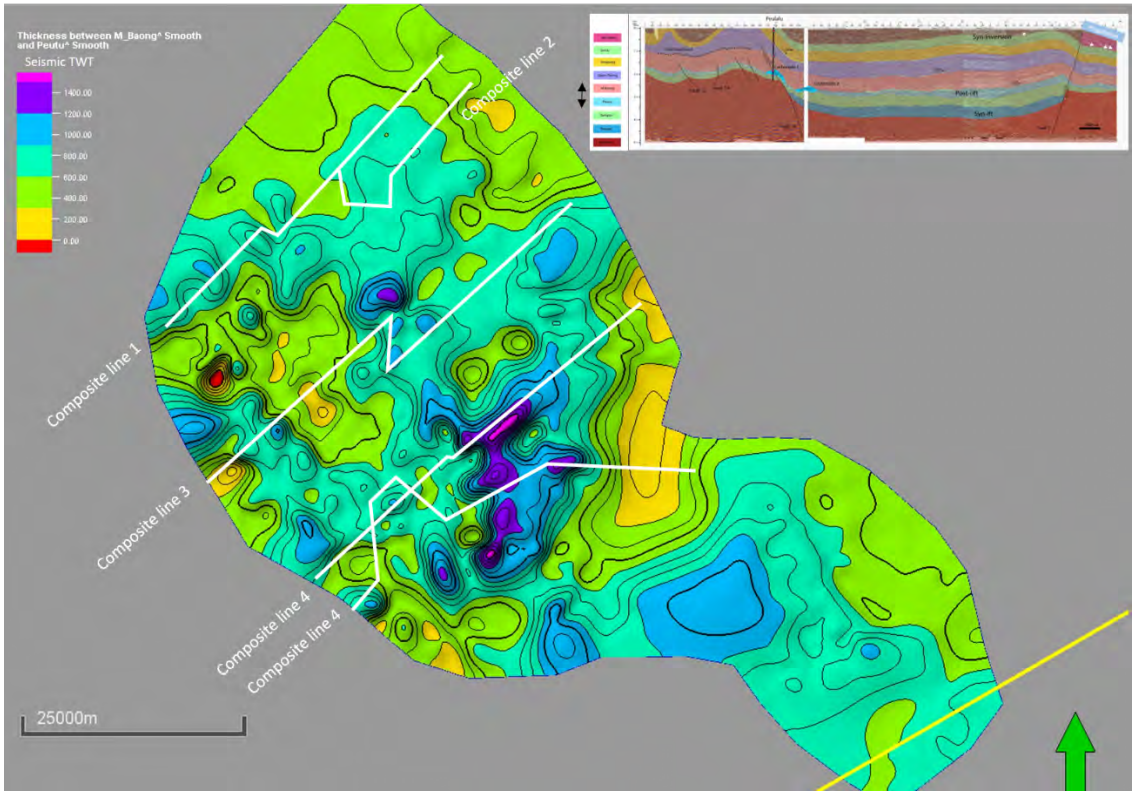

Figure 4-25 the thickness of the Middle Baong-Peutu formation. The green color shows lower thicknesses; meanwhile, blue is the highest thickness. The upper right is seismic composite line 2.

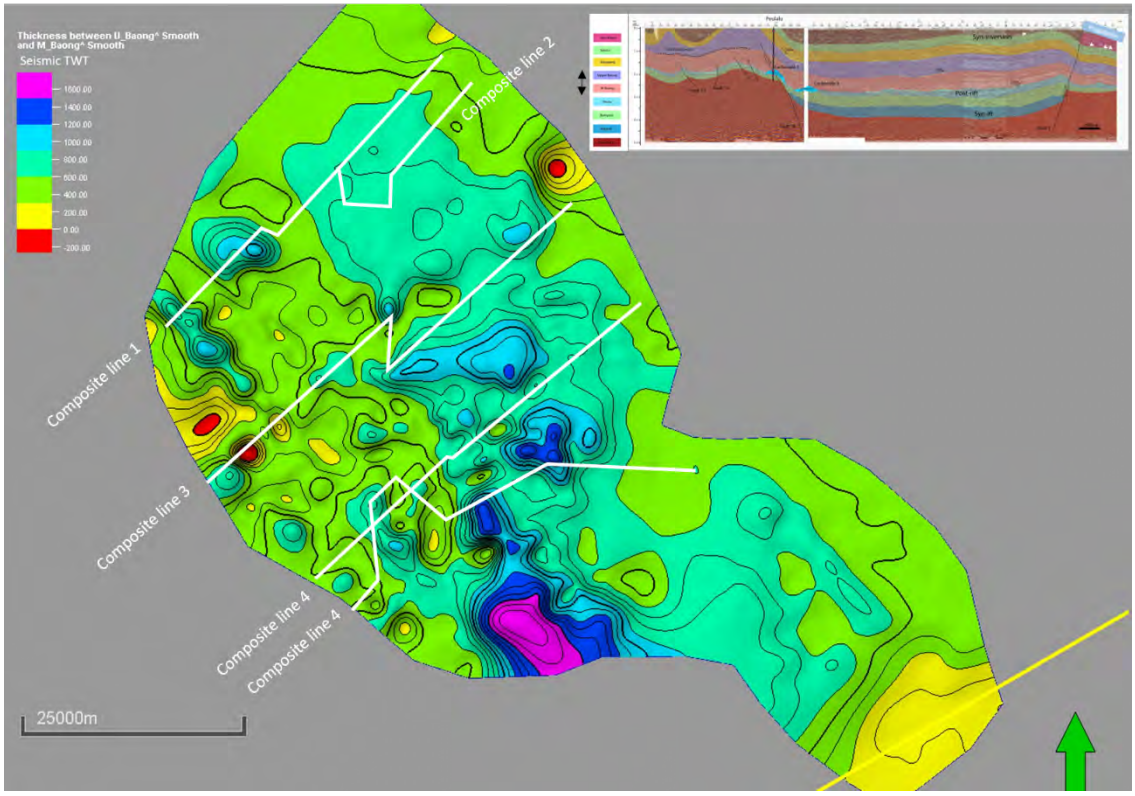

Figure 4-26 Isochron maps showing the thickness of Upper Baong-Middle Baong formation. The green colour shows a lower thickness; meanwhile, blue is the highest thickness. The upper right is seismic composite line 2.

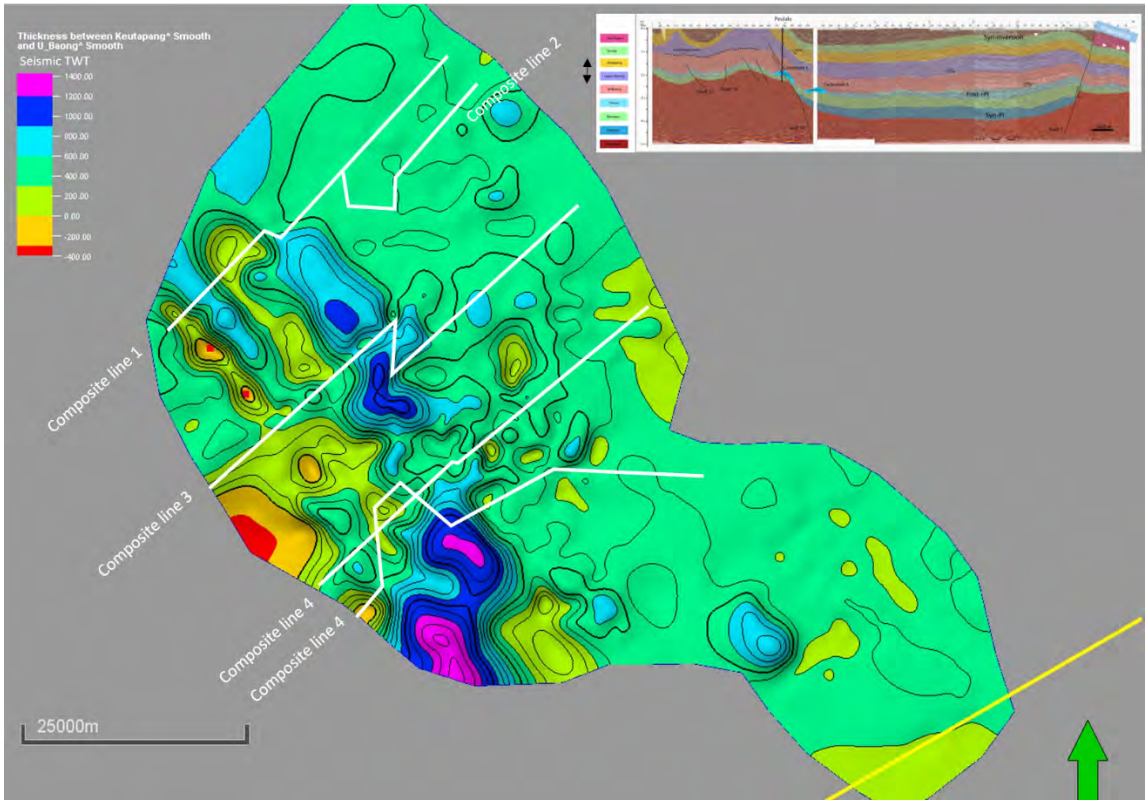

Figure 4-27 Isochron maps the thickness of Keutapang formation-Upper Baong formation. The green colour shows a lower thickness; meanwhile, blue is the highest thickness. The upper right is seismic composite line 2.

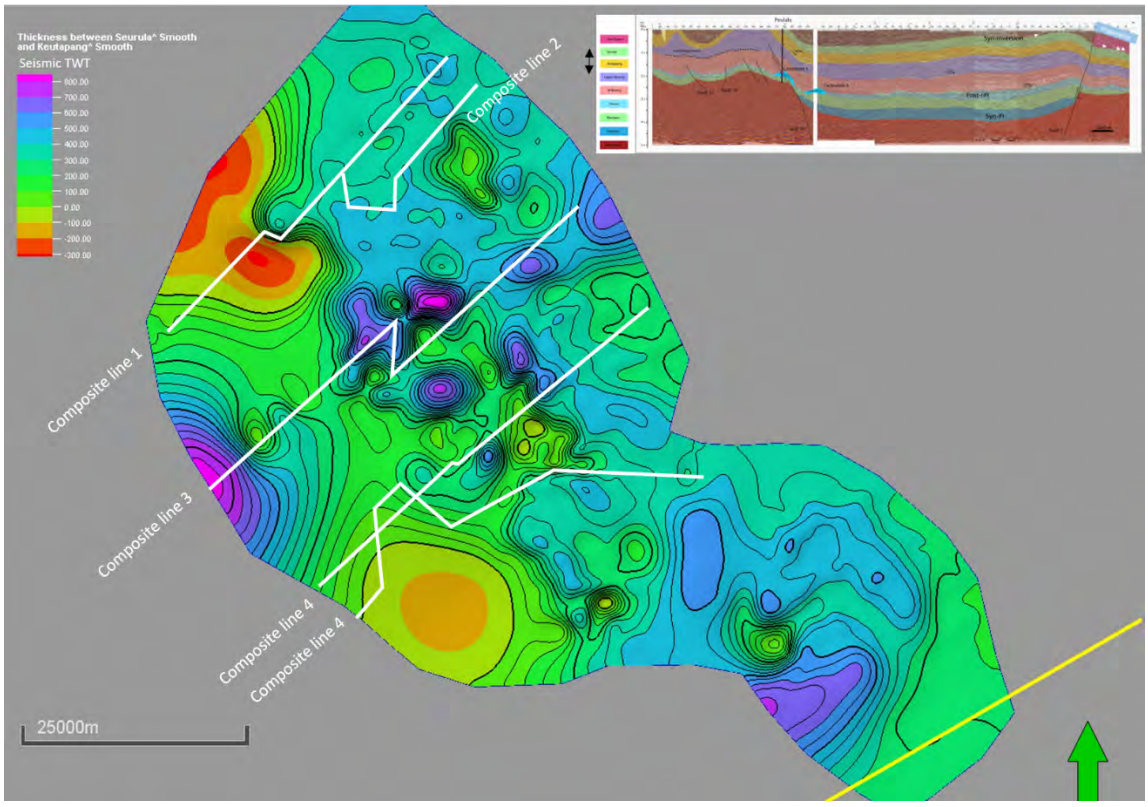

Figure 4-28 Isochron map Showing the thickness of Seurula-Keutapang formation. The green color shows lower thicknesses; meanwhile, purple is the highest thickness. The upper right is seismic composite line 2.

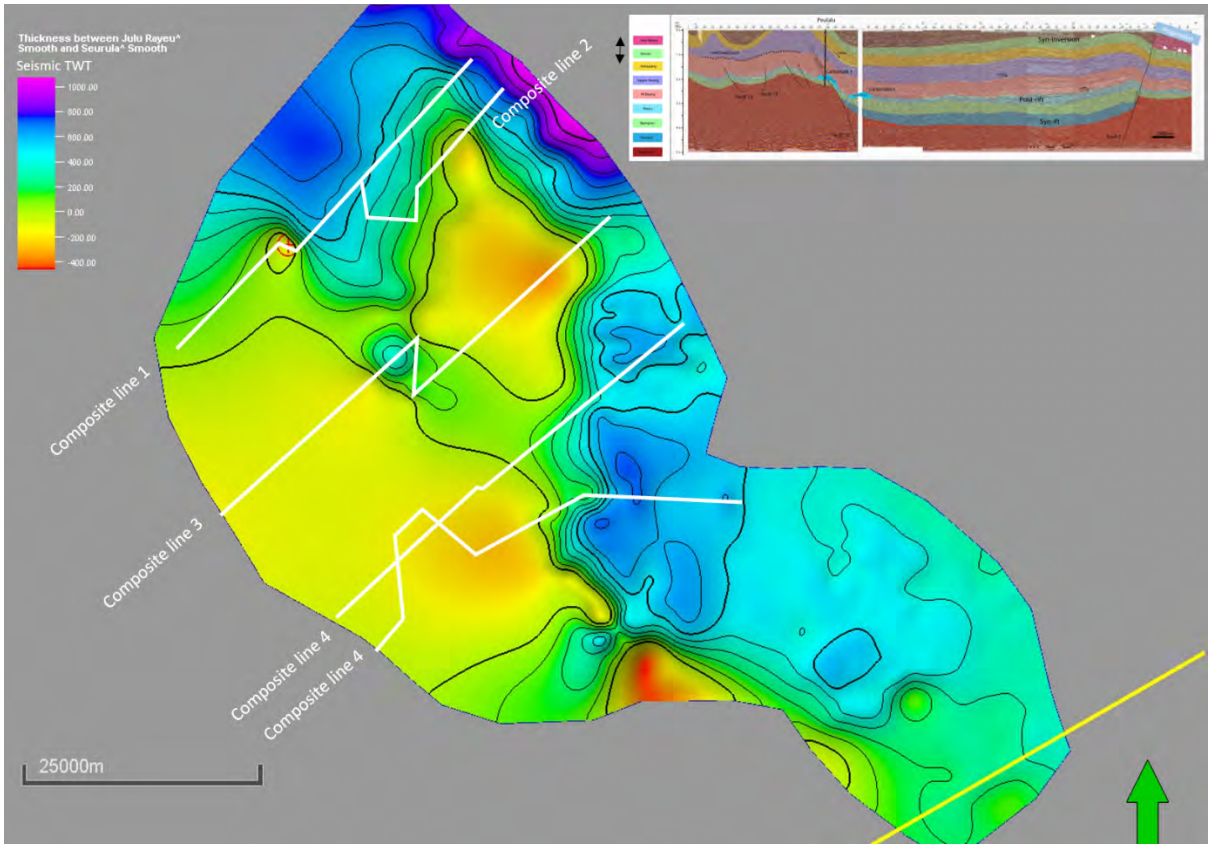

Figure 4-29 Isochron map showing the thickness of Julu Rayeu-Seurula formation. The green color shows lower thicknesses; meanwhile, blue is the highest thickness. The upper right is seismic composite line 2.

4.5 Recent Earthquakes

The earthquake catalog (USGS, 2022) shows that the deformation in the North Sumatra Basin onshore area is very active. Almost 40 earthquakes with a magnitude scale of 4 to 6 Mw occurred between 1950 to 2022. Most earthquakes are located in the Barisan Mountains and possibly related to the Sumatra Fault System (Figure 4-30). Earthquake depths vary from 150 km in the Barisan Mountains to 12 km in the onshore North Sumatra Basin. The earthquakes in the onshore area are categorized as shallow, while those in the Barisan Mountains are intermediate (Spence, Sipkin, & Choy, 1989).

Five onshore earthquakes are located in the study area and intersect the onshore seismic lines (Figure 4-30). The five earthquakes are:

1. The 1970 earthquake had a magnitude of 5.6 MW and a depth of 10 km. The epicenter is located southwest and adjacent to the Barisan foothills. There are no focal mechanisms or moment tensor records for this earthquake (Figure 4-30).
2. The 1982 earthquake with a magnitude of 5.4 MW and a depth of 52 km. The epicenter is located to the southeast of the first earthquake. The focal mechanism shows oblique reverse

movement with two possibile trends. The first is a northwest-southeast trend with a strike of 300° and a dip of 49°. The second is almost north-south, with a strike of 171° and a dip of 54°. The seismic lines and faults map shows that this epicenter is located in the same area as Fault 9 (Figures 4-30 and 4-31). Fault 9 also has a similar trend to the north-south direction of the focal mechanism (Figure 4-10). However, given the dip of the fault, it would be some distance from the epicentre at 10 km depth.

3. The January 2003 earthquake with a magnitude of 6.1 MW and a depth of 33 km. The location is close to the 1970 earthquake (Figure 4-30). There is no focal mechanism record for this earthquake.
4. The September 2003 earthquake with a magnitude of 5.3 MW and a depth of 15 km. The epicentre is north of the 1970 earthquake (Figure 4-30). The focal mechanism shows an oblique reverse fault with two possible trends. The first is almost north-south direction with a strike of 1°, and a dip of 68°. The second is a northwest-southeast with a strike of 103°, and a dip of 52°. This second trend is similar to the trend of Fault 16 (Fault 16 is shown on Figure 4-5 in composite seismic line 3). The earthquake epicentre is close to the location of Fault 16, as shown in the seismic lines (Figure 4-10).
5. The 2018 earthquake with a magnitude of 5.2 MW and a depth is 11.5 km. The epicentre is northeast of the 1970 earthquake (Figure 4-30). The focal mechanism shows an oblique reverse fault with two possible trends. The first is almost north-south, with a strike of 177° and a dip is 43°. The second trend is northwest-southeast, with the strike is 300° and a dip is of 63°. This earthquake epicentre is located close to Fault 7 (The fault 7 is shown in seismic composite 4 in figure 4-6 and its location is shown in Figures 4-10 and 4-30).

Another earthquake occurred near the Julu Rayeu sub-district but is not covered by seismic lines. The earthquake happened in 2007 with a magnitude of 5.2 MW and a depth of 12 km. This earthquake occurred due to compressive stress with the reverse/thrust fault oriented northwest-southeast, as shown by the focal mechanism (Figure 4-30).

Collectively, the earthquake data show that the North Sumatra Basin reamins in compression and that existing faults are still experiencing inversion. The data shows that oblique compression is the most common stress regime.

In general, the faults mapped (Fault 9, 7, and 16) in this study have similar trends and dips to the faults associated with earthquakes. These faults at the surface locations of the epicentres may not be directly linked with the earthquakes. However, they may also have the potential to be reactivated in future earthquakes.

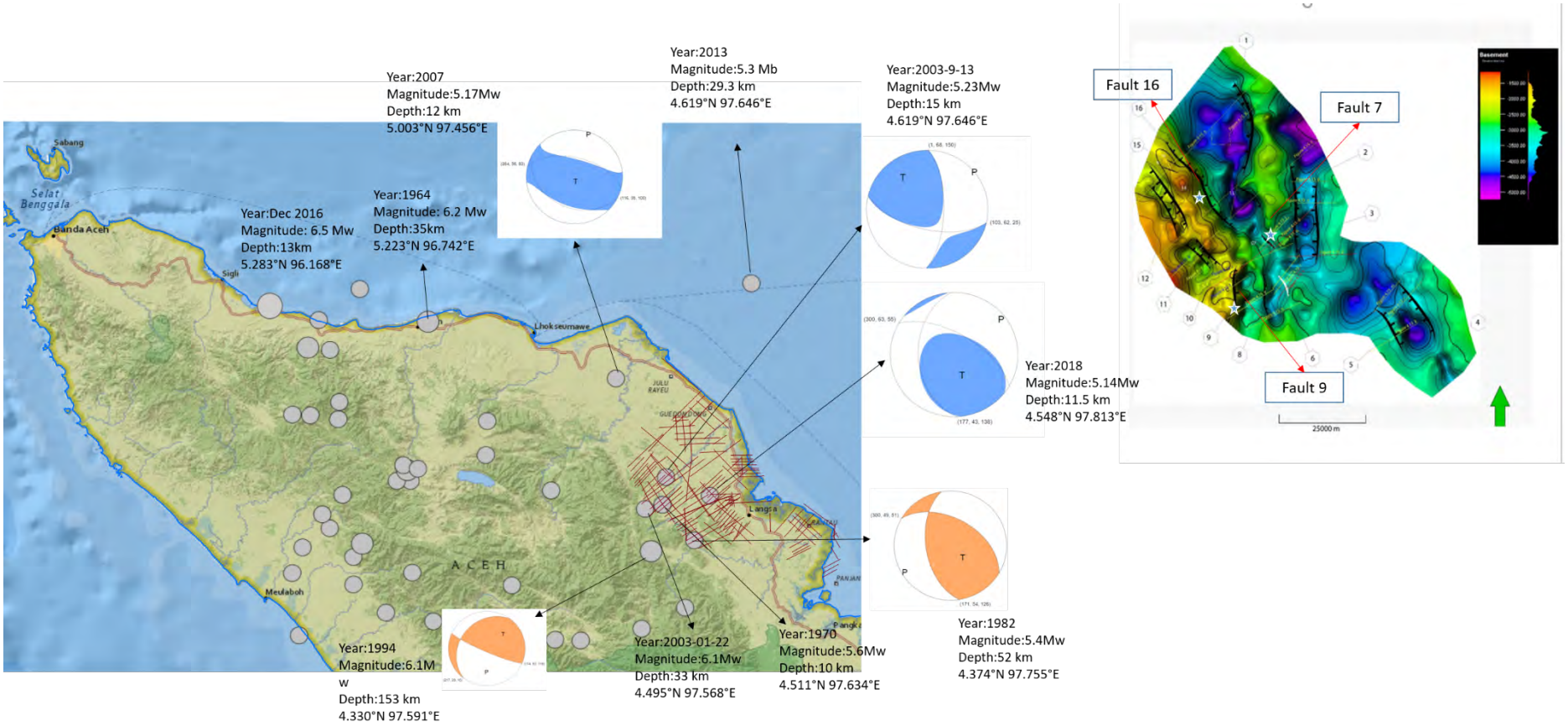

Figure 4-30 The Recent tectonic activities show the basin evolutions associated with the earthquakes. The top left shows the earthquake epicenter (white stars symbol) in the area of mapped faults, onshore North Sumatra Basin.

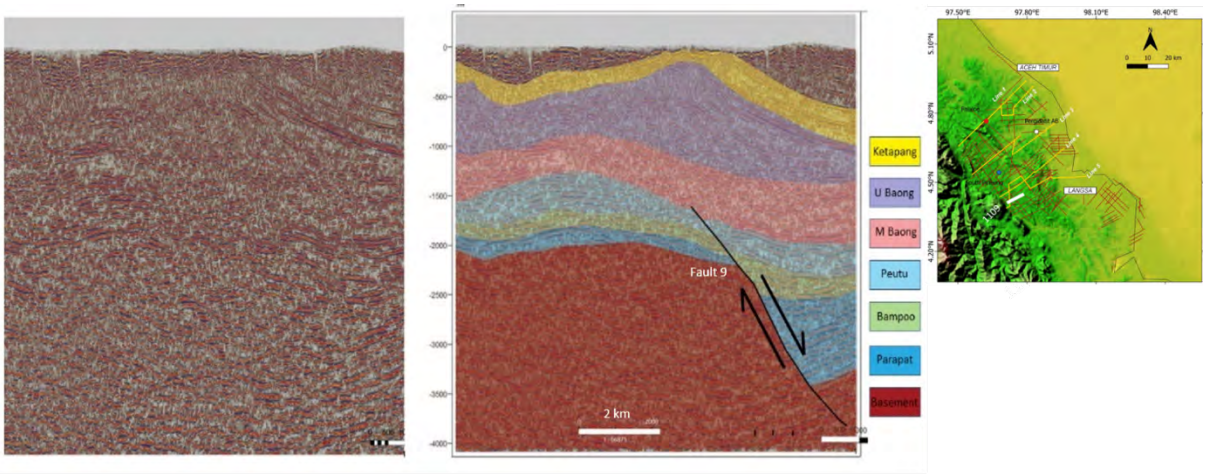

Figure 4-31 The Figure is intended to show faults 9 in Figure 4-10. The seismic line (1109) location is on the right (white line).

4.6 New Perspectives in the onshore area

The new perspectives are based on interpreting the 2D seismic data in the study area (Figure 4-1). The basement configuration shows a significant difference from the previous maps by several authors. (Anderson et al., 1993; Davies, 1984; Kamili et al., 1976; Sosromihardjo, 1988) (Figure 4-32). The previous maps are presented in conference publications the methodology they used is not clear, although it was probably based on seismic interpretation and Synthetic Aperture Radar data. This thesis also gives a new perspective of the geological cross-section constructed by (Pertamina/Beicip, 1985) (Figure 2-6).

4.6.1 Basement configuration

This thesis has filled a gap in the southwestern region of previous maps (Figure 4-33). The new map shows that the basement forms a shallow platform at about -1200 ms in the southwestern area close to the Barisan Mountains.

The map presented in this thesis also provides a more detailed interpretation of horst blocks compared to those presented by Anderson et al. (1993); (Kamili et al., 1976; Sosromihardjo, 1988) in Figure 4-335. This thesis's basement map proposes -1100 ms to -1900 ms, while, the old map uses a more general range from -2000 ms to -3000 ms.

In the new interpretation also extends the of intra-basinal horst and graben, which can now be seen to be more extensive. The North Depocentre does not appear to have been distinguished from the Perlak Platform on the older maps. The new map also shows that sediment packages in the

graben range from -4000 ms to -5200 ms. The horsts and graben have a similar north-south trend in both maps. This is important for understanding the extension regime in which the basin formed.

4.6.2 The Geological Section in the research area

The previous work by Pertamina/Beicip (1985) (Figure 4-34) shows that the deformation in the southwest relates to the strike strip faults. The faults cut the surface and accommodate the pop-up/anticline structure that causes the Baong Formation to outcrop. A low-angle reverse fault also causes the older formations (Peutu and Bampo formations) to be elevated in the Barisan foothills (Figure 4-34). By contrast, the seismic interpretation shows that these folds are related to a detachment within the Baong Formation, rather than being a result of strike-slip deformation.

The previous work also shows that the depression marking the central graben in the area (blue box in Figure 4-34) is part of a large scale monocline that is possibly related to inversion tectonics or to tectonic loading. In contrast, the interpreted seismic section shows that the graben/trough were shaped by major extensional basement bounding faults. The first is in the southwest, where the fault propagated until the Upper Baong. The second is in the northeast, which is interpreted as an inverted basement fault that propagates close to the surface. This is similar to the structure shown by Pertamina/Beicip (1985), although the geometry on the interpreted sesinic section is simpler.

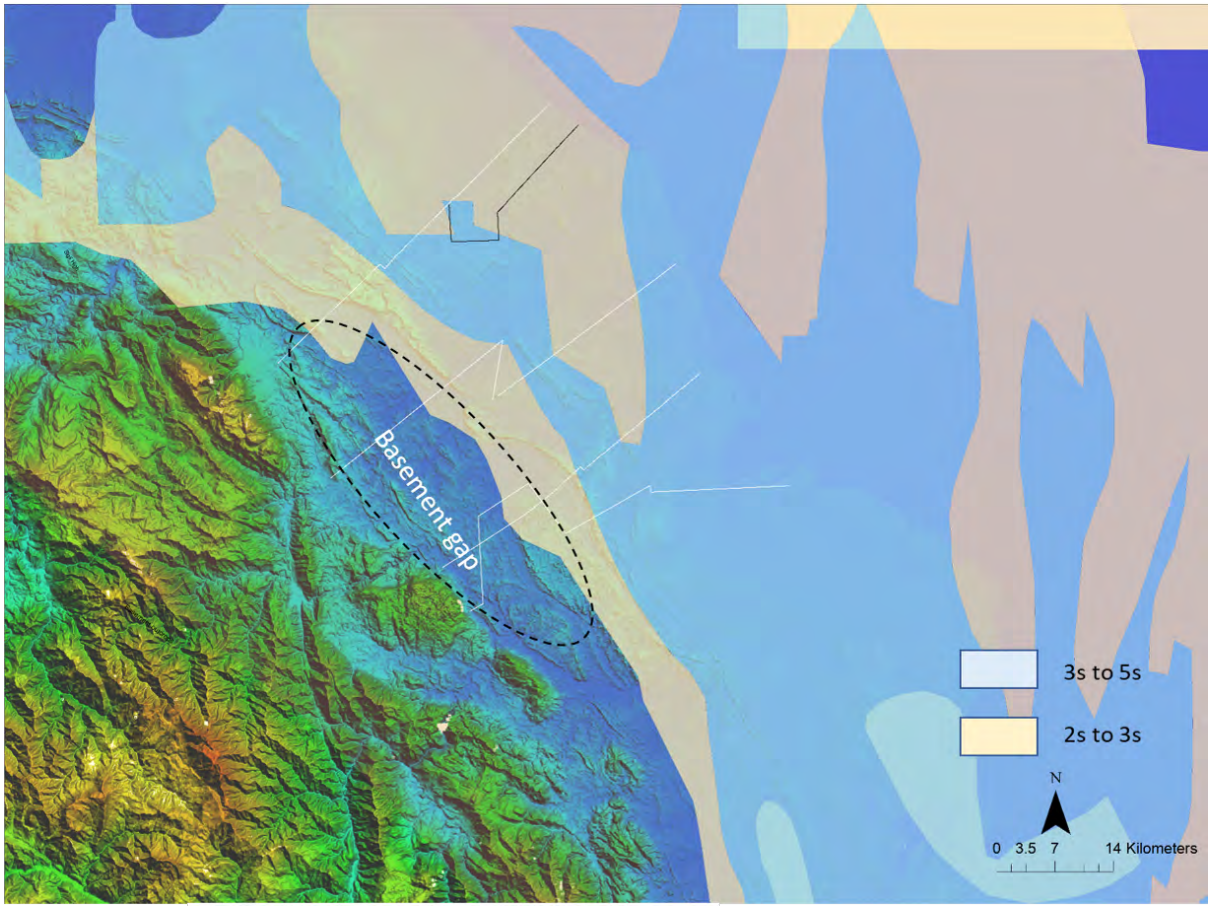

Figure 4-32 the basement map by (Anderson et al, 1993; Davies, 1984; Kamili et al., 1976; Sosromihardjo, 1988). The map shows basement horst (2s to 3s) and grabens (3s to 5s). There is a gap area that can be filled by this thesis.

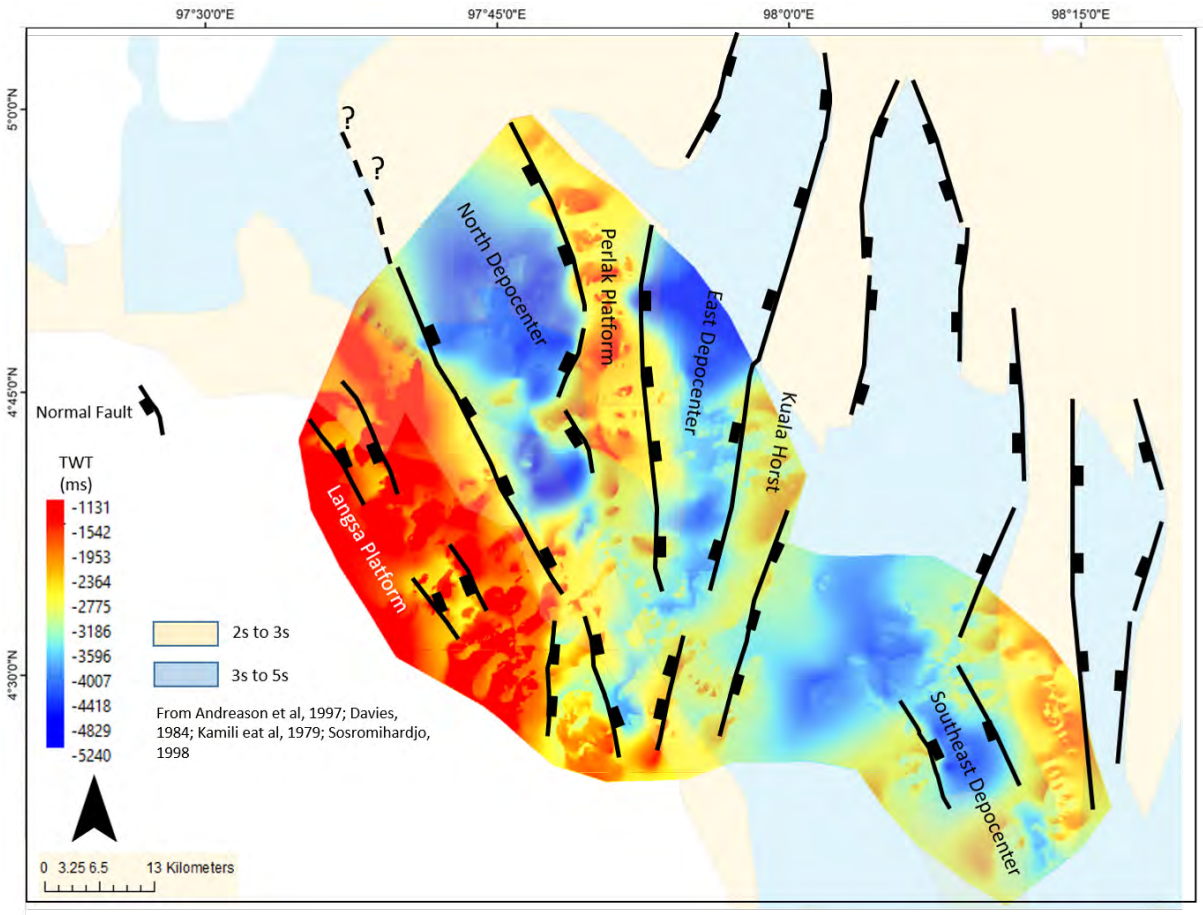

Figure 4-33 this thesis map overlay the previous map in Figure 4-32. This figure shows the comparison basement configuration map between this thesis and the previous map by some authors (Anderson et al, 1993; Davies, 1984; Kamili et al., 1976; Sosromihardjo, 1988). This thesis also filled the information gap in the Langsa Platform.

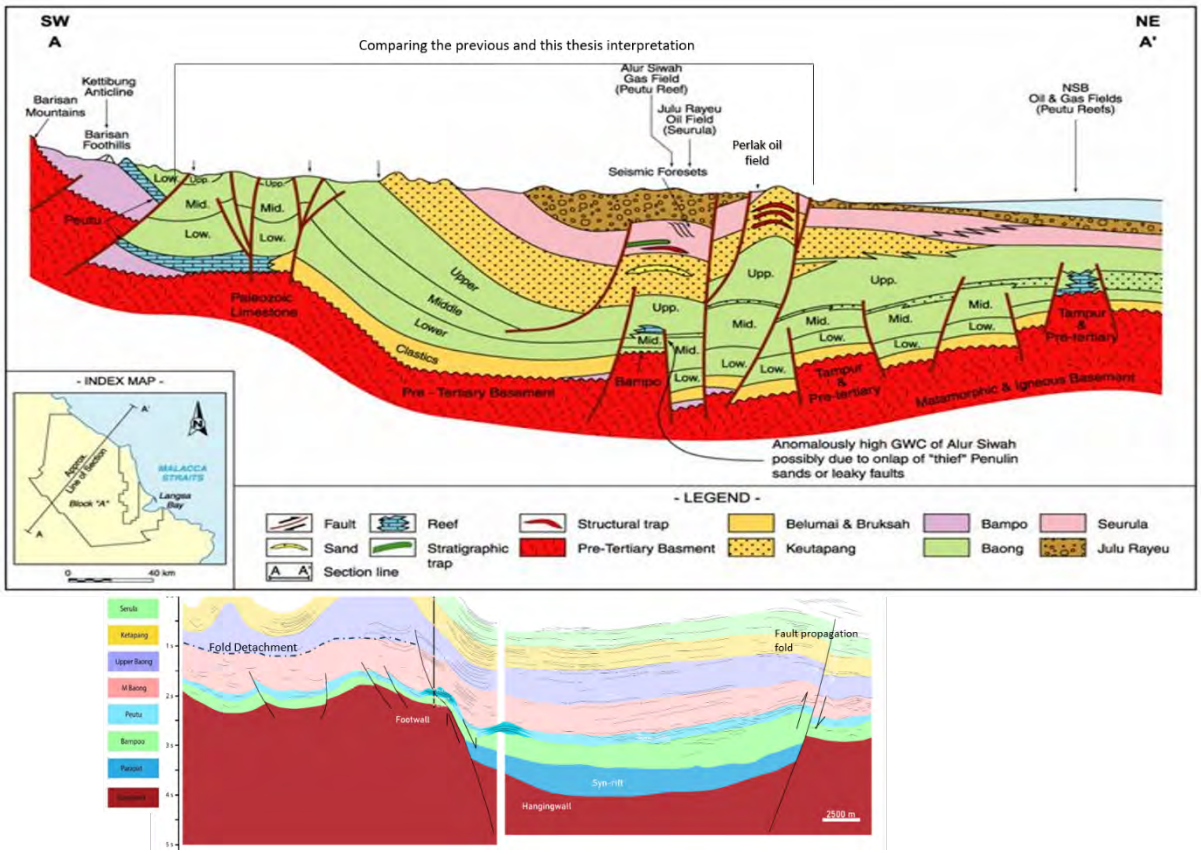

Figure 4-34 The comparison between the geological cross-section from this thesis (below) and the previous work by Pertamina& Beicip, 1984(above) from the paper by Caughey & Wahyudi, (1993).

4.7 Summary

The onshore North Sumatra Basin demonstrates several findings and gives new perspectives on structure elements and evolutions. These are among the findings:

1. The SRTM images associated with the seismic data revealed lineaments/morphology in the onshore area of the North Sumatra Basin. The contours are associated with the folds, synclines, and erosional beddings (surface beddings) exposed on the surface (Figure 4-18). Also, this thesis shows two areas with different surface expression of the anticlines: anticlines which expose Keutapang and older formations and with higher relief, in the Barian Foothills, and anticlines which expose younger formations than the Keutapang, have lower relief and occur further in to the basin (Figure 4-3, 4-4, 4-5, 4-6, and 4-7 respectively).
2. The updated geological section using the 2D seismic interpretation provides a new perspective compared to that published by Pertamina-Beicip (1984) (Figure 4-34). Their study shows that the anticlines were interpreted as flower structures associated with strike-slip faults. However, the seismic interpretation shows that the symmetrical anticlines in the southwest are due to the detachment faults. Also, the new interpretation shows that the Basin

depocenter was shaped by basin bounding basement fault and not by a large monocline. Also, there is also an oil field location mistake; the Perlak oil field is not to the northeast of the Alursiwah field. The Perlak is southeast of the Alur Siwah (Figure 4-34).

3. The basement horst and graben maps were also updated using the interpretation of the 2D seismic lines. The interpretation fills a gap in information to the southwest area adjacent to the Barisan Foothills. In addition, the interpretation proposed the new geometry of the basement horst and grabens, such as orientations and elevation (Figure 4-33).
4. The onshore North Sumatra Basin shows three different fold mechanisms related to the inversions relative to the Barisan Mountains. First is the northwest-southeast anticline direction adjacent to the Barisan foothills. This anticline is associated with the fold-detachment. Second is the anticline that is associated with the fault propagation fold. The anticline is located north of the study area in a northwest-southeast direction. The third is to the east of the study area with the association of fold detachment. The anticline is a north-south trend. All the detachment folds are due to the existence of a décollement within the Baong Formation (Figure 4-3, 4-4, 4-5, 4-6, and 4-7 respectively).
5. The fault styles in the onshore of the North Sumatra Basin include normal and reverse faults. The major normal faults are the basement bounding faults that shape basement horst and grabens during the Oligocene times (Figure 4-10). The primary reverse fault is observed in the north. This reverse fault was normal in Oligocene and later changed to reverse in the Pliocene time. There are also minor normal faults that cut the basement platforms (Langsa platform) during the Oligocene age and reactivated during the Miocene (Figure 4-3, 4-4, 4-5, and 4-10). In the east of the study area, the normal faults were associated with folds at the tip of them (Figure 4-3, and 4-18). These faults formed during Oligocene and reactivated in the Miocene.
6. This thesis proposed a different view about the timing of the Inversion of the onshore North Sumatra Basin. The previous works suggested the inversion was in the Middle-Late Miocene (Anderson et al., 1993; Davies, 1984; De Smet & Barber, 2005). However, based on the 2D seismic interpretation, the inversion occurred during the deposition of the Seurula and younger formation (Julu Rayeu) in the Pliocene age. The seismic 2D reconstruction also shows that the inversion initially occurred in the Pliocene and that the maximum inversion occurred during the late Pliocene (Figure 4-28, 4-29). The inversion in the onshore North Sumatra Basin was possibly related to the development of the Barisan Mountains.
7. The earthquake data demonstrate that the inversion of the onshore North Sumatra Basin is still progressing. The focal mechanism shows that the compression regime triggered the earthquakes. Furthermore, the earthquake epicentres are in the same locations of some mapped faults from the seismic lines, and the trends are also similar (4-30).

5 Offshore North Sumatra Basin

The offshore North Sumatra Basin is located in the marine waters of Aceh and North Sumatra Province, but it extends north into the Mergui Basin in Thailand and Malaysia (Figures 1-1 and 5-1). This part of the offshore includes a present day shelf where water depth ranges from 0 to 100 m, a shelf slope from 100 to 500 m, and a basinal area from 500 to 2500 m (Figures 1-2 and 5-1). In terms of structural elements, the offshore basin is situated between the Malacca platform to the east and the Mergui Platform and Andaman Sea to the west. The basin itself corresponds to the northward extension of the Lhoksukon Deep (Figure 2-5).

The general stratigraphy of the North Sumatra Basin was introduced by Tsukada et al. (1996) (Figure 5-2, general stratigraphy offshore NSB). They interpreted syn-rift successions in the Parapat and Bampo formations characterised by lacustrine and marine shales in the west with sandstone and conglomerate deposits toward the Malacca Platform in the east, as well as a carbonate deposit on local horst within the basin. The basin experienced subsidence during the Early Miocene and early Middle Miocene associated with the deposition of greater thickness of shale toward the Mergui Platform and thicker sands toward the Malacca Platform in the Belumai Formation. They also described inversion tectonics that occurred during the middle Miocene, as marking the basin's change in geometry to a foreland basin. During this period, the thicker sandstones were deposited in the west, towards the Mergui Platform, while, the shales are prevalent toward the Malacca Platform. Compression continued during the late Miocene when the Barisan Mountains onshore were uplifted. During this period, the sedimentary rocks filling the offshore North Sumatra Basin were mainly shales, with minor sands towards the Mergui platform.

In this thesis, the stratigraphy and structures of offshore NSB were interpreted and mapped on 2D seismic data using Petrel. Only one well was available (BLD) and was tied into the seismic to control the stratigraphic interpretation (Figure 3-4). The well was spudded on a basement high (horst) and penetrated pre-Paleocene sediment (basement). This means that there is less constraint on the age of sediments filling the grabens.

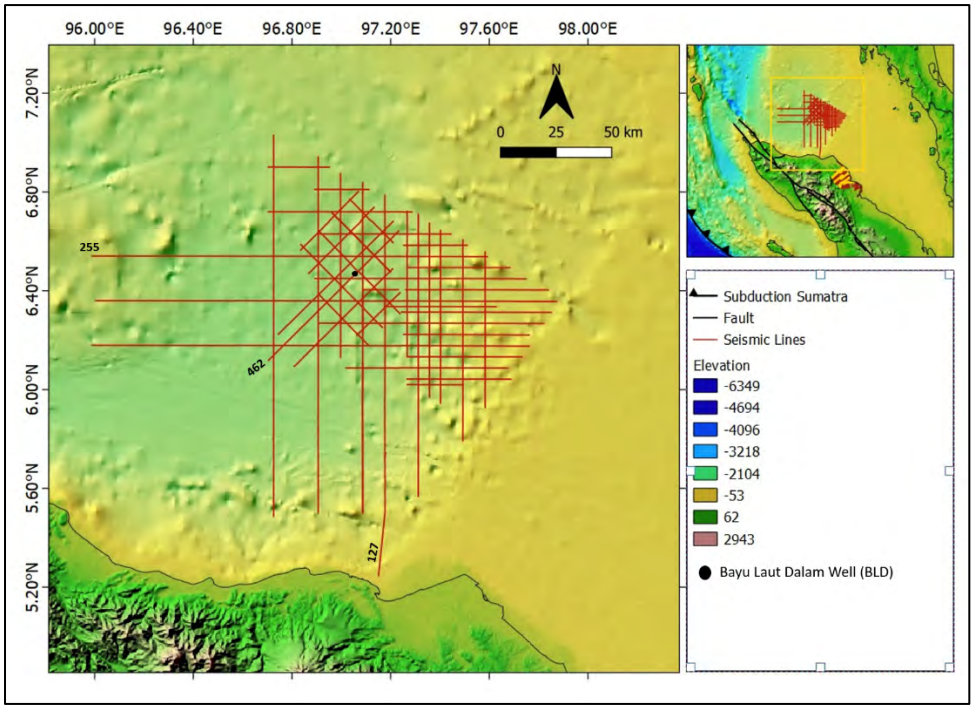

Figure 5-1 the offshore seismic lines are shown in red lines. The BLD well is located in the central area (red circle). The yellow box indicates the study area in offshore Aceh (top right).

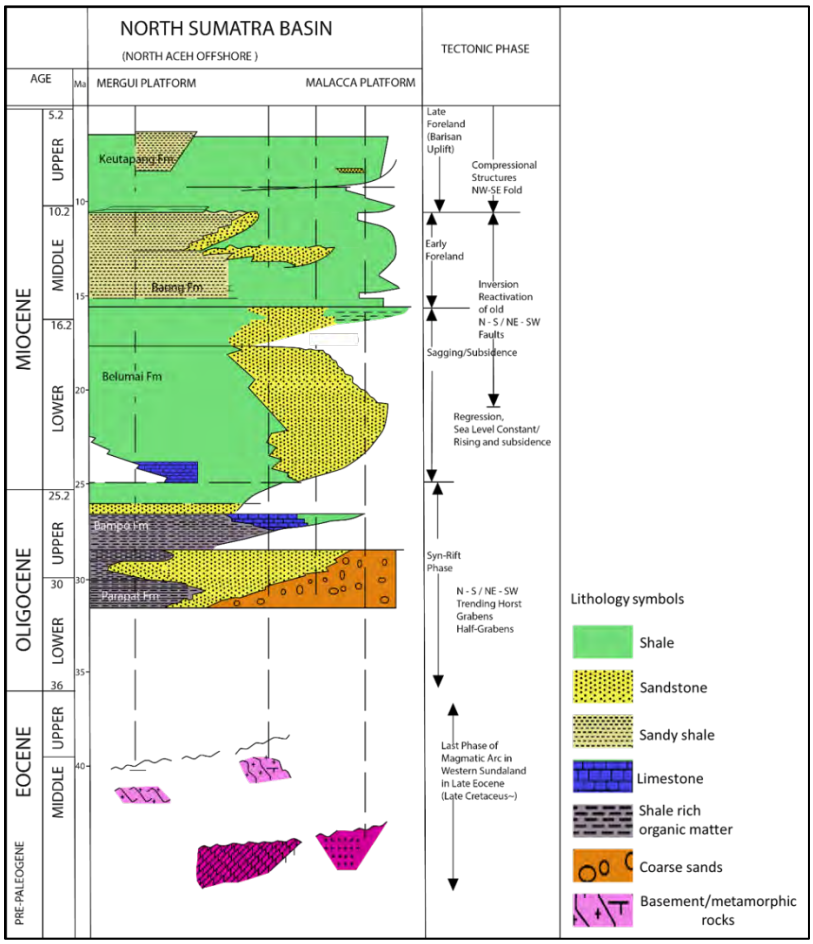

Figure 5-2 General Stratigraphy of offshore North Sumatra Basin from Mergui Platform in the west to the Malacca platform area in the east, adapted from (Tsukada et al., 1996).

5.1 Seismic Stratigraphy and Structure

North-south line 127 (Figure 5-3) and east-west line 225 (Figure 5-4) (location is in Figure 5-1) is used to illustrate the seismic stratigraphy due to their better resolution and because they are the longest lines in the area (Figures 5-3 and 5-4). Other seismic lines were also used to demonstrate the structural and stratigraphic features not covered by these lines.

Eight Paleogene to Neogene sequences have been recognized in the offshore North Sumatra Basin. These can be divided into pre, early, late, and post-rift (Figure 5-5). The seismic stratigraphy and structures of the offshore North Sumatra Basin are summarised in Figure 5-5.

5.1.1 Pre-rift/Basement (Pre-Paleocene)

This horizon is characterised by a lack of coherent reflectivity. The depth of the basement varies from 2 s twt to 5.5 s twt below sea level (Figure 5-6). Some major faults cut this sequence and define basement fault blocks. The faults also propagate into the younger units, such as the Parapat and Bampo Formations. The unconformity between the top basement and the base of the overlying sedimentary sequences is not well defined on seismic sections. The well reports provide very little information about the lithology and age of the basement rocks.

5.1.2 Parapat Formation (Early Oligocene)

The sediment unit that filled the grabens is known as the Parapat Formation of Oligocene age. This unit thins or is absent on basement highs, due either to erosion or non-deposition. The thickness varies from 0 to approximately 1500 ms (Figure 5-7). The thicker parts are in the graben while the thinner sequence is on the horst blocks. Thickening towards the faults, particularly at the northern end of line 127, shows that these are syn-kinematic sediments. The primary structures are extensional faults that cut basement (Figure 5-8). Besides, several minor normal faults were also observed within this package between the major faults that define the horsts and graben (Figure 5-4).

The Parapat succession is characterized by parallel and continuous reflectors. The upper part shows high amplitude, but the lower part shows medium to low amplitude. Based on the general offshore stratigraphy, the Parapat Formation consists of sandstones and shales (Bennett et al., 1981; Tsukada et al., 1996) (Figure 5-2).

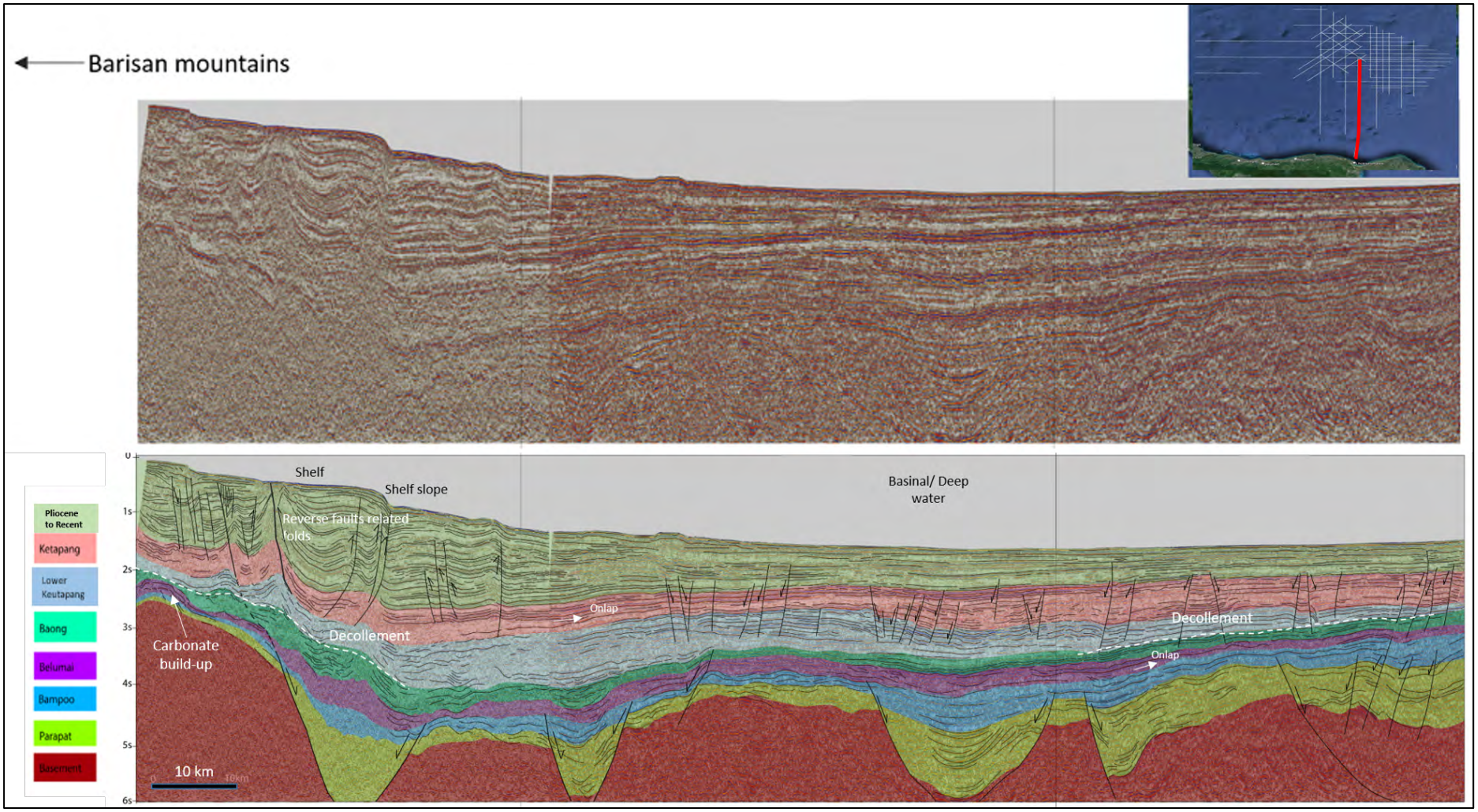

Figure 5-3 Regional Seismic line 127A-127B-127C. This composite seismic line covers south area, close to the onshore of Aceh, and north toward the Thailand water.

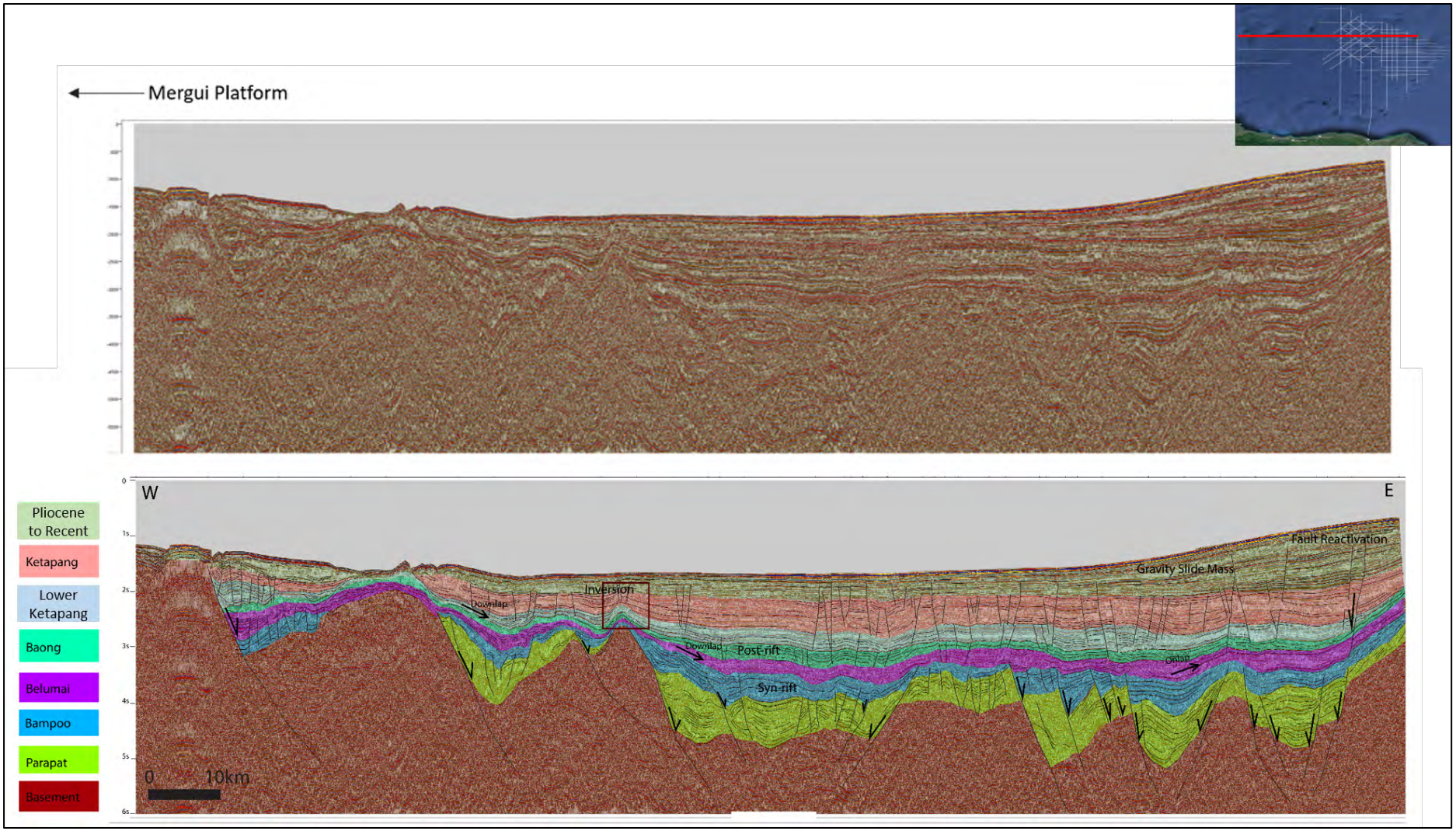

Figure 5-4 Regional Seismic line 255. This Regional seismic line covers east, close to the Malacca Platform, and west toward the Mergui ridge.

Horizons	Seismostratigraphy	Structures
Pliocene to Recent	• Moderate to high amplitude • Unconformity above the local fold to the west • Unconformity in the east	• Normal faults (fault reactivation? Or maybe polygonal faults) • Fold structure in the west • Canyon and channel at the sea bed
Upper Ketapang Fm.	• Moderate to high amplitudes • Parallel with good continuity reflectors • On lap sequence cutting the fold indicating the beginning of inversion	• Normal faults (planar and semi listric) • Fold structure to the west
Lower Ketapang Fm.	• Medium to high amplitude • Parallel with continuous reflectors • Thinning toward east and west • Thickening in the centre • Cut by younger faults	• Less deformations except in the centre • Normal faults with dip east and west
Baong Fm.	• Moderate amplitudes and low amplitudes in the western part • Parallel with semi continuous reflectors • Almost uniform thickness • Thicker above the trough in the centre area	• Almost no faults except in the centre area
Belumai Fm.	• Low to moderate amplitude in the centre and moderate to high in the basin edges • Parallel to elongated with semi continuous reflectors • Uniform thickness	• Almost no deformations
Bampoo Fm.	• Moderate to high amplitude • Sub-parallel with continuous reflectors in the upper part and complex discontinuity in the lower part • Thinning on the horst and thicker in the graben	• Basement bounding faults forming horst-graben structure dipping east and west • Minor normal faults
Parapat Fm.	• Low to moderate amplitude • Sub parallel with semi continuous reflectors and discontinuity reflector in the lower part • Deposited in the graben and possibly eroded on the horst	• Basement bounding faults forming horst-graben structure (initiation of syn-rift) • Minor normal faults and some faults cut through the basement.
Basement Fm.	• Chaotic with discontinuous reflectors	• Basement bounding faults and cut by the younger faults.

Figure 5-5 Summary Seismic Stratigraphy and structural of offshore NSB based on the line 255 in Figure 5-4.

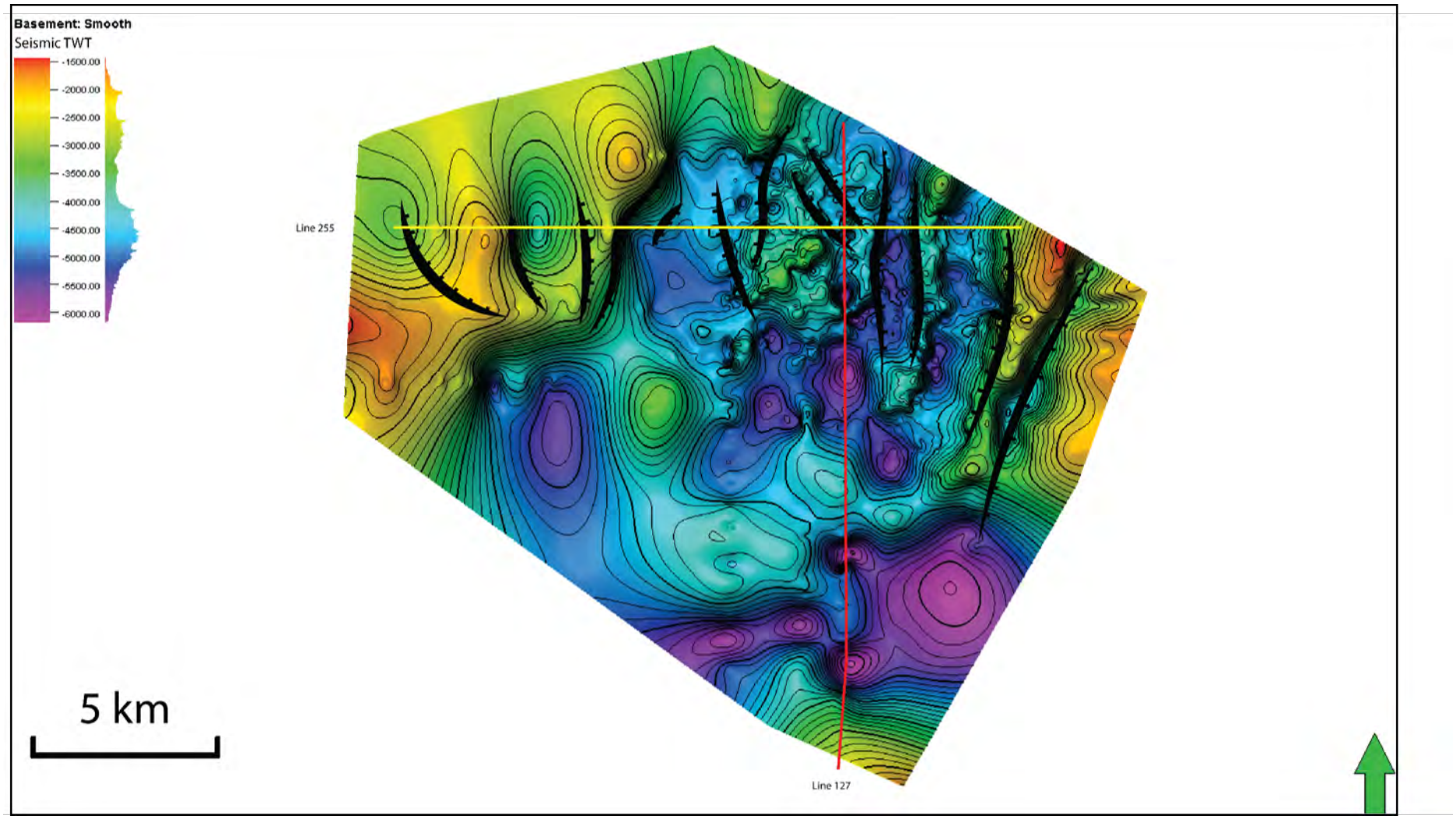

Figure 5-6 Basement time map offshore North Sumatra Basin. The red line is the composite seismic line 127A-B-C (Figure 5-3), and the yellow is seismic line 255 (Figure 5-4).

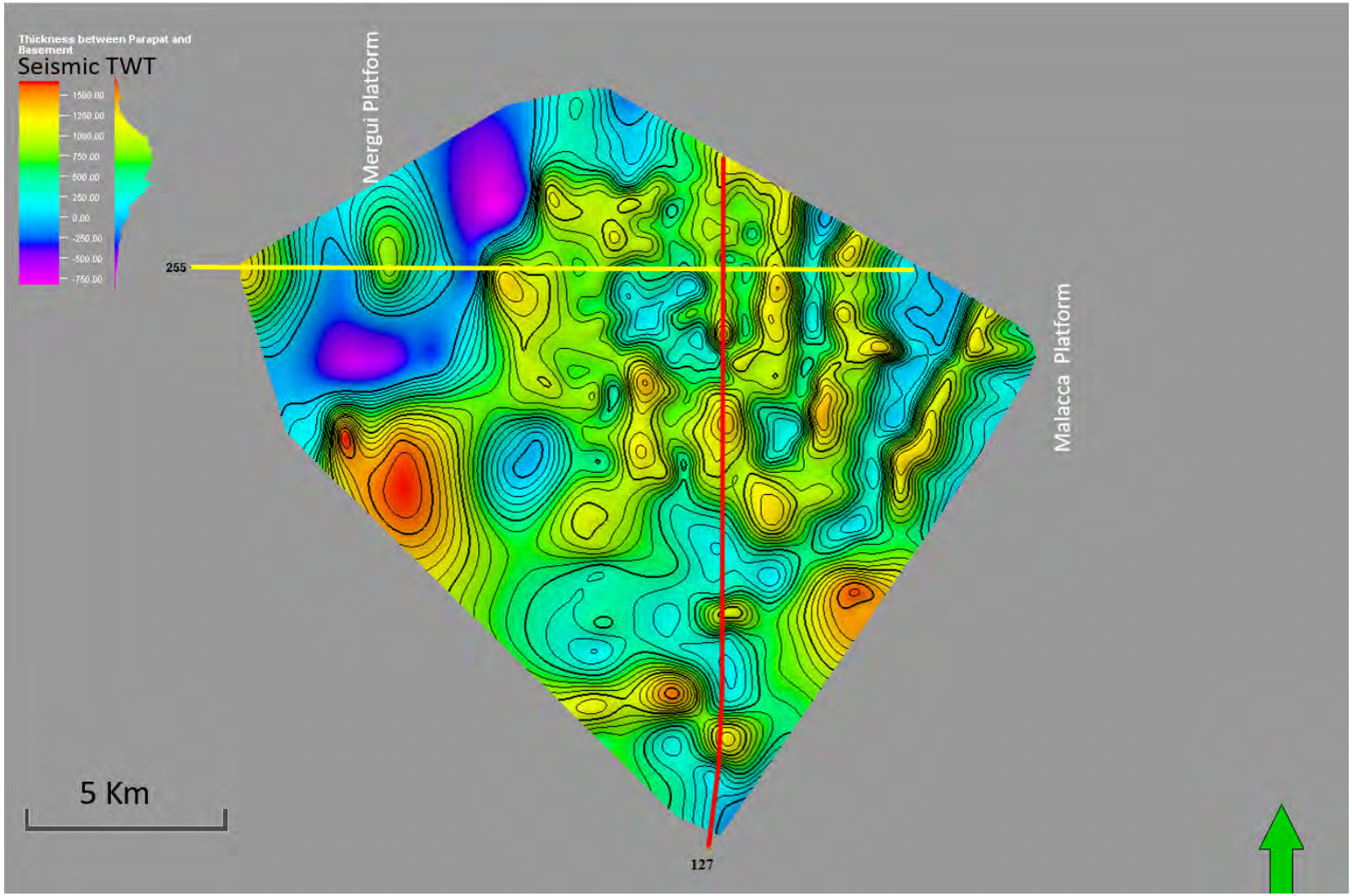

Figure 5-7 Isochron map of Parapat fm (Early Oligocene). The red line is the composite seismic line 127A-B-C (Figure 5-3), and the yellow is seismic line 255 (Figure 5-4).

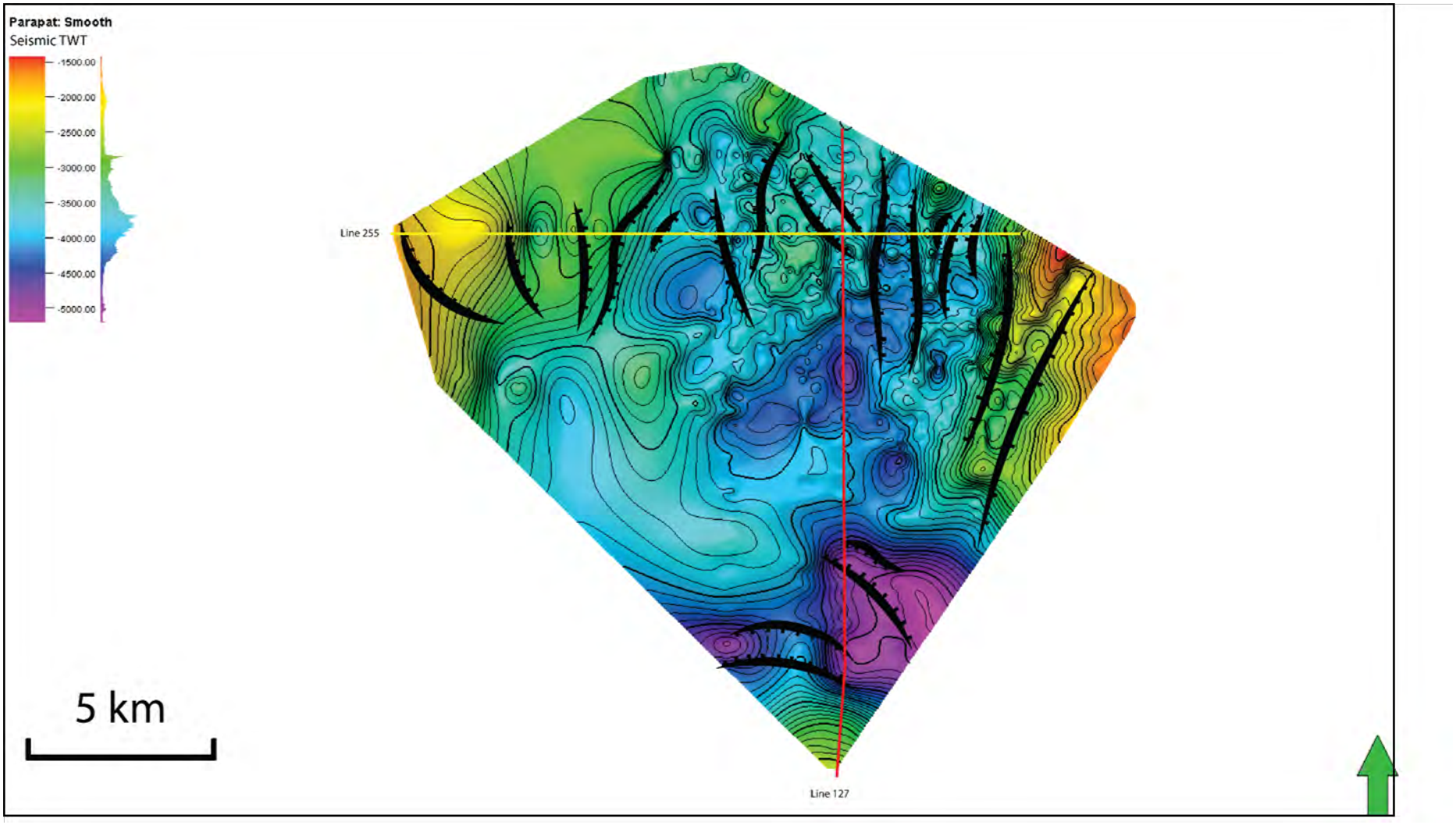

Figure 5-8 Parapat formation (Early Oligocene) time map offshore North Sumatra Basin. The red line is the composite seismic line 127A-B-C (Figure 5-3), and the yellow is seismic line 255 (Figure 5-4).

5.1.3 Bampo Formation (Late Oligocene)

The Bampo Formation conformably overlies the Parapat Formation, although it may be deposited unconformably above the basement on some horst blocks where the Parapat Formation is absent (e.g. close to the Mergui Platform. Figure 5-4). This unit is thicker towards the faults and thinner away from the faults and has a thickness range of 100 ms on the horst to 500 ms within the grabens (Figure 5-9), indicating that it is part of the syn-kinematic sequence. Extensional faults propagate to the top of this unit (Figure 5-4) showing that it also marks the end of the rifting stage in the late Oligocene (Figure 5-10).

This unit is characterized by parallel, continuous to discontinuous reflectors with high amplitudes, particularly in the centre of the graben. Lower amplitudes are shown closer to the faults and in the lower part of the sequence. (Figure 5-5). The lithology of this unit varies from sandstone to shales (Figure 5-2).

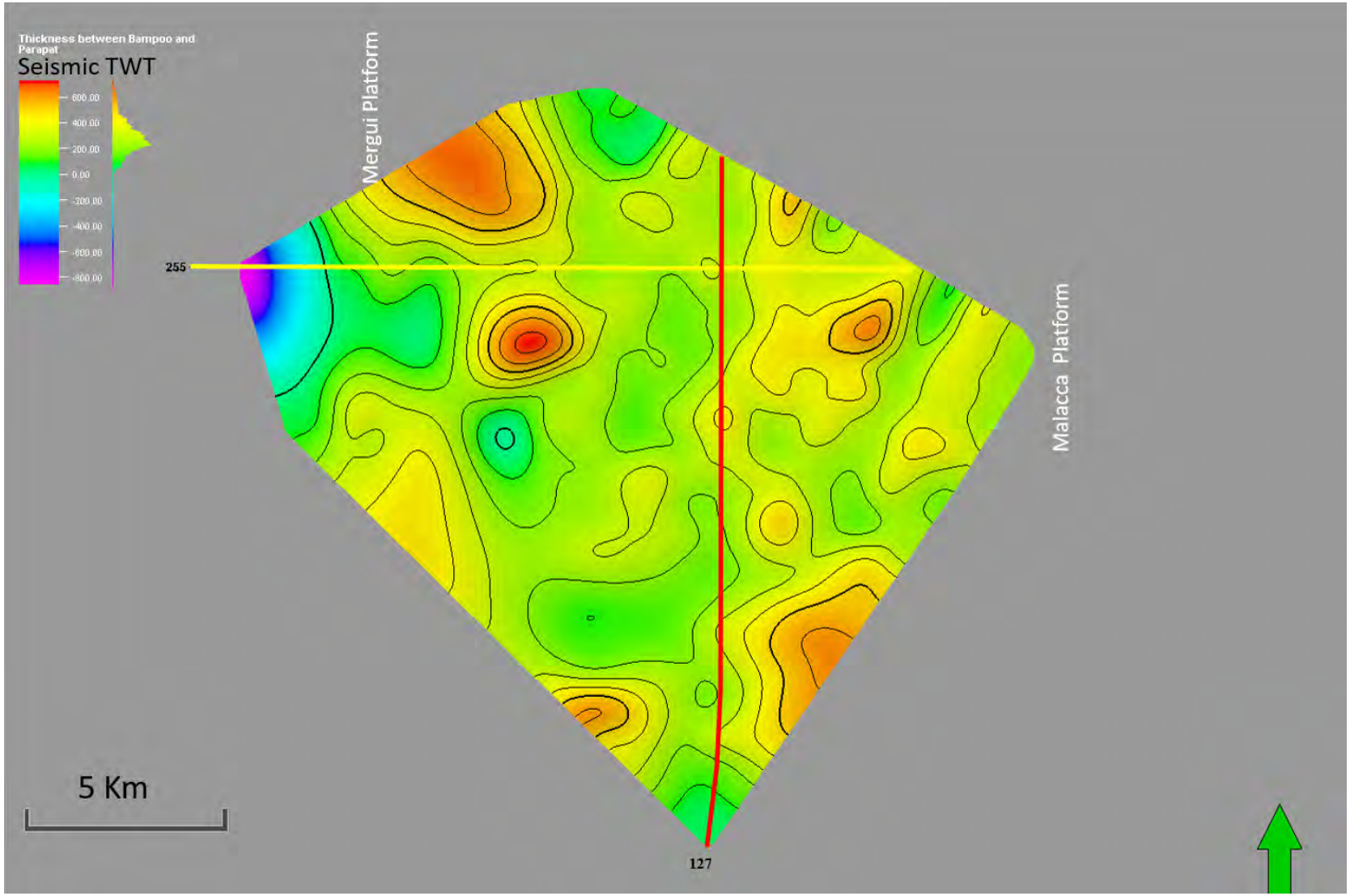

Figure 5-9 Isochron map of Bampo fm (Late Oligocene). The red line is the composite seismic line 127A-B-C (Figure 5-3), and the yellow is seismic line 255 (Figure 5-4).

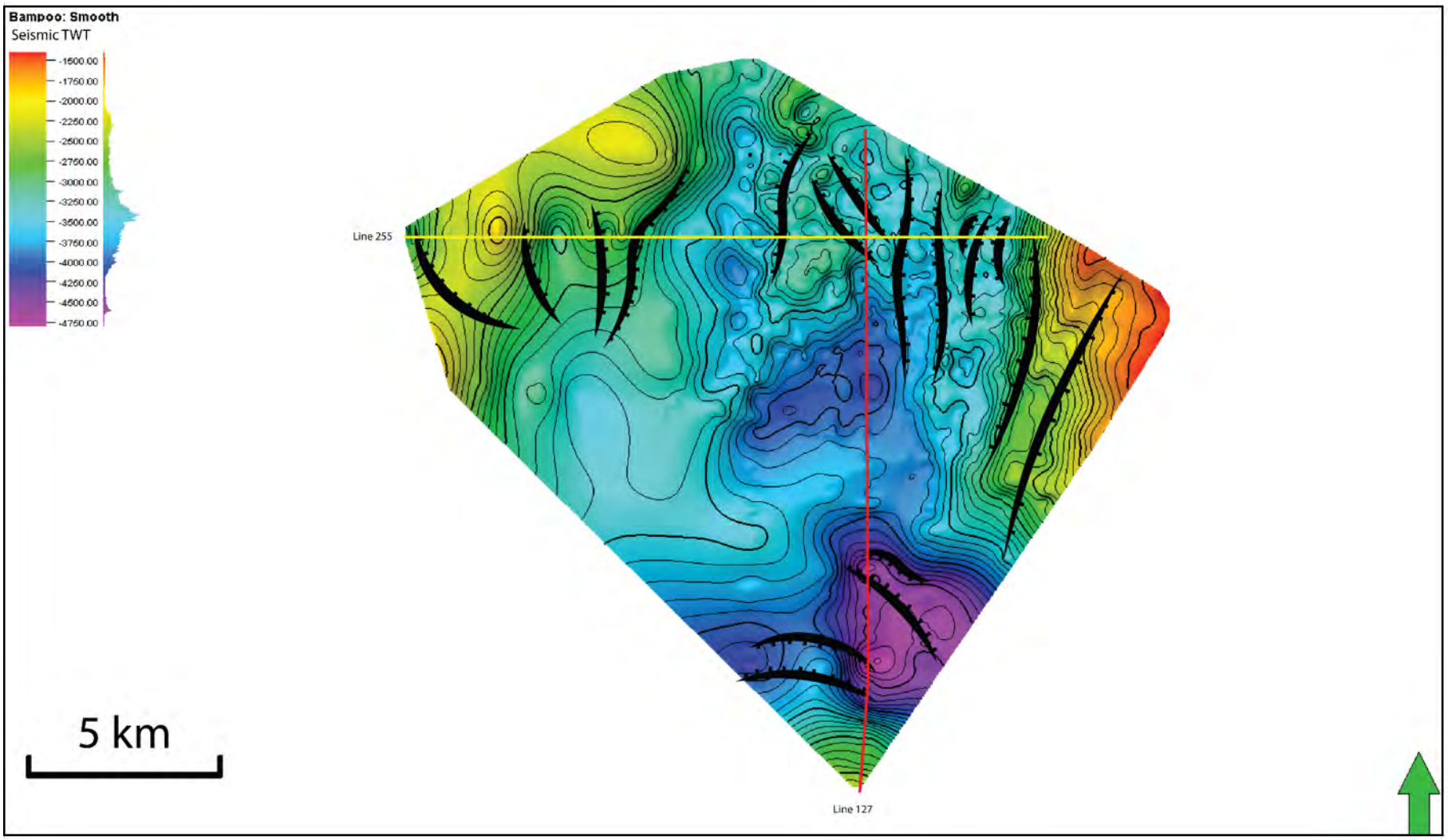

Figure 5-10 Bampo (Late Oligocene) time map offshore North Sumatra Basin. The red line is the composite seismic line 127A-B-C (Figure 5-3), and the yellow is seismic line 255 (Figure 5-4).

5.1.4 Belumai Formation (Early Miocene)

The Belumai Formation overlies the Bampo Formation in most of the basin, but it sits unconformably on the basement on some of the fault blocks that mark the edge of the Mergui Platform (Figure 5-4). There is little deformation that has affected this unit and it is of relatively uniform thickness, varying between 200 ms and 300 ms, with thinning observed on horst blocks, such as around the Mergui and the Malacca platforms (Figure 5-11). It is interpreted to mark the initiation of the post-rift sequence (Figure 5-12). In some places it is affected by folding that may indicate later inversion (Figure 5-4).

The Belumai Formation is characterised by low amplitude, parallel and discontinuous reflectors. Chaotic reflectors are also recognised in the slope and basinal areas (Figure 5-5). To the south reflectors are of high amplitude and define mounded shapes (Figure 5-3) which are probably related to carbonate platforms or build-ups. The stratigraphic well report shows that this unit is dominated by shales and sandstones in the deeper part of the basin (Figure 5-2).

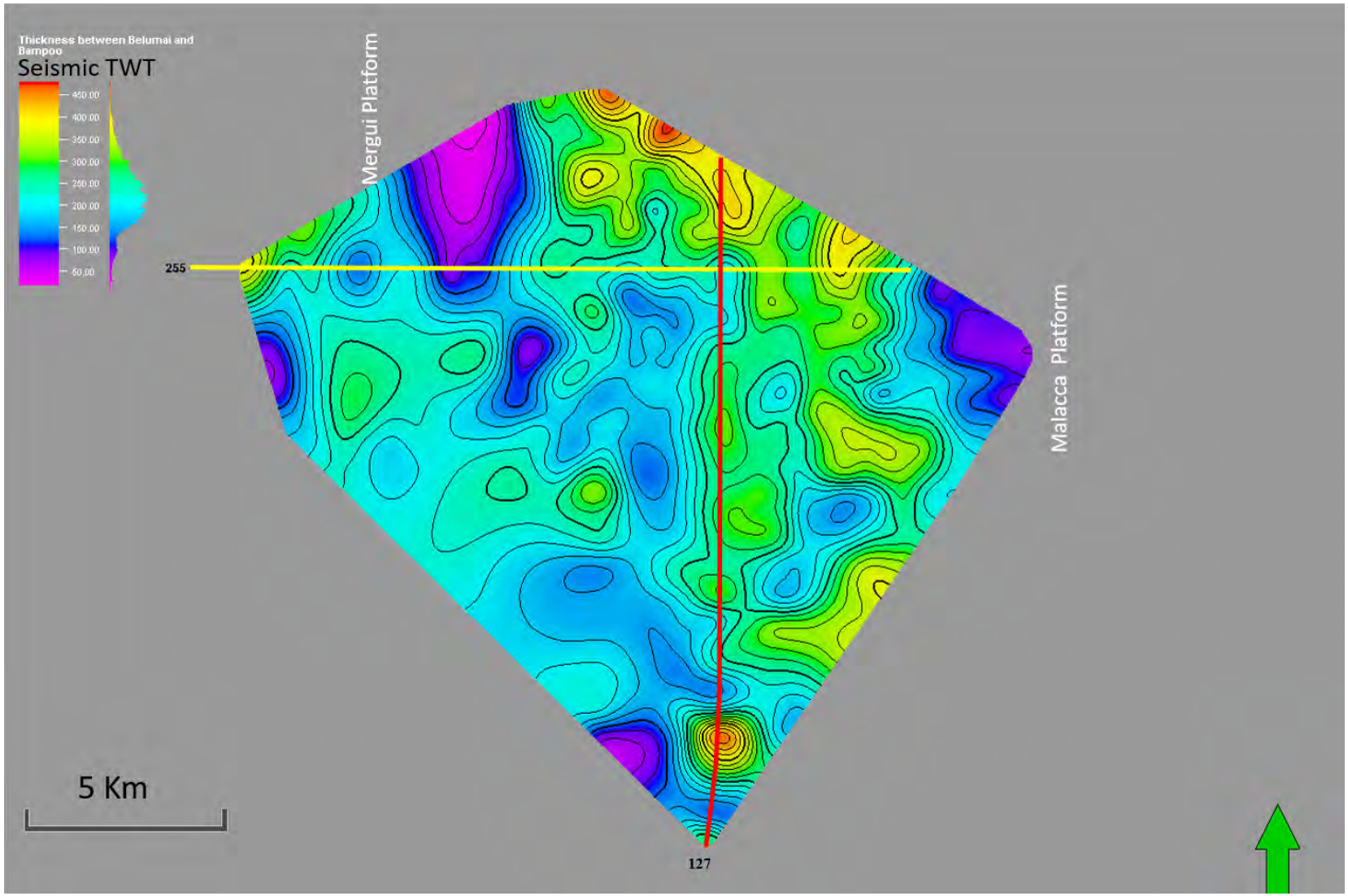

Figure 5-11 Isochron map of Belumai fm (Early Miocene). The red line is the composite seismic line 127A-B-C (Figure 5-3), and the yellow is seismic line 255 (Figure 5-4).

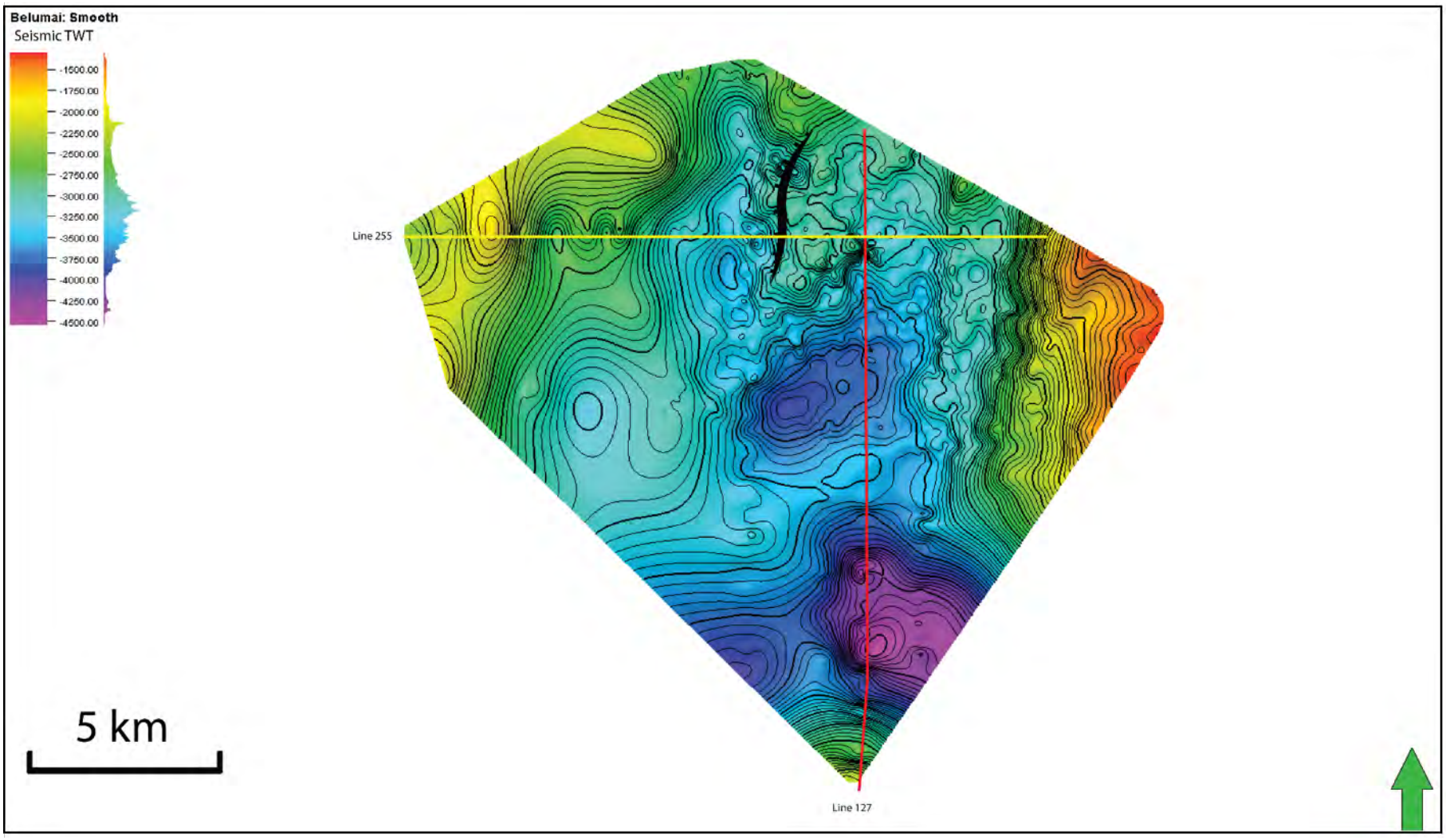

Figure 5-12 Belumai (Early Miocene) time map offshore North Sumatra Basin. The red line is the composite seismic line 127A-B-C (Figure 5-3), and the yellow is seismic line 255 (Figure 5-4).

5.1.5 Baong Formation (Middle Miocene)

The Baong Formation overlies the Peutu formation. The thickness of this unit is relatively uniform but it thickens in basinal areas, probably due to post-rift thermal subsidence, which created additional accommodation space in the basin centre (Figure 5-13).

The Baong Formation is characterized by moderate to high amplitude, continuous, and parallel reflectors (Figure 5-5) and it shows little evidence of deformation (5-14). From the stratigraphic well report, the lithology is dominated by sandstone to the west and shale to the east (Figure 5-2).

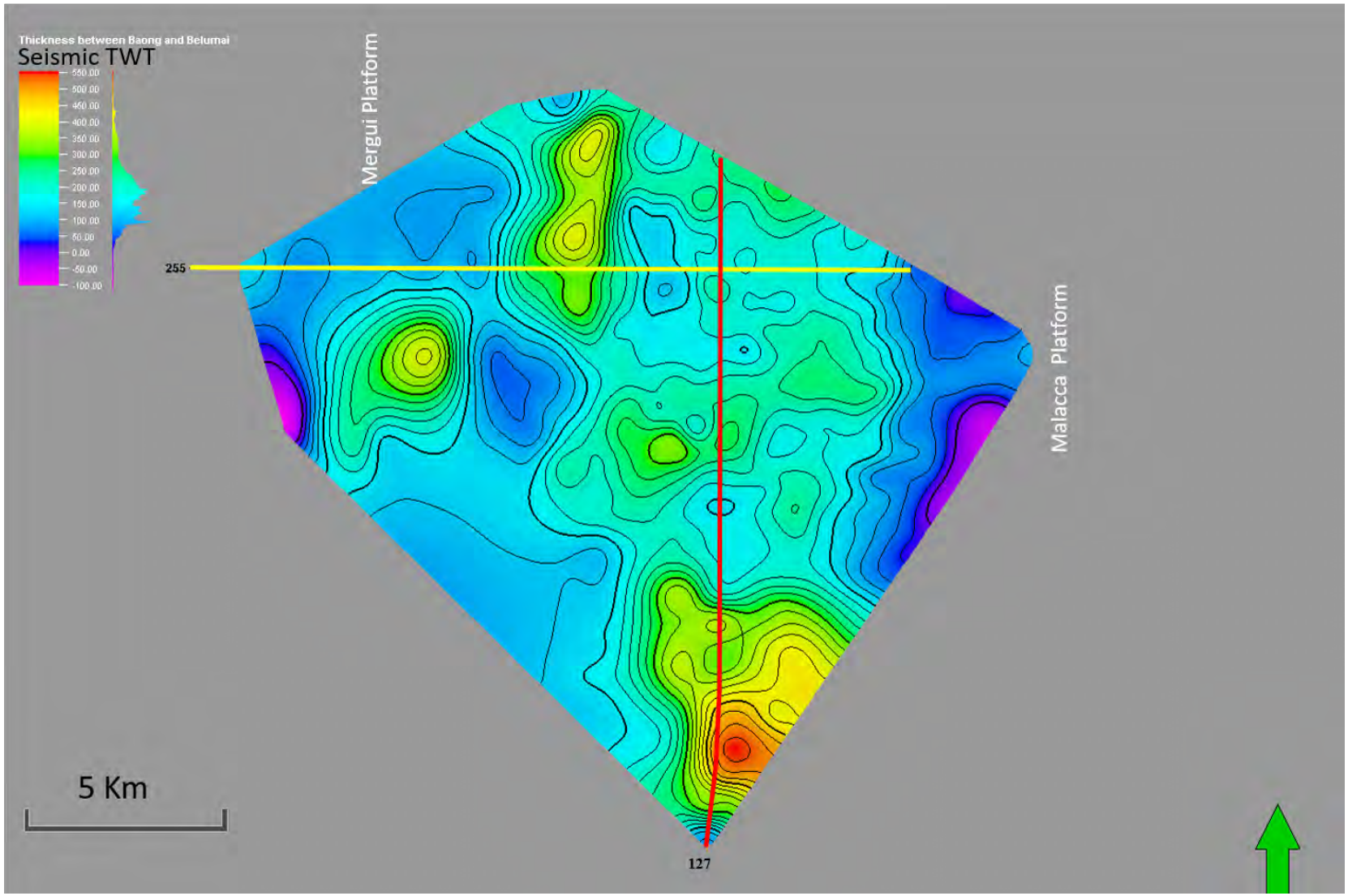

Figure 5-13 Isochron map of Baong fm (Middle Miocene). The red line is the composite seismic line 127A-B-C (Figure 5-3), and the yellow is seismic line 255 (Figure 5-4).

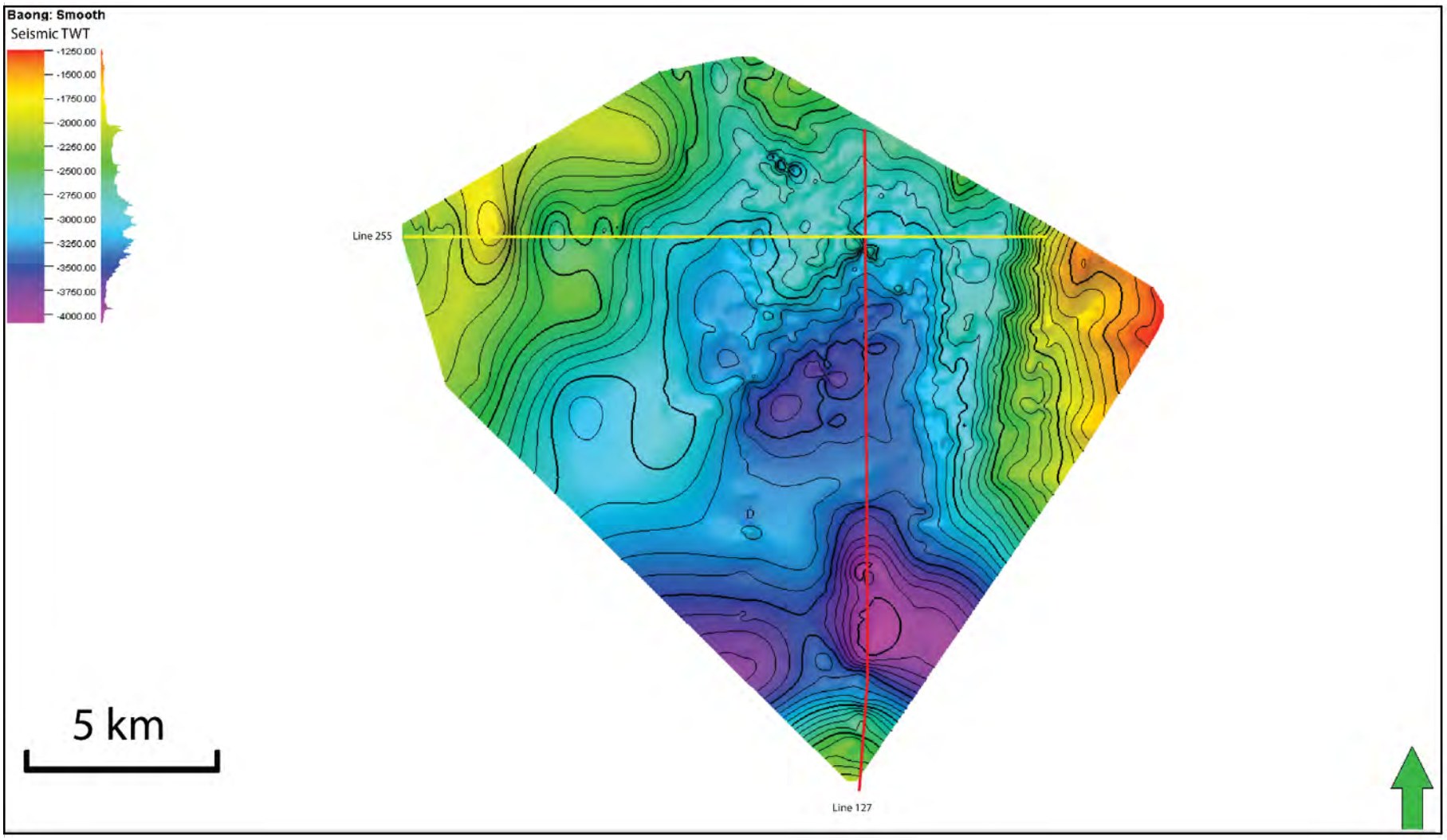

Figure 5-14 Baong (Middle Miocene) time map offshore North Sumatra Basin. The red line is the composite seismic line 127A-B-C (Figure 5-3), and the yellow is seismic line 255 (Figure 5-4).

5.1.6 Lower Keutapang Formation (Late Miocene)

The Lower Keutapang Formation was deposited conformably above the Baong Formation. The unit is of relatively uniform thickness (300 ms to 500 ms) (Figure 5-15). However, it is thicker in the south where it has been affected by folding (Figure 5-3). The base of the unit, and the underlying Baong Formation, is not folded which implies that there is a significant detachment within, or at the base of the Lower Keutapang Formation (Figure 5-3).

The Lower Keutapang Formation is characterized by low amplitude parallel, continuous reflectors in the south and high amplitude, parallel, continuous reflectors toward the north (Figure 5-5). The lithology of this unit is dominated by shales (Figure 5-2), which is associated with a marine environment. The presence of thick shale enables the development of detachment horizons.

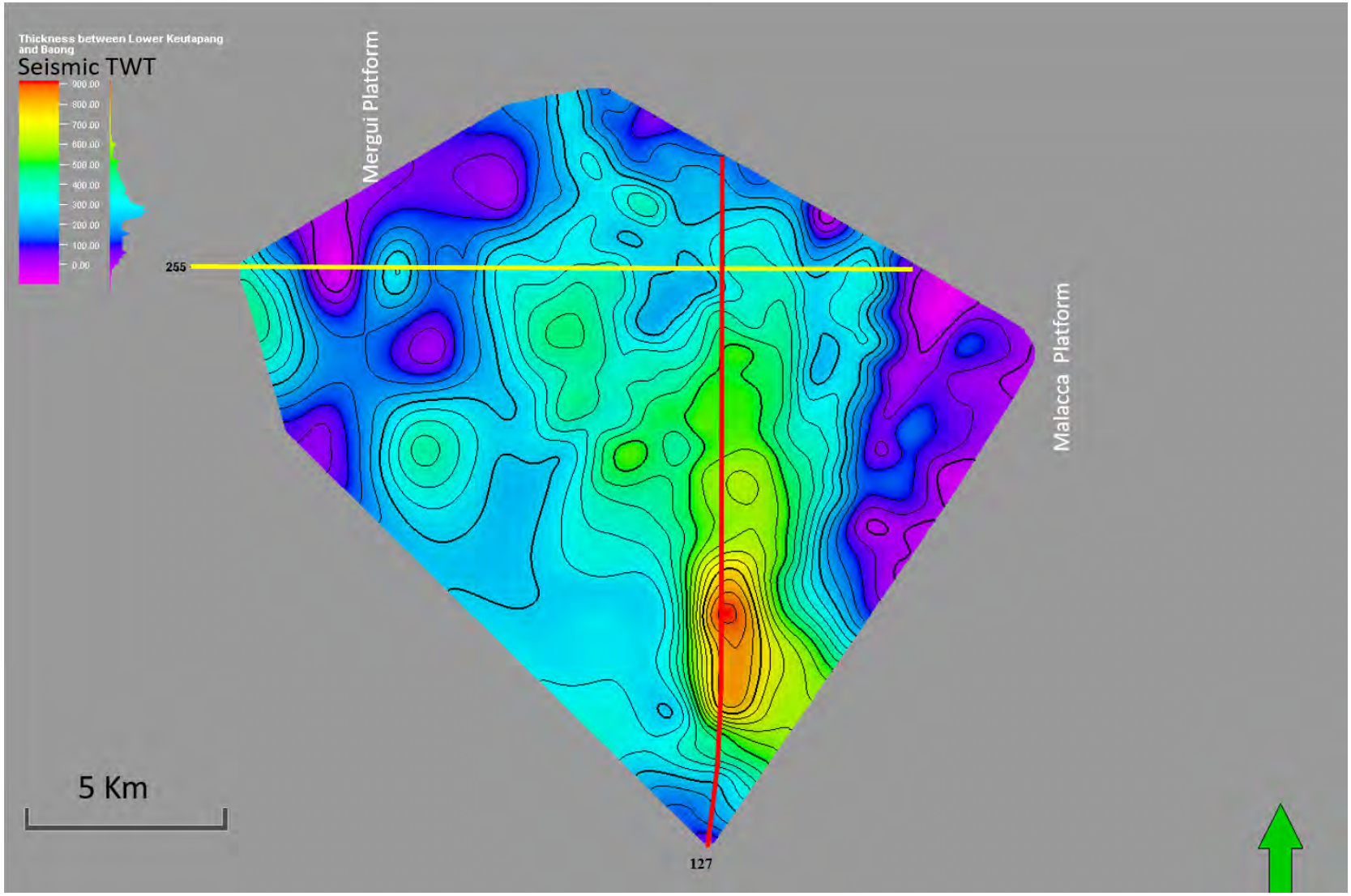

Figure 5-15 Isochron map of Lower Keutapang fm (Late Miocene). The red line is the composite seismic line 127A-B-C (Figure 5-3), and the yellow is seismic line 255 (Figure 5-4).

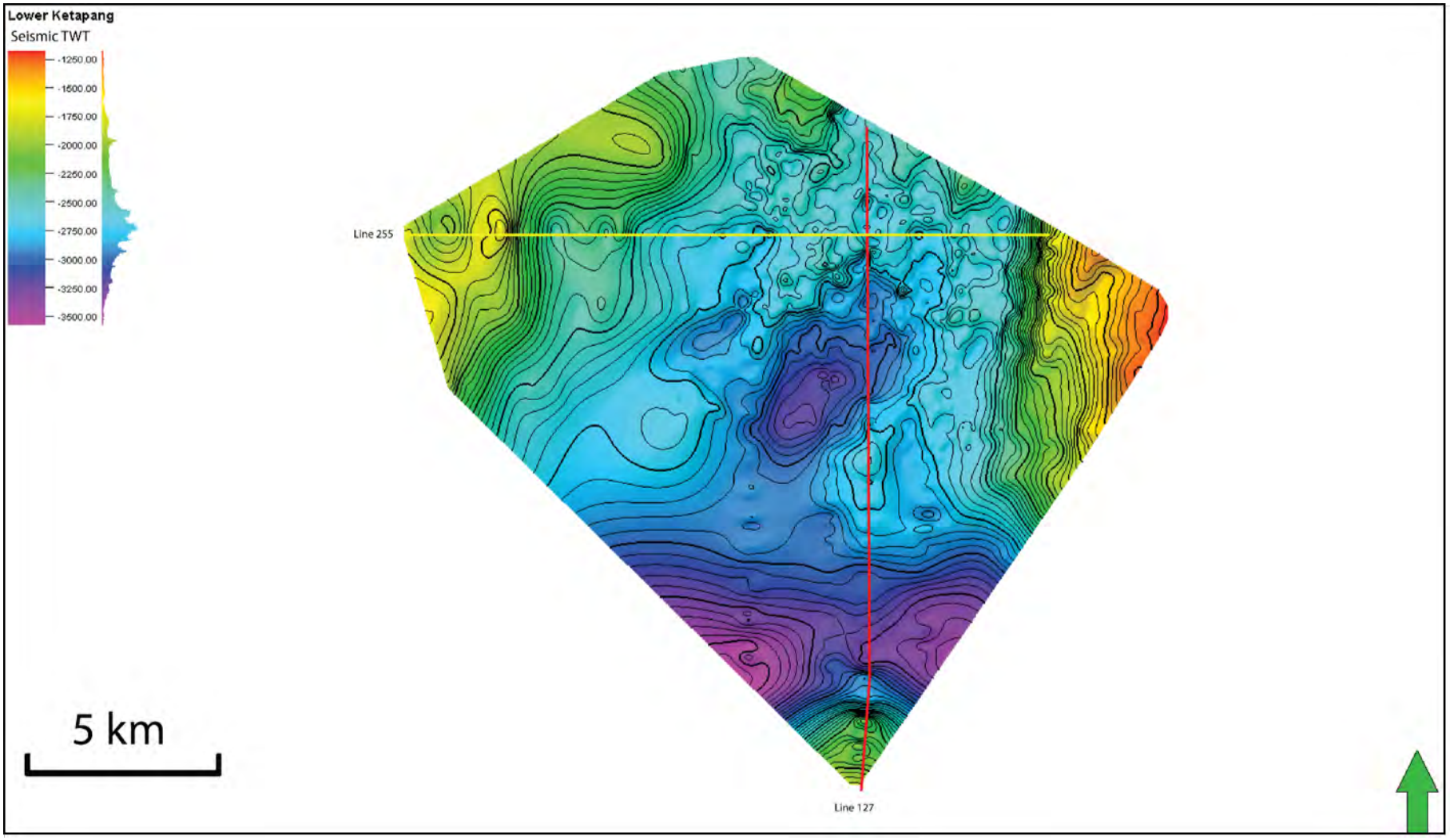

Figure 5-16 Lower Keutapang (Late Miocene) time map offshore North Sumatra Basin. The red line is the composite seismic line 127A-B-C (Figure 5-3), and the yellow is seismic line 255 (Figure 5-4).

5.1.7 Upper Keutapang Formation (Late Miocene)

The Upper Keutapang Formation is deposited conformably above the lower Keutapang Formation. It has a relatively uniform thickness of about 500 ms (Figure 5-17), but increases in thickness into the centre of the basin, again consistent with post-rift subsidence (Figure 5-3). The sequence also thickens to the south due to shortening and compression that occurred during the Pliocene-Pleistocene.

The first phase of compression in the basin is also recorded by a symmetrical anticline that developed towards the western margin of the basins (Figure 5-4). Onlap of the Upper Keutapang Formation onto the anticline indicates that it clearly began to form at this time (Figure 5-18 for illustration).

Several minor extensional faults are also present in both the Upper and Lower Keutapang formations. Most of the faults detach in the underlying Baong Formation, although some also propagated and reactivated major Oligocene rift faults (Figure 5-4).

The Upper Keutapang Formation is characterised by moderate to high amplitude parallel and continuous seismic reflectors. According to well reports, the unit is shale-dominated (Tsukada et al., 1996), although sandstone is also present in the upper part of the formation, towards the east (Figure 5-2).

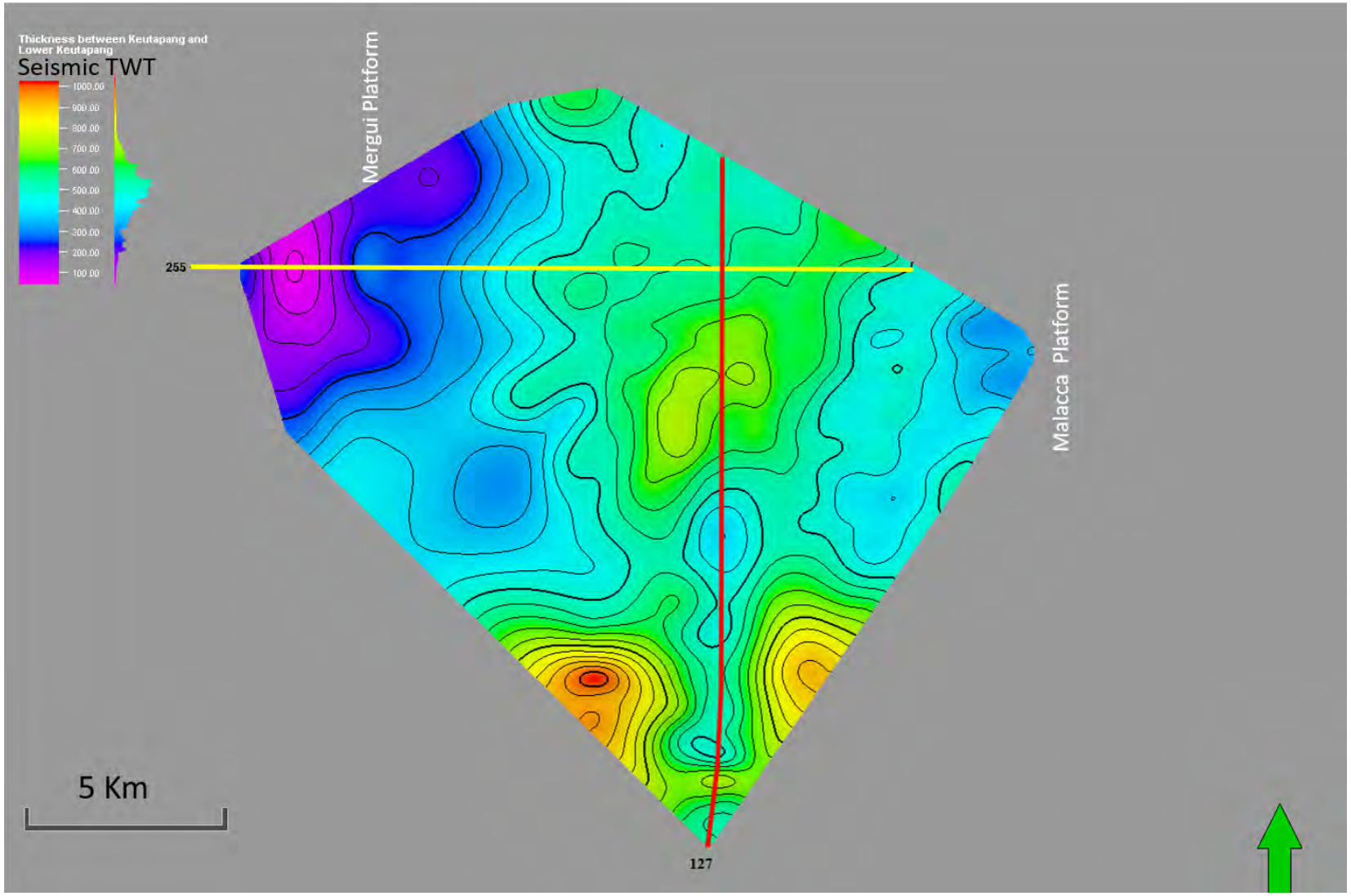

Figure 5-17 Isochron map of upper Keutapang fm (Late Miocene). The red line is the composite seismic line 127A-B-C (Figure 5-3), and the yellow is seismic line 255 (Figure 5-4).

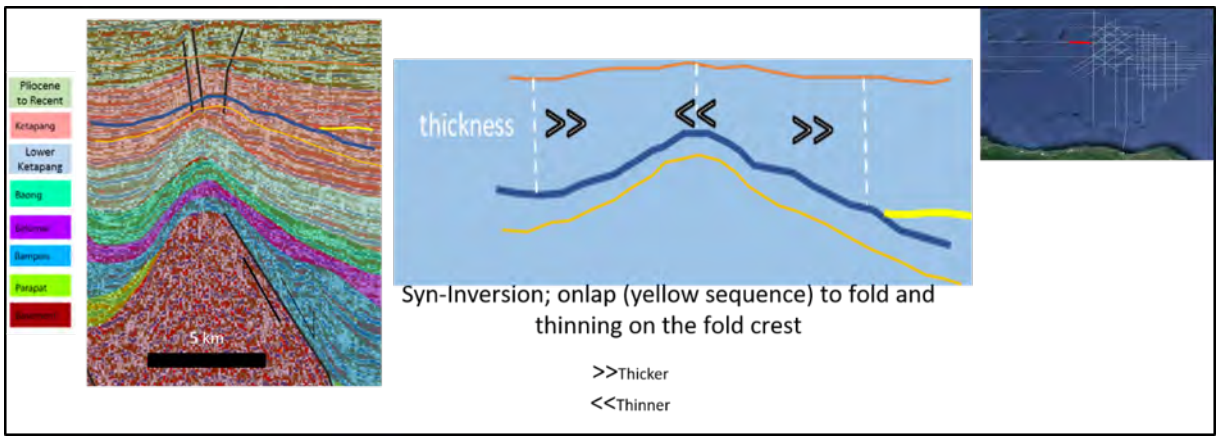

Figure 5-18 an illustration to explain the kinematic (late Miocene inversion) of syn-inversion in red box of line 255 Figure 5-4.

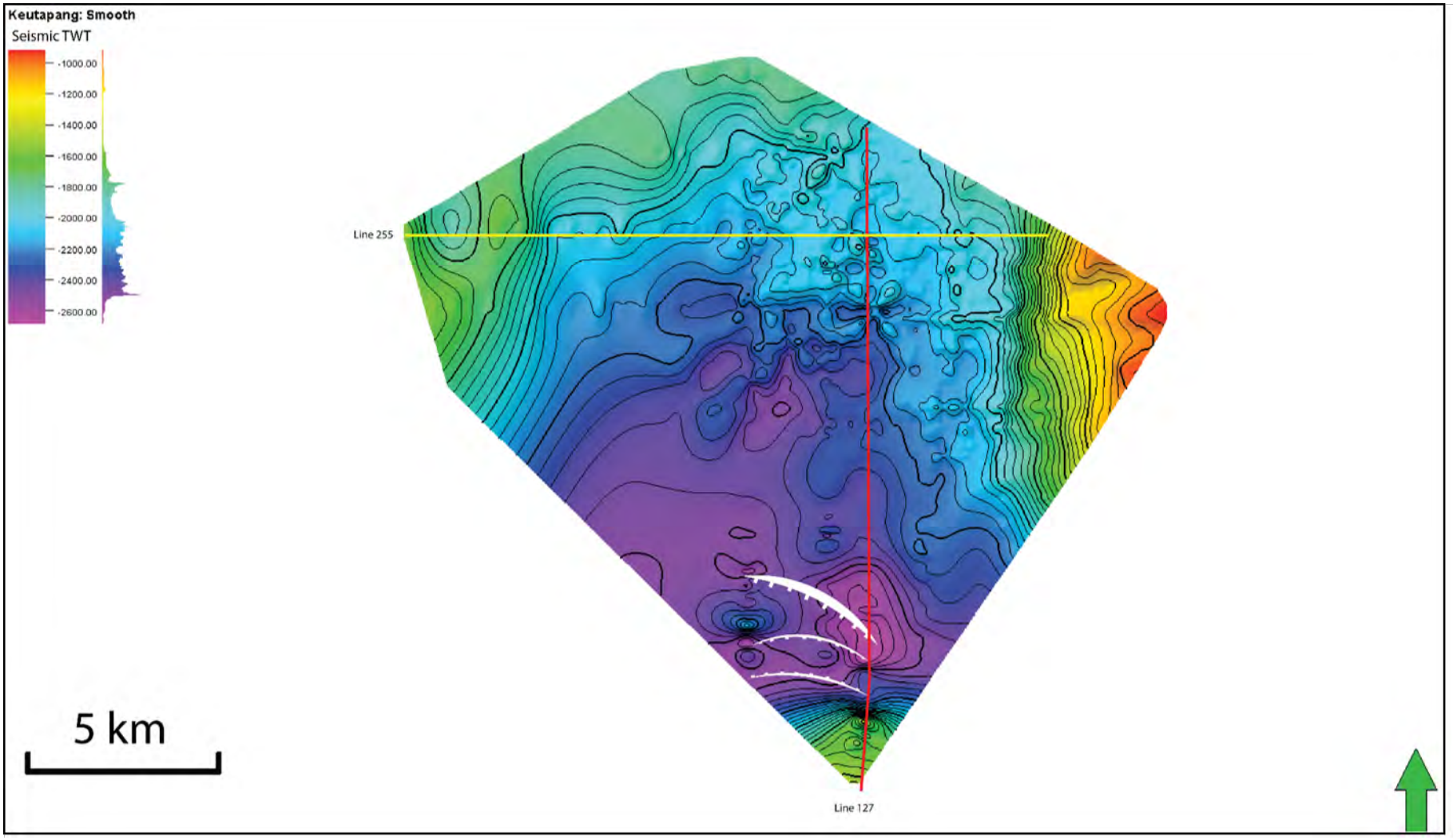

Figure 5-19 Upper Keutapang (Late Miocene) time map offshore North Sumatra Basin. The red line is the composite seismic line 127A-B-C (Figure 5-3), and the yellow is seismic line 255 (Figure 5-4).

5.1.8 Pliocene to Recent sediments

Sediments above the Keutapang Formation have not been allocated a formal lithostratigraphic name in the offshore North Sumatra Basin, but they are equivalent to the Seurula and Julu Rayeu Formations in the onshore basin. In the offshore, the thickness of this succession ranges from 1600 ms in the south to 300 ms in north (Figure 5-20) forming a distinct sediment wedge derived from the uplifted Barisan Mountains to the south.

This sequence is cut by reverse faults in the south of the area that propagate up to the seabed and define the geometry of the shelf and basinal areas (Figure 5-21). Folds are also present, with clear onlap in the upper part of this sequence (Figure 5-3), further indicating the relatively recent nature of this deformation. In contrast, the northern part of the basin is characterised by undeformed sediments or areas of minor extensional faulting (Figure 5-4).

This unit is characterised by high amplitude, continuous parallel reflectors. However, chaotic and transparent reflectors are identified at the base of the slope marking the edge of the Malacca Platform in the east (Figure 5-5). The lithology of this unit is a mixture of sandstones and shales (Tsukada et al., 1996), with the south part, close to onshore, dominated by sandstones (Figure 5-2).

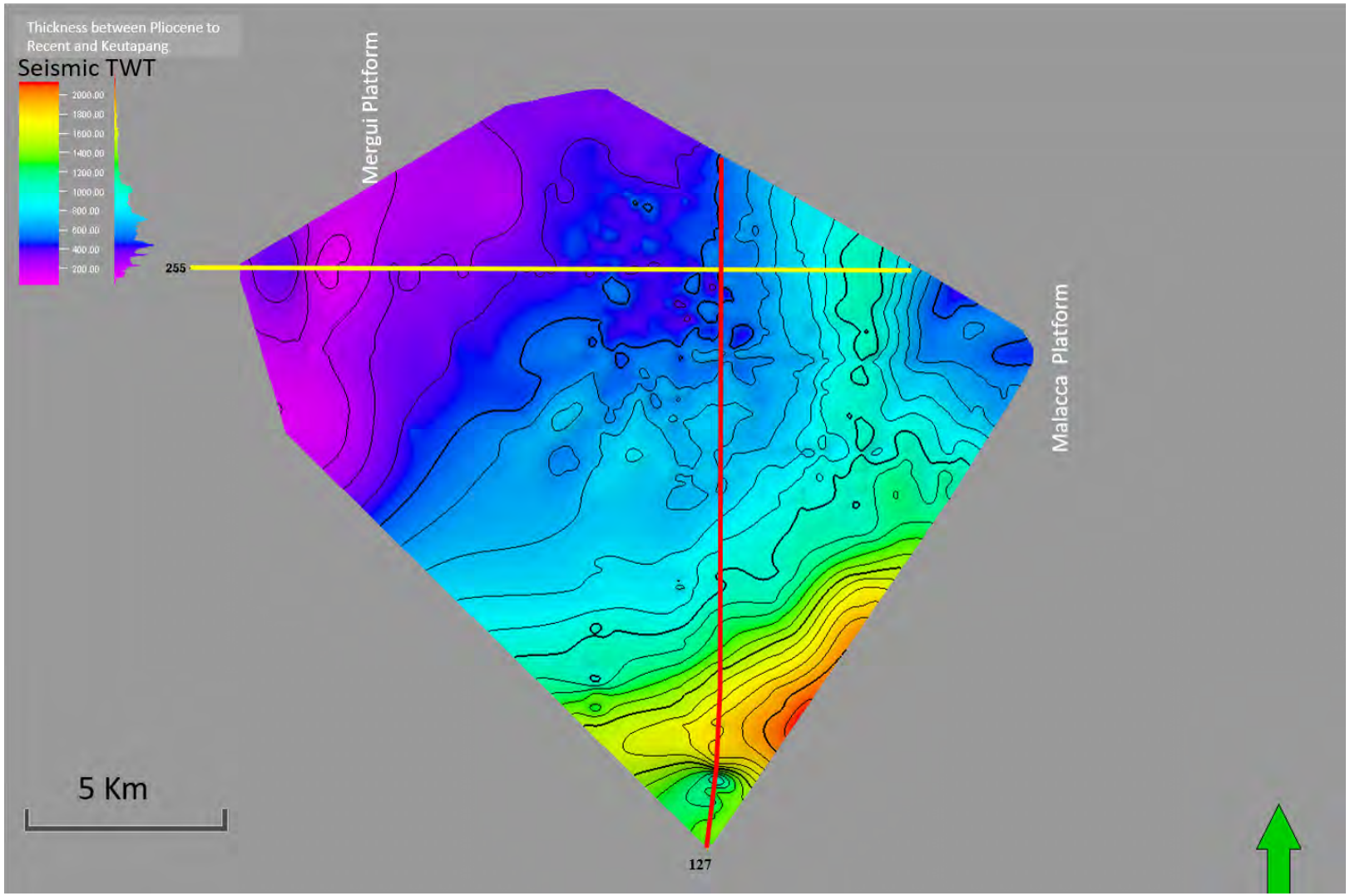

Figure 5-20 Pliocene-to recent Isochron map, offshore North Sumatra Basin. The red line is the composite seismic line 127A-B-C (Figure 5-3), and the yellow is seismic line 255 (Figure 5-4).

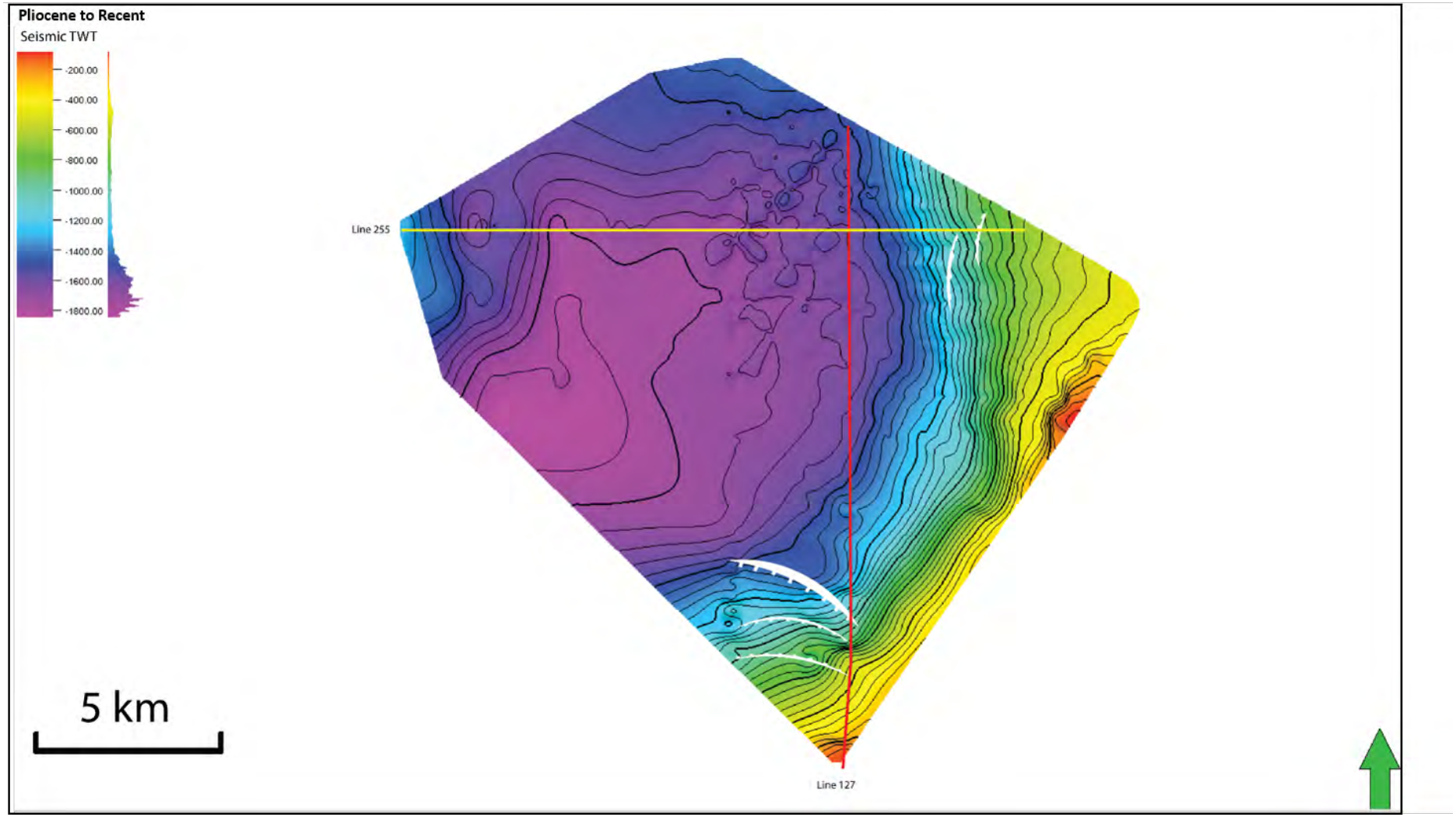

Figure 5-21 Pliocene-to recent time map offshore North Sumatra Basin. The red line is the composite seismic line 127A-B-C (Figure 5-3), and the yellow is seismic line 255 (Figure 5-4).

5.2 Structural Styles of Offshore NSB

5.2.1 Oligocene age extensional rift faults

Time structure maps of the Top Basement, Parapat and Bampo formations (Figures 5-6, 5-8 and 5-10) show the major extensional faults that define the Offshore North Sumatra Basin. The largest faults trend north-south and separate the North Sumatra Basin from the Malacca Platform in the east and the Mergui Platform in the west, while smaller faults divide the basin into a number of separate horsts and graben. The boundary of the Mergui Platform is characterised by domino style faults which define half graben structures (Figure 5-4), while the boundary of the Malacca Platform is defined by planar faults which define more symmetrical graben (Figure 5-4 and 5-22).

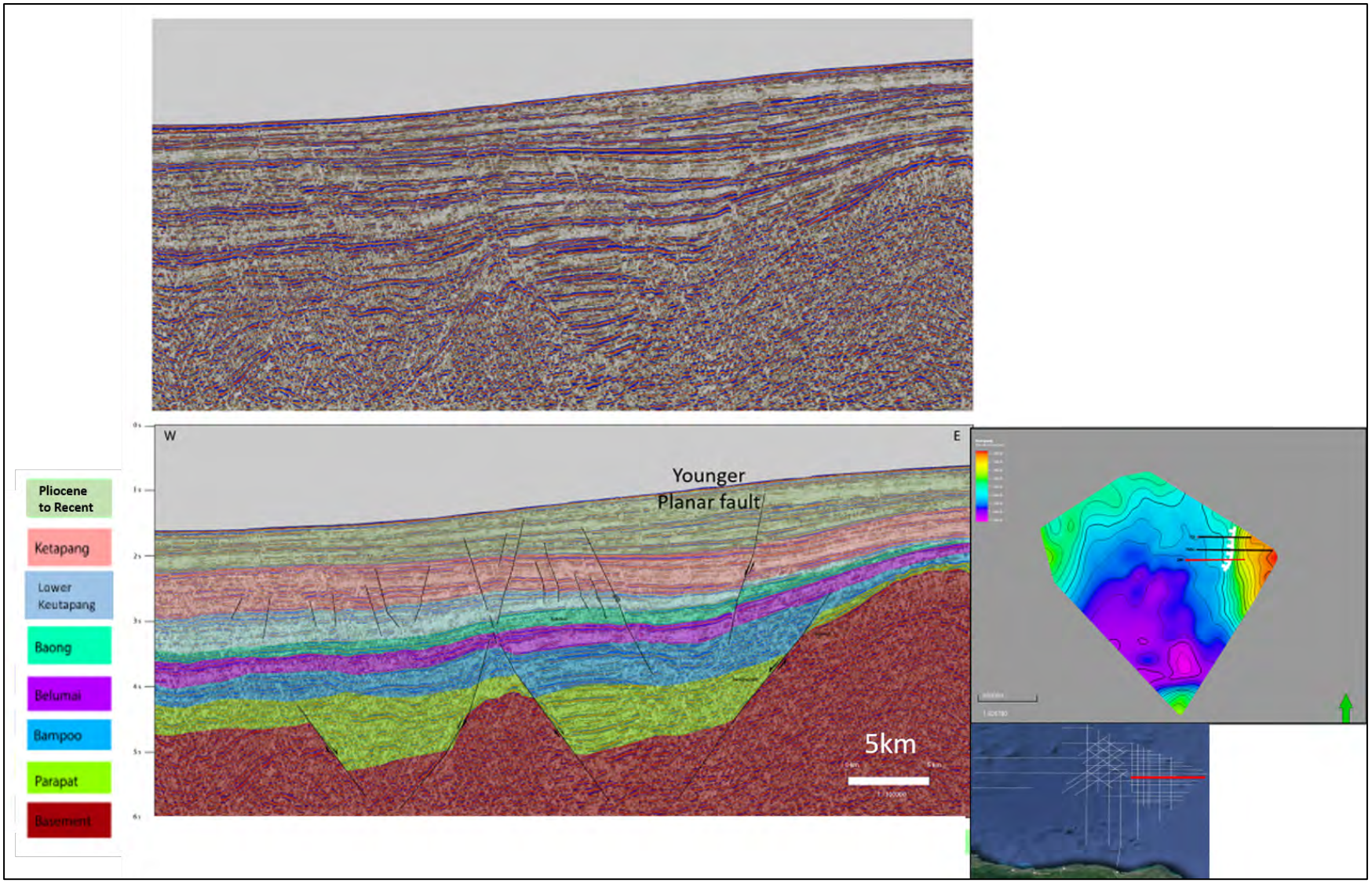

Figure 5-22 Seismic line 245. The line is located east toward the Malacca Platform, marked by the red line on the map (bottom right). The white polygon is the fault orientation (Younger (Pliocene/Pleistocene planar fault).

5.2.2 Younger extensional faults

The offshore seismic lines indicated that a large number of normal faults developed late Miocene (Ketapang Formation) and Pliocene-Pleistocene sequences. Most faults have small displacement and were difficult to correlate laterally, so they could not be mapped using the 2D seismic line with the sparse grids.

Late Miocene Normal faults

A dense network of normal faults developed in the late Miocene Ketapang Formation (Figure 5-4, line 255 pink formation). They can be seen on most of the seismic lines in the offshore North Sumatra Basin, but they are most common in the northern part of the basin, between the Mergui to Malacca platforms. For example, the seismic lines 465 and 460, located northwest offshore, indicate the faults developed in the upper Keutapang successions (pink formation in Figure 5-23 and 5-24).

Lines 245 and 249A, located northeast offshore of the North Sumatra Basin, also show that the faults occurred in a similar formation (pink formation Figure 5-30 and 5-29). Some of these faults propagated from older formations, and some were detached at the base of the same formation. It is difficult to say that these faults are tectonic faults because they are minor and are largely confined to the pink horizon. Thus, these faults may considered as polygonal faults relating to the dewatering.

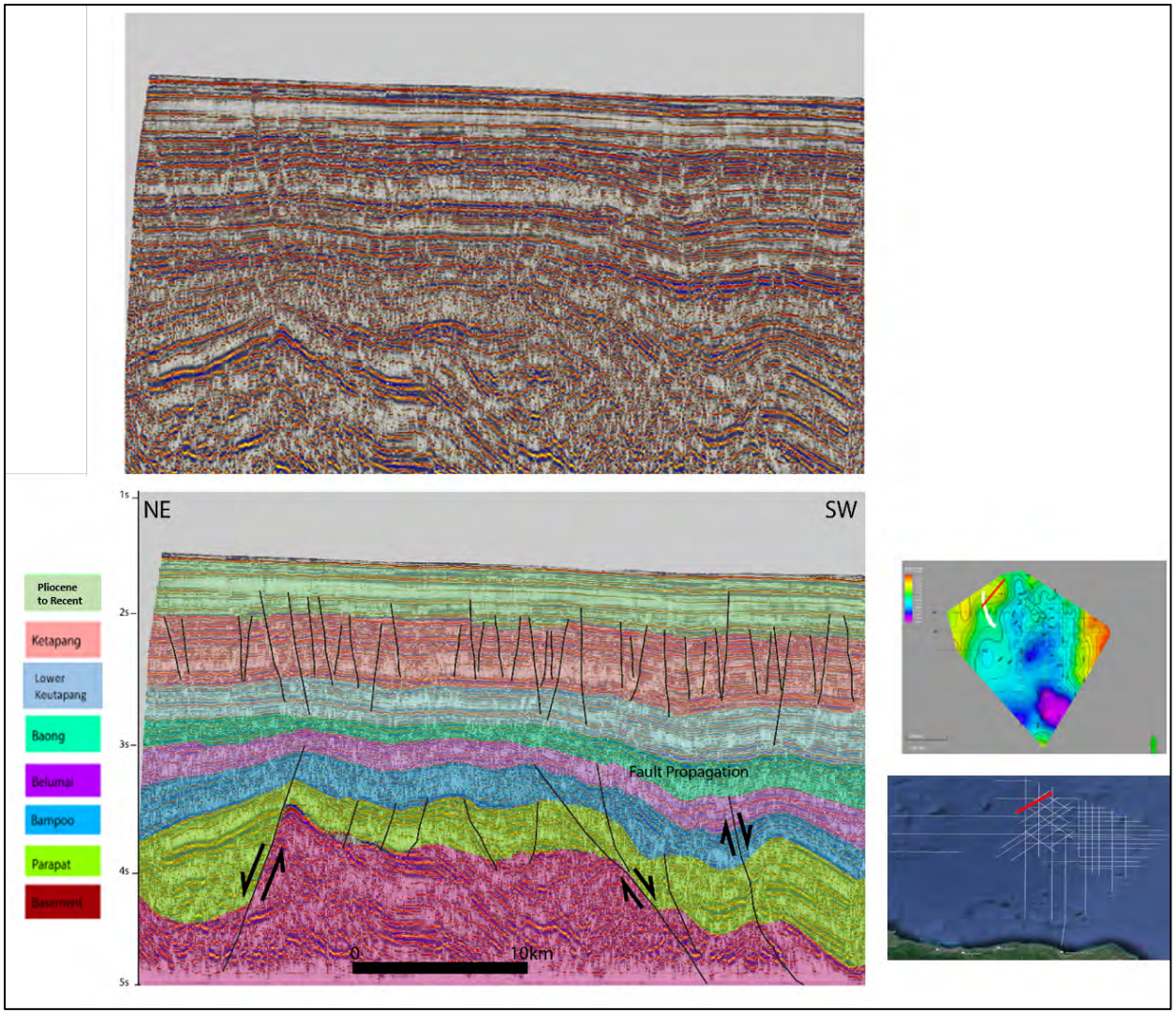

Figure 5-23 Seismic line 465 shows the polygonal faults within Ketapang sequence. This figure also show fault propagation fold formed during the Belumai depositing in the early Miocene. On the right is the time map of the Belumai formation (Early Miocene), showing the fault trend of a slightly oblique north-south (white polygon). The location of this line is guided by a red polygon that overlays the google map (bottom right).

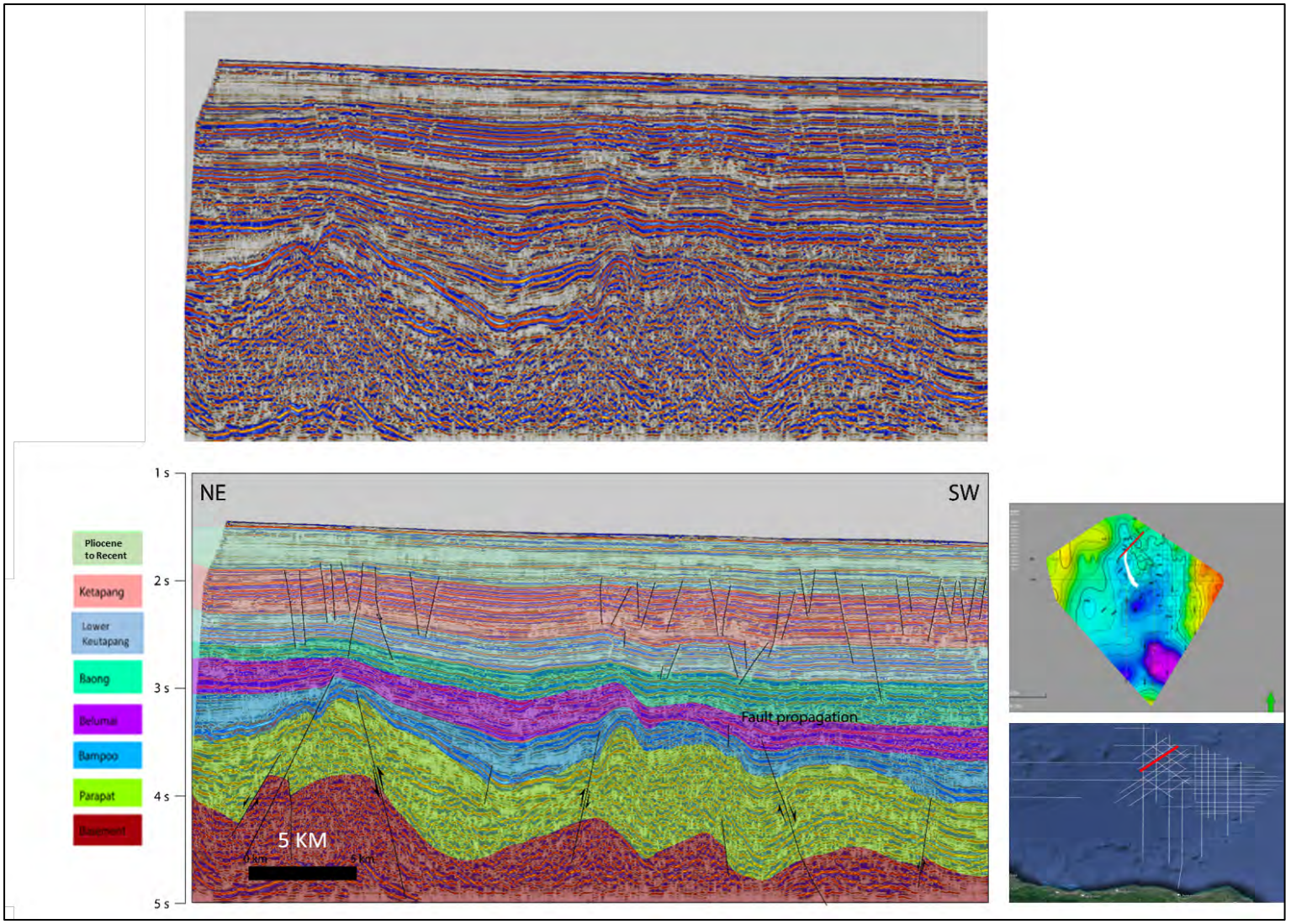

Figure 5-24 Seismic line 467 shows the polygonal faults within Ketapang sequence. This figure also show fault propagation fold formed during the Belumai depositing in the early Miocene . The line is located north, marked by the red line on the map (bottom right). The white polygon is the fault orientation (Early Miocene fault related to the fold).

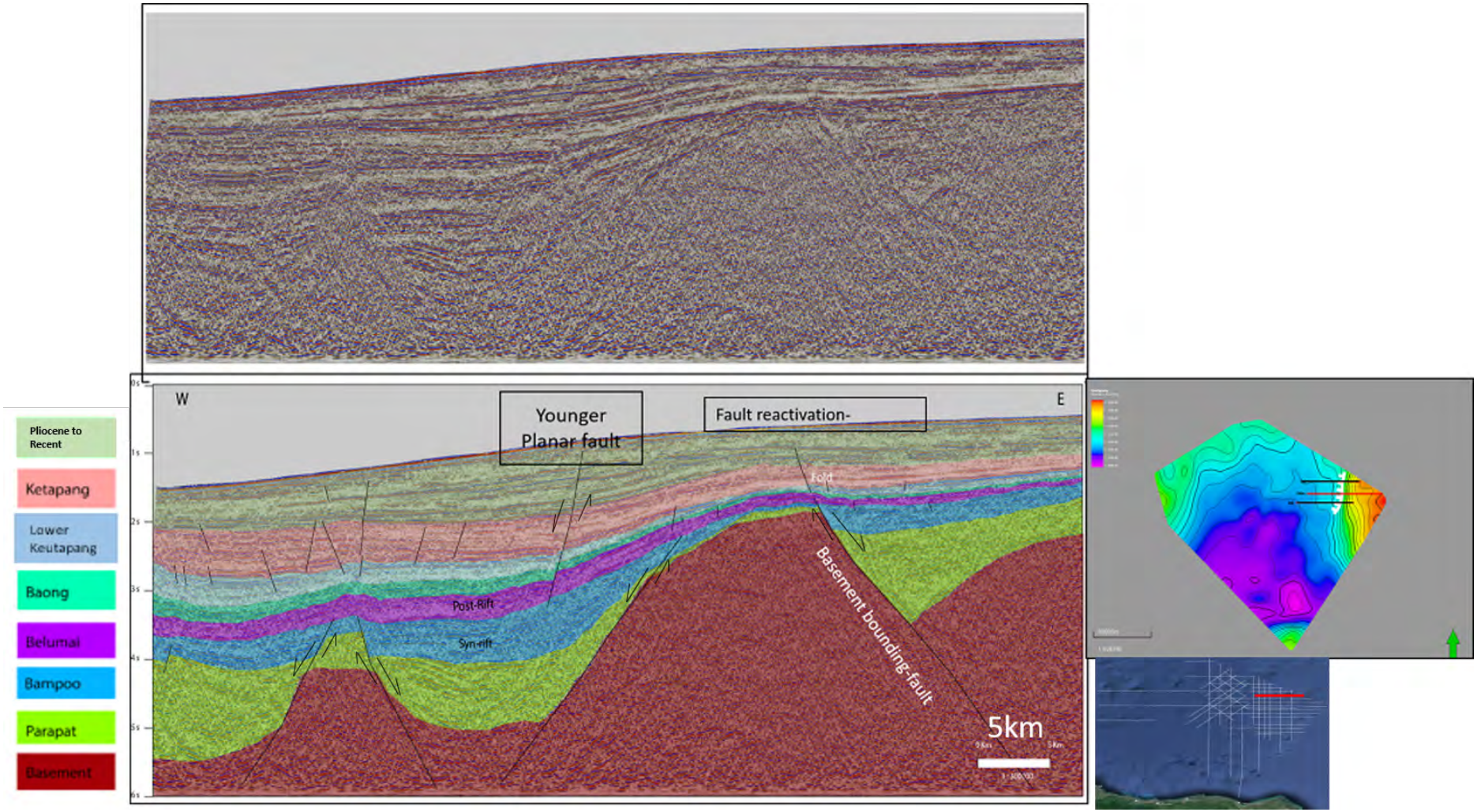

Figure 5-25 Seismic line 249A. The line is located northeast, marked by a red line on the map (bottom right). The white polygon is the fault orientation (Younger (Pliocene/Pleistocene planar fault).

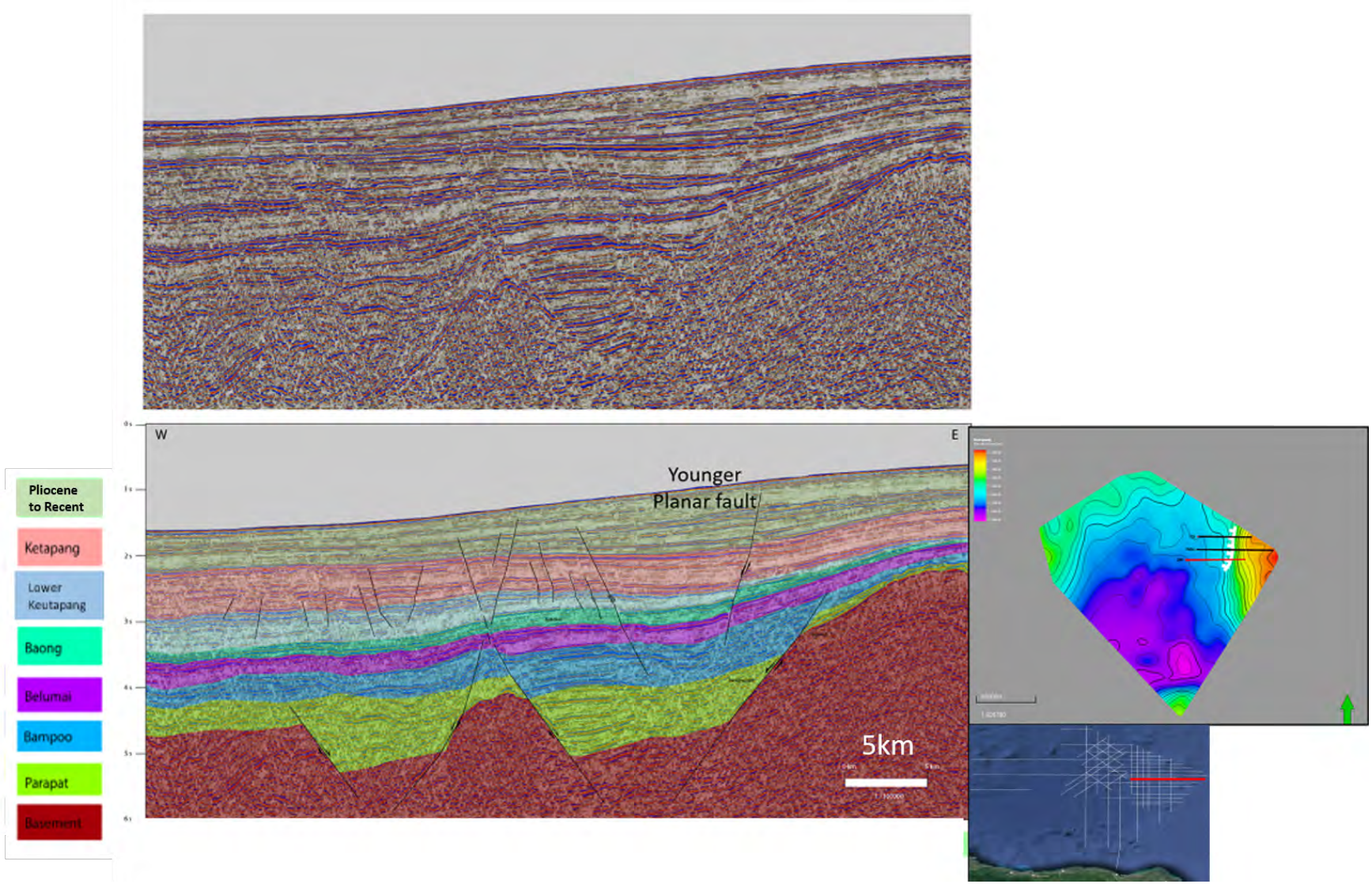

Figure 5-26 Seismic line 245. The line is located northeast, marked by the red line on the map (bottom right). The white polygon is the fault orientation (Younger (Pliocene/Pleistocene planar fault).

Pliocene-Pleistocene faults

Several extensional faults, such as planar and curved (listric) faults, were identified within the Pliocene/Pleistocene formations (light green formation in Figure 5-25, 5-26, and 5-27). The faults propagated through older sedimentary rocks, and some of them reactivated the older faults.

A large and apparently planar fault is located in the northeast of the offshore North Sumatra Basin, adjacent to the Malacca Platform. The fault is below the seabed and propagated up from the syn-rift succession. This fault has a north-south orientation and dips west (Figure 5-25 and 5-26, white polygon in the map).

Some other planar faults are relatively minor and could not be mapped due to the sparse data. In the main, these faults are confined to post-rift sequences (Figure 5-25, 5-26, and 5-27). However, there is evidence of fault reactivation to the east of the seismic line 235 (Figure 5-27). This fault propagated and reactivated the major extensional basement bounding fault. The reactivation also caused the minor folding at the tip of the major extensional fault in the form of a monocline (Figure 5-27). Figure 5-28 shows how such a monocline might form.

Another prominent feature is the listric growth fault shown in seismic line 235 (Figure 5-27). This fault cut propagated from the Bampo Formation and stopped within the upper part of the Pliocene/Pleistocene formations, just a few hundred milliseconds below the seabed. The syn-kinematic sediments along the hanging wall of this fault indicates that this fault was reactivated several times before the Pliocene/Pleistocene time. The first was during the deposition of the Baong Formation (Middle Miocene), and the second was during the deposition of the Keutapang Formation (Late Miocene). The fold also formed below this fault, within the Belumai Formation, probably to compensate for the reactivation of the older basement bounding fault.

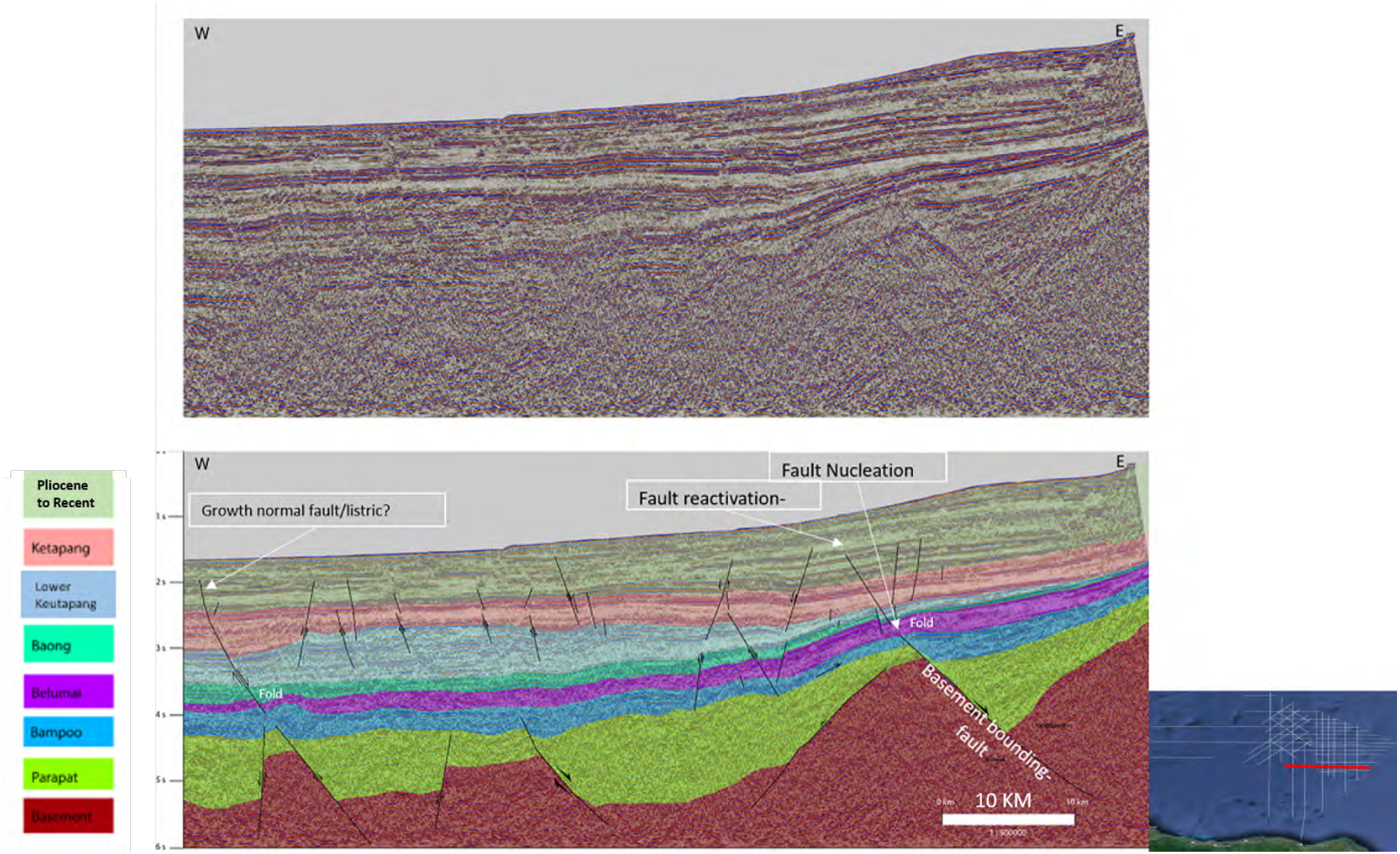

Figure 5-27 Seismic line 235. The line is located in the offshore area, marked by a red line on the map (bottom right).

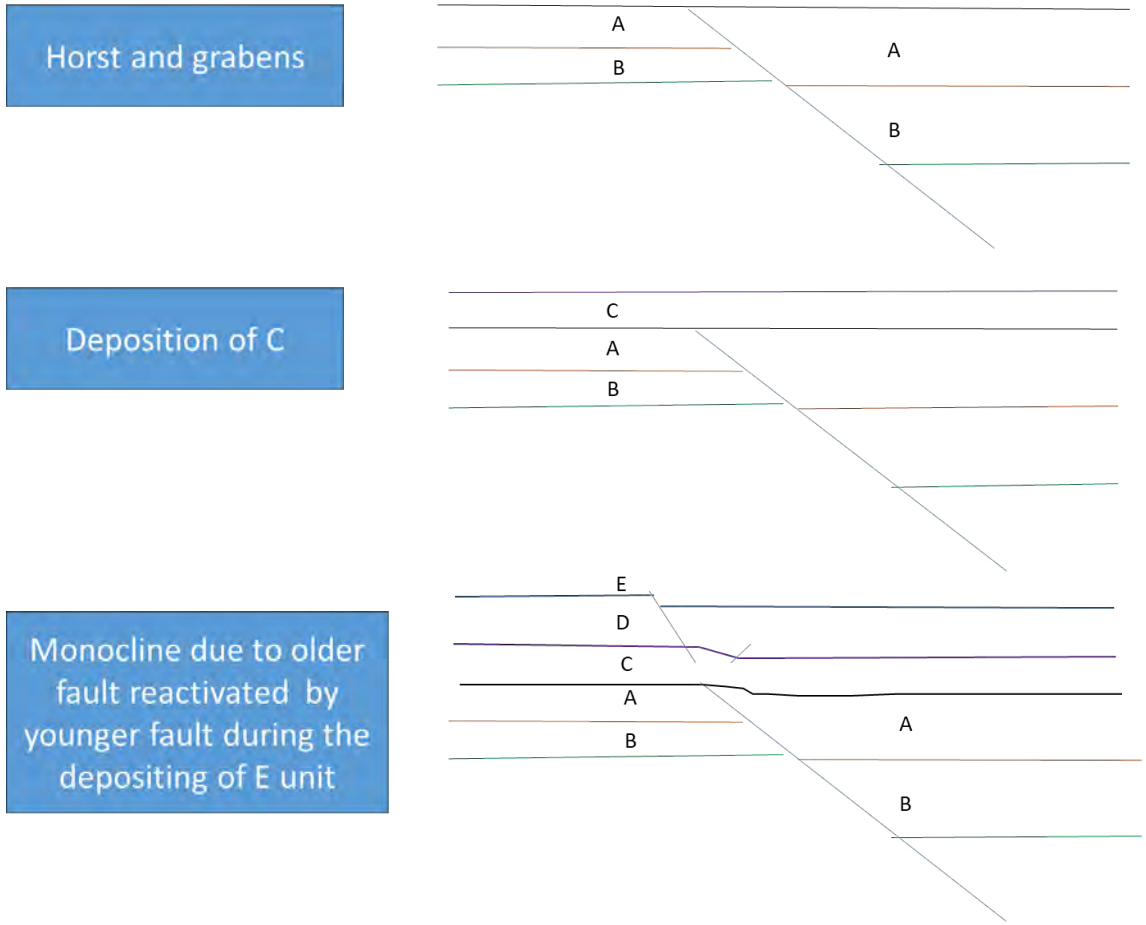

Figure 5-28 Illustration of minor monocline formed above the fault tip to explain the minor fault structure in Figure 5-27.

5.2.3 Folds related to basin inversion

Some folds related to the inversion were observed offshore of the North Sumatra Basin. These folds occurred in different periods of geological ages and mechanisms.

Early Miocene folds

Miocene fault propagation folds are observed in the north area of the offshore North Sumatra Basin. The Fault is slightly oblique to the north-south trend and dips southwest (see the white polygon in structural time map Figure 5-23 and 5-24).

Although the seismic quality is poor, the fault was evidenced by the offset of the sequence within the Parapat Formation (Figure 5-23). The offset indicates that the fault is the reverse fault.

The fault inverted the syn-rift successions of the Bampo and Parapat formations and deformed them to asymmetrical folds (anticline). The timing of the inversion is indicated by the difference in thickness of the Belumai formation (early Miocene) between the crest and flanks of the fold, thinning above the fold and thickening at the flanks (Figure 5-23, marked by the white box in the Belumai formation).

Folds structures related to inversion were also observed from an un-interpreted image of new 3D seismic (Figure 5-29). This image was published by PGS (PGS, 2022) without any information about the orientation, scale, and interpreted horizons. However, this new line comes from a similar area to some 2D seismic lines that have been interpreted in this study. This new line was compared to the best 2D seismic line, line 255 (Figure 5-4), to identify similarities based on the major sequences, such as post-rift and thickness. It is assumed that the seabed is at the top of this new seismic line. The new line was also interpreted based on stratigraphic events, such as unconformities associated with the observed tectonic events.

The new seismic line shows local symmetrical folds in the syn-rift successions which are interpreted as inversion structures (Figure 5-29). No faults are associated with the folds; thus, it is proposed that the folds are associated with detachments. However, the décollement horizons for this fold could not be identified because the seismic line was cut/incomplete in the lowest section.

Furthermore, the timing of the inversion is indicated by the syn-kinematic strata on and around the fold that possibly belong to the Belumai Formation. They show thinning above the fold, and

the thickening on the flanks (Figure 5-29, white box). These strata are interpreted as belonging to the Lower Miocene Belumai Formation as the underlying fold contains a direct hydrocarbon indicator and it was reported that the discovery was made in the Bampo Formation (figure 5-29, green box).

The inverted syn-rift sequences (Bampo Formation/late Oligocene) also establish the concept of a new hydrocarbon play in the offshore North Sumatra Basin. This play was proved by Harbour Energy that drilled the structure in August 2022 and by Mubadala in 2023 and made significant oil and gas discoveries. Before the test, the syn-rift sedimentary rocks, such as the Bampo Formation, were only known as the source rock (Anderson et al., 1993; Smet, 2007). Now, sands within the Bampo Formation, most likely of turbiditic origin, have also becomes the reservoir target in the offshore area (PGS, 2023).

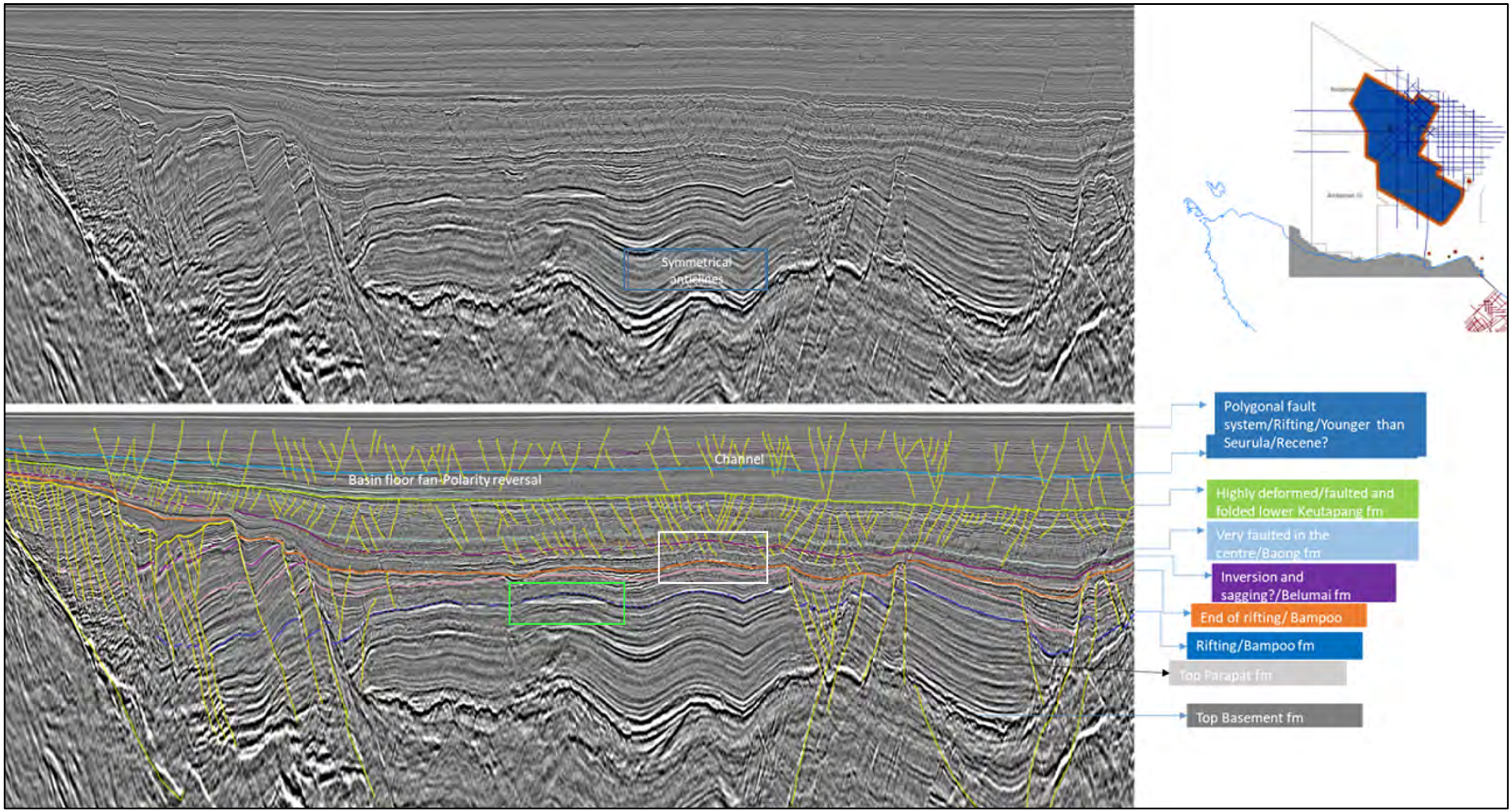

Figure 5-29 New Seismic 3D in the study area. This line was downloaded from the PGS website (PGS, 2022) without information such as directions, scales, and top geological formations. The line is offshore (Blue acreages on the right top). The white box indicates the syn-kinematic strata of inversion, while the green box indicates the anticline prospect that was successfully drilled and flowed the hydrocarbons.

Late Miocene fold

A fold structure associated with local inversion is located northwest of the North Sumatra Basin. The inversion caused the Oligocene to late Miocene strata on the horst block to be folded symmetrically. This feature was identified only from the western part regional seismic line 255 (Figure 5-4, line 255, red box, explained in Figure 5-18). Data limitations meant this fold trend could not be mapped, but it is still an interesting feature to address.

No fault was observed to have propagated to this symmetrical fold. However, there is a major extensional basement involved- fault adjacent to or below the fold. It has been recognized that this major fault forms the horst where the thin Oligocene sediments were deposited. A possibility is that the fault may have reactivated but failed to propagate into the younger strata due to the ductility/plastic behaviour of the Miocene successions.

The timing of this local inversion is indicated by the on-lapping sequence on the flank of the fold within the late Miocene Upper Keutapang formation (see Figure 5-18 for an illustration of syn-inversion). The syn-inversion sequence also shows a difference in thickness difference between the crest and the flank of the anticline within the late Miocene formation.

5.2.4 Thin-skinned fold and thrusts

Thin-skinned deformation refers shallow thrust faults and exclusively affects upper layers, usually composed of sedimentary rocks, without affecting the deeper basement rocks (Davidson, Reed, & Davis, 1997). Thin-skinned deformation in the offshore North Sumatra Basin is characterized by the presence of the décollement (basal detachment fault) that is associated with both compressional and extensional structures, recognized in a North-south regional seismic line (Figure 5-3). The line extends from the coast of Aceh in the south to Thailand's territorial water in the north.

The décollement relating to the compressional setting (fold propagation fault) is located south and within the late Miocene succession (at the base of the pink horizon/top of the light blue horizon) (Figure 5-3, south area). The seismic shows that the faults dip steeply south that terminate downwards in the lower Miocene strata and propagate upwards, with associated folds into the Pliocene-Pleistocene formations. Meanwhile, the décollement relating to the extensional faults is located north (Figure 5-3, north area). Several normal faults that developed within the pink horizon (Ketapang fm/late Miocene) detached at the top of the green horizon (Baong

Formation/middle Miocene) (Figure 5-3, in the north). Another seismic line also indicated that most of these faults discontinue at the top of the Baong Formation (Figure 5-30).

The youngest folds identified offshore of the North Sumatra Basin are located south, close to the coast of Aceh onshore. The folds/anticlines are asymmetrical and offset by the reverse fault; thus, they are associated with the fault propagation folds (Figure 5-23 and 5-24, the faults are shown by the labels RF1 and RF2). The folds have steep front and gentle back limbs and are asymmetric. The faults are oriented northwest-southeast and dip south (Figure 5-23, white polygons in the map) and detached within the late Miocene of the lower Keutapang Formation. The direction of the vergence is northward because the long limb has moved northwards with respect to shorter limb of the asymmetric folds. In addition, the magnitudes of the folds diminished to the north of offshore the North Sumatra Basin

The syn-kinematic strata within the upper part of green successions (probably Pleistocene age), just below the seabed (see Rf1 in Figure 5-24), indicates the timing of when the folds occurred. The seabed (or just slightly below the seabed) also marks the unconformity that eroded the top of the anticlines.

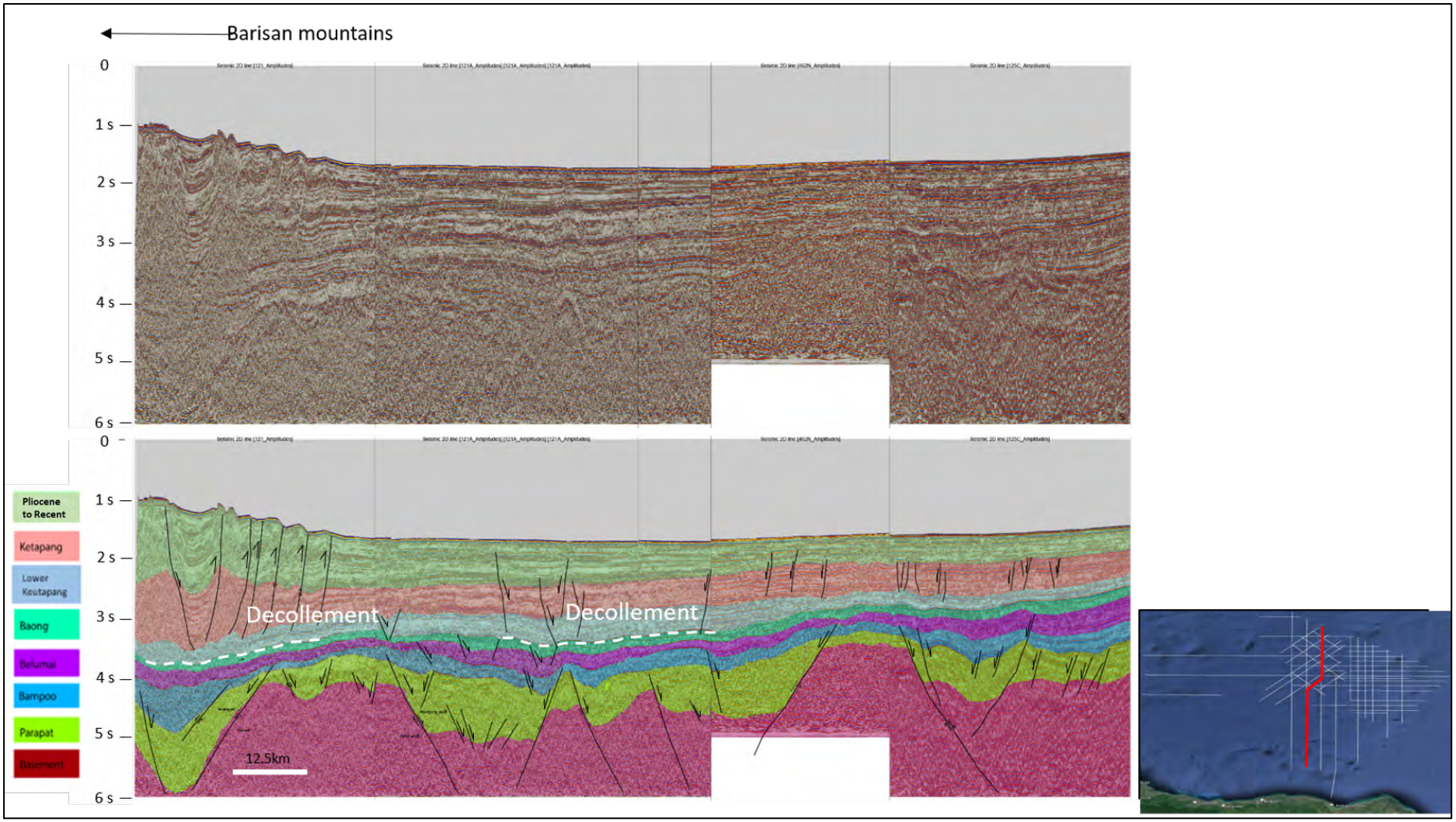

Figure 5-30 Seismic Regional line 121 shows the décollement strata between lower Ketapang and top Baong formation.

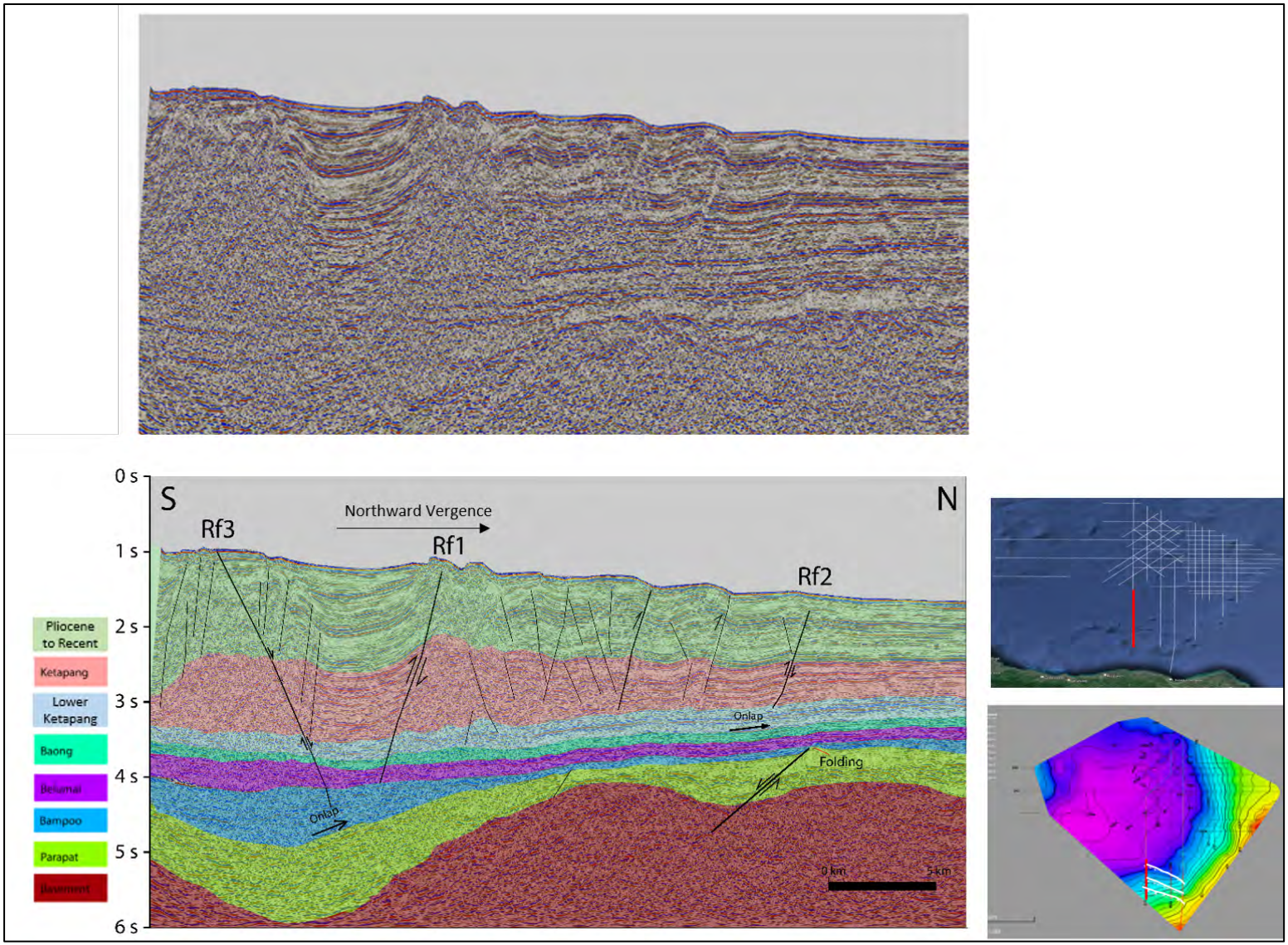

Figure 5-31 Seismic line 121A. The line is located south, marked by a red line on the map (bottom right).

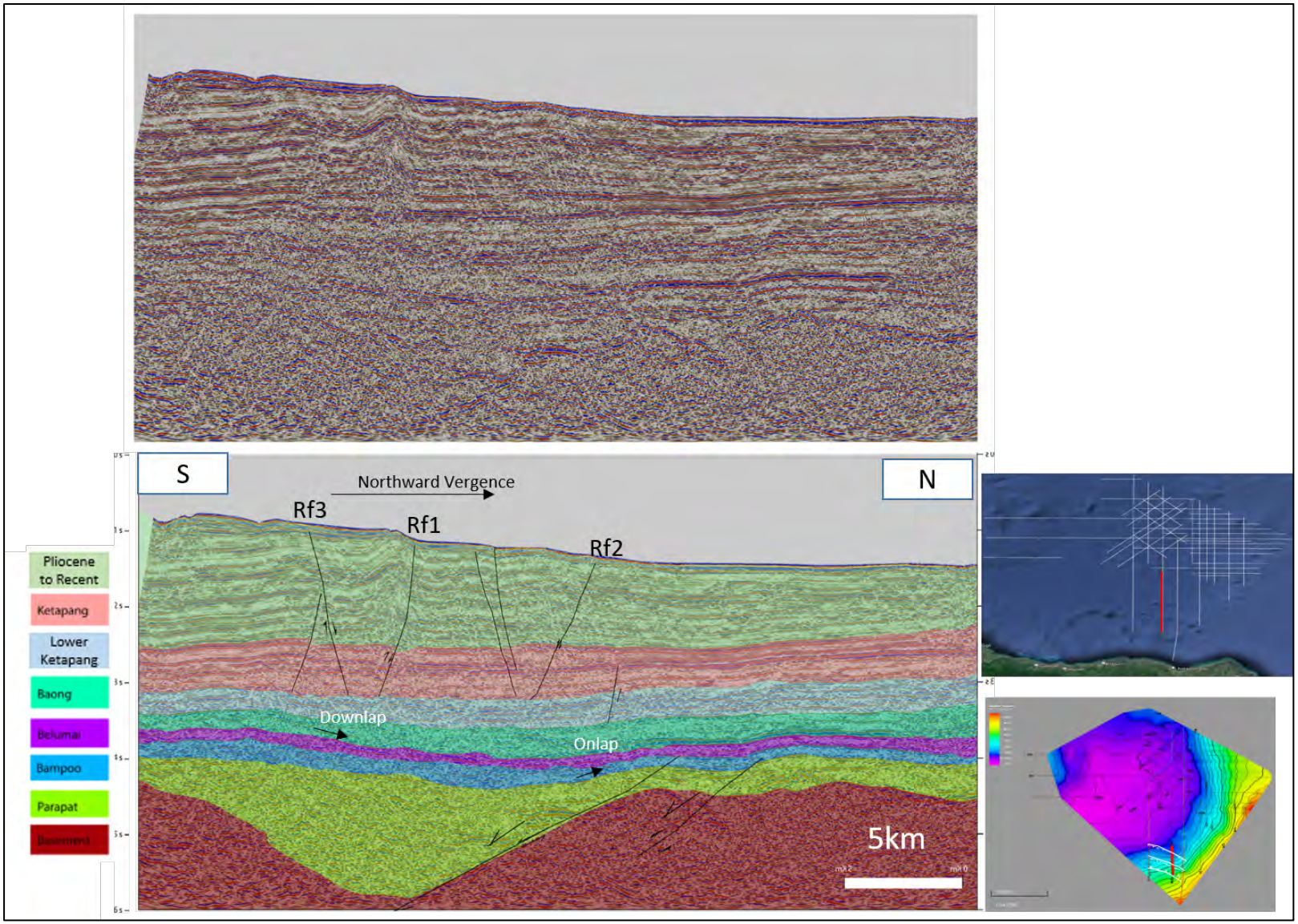

Figure 5-32 Seismic line 125A. The line is located south of the red line marks on the map (bottom right).

5.2.5 Strike-Slip Fault

The strike-slip fault, as the main structural element of the North Sumatra geology, is widely recognized due to its association with the main Sumatra fault system (Berglar et al., 2010; Mount & Suppe, 1992; Situmorang & Yulihanto, 1985; Wajzer, Barber, & Hidayat, 1991). For example, the restraining bends of the left and right stepping of the dextral Sumatra strike-slip fault are responsible for uplifted and intra-basinal areas along the Barisan Mountains (Figures 2-4 and 2-3). However, evidence of this fault style in the onshore North Sumatra Basin is not identified, particularly in this thesis research area. For example, in the geology cross section introduced by Pertamina-Beicip (1984), the interpretation shows the strike-slip faults associated with the anticline structures (Figure 4-34 above). In contrast, this thesis proposes that the anticlines are associated with fold detachment (Figure 4-34 below). The interpretation was based on the almost flat reflectors at the base of the dipping inward/onward reflectors of anticlines/synclines structure. There is no indication, such as seismic reflector displacement, that several minor faults (either normal or reverse faults) merged into one single main fault with a vertical dip forming a flower structure.

However, a possible flower structures indicating the extensional strike-slip fault are identified in the offshore area (Figure 5-33). The fault is located to the north offshore North Sumatra Basin. The fault could not be mapped in 2D because the fault was recognized by only one line, and the distance between the lines is large (line 130, Figure 5-31).

The Seismic reflectors show a consistent vertically stacked depression from the upper part of the Pleiocene-Pleistocene formation until the lower part of the Bampo Formation (Oligocene), terminating around the basement bounding fault. Along the depression, some minor extensional faults with high angles mimicking flower branches (shown by slight seismic reflectors break/displacement) intersect and merge into the main fault that dips vertically. The fault during the deposition of the Pliocene-Pleistocene Formation.

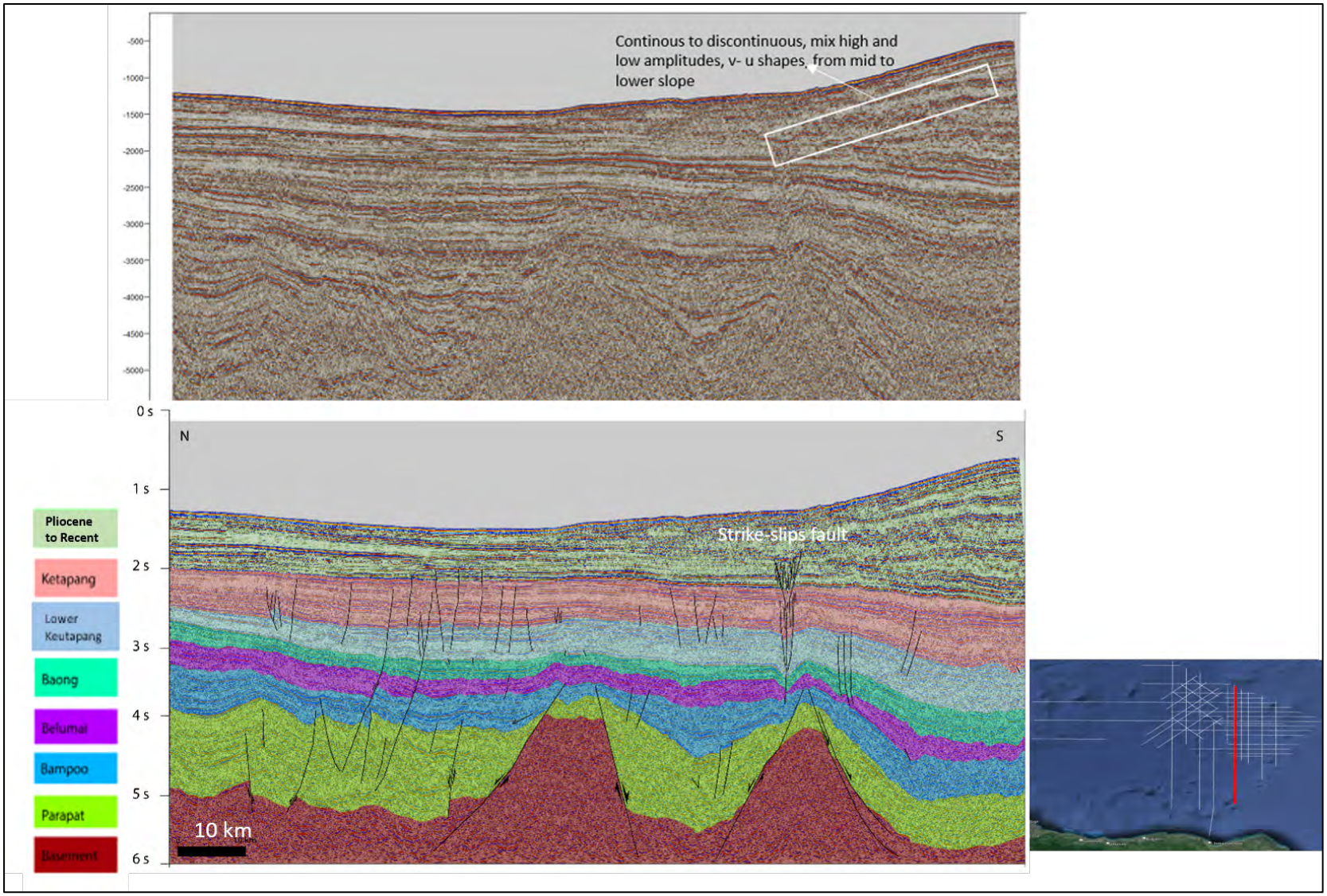

Figure 5-33 Seismic line 130, one of the single regional lines with a south-north orientation. The location is shown by a red line (bottom right).

5.2.6 Carbonate build-up

Carbonate build-up also exists in the offshore North Sumatra Basin. The carbonate is identified in a single line seismic and is located in the southern part of the offshore of North Sumatra Basin, toward the coastline of Aceh (Figure 5-3). The carbonate is in the Belumai formation and is 2 seconds TWT below the sea bed. Another carbonate is identified in a single line seismic located in the western part of the offshore of North Sumatra Basin, on the Mergui Platform (Figure 5-34). The carbonate is located at 1.5 seconds, just a few milliseconds under the seabed.

The feature is imaged by the seismic has similar characteristics to the carbonate build-ups in the onshore area (4-9) with the mounded geometry and strong amplitude as a result of the contrast between the top of the carbonate build-up from the surrounding successions. The younger sequences also on-lap to the flanks of this feature.

The carbonate is also a target reservoir for exploration in offshore areas. For example, Repsol targeted Oligocene carbonate located in the basin centre/trough of the offshore North Sumatra basin (Ascaria et al., 2019). In addition, in 2012, another company, Zaratex NV, drilled the early Miocene carbonate on a horst block, 25 km toward the coastal area Aceh, resulting in a dry hole (Hakim, Gunarto, Sompie, & Raharjo, 2014). However, the carbonate build-up along the Mergui platform, part of the offshore North Sumatra Basin, has never been drilled and may become a target for future exploration.

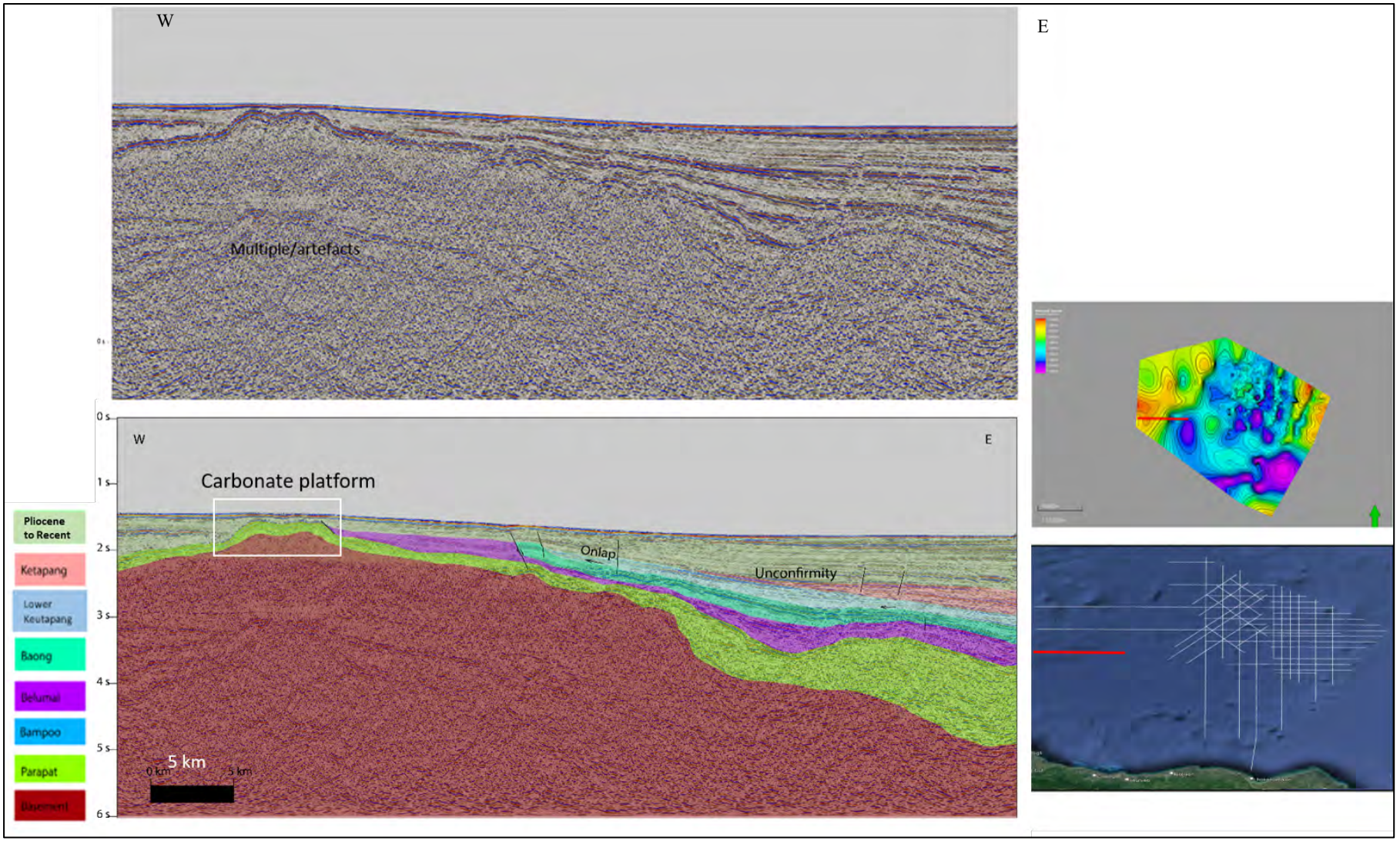

Figure 5-34 Seismic line 239A showing the Carbonate build-up on the basement platform high, part of the Mergui platform. The seismic line is in the western offshore North Sumatra Basin, marked by a red line (bottom right of the Figure).

5.3 Basin Evolutions

The evolution in the offshore North Sumatra Basin is demonstrated by reconstructing the 2D seismic line. The seismic line 255 was selected because the line is the longest and gives the better reflector quality among the other seismic lines. The line also covers the area from the Malaka Platform to the Mergui Ridge.

The isochron maps were also incorporated to give an idea of the thickness variation. The highest isochron values correlate to the thickness associated with the basinal/low areas where the sediments were deposited. The lower values relate to elevated areas with less sediment accumulation.

5.3.1 Pre-Rift

During the pre-rift, the basin was considered to form a plateau from the Mergui Platform to the Malaka Platform. (Figure 5-35a).

5.3.2 Early Oligocene

The rifting initiated by the basement faulting during the Early Oligocene. The horst and grabens developed between the Mergui and Malaka platforms. Most of the faults that created the horst and grabens are oriented North-South. The reconstruction demonstrates that the graben/trough in the center part of the Basin allows for the greatest sediment accumulation. During this period, the Parapat Formation was filling the basin, and the thicker succession was accumulating in the grabens. Meanwhile, the Parapat was deposited more thinly on the horsts (Figure 5-35b). During this period, the basin was compartmentalised into several sub-basin, horsts, and grabens (Figures 5-7 and 5-8).

5.3.3 Late Oligocene

Rifting continued during this period, associated with the growth of the faults. The reconstruction demonstrated half graben on the Mergui Platform develped at a later stage compared to other horsts. The rifting continues, as shown by deposition of the the Bampo Formation into the basin. On the horst, some of the Parapat Formation was not deposited and was replaced by the Bampo sequences. The top of the Bampo Formation marked the cessation of Oligocene rifting in the Basin (Figure 5-35c). The width of the basin was restricted, which was associated with the continuing development of horst and grabens (Figures 5-9 and 5-10).

5.3.4 Early Miocene

The reconstruction shows that, during the Early Miocene, the rifting stopped, marked by depositing the Belumai/Peutu formation. The reconstruction shows that this was a period of relatively quiescence, as shown by the absence of deformations such as faults (5-35d). However, in some places the first stages of inversion occurred during this period, indicated by asymmetrical folds (Figure 5-25). The other symmetrical folds were also observed (Figure 5-29). The kinematics of this fold is shown by the different thicknesses above and toward the anticline's crest (see Figure 5-18 for the illustration). The isochron map shows that thickness increases toward the Malacca platform, whereas in other places it is quite uniform (Figure 5-11).

5.3.5 Middle Miocene

The basin experienced subsidence during deposition of the Baong formations in the middle Miocene. The model demonstrates that the Baong is thicker in the center and thinned to the flanks, showing a classic post-rift subsidence geometry. Some Baong sequences also onlap to the Belumai Formation (Figure 5-35e). However, the fault activity was observed, as shown by the population of minor normal faults in some areas (Figure 5-29). The isochron map indicates the thickening in the center, south to north. In contrast, the thinning took place in the west (Mergui platform) and east (Malacca high) due to the areas being the topographic highs (Figure 5-13).

5.3.6 Late Miocene

Two major formations differentiate this Period: the lower and upper Keutapang.
The subsidence continued to occur during the deposition of the Lower Keutapang Formation. The subsidence resulted in the added overburden thickness in the basin (Figure 5-35f). In some parts, minor faults and folds also developed (Figure 5-29). The isochron map of the lower Keutapang shows a central thickening from south to north. In contrast, it is thinner on the western (Mergui platform) and eastern (Malaka platform) sides due to the topographically higher elevation (5-15).

The isochrone map of upper Keutapang shows that the thickening still occurs in the center while the thinner horizon is located in the west (Mergui Platform) (Figure 5-17). During this period, the inversion also occurred in the western part toward the Mergui platform. The inversion is shown by the upper Keutapang succession onlap and thinning above the fold crest (5-35g). This inversion probably developed locally in this area.

Widespread minor normal faults also developed throughout the offshore North Sumatra Basin at this time. Some of the faults also reactivated the older structures. The top of upper Keutapang marked the termination of faulting during this period. Another suggestion that those minor faults are polygonal faults that link to the tips of deeper normal faults. This because those minor faults represent the boundaries between areas of differential compaction.

5.3.7 Pliocene-recent

During this period, major and minor extensional faults were observed in some places that small scale extension (Figure 5-35h to 5-35i). Some major faults propagated from the older strata and caused some older faults to be reactivated. The inversion also occurred during this time in the south toward the coast of Aceh (Figure 5-3). The isochron map shows the south-north trend of the thickness. The highest thickness is south toward the onshore area, associated with the development of the thin-skinned fold and thrust belt while the thinner sequences is north and west of the offshore North Sumatra Basin probably reflect sediment input from the Barisan Mountains to the south (Figure 5-19).

Figure 5-35a. Reconstruction of east-west Seismic line 255. The model show the initiation of rifting in the basement.

Figure 5 35b. Depositing of Parapat fm (green sequence) while the rifting occurring during Early Oligocene.

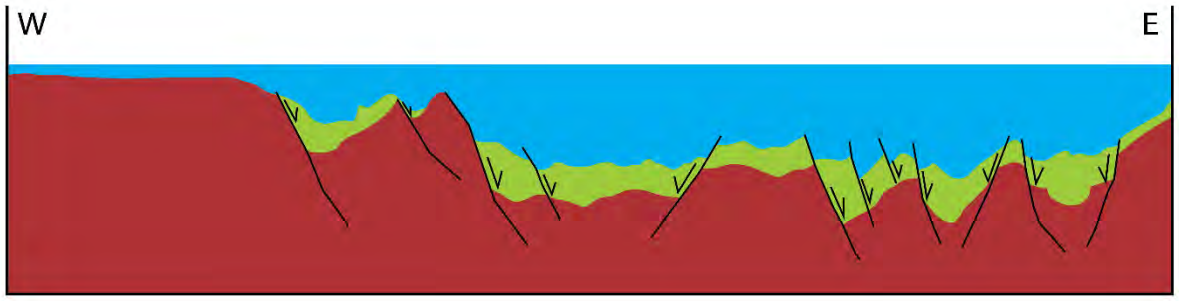

Figure 5 35c. Depositing of Bampo fm (Blue sequence) while the rifting continued during Late Oligocene.

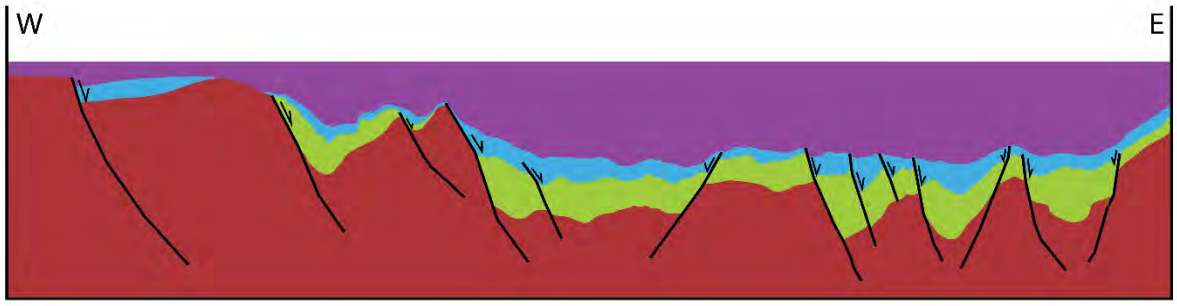

Figure 5-35d. Depositing of Belumai fm (Cyan sequence) during the Early Miocene marked the post-rift deposition of sedimentary rocks. No significant deformations occurred during this age. However, another seismic line shows evidence of inversion (Figure 5-24).

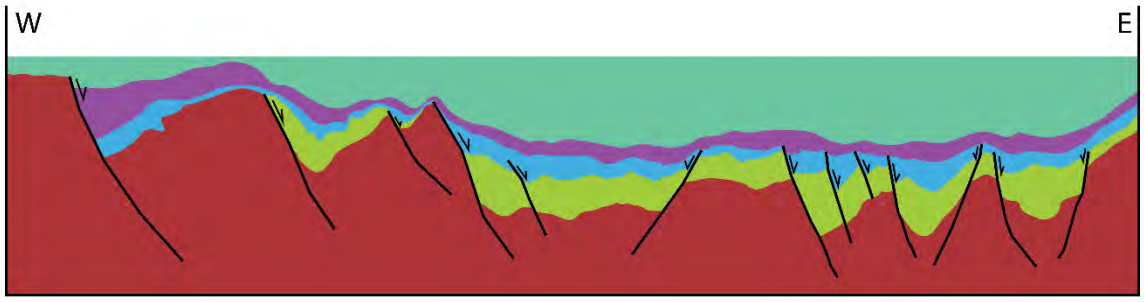

Figure 5-35e. Depositing of Baong fm (Dark green sequence/middle Miocene) while sagging due to subsidence during Middle Miocene.

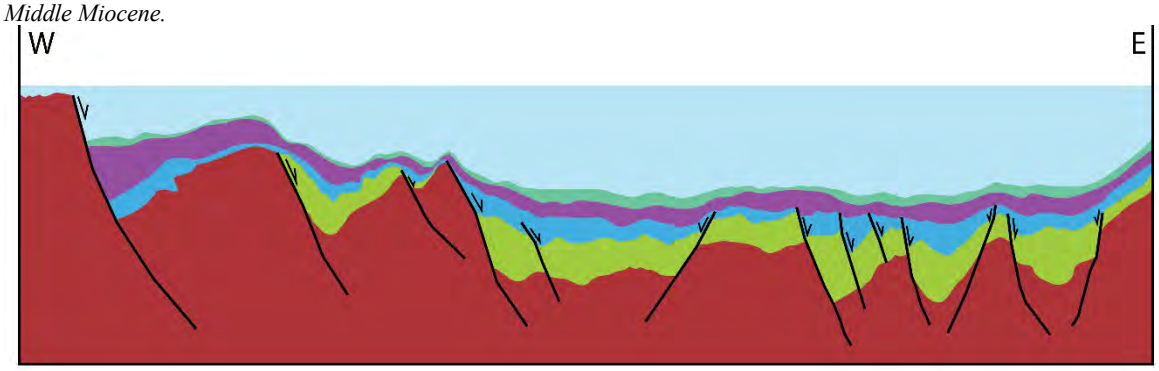

Figure 5-35f. Depositing of Lower Keutapang (light blue sequence/late Miocene) marked the end of subsidence during the late Miocene.

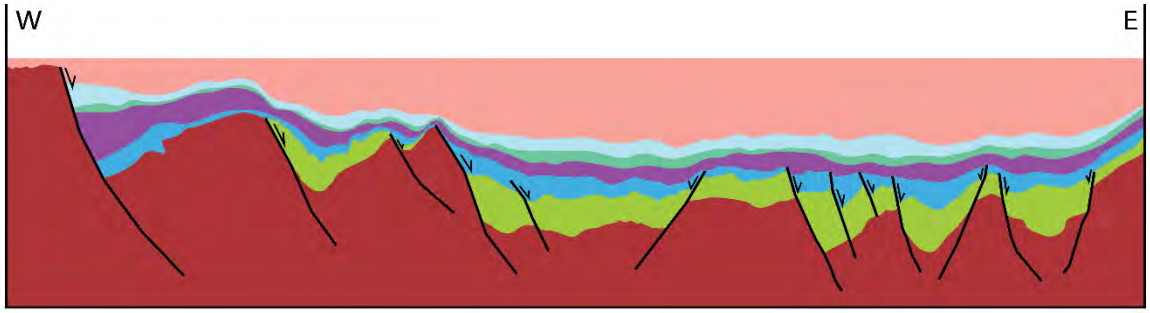

Figure 5-35g. Depositing of upper Keutapang (pink sequence/late Miocene) marked another inversion phase in offshore North Sumatra Basin during the late Miocene. While some extensional faults also occurred.

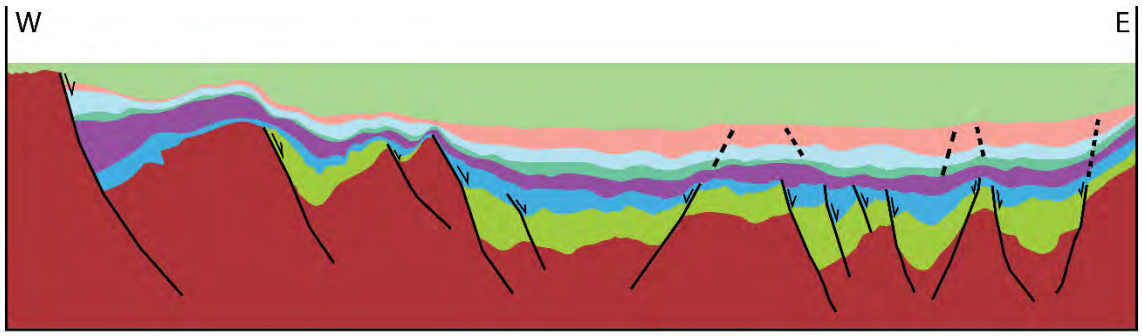

Figure 5-35h. Depositing of Pliocene to recent sediment (light green interval) marked another rifting phase in offshore North Sumatra Basin during Pliocene-Pleistocene. At the same time, some extensional faults reactivated the older faults.

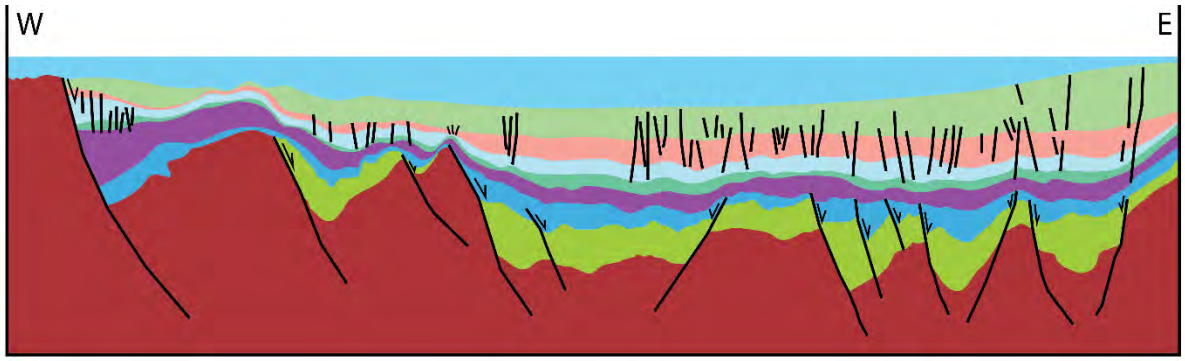

Figure 5-35i. Depositing of Holocene/recent sedimentary rock (the light blue colour). Little deformations were occurred during the deposition of the light blue horizon.

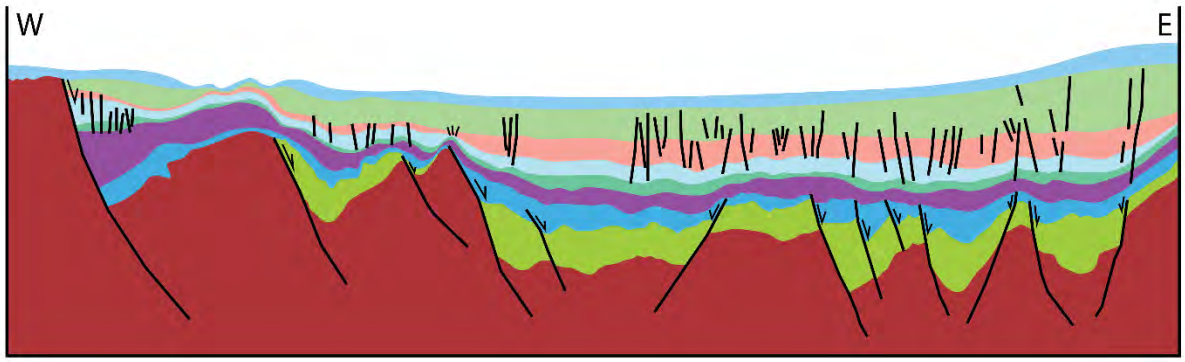

Figure 5-35j. The current geological profile of offshore NSB

5.4 Summary

Based on the data presented in this chapter, there are a number of findings that can be made about the Offshore North Sumatra Basin:

1. The evolution of offshore NSB began with rifting in the early Oligocene, creating a series of horst and grabens. The rifting event continued into the late Oligocene. The rifting controlled the localized sedimentary deposits that thicken in the grabens and thin on the horst blocks.

2. The Basin experienced multiple phases of inversion in different places. The first is in the Early Miocene, north of the offshore North Sumatra Basin, toward the Thailand water. This event inverted most syn-rift successions which were folded into anticline structures. This thesis, using 2D seismic lines, shows that the folds/anticlines were asymmetrical and associated with the fault reactivation. Elsewhere, new seismic evidence from PGS revealed symmetrical anticlines with no faults involved. The anticline also contained hydrocarbon and was successfully tested in June 2022. The second inversion developed during the late Miocene and is located northwest toward the Mergui ridge/platform. The inversion folded the post-rift sedimentary rocks on the high basement block.

3. Furthermore, the latest tectonic phase is the compression developed during the Pliocene-Pleistocene toward the coastline of Aceh, south of the offshore North Sumatra Basin. The compression is associated with the fault propagation folds, similar to the onshore North Sumatra Basin, and thrust faults. This is related to uplift and shortening in the Barisan Mountains.

4. The magnitude of folds caused by Pliocene-Pleistocene compression reduces from south to north in the offshore North Sumatra Basin. The reduction is probably related to northward propagation of deformation from the Barisan Mountains.

5. Most seismic lines show widespread minor extensional faults that developed during the late Miocene. Some younger extensional faults, particularly the major ones, reactivated the older faults. The reactivation also created a minor monocline structure on the tip of the older faults in some places.

6. The décollement associated with thin-skinned deformation was observed in the south region within the lower Keutapang formation (late Miocene). The décollement was associated with the reverse fault detachment that occurred during the Pliocene-Pleistocene time. Another

décollement was identified in the north region within the Baong formation. The décollement was associated with the extensional faults occurring in the late Miocene.

7. A strike-slip fault was observed in the north of the offshore Sumatra Basin adjacent to the Malacca platform. The structure was identified only by one seismic 2D line and could not be mapped laterally. The shows that the offshore North Sumatra Basin experienced little deformation related to the Sumatra Strike Slip fault system.

8. Carbonate build-ups were observed in the south and the western area offshore of the North Sumatra Basin, toward the Mergui platform. The southern carbonate is located at 2 s TWT under shallow water and the western carbonate is located at 1.5 seconds TWT and a few milliseconds below the seabed. These carbonates may act as a petroleum reservoir, although lack of seal for the shallow carbonate is a significant risk.

6 Passive Seismic for Hydrocarbon Indication in the Western Margin of the North Sumatra Basin

6.1 Background

The North Sumatra Basin is mature due to its long oil and gas exploration history. Significant oil and gas fields such as Arun, Alur Siwah, and South Lhoksukon (see Figure 1-3 and 6-1 for the location of the fields) were discovered in the 1960s, 1970s, and 1980s. After this, exploration ceased due to the local conflicts between the Free Aceh Movement and the Government of Indonesia.

In 2005, just after the mega Tsunami that occurred on 26 December 2004, a peace agreement between the parties who had been involved in the conflict was signed. Hence the province became stable. Due to this improved political situation, several companies, such as Talisman (Repsol), Zaratex, Premier Oil (Harbour Energy) and Mubadala Energy, acquired hydrocarbon exploration blocks offshore Aceh. At the time this thesis was being written, these companies are actively involved in exploration, conducting seismic acquisition and exploration drilling.

However, the western margin of the basin, is a low priority for companies to study and explore. Only limited seismic data and wells are available west of Arun's giant gas field, from Bireun to Sigli. The data limitations are also reflected by the absence of hydrocarbon fields in the area (Figure 1-3 and 6-1).

Passive seismic is a simple method for hydrocarbon exploration which uses low seismic frequencies between 1 to 10 Hz (Ali, Berteussen, Small, & Barkat, 2007, 2010; Ali, Berteussen, Small, Barkat, & Pahlevi, 2009; Dangel et al., 2003). Because oil and gas absorb this frequencies in this range, some authors (Peterson, 1993; Saenger et al., 2009; Van Mastrigt & Al-Dulaijan, 2008) have suggested that the presence of a hydrocarbon reservoir correlates with a spectral anomaly of 1 to 6 Hz recorded by surface seismographs. This frequency window is a typical noise trough in the low-frequency spectrum wherever hydrocarbon-related effects are observable (Peterson, 1993) (see Figure 6-2 for the illustration). The arithmetic area below the Power Spectral Density (PSD) curve between 1 to 6 Hz is then calculated to measure the anomaly.

This chapter highlights the use of passive seismic to indicate the presence of hydrocarbon at the western part of North Sumatra Basin, part of Sigli high. There is a well that drilled by Mobil Oil in 1975 (Carbonate X reservoir), (Figure 6-1).

6.2 Regional Seismic line from Bireun to Sigli

An image of a 2D line has been interpreted manually to identify the structures and horizons in the area (Figure 6-3). The line length is approximately 48 kilometres, with a record length of 4500 milliseconds of two-way time. The line has an east-west orientation and moderate to poor seismic imaging quality. This is probably due to poor processing and the complexity of the surface geology (Figure 6-4). Five horizons were interpreted based on the regional stratigraphy of North Sumatra Basin, the stratigraphic study of the Sigli-B1 well, and the characteristic of the seismic data itself (Figure 6-3). The five horizons are described as follows:

Basement

The Basement horizon is characterized by a low amplitude reflector above a package of discontinuous chaotic reflectors. A graben is present between two basements highs marked by major extensional faults. To the west, the fault propagates from the basement deep and stops at the base of Peutu Formation (early Miocene), while the fault in the east propagates up to late Miocene horizons, and may even be present at the surface (Figure 6-4). Hence, the eastern fault may be associated with the fold structure.

Bampo Formation (Oligocene).

The Bampo Formation is inferred to form the syn-rift packages that fills the graben between Bireun and Sigli, although it is absent from the horsts. It is characterized by the changes between low amplitude reflectors (below) and high amplitude reflectors (above). The reflectors are parallel and continuous. There is also a mound with a high amplitude that is interpreted as a carbonate/reef in the central deep.

Peutu Formation (Early Miocene).

This formation is characterized by strong amplitudes on the west horst and which pass laterally to low amplitudes in the centre of the graben. The strong amplitudes relate to the carbonate platform that was been tested by Mobil oil in 1976 (carbonate X, Figure 6-3). A similar carbonate was also interpreted west of the Sigli-well, but has not been tested (carbonate Y, Figure 6-3). Reflector continuity is fair to good with the discontinuous reflector packages towards the Bireun area.

Baong (Middle Miocene).

The Baong Formation is characterised by low amplitudes seismic reflectors and is seismically transparent in the central graben area, which may be due to the presence of overpressure shale.

Previous authors noted drilling problems associated with the Baong Formation due to the presence of thick shales (De Smet, 2007).

Keutapang Formation (Late Miocene).

The Keutapang formation fills the upper part of this basin. It is characterised by low amplitudes in the west and higher amplitudes to the east. Folding is evident in the Keutapang Formation, possibly due to the location of the seismic line close to the Barisan foothills (Figure 6-1) and may be associated with older reactivated the structure that formed in the Bampo and the Peutu formations.

6.3 Surface geological map

The surface geological map also constrains the structure (Figure 6-4). It shows that large parts of the area, particularly around the Sigli well, are covered by alluvium. Elsewhere, local lithostratigraphic formation names based on local villages or sub-districts are used, rather than more widely used lithostratigraphic scheme based on well data from the North Sumatra Basin. However, the outcrop of Miocene sandstones of the locally named Kotabakti Formation is consistent with the presence of folds interpreted in the Keutapang Formation on the seismic section.

6.4 Passive Seismic acquisition

Based on the Seismic Interpretation (Figure 6-3), Carbonate Y was selected as having the best potential for the storage of hydrocarbons, given that Carbonate X was previously tested dry. Also, Carbonate Y is in a higher position than Carbonate X so is better situated assuming that the hydrocarbon migrated up dip and filled a higher position.

A Raspberry RS3D portable three-component (3-C) seismometer with a frequency range of 0.6–39 Hz and a sampling rate of 100 samples per second (SPS) was used to collect 78 measurements of the passive seismic wave field at the surface over an area of approximately 64 km^2 covering the area of both Carbonate X and Y. The measurements took 45 minutes for each location and required 15 minutes for tool preparation and recording. The total time for the survey was ten days.

The frequency data recorded was then filtered to 1 to 6 Hz to determine the PSD anomaly by calculating the arithmetic average below the PSD curve (the PSD anomaly value is dimensionless) (Figure 6-2a, PSD anomaly area). The PSD associated with a proven

hydrocarbon well in East Aceh has also put constraints on the result of this acquisition (Setiawan, Muchlis, Arsyi, & Ardhie, 2021).

This methodology is a swift method for obtaining a preliminary indication of the presence of hydrocarbon. Another advantage is that it does not need an artificial sources such as dynamite and vibroseis, which can take up most of the cost of a conventional seismic survey.

6.5 Result and Discussion

The acquired data from 78 measurements were filtered to gain the PSD anomaly of 1 Hz to 6 Hz. The results are presented in Figure 6-5. A map was also created to show the distribution and lateral variation in PSD values (Figure 6-6).

Results of the calculation are as follow: a) most of the area of the PSD anomaly between 1.0 Hz and 6.0 Hz is below 1000; b) the highest PSD anomaly is at the location T-10 is approximately 7000, whereas the second highest is at T-25 and is approximately 5000; c) the value at T-59, the location of Carbonate X (dry well), is 715 square, and at T-74 (Carbonate Y) is 344; d) the lowest value is at location T-37 and is approximately 194 square area.

The results provide a surprising outcome, as Carbonate Y has a lower value than Carbonate X and does not meet initial expectation that Carbonate Y would be more likely to contain hydrocarbons. We expected that the hydrocarbon migrated to the Carbonate Y due to its higher position.

Furthermore, for a benchmark, the results of this survey were compared to the PSD curve from the hydrocarbon well in east Aceh (Figure 6-2b). The comparison suggested that locations T-10 and T-25 are potential areas of hydrocarbon accumulation due to their high PSD anomaly (Figure 6-5).

T-10 and T-25 are located north of T-59, where Carbonate X is situated. Hence, T-59, T-10, and T-25 form a south-north trend which possibly follows the edge of the Sigli High and continue offshore towards the carbonate platform imaged in Figure 5-34. Carbonate platforms are developed adjacent to other north-south trending basement highs in the North Sumatra Basin, such as the north-south trend of the Arun field (Figure 6-1). It is therefore possible that T-10 and T-25 are separate carbonate build ups along the same basin margin trend as Carbonate X. A possible reason why the Sigli-1 well did not encounter the hydrocarbon in the Carbonate X

reservoir at location T-59 may be the absence or breaching of a seal, perhaps caused by fault reactivation.

In addition to the areas covered by the passive seismic survey, the western part of the North Sumatra Basin also shows other potential prospects. For example, the carbonate within the depocenter was interpreted on the seismic line due to its similar characteristic to Carbonate X (Figure 6-3). However, this possible carbonate is Oligocene age and is part of the syn-rift sequence which developed during the initiation of rifting in the North Sumatra Basin. So far, only the Miocene carbonate has been drilled and produced significant hydrocarbons (Meckel, 2013). Syn-rift carbonate of Oligocene age is a potential new play in North Sumatra Basin.

Another play is anticlinal structures that are also prominent in this region, similar to the eastern part of the onshore North Sumatra Basin around Tamiang (Figure 1-1, location of the study area). The regional seismic line (Figure 6-3) shows that toward the Bireun area, major extensional fault propagated folds and developed shallow anticlines, indicating that inversion occurred in this area. These anticlines may also act as hydrocarbon traps if source rock exists in this area, and oil and gas seeps are known to be present in the Bireun area (Meckel III & Banukarso, 2016). Hydrocarbon seals such as thick shale rocks are also present with the Baong Formation (De Smet, 2007). Therefore, all the elements of the petroleum systems are present in the western margin of North Sumatra, with the faults acting as a pathway for the hydrocarbon to migrate from the source rock to the reservoir.

6.6 Future Work and Recommendation

For all the reasons given above, this thesis proposes that the government should attract companies to come and explore. One option would be sponsoring the acquisition of passive seismic data on the leads identified in the existing 2D lines. This method has been known to provide a low cost, fast evaluation with no adverse environmental impacts.

The passive seismic imaging can be used also for geothermal exploration (Foulger, 1982; Warren, et al 2018). In Aceh there is some geothermal potential that can be sourced from inactive volcanoes such as the Geureudong, and Seulawah volcano (Figure 6-1).

The government should develop geothermal energy because Indonesia has been importing almost 1 million barrels of oil per day to tackle the energy consumption (Rahman et al, 2021). Besides, the geothermal energy can provide a long and sustainable source for energy resilience.

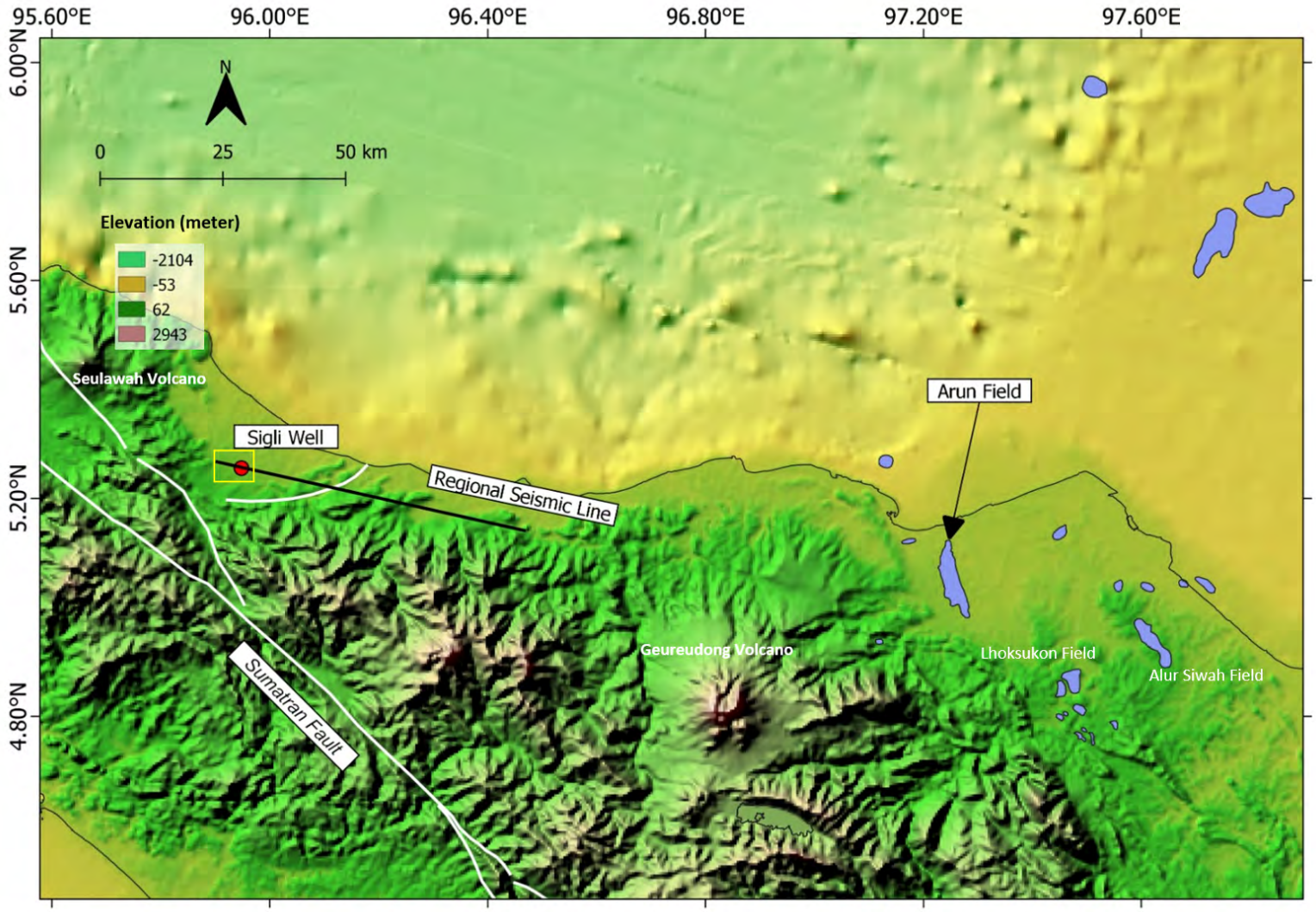

Figure 6-1 Location of the passive seismic survey is in the orange box, while the well (containing the Carbonate X reservoir) is indicated by the red dot, while the black line indicates the seismic location. This map shows absence of the hydrocarbon fields west of Arun field, the western part of the North Sumatra basin.

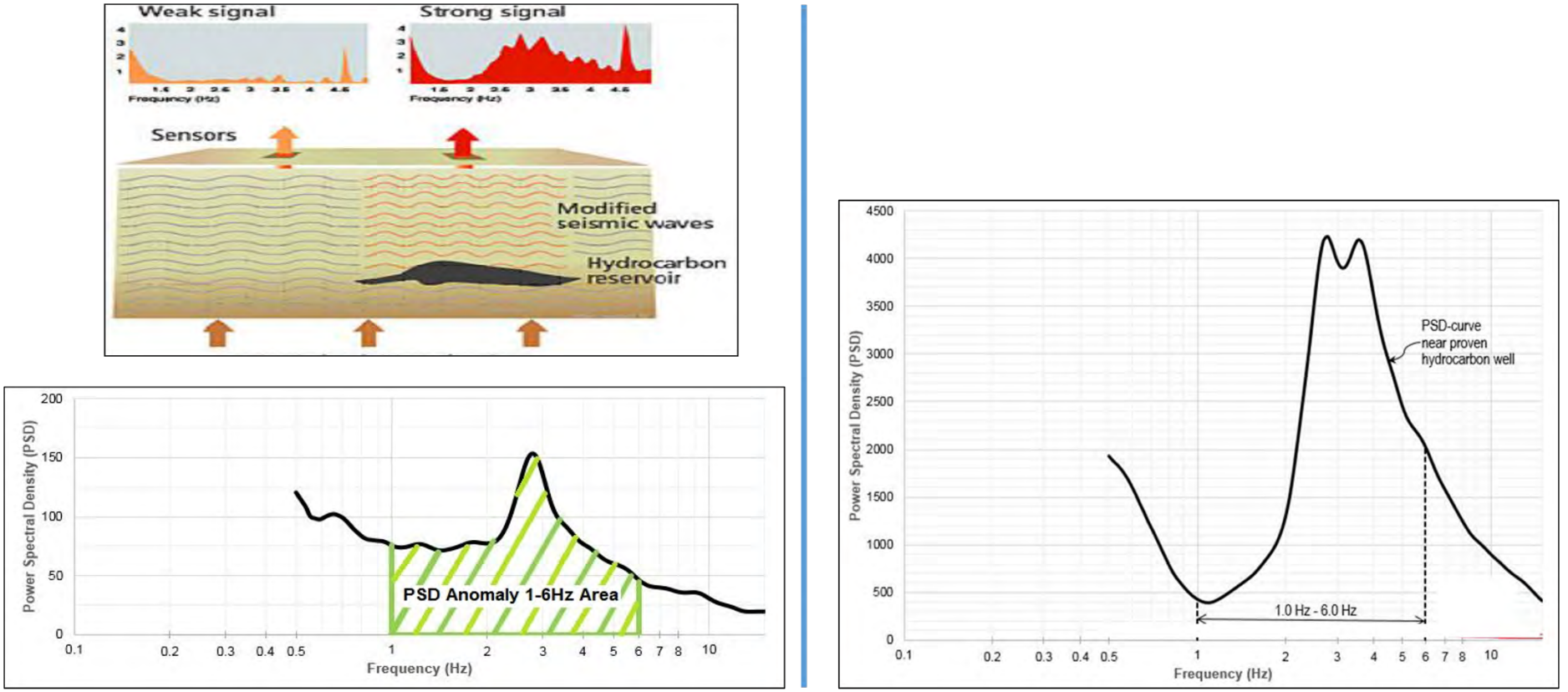

Figure 6-2 a. Illustration of Spectral frequency 1-6 Hz is vital for the hydrocarbon reservoir; b. response of Power Spectral Density (PSD) near a production well in East Aceh.

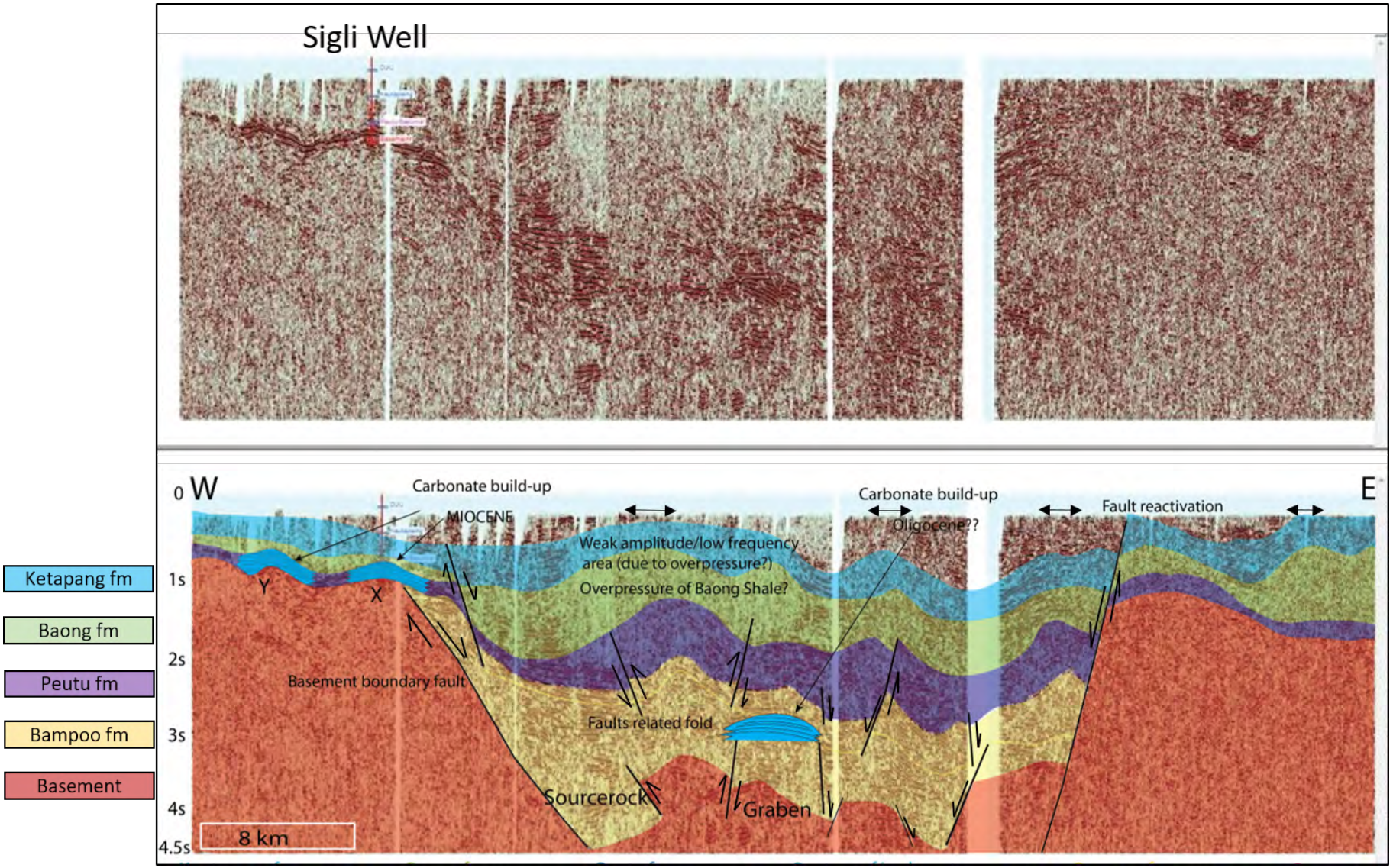

Figure 6-3 Regional Seismic line above; un-interpreted seismic with length approximate 58 km, below the seismic interpretation profile. The hydrocarbon leads are Carbonate X and Y.

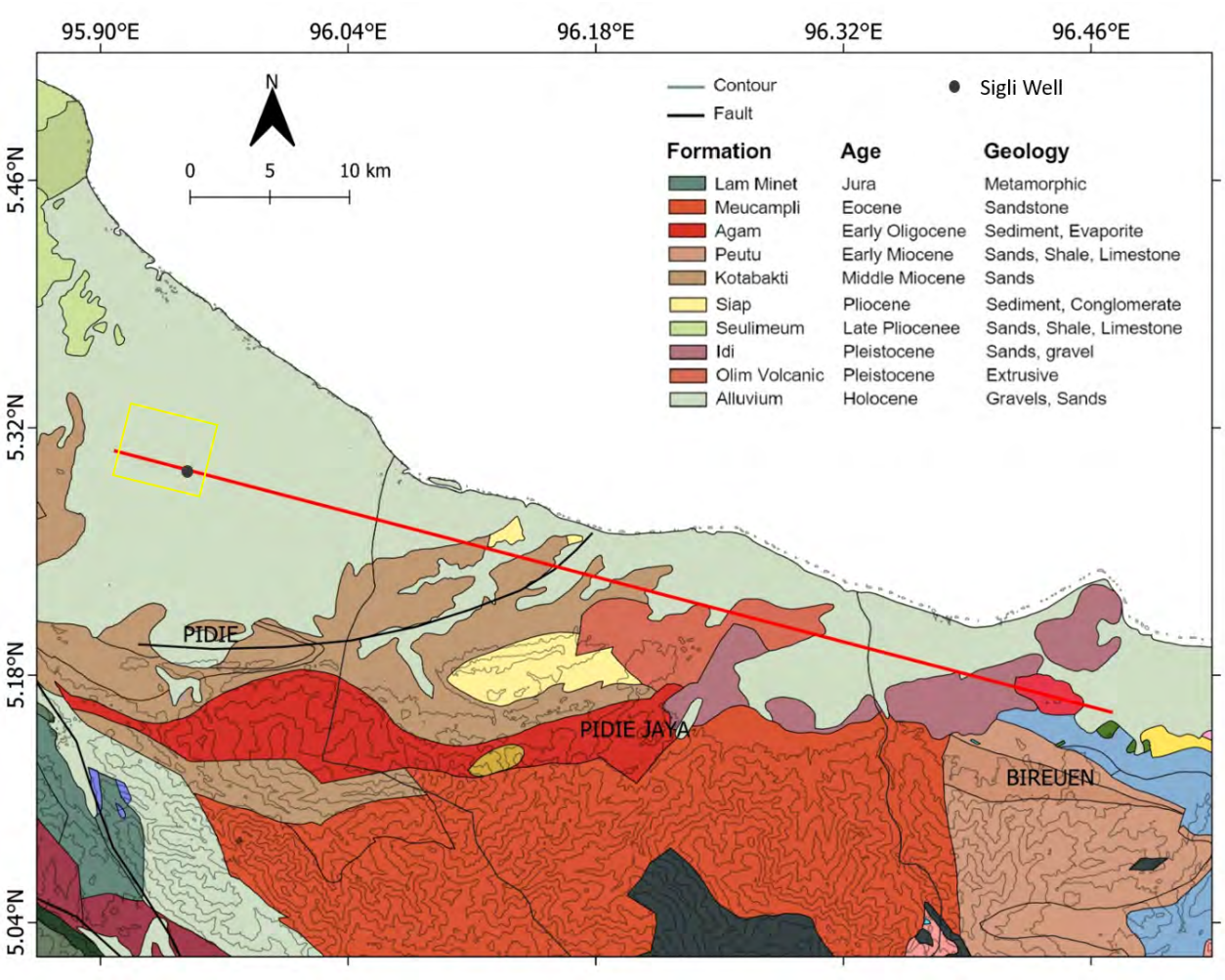

Formations from well	Ages	Lithology
Ketapang	Late Miocene	Sands, Shales
Baong	Middle Miocene	Shale
Peutu	Early Miocene	Sands, Shale, limestone
Bampo	Oligocene	Shales
Basement	?	?

Figure 6-4 Surface geological map Bireun-Sigli area from (Bennet et al, 1983., Keats et al, 1981). The long red line is the location of the seismic profile from Figure 6-2 while the yellow box is the survey area.

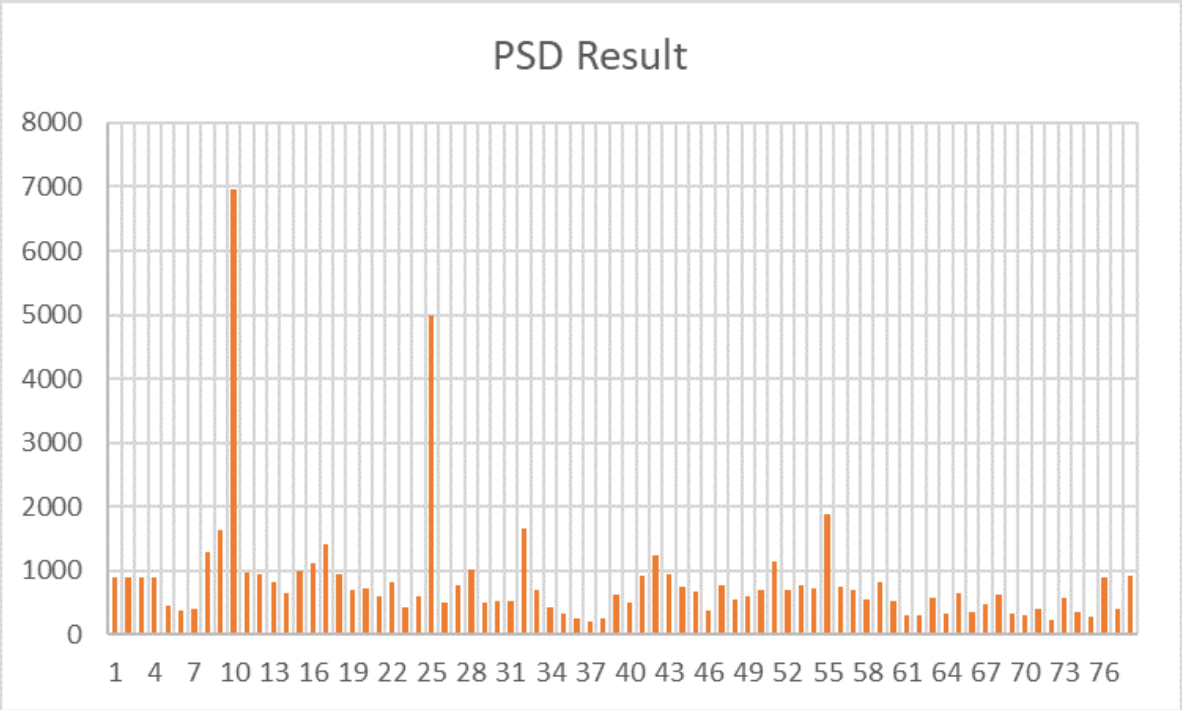

Figure 6-5 Results of PSD for each measurement. The value shows that the highest PSD is T-10, and the second is T-25. Meanwhile, T-59 and T-74 give low PSD.

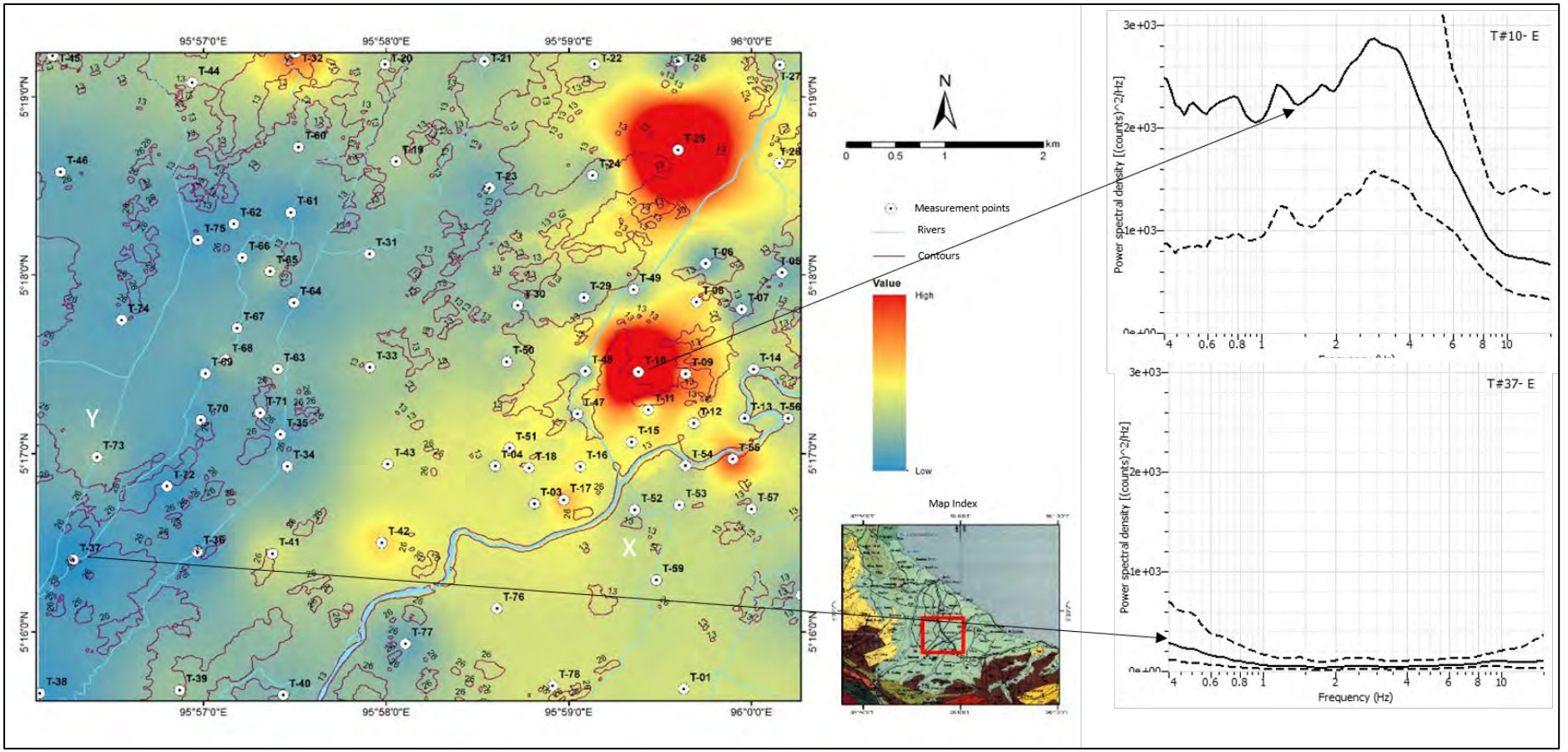

Figure 6-6 Map of PSD anomaly based on PSD result in table 6-2. On the right, the curve of frequency anomaly of 1-6 Hz at T-10 shows the highest PSD. Meanwhile, T-37 shows the lowest value.

7 Discussion and Conclusions

7.1 Comparison of Onshore and Offshore North Sumatra Basin

The North Sumatra Basin is a large basin in terms of its size (approximately 60,000 km2 in Indonesia alone), geometry (it contains up to 6 km of sediment), and its position that covers both onshore and offshore areas (Tampubolon et al., 2017). In terms of its tectonic context, it sits inboard of the Indian Ocean subduction trench. The Barisan Mountains and the strike-slip Sumatra Fault System separate the North Sumatra Basin from the subduction trench, while the Andaman spreading centre lies to the north-west.

Analysis of the basin history and structural styles of the onshore (Chapter 4) and offshore (Chapter 5) NSB has revealed some similarities and some differences which are summarised in Figure 7-1. These can also be related to some of the regional tectonic events described in Chapter 2 and address the knowledge gaps and research questions identified in that chapter:

1. How does the timing of the onset of extension in the North Sumatra Basin compare to other basins in the region, and can it be linked to similar back-arc processes*?*. The North Sumatra Basin initiated as an extensional basin in the Oligocene (Chapter 4.3.1, Chapter 5.2.1). Basin formation was widespread throughout Sundaland at this time (Pubellier & Morley, 2014, Doust & Noble 2008), although the age of basin initiation varies from Palaeocene to Oligocene. This variation in age suggests different controls on basin formation, with Pubellier & Morley (2014) linking basin formation in western Sundaland to subduction rollback along the Andaman–Sumatra–Java–Sulawesi subduction zone, supported by tomographic images that show a steeply dipping subducting slab (Widiyantoro and van der Hilst (1996). The margin of the onshore NSB contains NW-SE trending extensional faults (Chapter 4.3.1), parallel to the main structural trends the dominate Sumatra Island and which may reflect tectonic fabrics associated with the accretion of terranes to this part of the Sundaland margin (Hall, 2012). Further outboard, and in the offshore NSB, north-south oriented faults dominate (Chapter 4.3.1, Chapter 5.2.1). This implies an extension direction oblique to the trend of the subduction zone offshore Sumatra. If subduction roll back is the mechanism driving basin formations, then it is more likely related to the Andaman section of the subduction zone, and possibly to events in the Andaman Sea, rather than to the formation of the North Sumatra Basin.

   The onshore and offshore NSB both entered a phase of thermal subsidence and tectonic quiescence in the early Miocene (Chapter 4.4.3, Chapter 5.3.4). This is also widely observed

in other basins in Sundaland at this time (Pubellier & Morley, 2014, Doust & Noble 2008). Pubellier & Morley (2014) explain this as consequence of the end of subduction roll back. The reason for this is not clear, although it may correspond to end of rifting in the South China Sea and the collision of Greater India with Eurasia (Doust & Noble 2008).

2. How is the compression associated with the formation of the Barisan Mountains expressed in the North Sumatra Basin, and how does it vary with distance from the Barisan Foothills? The Middle Miocene marks the onset of inversion in many basins in Sundaland (Doust & Noble 2008) and in Sumatra corresponds to the onset of uplift in the Barisan Mountains (Morton et al., 1994). Despite this, there is no evidence of any compressional structures developing at this time in the onshore North Sumatra Basin, despite its proximity to the Barisan Mountains. However, the initial stages of inversion are observed in the offshore North Sumatra basin at this time (Chapter 5.2.3). Pubellier & Morley (2014) suggest that the Sumatra-Java subduction zone is the source of these compressive stresses, based on their consistency with present day stress distributions, and might also correspond to collisions elsewhere along the margin and in eastern Indonesia.

   Thin-skinned Pliocene-Pleistocene deformation is evident in both the onshore and offshore North Sumatra Basin. In the onshore NSB these take the form of detachment folds that are most common on the Langsa Platform, in the footwall of the fault that marks the edge of the Northern Depocentre (Chapter 4.3.2). It is possible that this fault represents a fundamental structure that prevented earlier inversion propagating further into the basin. Uplift associated with this deformation resulted in exposure of the Miocene sequences in the Barisan Foothills. A similar style of deformation is observed at the southern edge of the offshore NSB, although thrust faults are also present in this area. Also, the folds remain below sea level, indicating less uplift. In both areas the folds and thrusts detach in thick Miocene shales and they appear to represent propagation of the deformation associated with uplift of the Barisan Mountains into the NSB.

   The earthquake data shows that compressional deformation is still progressing in the onshore North Sumatra Basin. In the offshore area there is less present day deformation, indicated by fewer earthquakes. Furthermore, the 2D seismic lines show that the upper part of the sequence in the northern offshore north area is dominated by the extensional faults.

3. Is there any evidence that strike-slip deformation associated with the Sumatra Fault extends into the North Sumatra Basin*?* This thesis also proposes a new geological cross-section that

combines observations from the onshore to the offshore area (Figure 7-1). The main new insights compared to previous structural interpretations (e.g. Caughey & Wahyudi, 1993; Figure 2-6) are the presence of a detached fold and thrust system on the southern margin of the basin, rather than the previously interpreted positive flower structures. In addition, large scale extensional faults control variations in the depth to basement, rather than large scale monoclinal folds. The North Sumatra Basin was initiated as a rift basin and transformed into an inverted basin that started during the Miocene, but which only became strongly developed during the Pliocene-Pleistocene (Figure 7-1)

4. There are no comprehensive and integrated studies which link the onshore and offshore parts of the basin. The thickness of sedimentary sequences in the offshore and onshore North Sumatra Basin is comparable from the Oligocene until the late Miocene. However, a significant contrast was noticed from the late Miocene onward. The thickness reduction in the onshore area was probably related to the Pliocene-Pleistocene compression tectonics, which uplifted and eroded the late Miocene and Pliocene-Pleistocene successions. In contrast, similar successions were preserved in the offshore NSB, as shown by the increasing trend during those periods (Figure 4-2).

.

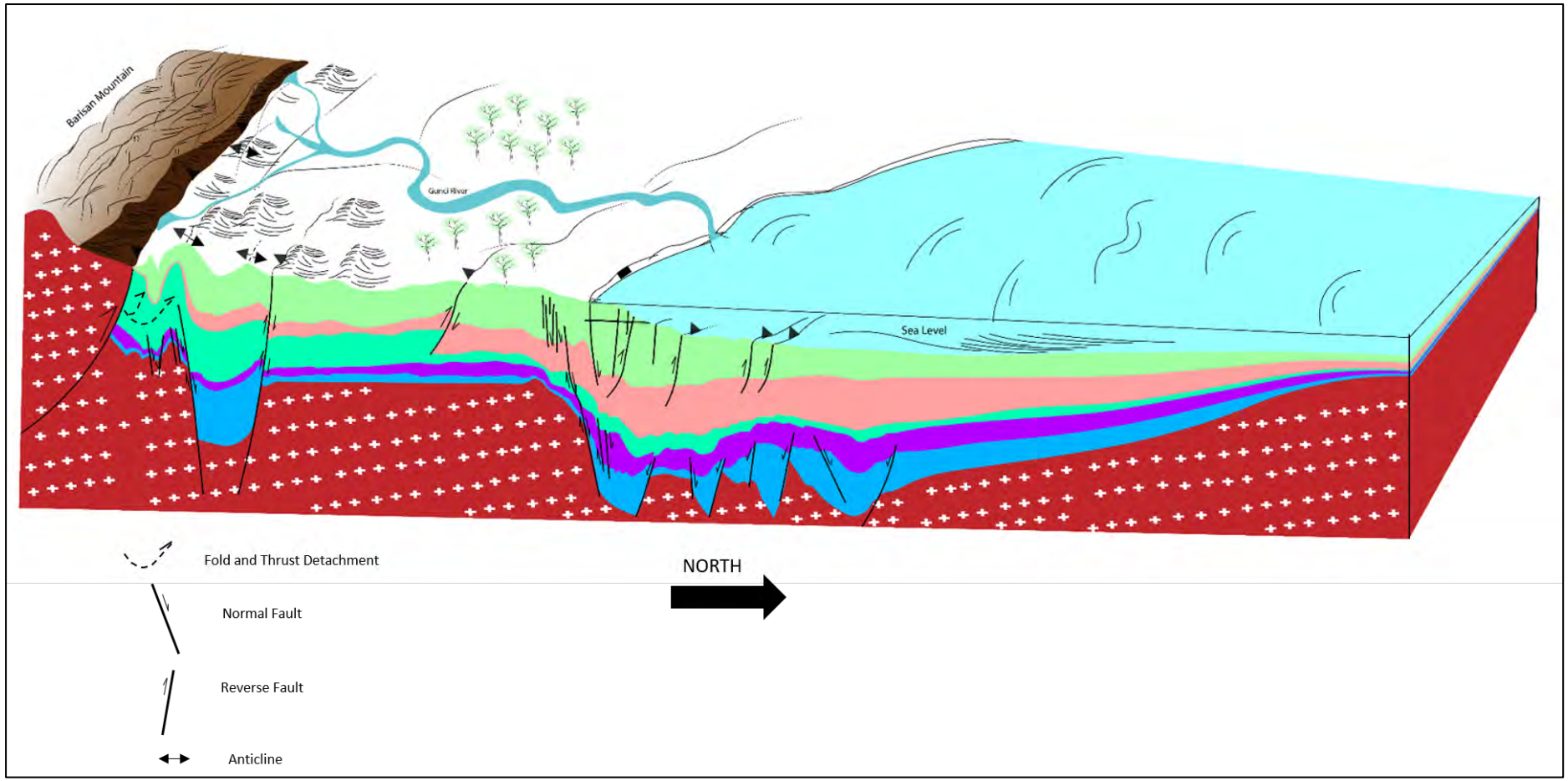

Figure 7-1 A schematic cross-section of south-north geological structure and stratigraphy from the Barisan foothills to the deep-water area offshore North Sumatra Basin.

7.2 Conclusion

This thesis has documented the complete findings of the structural and stratigraphic evolution and structural styles of the North Sumatra Basin, onshore and offshore. This thesis also revealed the timing of multi-phase deformation in the area from the Oligocene to recent tectonic events which all contribute to the complexity of the basin. Several conclusions can be made based on the data analysis and discussion presented in this thesis:

1. The North Sumatra Basin, the onshore and offshore areas, was initiated as a rifted basin during the Oligocene, while in the offshore North Sumatra Basin, where the seismic image are of better quality, the progression of rifting from the early and late Oligocene can be observed. Both areas also experienced tectonic quiescence during the early Miocene.

2. It has been possible to extend the mapping of horst and graben structures, particularly in the onshore area adjacent to the Barisan Mountains, where the basement platform high was defined by a northwest-southeast fault and enclosed by a north-south fault.

3. The onshore and offshore North Sumatra Basin has a different history relating to inversion structures. The inversion only occurred regionally during the Pliocene or younger time in the onshore research area. Meanwhile, the offshore area had a multi-phase inversion in the early Miocene, Late Miocene, and Pliocene-Pleistocene times. The inversions occurred only in certain places, such as the late Miocene fold that occurred northwest, toward the Mergui platform; and, during the Pliocene-Pleistocene, to the south toward the onshore area of North Sumatra Basin.

4. The structural movements controlled the stratigraphy onshore and offshore of North Sumatra Basin. For example, the local thickness during the Oligocene was controlled by extensional faults that created horst and grabens. Also, in the onshore area, the inversion during Pliocene or younger provides the space for younger sedimentary rocks to be deposited.

5. This thesis's findings update previous work conducted on the North Sumatra Basin. For example, the geological cross-section and the basement configuration in the onshore North Sumatra Basin emphasises the importance of large scale extensional faults and the thin skinned nature.

6. In the North Sumatra Basin there are still opportunities to explore hydrocarbon resources, especially in the western part where no hydrocarbon fields exist. In addition, the carbonate reservoir is still a potential target for future hydrocarbon exploration.

7.3 Recommendations for future works

1. This thesis has updated previous work done on this area/topic over many years. However, much work needs to be done regarding the structures and stratigraphy of the North Sumatra Basin, onshore and offshore. Due to the data gaps between those areas, the link from onshore to offshore could not be directly done to see the transformation of the structures and stratigraphy. Therefore, future work is needed on seismic data that connects onshore and offshore areas.

2. Some structural styles, such as Strike-slip faults, were identified in the Barisan Mountains, but not in the onshore and offshore areas using the 2D Seismic data in this thesis. Further research with better data, such as the 3D seismic surveys that have been acquired offshore, will make it possible to assess the significance, or otherwise, of this style of deformation.

3. This thesis provides foundation information for future study regarding resources and geo-hazard risks, although significant base line research is also needed. Therefore, it is essential to present and socialize the findings to the government in Indonesia, especially the Aceh Province.

4. This thesis justifies a request the government to map the surface and subsurface of the geological features to capture more data and bring new geological knowledge to the area.

5. New seismic data can be used to map the structures, especially the minor and detailed structures that could not be covered in this thesis's map. Also, the 3D Seismic data can precisely map facies, properties, and even hydrocarbon accumulation.

6. The above-mentioned recommendations are all needed in the North Sumatra Basin so as to attract companies to come and explore opportunities with considerable potential to bring prosperity to the people of Aceh.

7. The North Sumatra Basin is considered to be a Paleogene-Neogene basin because the oldest sedimentary rocks filling the Basin are Oligocene in age, constrained by well information. However, the wells only penetrated the horst area, which may erode the oldest sedimentary rocks overlying the basement. Thus, new 3D data with more record length would be an advantage to revisit the stratigraphy filling the graben areas.

8. The acquisition of new data, such as 3D seismic surveys, must be conducted in the onshore area of the North Sumatra Basin. The benefits are not only for research purposes but also for economic reasons. The new 3D will reveal the hidden structures and stratigraphy that may not be visible in the old 2D seismic data.

8 References

Acocella, V., Bellier, O., Sandri, L., Sébrier, M., & Pramumijoyo, S. (2018). Weak tectono-magmatic relationships along an obliquely convergent plate boundary: Sumatra, Indonesia. Frontiers in Earth Science, 6, 3.

Ali, M. Y., Berteussen, K. A., Small, J., & Barkat, B. (2007). A low frequency, passive seismic experiment over a carbonate reservoir in Abu Dhabi. *first break, 25*(11).

Ali, M. Y., Berteussen, K. A., Small, J., & Barkat, B. (2010). Low-frequency passive seismic experiments in Abu Dhabi, United Arab Emirates: implications for hydrocarbon detection. *Geophysical Prospecting, 58*(5), 875-899.

Ali, M. Y., Berteussen, K. A., Small, J., Barkat, B., & Pahlevi, O. (2009). Results from a low frequency passive seismic experiment over an oilfield in Abu Dhabi. *first break, 27*(4).

Anderson, B., Bon, J., & Wahono, H. (1993). Reassessment of the Miocene stratigraphy, paleogeography and petroleum geochemistry of the Langsa Block in the offshore North Sumatra Basin. *Indonesia Petroleum Association Proceedings of the 22nd Annual Convention, 22*, 169-189.

Andreason, M. W., Mudford, B., & Onge, J. E. S. (1997). Geologic evolution and petroleum system of the Thailand Andaman Sea basins. Indonesia Petroleum Association Proceedings of the 16 th Annual.

Ascaria, A., Herrero, D. R., Mesquita, R., Kajatmo, A., Maria, V. O., Hidayat, W., . . . Adrianto, S. (2019). Extended Carbonate Play Revealed by High Quality New 3D Data, Deep Water Offshore North Sumatra Basin.

Bahesti, F., Subroto, E., Manaf, N., Sadirsan, W., & Wahyudin, M. (2013). *Integrated geochemical, geomechanical and geological (3G) study of Lower Baong Shale Formation for preliminary shale gas prospectivity in the North Sumatra Basin.* Paper presented at the SPE Unconventional Resources Conference and Exhibition-Asia Pacific.

Bahesti, F., Taufiqurrahman, R., Nuri, F., & Wahyudin, M. (2013). Shale Diapir Tectonic Evolution of the Baong Formation as a Potential Hydrocarbon Seal in the North Sumatra Basin.

Bennett, J., Bridge, D. M., Cameron, N., Djunuddin, A., Ghazali, S., Jeffrey, D., . . . Thompson, S. (1981). The Geology of the Calang Quadrangle, Sumatra (1: 250 000). *Geological Research and Development Centre, Bandung*.

Berglar, K., Gaedicke, C., Franke, D., Ladage, S., Klingelhoefer, F., & Djajadihardja, Y. S. (2010). Structural evolution and strike-slip tectonics off north-western Sumatra. *Tectonophysics, 480*(1-4), 119-132.

Brune, S., Williams, S. E., Butterworth, N. P., & Müller, R. D. (2016). Abrupt plate accelerations shape rifted continental margins. *Nature, 536*(7615), 201-204.

Buck, S. P., & McCulloh, T. H. (1994). Bampo-Peutu (!) Petroleum System, North Sumatra, Indonesia: Chapter 38: Part VI. Case Studies--Eastern Hemisphere.

Buntoro, A., Rahmad, B., Asmorowati, D., Lukmana, A. H., Fattah, E. F., & Anuraga, E. (2022). Overpressure mechanism prediction based on well log and mineralogy analysis from drill cuttings of well NSE-001 in the North Sumatra Basin area, Indonesia. *Journal of Petroleum Exploration and Production Technology, 12*(10), 2801-2815.

Cameron, N. R., Clarke, M., Aldiss, D., Aspden, J., & Djunuddin, A. (1980). The geological evolution of northern Sumatra. *Indonesia Petroleum Association Proceedings of the 9th Annual Convention, 9*, 149-187.

Caughey, C. A., & Wahyudi, T. (1993). Gas reservoirs in the Lower Miocene Peutu Formation, Aceh Timur, Sumatra. Indonesia Petroleum Association Proceedings of the 22nd Annual.

Collins, J., Kristanto, A., Bon, J., & Caughey, C. A. (1996). Sequence stratigraphic framework of Oligocene and Miocene carbonates, North Sumatra Basin, Indonesia.

Dangel, S., Schaepman, M., Stoll, E., Carniel, R., Barzandji, O., Rode, E.-D., & Singer, J. (2003). Phenomenology of tremor-like signals observed over hydrocarbon reservoirs. *Journal of Volcanology and Geothermal Research, 128*(1-3), 135-158.

Davidson, J. P., Reed, W. L., & Davis, P. M. (1997). Exploring earth: an introduction to physical geology.

Davies, P. R. (1984). Tertiary structural evolution and related hydrocarbon occurrences, North Sumatra Basin.

De Smet, M., & Barber, A. (2005). Tertiary stratigraphy. *Geological Society, London, Memoirs, 31*(1), 86-97.

Doust, H., & Sumner, H. S. (2007). Petroleum systems in rift basins–a collective approach inSoutheast Asian basins. *Petroleum Geoscience, 13*(2), 127-144.

Fan, J.-J., Niu, Y., Liu, Y.-M., & Hao, Y.-J. (2021). Timing of closure of the Meso-Tethys Ocean: Constraints from remnants of a 141–135 Ma ocean island within the Bangong–Nujiang Suture Zone, Tibetan Plateau. *GSA bulletin, 133*(9-10), 1875-1889.

Foulger, G. (1982). Geothermal exploration and reservoir monitoring using earthquakes and the passive seismic method. Geothermics, 11(4), 259-268.

Fuse, A., Tsukada, K., Kato, W., Honda, H., Sulaeman, A., Troyer, S., . . . Lunt, P. (1996). Hydrocarbon Kitchen and Migration Assessment of North Aceh Offshore Basin, North Sumatra, Indonesia from Views of Sequence Stratigraphy and Organic Geochemistry.

Geospasial, B. I. (2018). DEMNAS seamless digital elevation model (DEM) dan Batimetri Nasional. *Badan Informasi Geospasial*.

Hakim, F., Gunarto, M., Sompie, M., & Raharjo, S. (2014). Bireun High Complex, a Rejuvenated Carbonate Province in Offshore North Sumatra Basin.

Hakim, F., Sibarani, F., & Syaiful, M. (2019). Understanding Seafloor and Recent Seismic Architectures to Depositional Models for Deepwater Exploration in the North Sumatra Basin, Offshore.

Hall, R. (2002). Cenozoic geological and plate tectonic evolution of SE Asia and the SW Pacific: computer-based reconstructions, model and animations. *Journal of Asian Earth Sciences, 20*(4), 353-431.

Hall, R. (2012). Late Jurassic–Cenozoic reconstructions of the Indonesian region and the Indian Ocean. *Tectonophysics, 570*, 1-41.

Jordan Jr, C. F., & Abdullah, M. (1992). Arun Field--Indonesia North Sumatra Basin, Sumatra.

Kamili, Z., Kingston, J., Achmad, Z., Wahab, A., Sosromihardjd, S., & Crausaz, C. (1976). Contribution to the Pre–Baong Stratigraphy of North Sumatra.

Kingston, J. (1978). Oil and gas generation, migration and accumulation in the North Sumatra Basin.

Kirby, G., Situmorang, B., & Setiardja, B. (1989). Seismic stratigraphy of the Baong and Keutapang Formations, North Sumatra Basin.

Kurniawan, K. (2018). Pelaksanaan Tugas Dan Fungsi Badan Pengelolaan Migas Aceh Menurut Peraturan Pemerintah Nomor 23 Tahun 2015 Tentang Pengelolaan Bersama Sumber Daya Alam Minyak Dan Gas Bumi Di Aceh. *Jurnal Ilmiah Mahasiswa Bidang Hukum Kenegaraan, 2*(4), 709-718.

Lanin, E., & Sone, H. (2022). *Geomechanical analysis of some potential shale reservoir formations in North Sumatra Basin, Indonesia.* Paper presented at the ARMA US Rock Mechanics/Geomechanics Symposium.

McArthur, A., & Helm, R. (1982). Miocene carbonate buildups, offshore North Sumatra. *Indonesia Petroleum Association, Proceedings of the 11th Annual Convention, 11*, 127-146.

McCaffrey, R. (2009). The tectonic framework of the Sumatran subduction zone. *Annual Review of Earth and Planetary Sciences, 37*(1), 345-366.

McNeill, L. C., & Henstock, T. J. (2014). Forearc structure and morphology along the Sumatra-Andaman subduction zone. *Tectonics, 33*(2), 112-134.

Meckel III, L. D. (2013). Late Syn-Rift Turbidite Systems in the North Sumatra Basin. Berita Sedimentologi, 27(1), 15-17.

Meckel III, L. D., & Banukarso, M. (2016). Exploring Indonesia's Mature Basins: North Sumatran Carbonates. Indonesia Petroleum Association Proceedings of the 45th Annual.

Meckel, L. D., Gidding, M., Sompie, M., Banukarso, M., Setoputri, A., Gunarto, M., . . . Sim, D. (2012). Hydrocarbon systems of the offshore North Sumatra basin, Indonesia. Indonesia Petroleum Association Proceedings of the 41st Annual.

Morley, C. (2001). Combined escape tectonics and subduction rollback–back arc extension: a model for the evolution of Tertiary rift basins in Thailand, Malaysia and Laos. Journal of the Geological Society, 158(3), 461-474.

Morley, C. (2002). A tectonic model for the Tertiary evolution of strike–slip faults and rift basins in SE Asia. *Tectonophysics, 347*(4), 189-215.

Morley, C., & Alvey, A. (2015). Is spreading prolonged, episodic or incipient in the Andaman Sea? Evidence from deepwater sedimentation. Journal of Asian Earth Sciences, 98, 446-456.

Morton, A. C., Humphreys, B., & Dharmayanti, D. A. (1994). Palaeogeographic implications of the heavy mineral distribution in Miocene sandstones of the North Sumatra Basin. *Journal of Southeast Asian Earth Sciences, 10*(3-4), 177-190.

Mount, V. S., & Suppe, J. (1992). Present-day stress orientations adjacent to active strike-slip faults: California and Sumatra. *Journal of Geophysical Research: Solid Earth, 97*(B8), 11995-12013.

Mulhadiono, P. H., & Soedaldjo, P. (1978). The middle Baong sandstone unit as one of the most prospective units in the Aru area, North Sumatra. *Indonesia Petroleum Association Proceedings of the 7th Annual Convention, 7*, 107-132.

Pertamina/Beicip. (1985). Hydrocarbon Potential of Western Indonesia. *Pertamina report,*, 275.

Peterson, J. R. (1993). *Observations and modeling of seismic background noise* (2331-1258). Retrieved from US Geological Survey. Open-File Report, vol. 93-322. 42 pp

PGS (Producer). (2022). PGS MultiClient Data in the North Sumatra Basin Yields Successful Results for Harbour Energy. Retrieved from https://www.pgs.com/company/newsroom/news/pgs-multiclient-data-in-the-north-sumatra-basin-indonesia-yields-successful-results-for-harbour-energy/

Prawirodirdjo, L., Bocl, Y., McCaffrey, R., Genrich, J., Calais, E., Stevens, C., . . . Zwick, P. (1997). Geodetic observations of interseismic strain segmentation at the Sumatra subduction zone. *Geophysical research letters, 24*(21), 2601-2604.

Pubellier, M., & Morley, C. (2014). The basins of Sundaland (SE Asia): Evolution and boundary conditions. Marine and Petroleum Geology, 58, 555-578.

Putuhena, M. I. F. (2015). Politik Hukum Participating Interest dalam Pengelolaan Migas (Pendekatan Pasal 33 UUD NRI Tahun 1945). *Jurnal Hukum dan Bisnis (Selisik), 1*(2), 66-81.

Rahman, A., Dargusch, P., & Wadley, D. (2021). The political economy of oil supply in Indonesia and the implications for renewable energy development. Renewable and Sustainable Energy Reviews, 144, 111027.

Rangin, C., Le Pichon, X., Mazzotti, S., Pubellier, M., Chamot-Rooke, N., Aurelio, M., . . . Quebral, R. (1999). Plate convergence measured by GPS across the Sundaland/Philippine Sea Plate deformed boundary: the Philippines and eastern Indonesia. *Geophysical Journal International, 139*(2), 296-316.

Rizky, A., Fahmi, B., Amijaya, D. H., & Anggara, F. (2018). geochemistry characteristic implication to brittleness index of lower baong formation, southern north sumatra basin. Indonesia Petroleum Association Proceedings of the 47th Annual

Ronoatmojo, I. S., Burhannudinnur, M., & Titaley, G. S. (2020). The influence of tectonic forces on the coupling ratio of sand Z-600, Keutapang formation, North Sumatra Basin. Paper presented at the AIP Conference Proceedings.

Rory, R. (1990). Geology of the South Lho Sukon'A'Field North Sumatra, Indonesia. Indonesia Petroleum Association Proceedings of the 21th Annual

Ryacudu, R., & Sjahbuddin, E. (1994). Tampur Formation, the Forgotten Objective in the North Sumatra Basin?

Saenger, E. H., Schmalholz, S. M., Lambert, M.-A., Nguyen, T. T., Torres, A., Metzger, S., . . . Méndez-Hernández, E. (2009). A passive seismic survey over a gas field: Analysis of low-frequency anomalies. *Geophysics, 74*(2), O29-O40.

Setiawan, B., Muchlis, I. H., Arsyi, H., & Ardhie, M. (2021). Application of Anomaly Spectral Density (ASD) for Hydrocarbon Prospecting.

Setyobudi, P. T., Suandhi, P. A., Tarigan, Z. L., Bachtiar, A., Jayanti, A. G. R., & Budin, L. (2016). Sedimentology And Limnology Of Singkarak And Toba Lakes, Sumatra, Indonesia: Depositional And Petroleum System Model For Tropical Fluvio-Lacustrine And Volcanic Related Rift Basins In Southeast Asia. Indonesia Petroleum Association Proceedings of the 44th Annual

Sidauruk, R., & Hamdi, M. (2015). *Mendorong pembentukan kebijakan dan implementasi data terbuka di Indonesia*: Institute for Criminal Justice Reform.

Situmorang, B., & Yulihanto, B. (1985). The role of strike slip faulting in structural development of the North Sumatra basin.

Sjahbuddin, E., & Djaafar, R. (1993). Hydrocarbon source rock characteristics and the implications for hydrocarbon maturation in the North Sumatra Basin.

Sosromihardjo, S. (1988). Structural analysis of the North Sumatra Basin-with emphasis on Synthetic Aperture Radar data.

Spence, W., Sipkin, S. A., & Choy, G. L. (1989). Measuring the size of an earthquake. *Earthquake Information Bulletin (USGS), 21*(1), 58-63.

Syafrin, K. N. (1995). Deposition of Middle Baong Sandstone as Post-Rift Incised Valley Fill Sequence, Aru Onshore Area, North Sumatra.

Tampubolon, R. A., Ozza, T., Arifin, M. T., Hidayatillah, A. S., Prasetio, A., & Furqan, T. (2017). A Review of Regional Geology of the North Sumatra Basin and Its Paleogene Petroleum System. Berita Sedimentologi, 37(1), 23-29.

Tarigan, Z. L., & Silaen, R. T. (2013). Dolomite Diagenesis of Tampur Formation Along Tampur River, Southeast Aceh.

Tsukada, K., Fuse, A., Kato, W., Honda, H., Abdullah, M., Wamsteeker, L., . . . Bon, J. (1996). Sequence stratigraphy of the North Aceh offshore area, North Sumatra, Indonesia.

USGS. (2022). Earthquakes map of East Aceh from 1950 to 2022

Van der Pluijm, B. A., & Marshak, S. (2004). Earth structure: An introduction to structural geology and tectonics. WW Norton and Company. Inc, New York.

Van Mastrigt, P., & Al-Dulaijan, A. (2008). *Seismic spectroscopy using amplified 3C geophones*. Paper presented at the 70th EAGE Conference and Exhibition incorporating SPE EUROPEC 2008.

Wajzer, M., Barber, A., & Hidayat, S. (1991). Accretion, collision and strike-slip faulting: the Woyla Group as a key to the tectonic evolution of North Sumatra. *Journal of Southeast Asian Earth Sciences, 6*(3-4), 447-461.

Warren, I., Gasperikova, E., Pullammanappallil, S., & Grealy, M. (2018). Mapping geothermal permeability using passive seismic emission tomography constrained by cooperative inversion of active seismic and electromagnetic data. Paper presented at the Proceedings of the 43rd Stanford Workshop on Geothermal Reservoir Engineering, Stanford, CA, USA.

Watkinson, I., Elders, C., & Hall, R. (2008). The kinematic history of the Khlong Marui and Ranong Faults, southern Thailand. Journal of Structural Geology, 30(12), 1554-1571.

Wicaksono, A. F., Sijabat, H., Usman, T. K., Susanti, D. N., & Indrajaya, H. (2016). Defining Pre-Tertiary Petroleum System of Langkat Area, North Sumatera Basin, Indonesia.

Widiyantoro, S., & van der Hilst, R. (1996). Structure and evolution of lithospheric slab beneath the Sunda arc, Indonesia. *Science, 271*(5255), 1566-1570.